PHOSPHATE INTERACTIONS WITH PROTEINS

Wayne J. Fairbrother

A thesis submitted to the Board of the Faculty of Physical Sciences (Chemistry) of the University of Oxford in partial fulfilment of the requirements for the Degree of Doctor of Philosophy.

Wolfson College
Oxford

Trinity Term
1989

ABSTRACT

Phosphate Interactions With Proteins

Wayne J. Fairbrother
Wolfson College, Oxford

Submitted for the Degree of Doctor of Philosophy

Trinity Term, 1989

Proton nuclear magnetic resonance (NMR) spectroscopy has been used to investigate the interaction of yeast phosphoglycerate kinase (PGK) with its phosphate containing substrates, ATP and 3-phosphoglycerate (3-PG). The application of one-dimensional and, for the first time, two-dimensional proton NMR techniques to this large protein has enabled specific resonance assignments to be made. Assignment has been aided by the investigation of specifically deuterated protein and site-specific mutant forms of the protein, including the isolated N- and C-domains.

The effects of ATP and 3-PG binding on the proton NMR spectrum of yeast PGK have been characterised and the assigned resonances used as local probes of structural and dynamic changes. Two binding sites have been determined for the nucleotide substrate, ATP, the occupancies of which are dependent on Mg^{2+} concentration. One site corresponds to the catalytic site determined crystallographically. A single binding site was found for 3-PG. This binding was shown to cause highly specific conformational changes throughout the N-domain and the interdomain region, which involve the relative movement of at least three α-helices. Investigation of 3-PG binding to several site-specific mutant forms of yeast PGK revealed a critical role for arginine 168 in the propagation of these changes.

The general binding of anions to yeast PGK was investigated using the paramagnetic probes $[Cr(CN)_6]^{3-}$ and $[Fe(CN)_6]^{3-}$, and the diamagnetic anion $[Co(CN)_6]^{3-}$. The primary anion binding site was determined from $[Cr(CN)_6]^{3-}$ broadening data and found to share some side-chains involved in 3-PG binding, namely histidine 62 and arginine 168. Evidence for a secondary anion site was found. The anion binding data is discussed in view of the complex activation/inhibition effects of anions on the catalytic activity.

Investigation of the isolated N- and C-domains showed that both can fold independently and confirmed that the C-domain is a nucleotide binding domain. It appears that the presence of the interdomain residues and/or the C-terminal peptide are neccessary for 3-PG binding to the N-domain.

This work shows that the specificity of the substrates is in binding, as expected, but also in the motions induced in the protein as a whole.

CONTENTS

PUBLICATIONS

Some of the work from this thesis has been published under the following titles :-

"Anion binding study of yeast phosphoglycerate kinase by nuclear magnetic resonance and site-specific mutagenesis".

Fairbrother, W.J., Hall, L., Littlechild, J.A., Minard, P., Watson, H.C. and Williams, R.J.P. (1987) *Biochem. Soc. Trans. 15,* 868.

"Probing the 3-phosphoglycerate binding site of yeast phosphoglycerate kinase using site-specific mutants and nuclear magnetic resonance".

Fairbrother, W.J., Hall, L., Littlechild, J.A., Walker, P., Watson, H.C. and Williams, R.J.P. (1988) *Biochem. Soc. Trans. 16,* 724.

"NMR analysis of site-specific mutants of yeast phosphoglycerate kinase - an investigation of the triose binding-site".

Fairbrother, W.J., Walker, P., Minard, P., Littlechild, J.A., Watson, H.C. and Williams, R.J.P. (1989) *Eur. J. Biochem.,* in press.

"Nuclear magnetic resonance studies of isolated domains of yeast phosphoglycerate kinase".

Fairbrother, W.J., Minard, P., Hall, L., Betton, J.-M., Missiakas, D., Yon, J.M. and Williams, R.J.P. (1989) *Protein Eng. 3,* in press.

"One- and two-dimensional NMR studies of yeast phosphoglycerate kinase".

Fairbrother, W.J., Bowen, D., Hall, L. and Williams, R.J.P. (1989) *Eur. J. Biochem.,* in press.

"An NMR analysis of the binding of inhibitors to yeast phosphoglycerate kinase".

Boyle, H.A., Fairbrother, W.J. and Williams, R.J.P. (1989) *Eur. J. Biochem.,* in press.

SYMBOLS AND ABBREVIATIONS

Symbols

Ala, A	alanine
Arg, R	arginine
Asn, N	asparagine
Asp, D	aspartic acid
β	Bohr magneton
Cys, C	cysteine
δ	chemical shift
$\Delta\delta$	change in chemical shift
Δp	change in peak height
$\Delta\nu$	line width (in Hz)
$\Delta\nu_p$	line width contribution due to presence of paramagnetic ion
g	Landé g-factor
g_x, g_y, g_z	components of g
$g_{\parallel} = g_z$	component of g along z axis, if g is axially symmetric
$g_{\perp} = g_x, g_y$	component of g along x or y axis, if g is axially symmetric
Gln, Q	glutamine
Glu, E	glutamic acid
γ_I	magnetogyric ratio of nucleus of spin I
$\hbar = h/(2\pi)$	Planck constant
His, H	histidine
Ile, I	isoleucine
K_d	dissociation constant
K_{eq}	equilibrium constant
K_m	Michaelis constant
$k_{cat.}$	catalytic rate constant
k	Boltzmann constant
Leu, L	leucine

Lys, K	lysine
M	molecular mass
Met, M	methionine
M_r	relative molecular mass
μ_o	permeability of vacuum
η	viscosity
Phe, F	phenylalanine
pK_a	-log(acid dissociation constant)
Pro, P	proline
r	distance of nucleus from a second nucleus or from a perturbing (*e.g.* paramagnetic) centre
R	gas constant
$s_{20,w}$	sedimentation constant (temperature = 20°C, medium = water)
S	total electron spin
Ser, S	serine
T	absolute temperature (K)
t_1	time-domain one in two-dimensional NMR experiments (evolution time)
t_2	time-domain two in two-dimensional NMR experiments (aquisition time)
T_1	longitudinal relaxation time
T_2	transverse relaxation time
$1/T_{2,A}$	transverse relaxation rate of bulk site
$1/T_{2,M}$	transverse relaxation rate of bound site
$1/T_{2,P}$	paramagnetic contribution to transverse relaxation rate
Thr, T	threonine
Trp, W	tryptophan
Tyr, Y	tyrosine
τ_c	dipolar correlation time
τ_M	chemical exchange life-time

τ_R	rotational correlation time
τ_S	electron spin relaxation time
$\bar{V}$	partial specific volume
Val, V	valine
ω_I	nuclear Larmor frequency
ω_S	electron Larmor frequency
$\Delta\omega_M$	chemical shift of nucleus in bound state

Abbreviations

1,3-P_2G	1,3-bisphosphoglycerate
1D	one-dimensional
2D	two-dimensional
3-PG	3-phosphoglycerate
ADP	adenosine 5′-diphosphate
AMP	adenosine 5′-monophosphate
APP(CF_2)P	adenosine 5′-(β,γ-difluoromethylene)triphosphate
APP(NH)P	adenosine 5′-(β,γ-imido)triphosphate
ATP	adenosine 5′-triphosphate
CIDNP	chemically induced dynamic nuclear polarisation
COSY	2D correlated spectroscopy
D372N	mutant form of yeast PGK in which apartic acid 372 is replaced by asparagine
(d_5-Phe)PGK	phosphoglycerate kinase in which the phenylalanine side-chains are deuterated
Δ51-56	mutant form of yeast PGK in which the residue 51-56 have been replaced by the analogous sequence from *Thermus thermophilus* PGK
EDTA	ethylenediaminetetraacetate
FID	free induction decay
FPLC	fast protein liquid chromatography

G-3-P	glyceraldehyde-3-phosphate
GAPDH	glyceraldehyde-3-phosphate dehydrogenase (E.C. 1.2.1.12)
H62Q	mutant form of yeast PGK in which histidine 62 has been replaced by glutamine
H170D	mutant form of yeast PGK in which histidine 170 has been replaced by aspartic acid
H388Q	mutant form of yeast PGK in which histidine 388 has been replaced by glutamine
HEPES	4-(2-hydroxyethyl)-1-piperazineethanesulphonic acid
MES	4-morpholineethanesulphonic acid
NAD^+, NADH	nicotinamide-adenine dinucleotide (oxidised and reduced forms)
NMR	nuclear magnetic resonance
NOE	nuclear Overhauser effect
NOESY	2D nuclear Overhauser and exchange spectroscopy
PAGE	polyacrylamide gel electrophoresis
PGK	phosphoglycerate kinase (E.C. 2.7.2.3)
ppm	parts per million
R168K	mutant form of yeast PGK in which arginine 168 has been replaced by lysine
R168M	mutant form of yeast PGK in which arginine 168 has been replaced by methionine
RCT	2D relayed coherence transfer spectroscopy
RPM	revolutions per minute
SDS	sodium dodecyl sulphate
Tris	2-amino-2-hydroxymethylpropane-1,3-diol (tris(hydroxymethyl)aminomethane)
UV-vis	ultra violet-visible
WT	wild-type protein

Chapter 1

INTRODUCTION

1.1. General introduction

Enzyme-catalysed phosphoryl transfer is ubiquitous in intermediary metabolism (Knowles, 1980) and is involved in the regulation of cellular activity at all levels (Cohen, 1985). The enzymes which catalyse the transfer from phosphoric monoesters can be categorised into three classes: the phosphatases, where water is the acceptor of the phosphoryl group; the mutases, where the acceptor is another functional group on the donor molecule; and the kinases, which catalyse the transfer of the γ-phosphoryl group of a nucleoside triphosphate (usually adenosine 5′-triphosphate; ATP) to an acceptor molecule other than water. The subject of this thesis is a glycolytic enzyme in the latter class, 3-phosphoglycerate kinase (EC 2.7.2.3; PGK) from yeast.

Glycolysis is the reversible metabolic pathway that converts glucose into pyruvate, with the concomitant production of ATP providing a means of conserving chemical energy. All the intermediates of glycolysis (between glucose and pyruvate) are phosphorylated compounds. The phosphate moieties of the glycolytic intermediates serve as binding/recognition groups in the formation of substrate.enzyme complexes and are essential for energy conservation since they ultimately become the γ-phosphoryl groups of ATP. PGK catalyses the first ATP generating reaction in glycolysis, in which the acyl phosphoryl group of the unstable, high-energy intermediate 1,3-bisphosphoglycerate (1,3-P_2G) is transferred to adenosine 5′-diphosphate (ADP) to produce 3-phosphoglycerate (3-PG) and ATP (Scopes, 1973). The catalytic reaction has an absolute requirement for a divalent metal ion (usually Mg^{2+} *in vivo*):

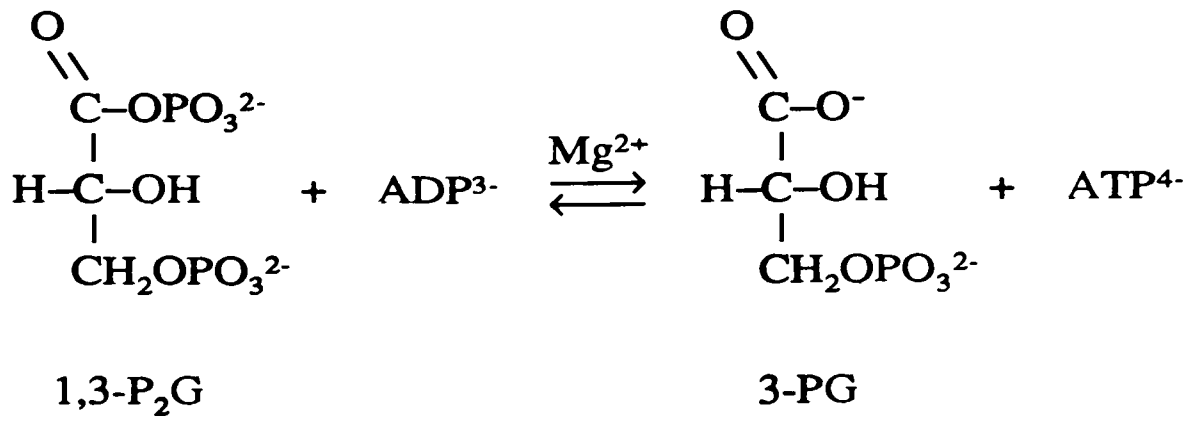

1,3-P_2G 3-PG

The equilibrium of the overall reaction is predominantly in favour of ATP production with K_{eq} = 2.8-3.1 × 10^{-4} at 25 °C (Krietsch & Bücher, 1970) and ΔG = -4.8 kcal mol^{-1}.

In addition to its role in glycolysis, PGK is involved in carbon fixation in many plant tissues since 3-PG is an early intermediate formed from CO_2 in a reaction catalysed by ribulosediphosphate carboxylase (Zelitch, 1975).

1.2. 3-Phosphoglycerate kinase (PGK)

1.2.1. *Structural studies*

The enzyme, from a variety of sources, has been shown to be monomeric with a molecular mass of about 45 kDa (Fifis & Scopes, 1978). Observation of similar amino acid compositions and catalytic properties led Fifis & Scopes (1978) to suggest that PGK has a highly conserved molecular and active site structure.

X-ray crystallographic studies of PGK from yeast (Bryant *et al.*, 1974; Watson *et al.*, 1982) and horse-muscle (Blake & Evans, 1974; Banks *et al.*, 1979; Blake & Rice, 1981) show a close structural homology. The most characteristic feature of the crystal structures is the presence of two widely separated domains, of approximately equal size, with a deep cleft between them (Figure 1-1). The domains correspond to the N-terminal and C-terminal portions of the molecule with the last ten residues of the C-terminus packed in the N-terminal domain. There are therefore two connections between the

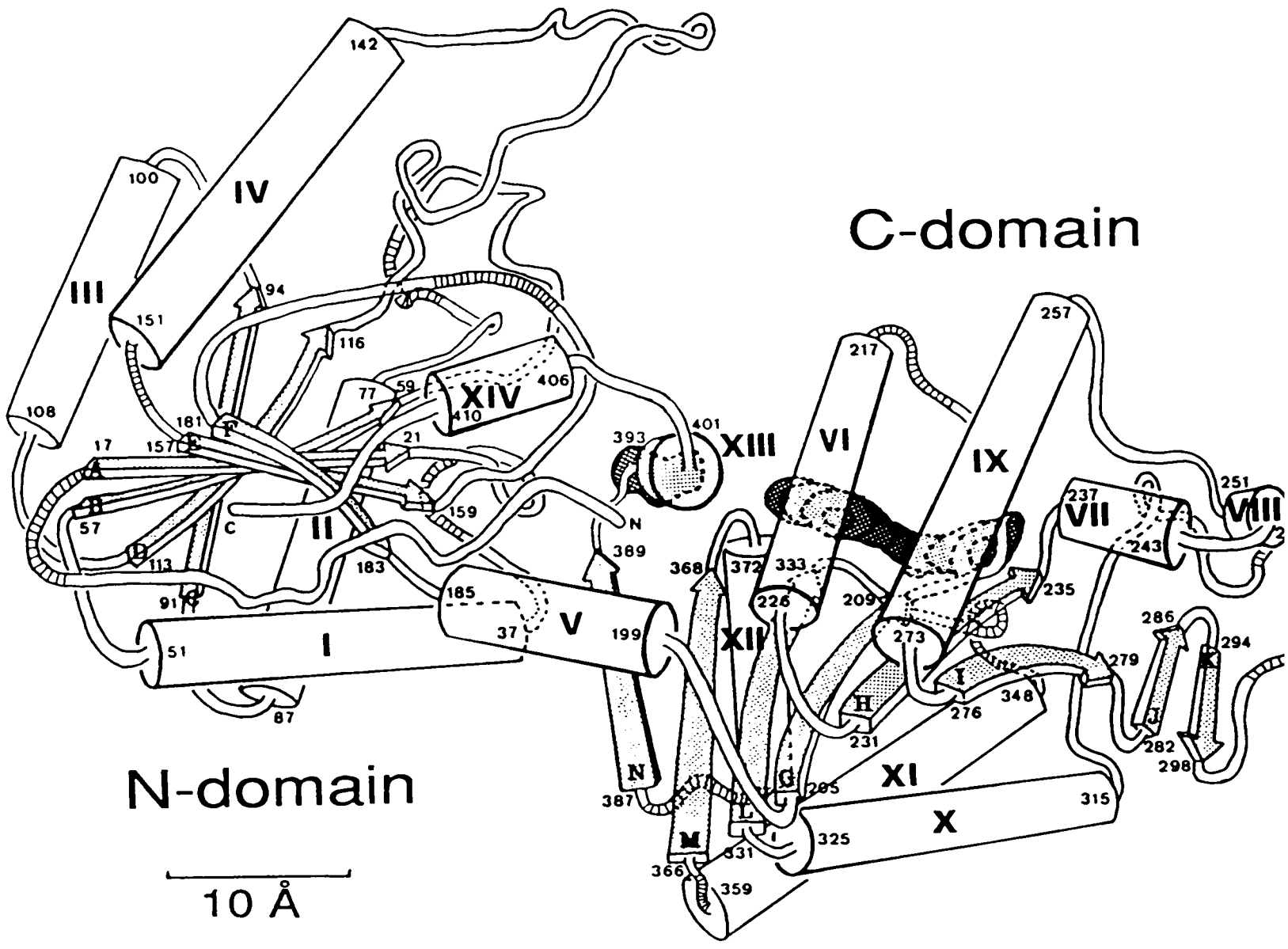

Figure 1-1: A schematic drawing of the crystal structure of yeast PGK. The α-helices are denoted by cylinders and the β-sheet strands by arrows. The crystallographically determined binding position for Mg.ATP is shown behind α-helices VI and IX, while that for 3-PG is behind helix XIII. (After Watson *et al.*, 1982).

domains. One, α-helix V (residues 185-199), runs from the N-domain to the C-domain, while the other involves residues 402-406 that link α-helices XIII and XIV (see Figure 1-1). The topology of the C-terminal domain of PGK is identical to the dinucleotide binding domain of the dehydrogenases, while that of the N-terminal domain is closely similar (Blake & Rice, 1981).

PGK crystals soaked in Mg.ADP and Mg.ATP have been shown to bind the nucleotides at a single site in the C-terminal domain (Banks *et al.*, 1979; Watson *et al.*, 1982). Experiments with yeast PGK, using data collected from crystals soaked in Mn.adenosine 5′-(β,γ-imido)triphosphate (Mn.APP(NH)P) at pH 9 (to minimise effects of sulphate ions on binding) have revealed the conformation of the bound nucleotide (Watson *et al.*, 1982). Its location is shown schematically in Figure 1-2. The adenine moiety lies in a shallow hydrophobic cleft defined by Gly 211, Ala 212, Phe 289, Leu 311, Gly 338 and Val 339. The ribose ring lies between Pro 336 and Gly 338 with its 2′- and 3′-OH groups coordinated to Glu 341 and Asp 372 respectively. The α- and β-phosphates interact with Lys 213 and Lys 217 respectively, while the γ-phosphate forms hydrogen-bonds with the main chain NH of Asp 372 and probably Gly 371, situated at the N-terminal end of α-helix XII. The crystallographic nucleotide binding site described for yeast PGK is essentially the same as that reported for crystals of horse-muscle PGK (Banks *et al.*, 1979).

The triose substrate binding site is less well defined. Blake and collaborators (Banks *et al,* 1979; Blake & Rice, 1981) were unable to identify the mode of 3-PG binding to crystals of horse-muscle PGK, although they postulated binding between Arg 38 and Arg 168 (170 in horse sequence). These residues form part of the positively charged face of the N-terminal domain defined by Arg 21, 38, 65 and 168, and His 62, 167 and 170. Three histidine residues were known to be close to the 3-PG site from NMR studies (Tanswell *et al.*, 1976). Binding in this position would place the substrate

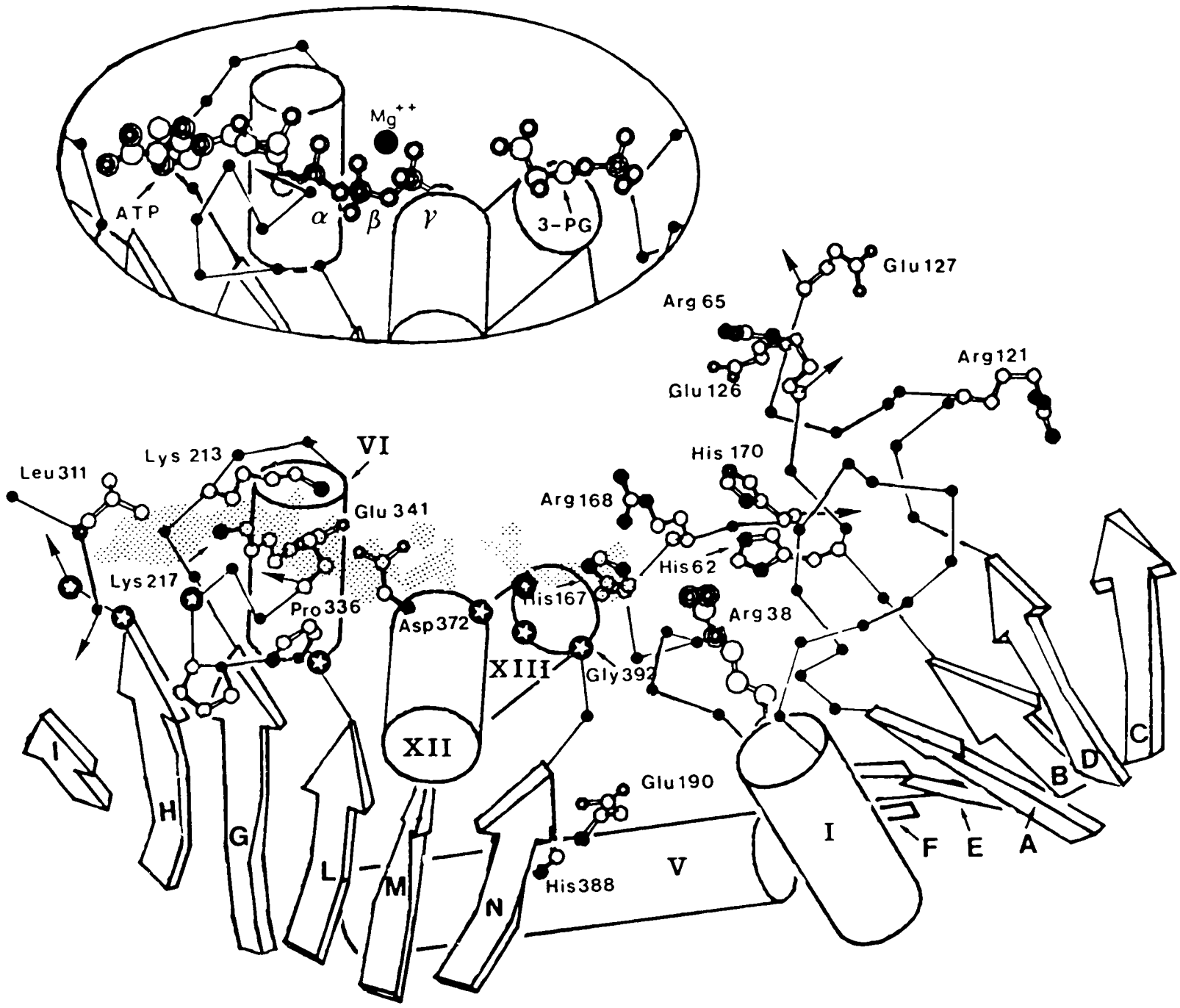

Figure 1-2: A schematic drawing of the active-site cleft of yeast PGK showing the binding site for Mg.ATP as determined by soaking crystals of the enzyme in solutions containing nucleotide substrates. The figure also includes the crystallographically determined 3-PG binding site. (After Wilson *et al.*, 1988).

12-15 Å from the γ-phosphate of ATP, a distance too large for the in-line attack mechanism proposed by Webb & Trentham (1980). Watson *et al.* (1982), on the other hand, have defined a 3-PG binding site involving the phosphate and 2′-OH moieties of the substrate, and the triple Gly sequence 392-394, Thr 391, and Arg 38 of the protein. The position of this crystallographically determined binding site is shown schematically in Figure 1-2. One of the carboxyl oxygens of bound 3-PG is only ~ 4 Å from, and in a suitable position to make an in-line attack on, the γ-phosphate of ATP.

It has been proposed that a substrate induced conformational change, resulting in the closure of the active site cleft between the two domains, is essential for the catalytic mechanism of the enzyme (Banks *et al.*, 1979; Anderson *et al.*, 1979) *i.e.* the crystal structure determined for yeast and horse-muscle PGKs represent an 'open' conformation. It has been pointed out that kinases in general have a need to exclude water from their active sites in order to facilitate phosphoryl transfer (Anderson *et al.*, 1979). Domain closure, as illustrated in Figure 1-3, would have the effect of shielding the substrates from water, thereby preventing phosphatase activity (yeast PGK has been shown to have no ATPase activity; Larsson-Raźnikiewicz & Schierbeck, 1974). Exclusion of water would also result in a lower dielectric environment to help promote the nucleophilic attack of the phosphoryl acceptor on the phosphoryl group to be transferred. Strong evidence for substrate induced conformational change has been obtained from solution studies, including NMR (Tanswell *et al.*, 1976; Wilson *et al.*, 1988), low angle X-ray scattering (Pickover *et al.*, 1979; Ptitsyn *et al.*, 1986; Sinev *et al.*, 1989) and analytical ultracentrifugation (Roustan *et al.*, 1980).

The amino acid sequences of a number of PGKs from both eukaryotes and prokaryotes have been determined (see Appendix 1). Comparison of the sequences reveals a high degree of homology between eukaryotic and prokaryotic enzymes. Regions of the molecule which are highly conserved can

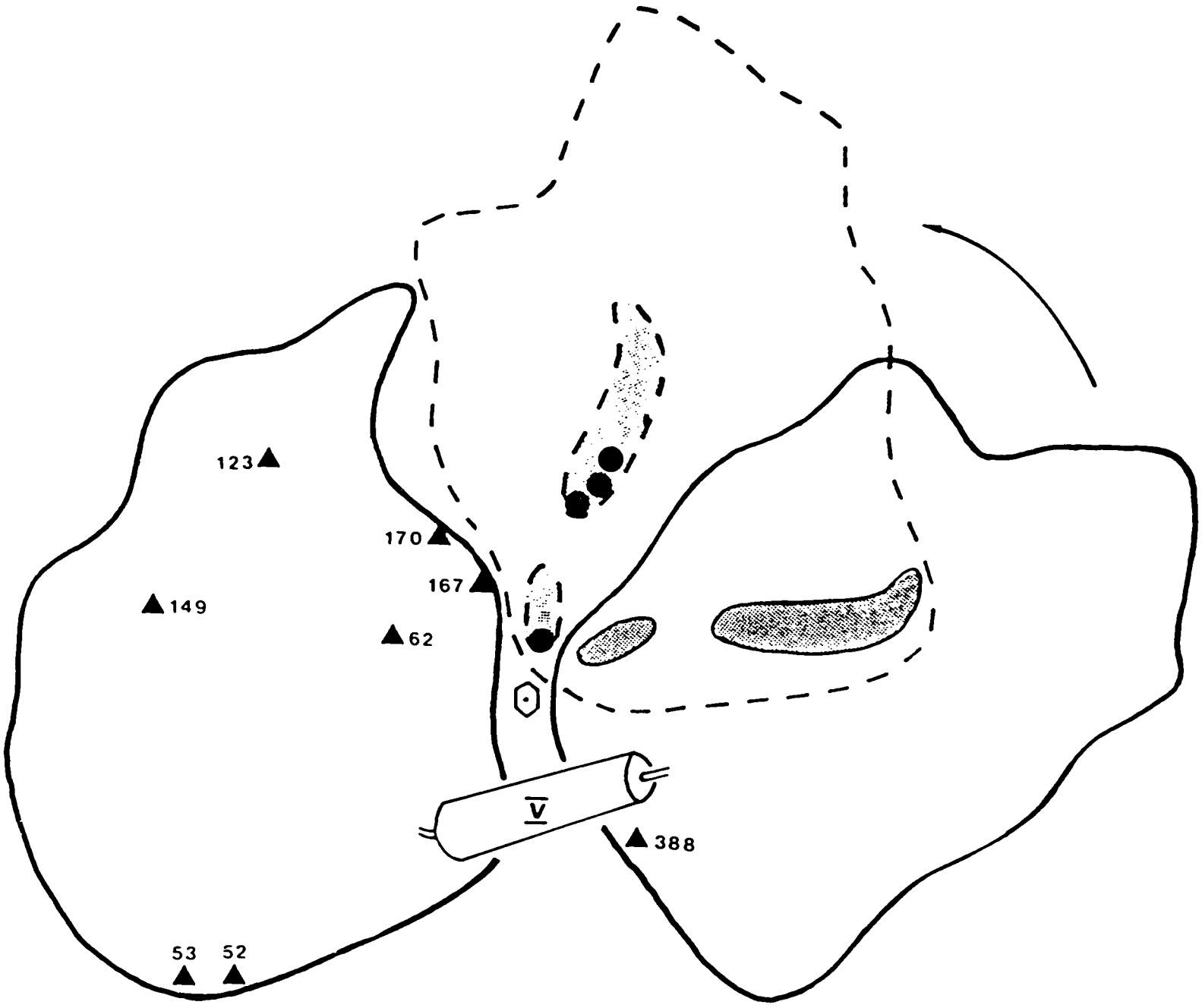

Figure 1-3: Outline of the yeast PGK molecule showing the crystallographic 'open' form and the proposed 'closed' form (broken line). The relative positions of the eight histidine residues (▲) and the substrates as observed in the crystal structure of the 'open' form of the enzyme are indicated. The positions of the phosphate groups (●) in the presumed 'closed' form are also shown. (After Watson & Gamblin, 1985).

be considered to be of structural and/or catalytic (mechanistic) importance. Alignment of the amino acid sequences of 21 PGKs (J.A. Littlechild, personal communication) indicates 68 residues which are totally conserved and a larger number of conservative substitutions. When the positions of the totally conserved amino acids are examined with respect to the crystal structure of yeast PGK (Figure 1-4) it is clear that the interdomain region and the active site faces of the N- and C-terminal domains are highly conserved.

1.2.2. *Kinetic studies*

There is a large amount of contradictory information in the literature regarding the kinetic properties of PGK. Most of the steady state kinetic determinations of substrate catalytic and inhibition parameters have been carried out by Larsson-Raźnikiewicz and her collaborators on the yeast enzyme. The results are, however, difficult to interpret in relation to known structural and functional properties of the enzyme, due mainly to the complexity of the system. The following points summarise the main conclusions:

(a) the reaction proceeds via a ternary complex between the enzyme and its two substrates when studied in the 'back' direction *i.e.* the direction of gluconeogenesis (Larsson-Raźnikiewicz, 1964, 1967; Larsson-Raźnikiewicz & Arvidsson, 1971; Larsson-Raźnikiewicz & Schierbeck, 1974).

(b) it has been possible to describe the mechanism as being of rapid equilibrium random order (Larsson-Raźnikiewicz & Arvidsson, 1971).

(c) at high concentrations of Mg^{2+} it appears that substrate activation occurs (Larsson-Raźnikiewicz, 1967). This result must be treated with caution, however, since $MgSO_4$ was used. Subsequent studies have shown multivalent anions, including sulphate, to activate PGK at low concentrations and inhibit at higher concentrations (Larsson-Raźnikiewicz & Jansson, 1973; Scopes, 1978a). Scopes (1978b) suggested that a single anion binding site, located at the active centre, could account for the observed activation and inhibition. In

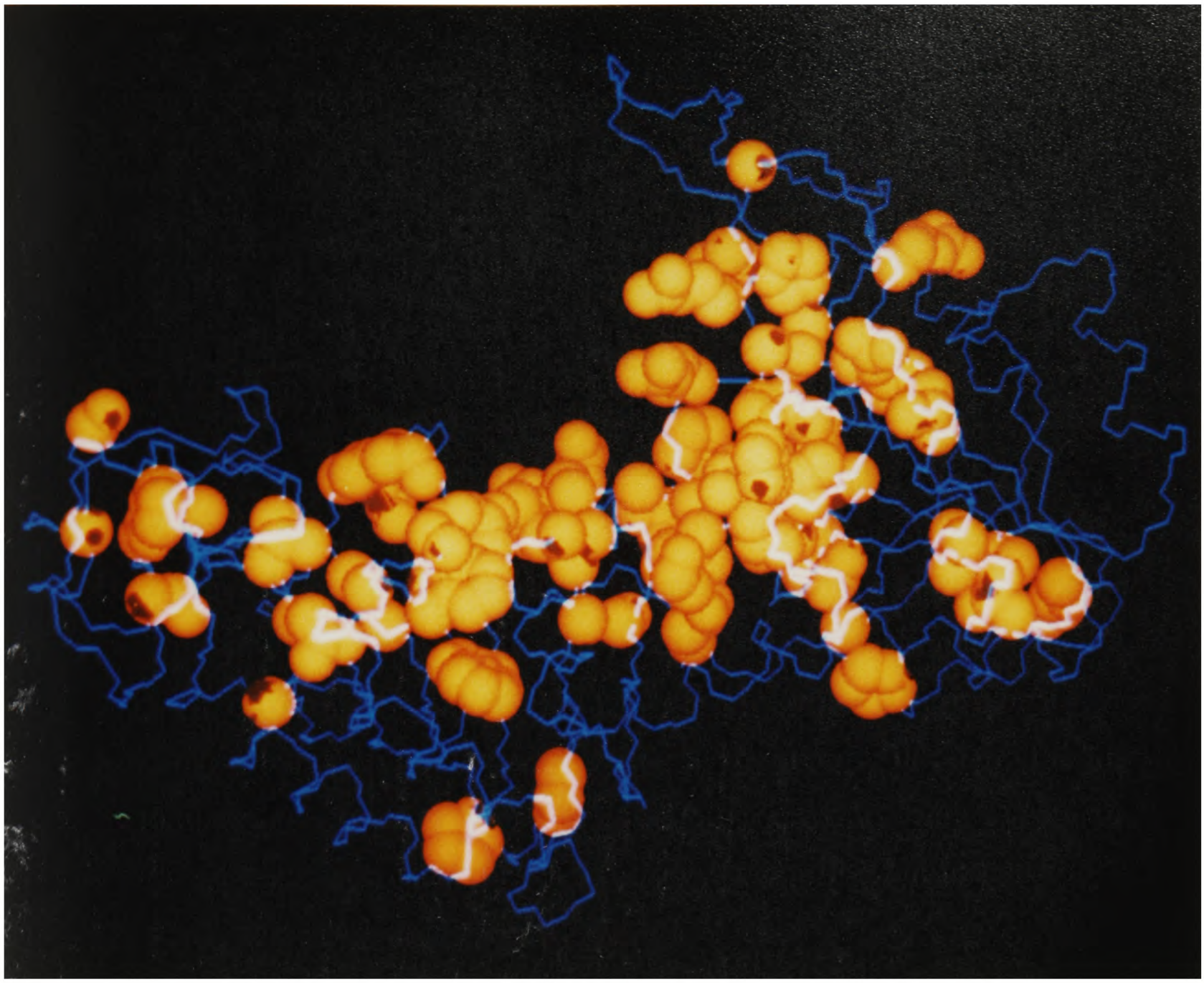

Figure 1-4: The positions of the totally conserved amino acid side-chains (drawn in orange space-filling mode) superposed on the main-chain (blue) of the crystal structure of yeast PGK. Totally conserved residues were determined from a sequence alignment of 21 PGKs (J.A. Littlechild, personal communication).

contrast, Khamis & Larsson-Raźnikiewicz (1981) proposed at least two anion sites, one being a general anion binding site, and a second being the catalytic centre.

(d) PGK has no ATPase activity (Larsson-Raźnikiewicz & Schierbeck, 1974).

(e) Mg^{2+} can be replaced as the divalent cation in the following order of activity, $Mg.ATP^{2-} \geq Mn.ATP^{2-} > Co.ATP^{2-} \sim Ca.ATP^{2-} > Zn.ATP^{2-} > Cd.ATP^{2-} > Ni.ATP^{2-}$. No measurable activity was found for Be^{2+} or Fe^{3+} (Larsson-Raźnikiewicz, 1970). The free divalent metal ions showed varying patterns of inhibition.

(f) ADP^{3-} and $Mg.ADP^{-}$ are competitive inhibitors, and AMP^{2-} is a non-competitive inhibitor of 3-PG (Larsson-Raźnikiewicz & Arvidsson, 1971). This, together with the fact that ATP^{4-} causes activation of the enzyme in the backward reaction (Larsson-Raźnikiewicz & Schierbeck, 1977) and the results of equilibrium studies on ATP^{4-} and 3-PG binding to PGK (Larsson-Raźnikiewicz, 1973), have been used as evidence for two binding sites for each substrate.

(g) further product inhibition studies appeared to confirm that multiple binding sites exist and a regulatory role was proposed (Schierbeck & Larsson-Raźnikiewicz, 1979).

Equlibrium gel filtration studies by Scopes (1978b) supported the conclusion that there are two adenine nucleotide binding sites but found only one site for 3-PG and 1,3-P_2G (with dissociation constants of ~ 33 μM and 0.6 μM respectively).

1.3. Objectives of the present work

The principle aim of this work is to use high field nuclear magnetic resonance (NMR) spectroscopy to address the following specific questions with regard to the structure-function relationships of yeast PGK in solution:

(a) which specific amino acid residues are involved in ligand binding to the

protein? In particular, the mode of binding of the triose substrate, 3-PG, and activating/inhibiting anions will be investigated.

(b) what is the extent of protein and ligand conformational changes (both local and long range) induced by ligand binding? Such conformational changes in proteins are not only important for enzyme catalysis but also for specificity and regulatory control (Williams, 1979; Karplus & McCammon, 1983; Williams, 1987).

(c) what is the number and nature of ligand (substrate, inhibitor, activator) binding sites on the protein?

Proton NMR spectroscopy is a powerful technique with the potential capability of probing into the structural and dynamic properties of all regions of a protein in solution. Every proton in the sample being studied will contribute differentially, depending on its chemical (and magnetic) environment and any temporal variations in that environment, to the observable NMR spectrum. Useful introductions into NMR spectroscopy are given by Shaw (1984) and Derome (1987), while a more detailed description is given by Ernst *et al.* (1987). The applications of NMR techniques to the study of proteins in solution, as in this thesis, are covered in detail in Dwek (1973), James (1975), Jardetzky and Roberts (1981) and Wüthrich (1986).

NMR has a number of advantages over the complimentary structural technique of X-ray crystallography, the first being that studies can be carried out in solution, under a wide variety of conditions (*e.g.* pH, temperature, ionic strength, ligand concentration, *etc.*). Information about protein and ligand dynamics is also readily available. NMR methods are restricted, however, in the case of large proteins due to the inability to resolve the increasing number of resonances which will be relatively broad.

The feasability of using NMR spectroscopy to study yeast PGK in solution has been demonstrated in previous studies (Tanswell *et al.*, 1976; Scheffler & Cohn, 1986; Wilson *et al.*, 1988), despite the fact that it has ~ 3000

potentially observable protons and a molecular mass of ~ 45 kDa. In the earlier 270 MHz study Tanswell *et al.* (1976), in the absence of a sequence and independently from the crystallographic studies, were able to define the 3-PG binding site in terms of three histidine residues. From experiments with paramagnetic shift and relaxation probes these three histidine residues were also found to be in close proximity to the phosphate binding sites of the bound nucleotide substrates. These results were found to be consistent with the subsequent crystallographic structure determinations (see § 1.2.1) if it was assumed that the NMR results related to a 'closed' conformation (Watson & Gamblin, 1985). More recent work has led to the suggestion that in solution the molecule fluctuates between many states including several 'open' or substrate binding forms in addition to the 'closed' and supposedly catalytically competent form (Wilson *et al.*, 1988). The occupancy of the various states appeared to be affected by several anions as well as substrates and their analogues. A number of tentative assignments have also been made to surface amino acids by comparison of NMR parameters with the X-ray structure (Wilson *et al.*, 1988) and with the use of photochemically induced dynamic nuclear polarisation (photo-CIDNP; Scheffler & Cohn, 1986).

The current work extends the previous analyses, principally through the use of higher-field spectrometers (500 MHz and 600 MHz) and site-specific mutagenesis (in collaboration with Drs H.C. Watson & L. Hall, Department of Biochemistry, University of Bristol).

In Chapter 2 the ^{1}H NMR spectrum is described in detail and two-dimensional (2D) techniques are applied to yeast PGK for the first time. The number of assignments, mainly to aromatic residues, is increased. The increased number of assignments allows more detailed interpretation of ligand induced effects in the spectrum.

In Chapter 3 the binding of the triose substrate, 3-PG, is reinvestigated in light of the new assignments and with the aid of 2D spectroscopy. Triose

binding is further investigated in Chapter 4 with the use of site-specific mutants of yeast PGK.

Metal hexacyanide probes ($[Cr(CN)_6]^{3-}$, $[Fe(CN)_6]^{3-}$ and $[Co(CN)_6]^{3-}$) are used in paramagnetic studies (Chapter 5) to define the general anion binding site of the protein. Results from this chapter are interpreted in view of the activatory/inhibitory effect of anions on the activity of PGK.

Chapter 6 and 7 concern the location of ATP binding to the protein and the effect of Mg^{2+} concentration. The paramagnetic cation, Mn^{2+}, is used to probe nucleotide binding in an analogous way to which Gd^{3+} was used in the previous studies (Tanswell *et al.*, 1976; Wilson *et al.*, 1988) and the results reevaluated.

The individual domains of yeast PGK have been produced using site-directed mutagenesis (Minard *et al.*, 1989) and are investigated using 1D and 2D NMR techniques in Chapter 8.

In the final chapter of this thesis the results are summarised and discussed in terms of the conformational and dynamic properties of the enzyme.

1.4. References

Anderson, C.M., Zucker, F.H. & Steitz, T.A. (1979) *Science 204,* 375-380.

Banks, R.D., Blake, C.C.F., Evans, P.R., Haser, R., Rice, D.W., Hardy, G.W., Merrett, M. & Phillips, A.W. (1979) *Nature (Lond.) 279,* 773-777.

Blake, C.C.F. & Evans, P.R. (1974) *J. Mol. Biol. 84,* 585-601.

Blake, C.C.F. & Rice, D.W. (1981) *Phil. Trans. R. Soc. Lond. A. 293,* 93-104.

Bryant, T.N., Watson, H.C. & Wendell, P.L. (1974) *Nature (Lond.) 247,* 14-17.

Cohen, P. (1985) *Eur. J. Biochem. 151,* 439-448.

Derome, A.E. (1987) *Modern NMR Techniques for Chemistry Research,* Pergamon Press, Oxford.

Dwek, R.A. (1973) *Nuclear Magnetic Resonance in Biochemistry,* Clarendon Press, Oxford.

Ernst, R.R., Bodenhausen, G. & Wokaun, A. (1987) *Principles of Nuclear Magnetic Resonance in One and Two Dimensions,* Clarendon Press, Oxford.

Fifis, T. & Scopes, R.K. (1978) *Biochem. J. 175,* 311-319.

James, T.L. (1975) *NMR in Biochemistry,* Academic Press, New York.

Jardetzky, O. & Roberts, G.C.K. (1981) *NMR in Molecular Biology,* Academic Press, New York.

Karplus, M. & McCammon, J.A. (1983) *Ann. Rev. Biochem. 53,* 263-300.

Khamis, M.M. & Larsson-Raźnikiewicz, M. (1981) *Biochim. Biophys. Acta 657,* 190-194.

Knowles, J.R. (1980) *Ann. Rev. Biochem. 49,* 877-919.

Krietsch, W.K.G. & Bücher, T. (1970) *Eur. J. Biochem. 17,* 568-580.

Larsson-Raźnikiewicz, M. (1964) *Biochim. Biophys. Acta 85,* 60-68.

Larsson-Raźnikiewicz, M. (1967) *Biochim. Biophys. Acta 132,* 33-40.

Larsson-Raźnikiewicz, M. (1970) *Eur. J. Biochem. 17,* 183-192.

Larsson-Raźnikiewicz, M. & Arvidsson, L. (1971) *Eur. J. Biochem. 22,* 506-512.

Larsson-Raźnikiewicz, M. (1973) *Arch. Biochem. Biophys. 158,* 754-762.

Larsson-Raźnikiewicz, M. & Jansson, J.R. (1973) *FEBS Lett. 29,* 345-347.

Larsson-Raźnikiewicz, M. & Schierbeck, B. (1974) *Biochem. Biophys. Res. Commun. 57,* 627-634.

Larsson-Raźnikiewicz, M. & Schierbeck, B. (1977) *Biochim. Biophys. Acta 481,* 283-287.

Minard, P., Hall, L., Betton, J.-M., Missiakas, D. & Yon, J.M. (1989) *Protein Eng. 3,* in press.

Pickover, C.A., McKay, D.B., Engelman, D.M. & Steitz, T.A. (1979) *J. Biol. Chem. 254,* 11323-11329.

Ptitsyn, O.B., Pavlov, M.Y., Sinev, M.A. & Timchenko, A.A. (1986) in *Multidomain Proteins,* (Patthy, L. & Friedrich, P. eds) pp. 9-25, Akadémiai Kiadó, Budapest.

Roustan, C., Fattoum, A., Jeanneau, R. & Pradel, L.-A. (1980) *Biochem. 19,* 5168-5175.

Scheffler, J.E. & Cohn, M. (1986) *Biochem. 25,* 3788-3796.

Schierbeck, B. & Larsson-Raźnikiewicz, M. (1979) *Biochim. Biophys. Acta 568,* 195-204.

Scopes, R.K. (1973) in *The Enzymes,* vol. 8. 3rd edn. (Boyer, P.D., ed.) pp. 335-351, Academic Press, New York.

Scopes, R.K. (1978a) *Eur. J. Biochem. 85,* 503-516.

Scopes, R.K. (1978b) *Eur. J. Biochem. 91,* 119-129.

Shaw, D. (1984) *Fourier Transform NMR Spectroscopy,* 2nd ed., Elsevier, Amsterdam.

Sinev, M.A., Razgulyaev, O.I., Vas, M., Timchenko, A.A. & Ptitsyn, O.B. (1989) *Eur. J. Biochem. 180,* 61-66.

Tanswell, P., Westhead, E.W. & Williams, R.J.P. (1976) *Eur. J. Biochem. 63,* 249-262.

Watson, H.C., Walker, N.P.C., Shaw, P.J., Bryant, T.N., Wendell, P.L., Fothergill, L.A., Perkins, R.E., Conroy, S.C., Dobson, M.J., Tuite, M.F., Kingsman, A.J. & Kingsman, S.M. (1982) *EMBO J. 1,* 1635-1640.

Watson, H.C. & Gamblin, S.J. (1985) *Proc. Int. Symp. Biomol. Struct. Interactions, Suppl. J. Biosci. 8,* 499-506.

Webb, M.R. & Trentham, D.R. (1980) *J. Biol. Chem. 255,* 1775-1778.

Williams, R.J.P. (1979) *Biol. Rev. 54,* 389-437.

Williams, R.J.P. (1987) *Carlsberg Res. Commun. 52,* 1-30.

Wilson, H.R., Williams, R.J.P., Littlechild, J.A. & Watson, H.C. (1988) *Eur. J. Biochem. 170,* 529-538.

Zelitch, I. (1975) *Ann. Rev. Biochem. 44,* 123-145.

Chapter 2

^{1}H NMR STUDIES OF YEAST PHOSPHOGLYCERATE KINASE

2.1. Introduction

Recent advances in NMR spectroscopy (Ernst *et al.*, 1987) have made possible the assignment of proton resonances of small proteins (M_r < 15000) and subsequent determination of their structures in solution (for recent reviews see Wüthrich, 1986; Clore & Gronenborn, 1987; Cooke & Campbell, 1988; Wüthrich, 1989). Sequential techniques are severely limited in the case of larger proteins, where the increased number of protons leads to severe spectral overlap and the larger molecular mass results in increased rotational correlation times and consequently broader linewidths. Further problems may also be encountered with concentration dependent aggregation of many larger proteins, which imposes limits on sample concentrations.

It is possible, however, that even large proteins will contain mobile regions that give rise to relatively well resolved resonances. These may be distinguished from those resonances originating from the remainder of the protein on the basis of their relaxation properties (Campbell *et al.*, 1975). This has been demonstrated recently for the multidomain fibrinolytic protein urokinase (M_r ~ 54000) (Oswald *et al.*, 1989).

A number of ^{1}H NMR studies of yeast PGK, which is a monomeric enzyme with M_r ~ 45000 (see Chapter 1), have been carried out and it has been noted that the spectrum contains a number of well dispersed, relatively sharp peaks in addition to the broad envelope typical of a larger protein (Tanswell *et al.*, 1976; Scheffler & Cohn, 1986; Wilson *et al.*, 1988). The crystallographic structures of both yeast (Watson *et al.*, 1982) and horse-muscle (Blake & Rice, 1981) enzymes show that PGK consists of two distinct domains. It has been suggested that the more mobile parts of the protein are associated with the

interdomain region, and that this region (in addition to some mobile side-chains on the protein surface) gives rise to the relatively well resolved resonances which are distinct from those originating from the less mobile cores of the two domains (Wilson *et al.*, 1988).

An extensive application of ^{1}H NMR spectroscopy to the investigation of structure-function relationships of PGK in solution is clearly dependent on the number of peak assignments available. Only a limited number of assignments have been made in the one-dimensional (1D) spectrum and these are mainly to sharp singlets of surface histidine residues (Scheffler & Cohn, 1986; Wilson *et al.*, 1988).

In this chapter a detailed description of the ^{1}H NMR spectrum of yeast PGK is given. It is shown that a combination of two-dimensional (2D) ^{1}H NMR methods and selective deuteration of phenylalanine residues allows improved resolution of selected resonances in the aromatic region of the spectrum. This has enabled the number of assignments to amino acid type to be increased, and further sequence specific assignments to be made. The use of site-specific mutagenesis for assignment purposes is also demonstrated.

2.2. Experimental methods

2.2.1. *Preparation of phosphoglycerate kinase*

The yeast PGK enzyme used in this study was either purchased from Boehringer Mannheim GmbH or prepared in the laboratories of Drs L. Hall and H.C. Watson (Department of Biochemistry, University of Bristol) from an overproducing yeast strain. The host yeast strain MD40/4C was transformed using a lithium acetate procedure (Ito *et al.*, 1983) with a modified yeast vector based on that described as pMA27 (Dobson *et al.*, 1982). The new expression vector pYE-PGK (Minard *et al.*, 1989) is based on the bacterial plasmid pAT153 and has the yeast 2μ origin of replication and the PGK gene

flanked on either side by a *Bam*HI site to enable easy transfer of the PGK gene in and out of the vector. The transformed yeast cells were grown on a leucine deficient selective growth medium to allow for selection of the cells containing the plasmid vector (Wilson *et al.*, 1987; Minard *et al.*, 1989). The composition of the growth medium is given in Table 2-1.

2.2.2. *Extraction and purification of (d_5-Phe)PGK*

In order to prepare the deuterated PGK protein, phenylalanine in the growth medium was substituted with the deuterated amino acid (L-Phenyl-d_5-alanine, 98.6 atom %, Merck, Sharp and Dohme). Two 4 litre cultures of cells were grown at 29 °C to an $A_{560\ nm}$ of 1.2-1.4 (21 hours after inoculation). The cells were harvested by centrifugation, broken by freeze fracturing in liquid nitrogen and resuspended in an extraction buffer containing 0.01 M Tris/HCl (pH 7.5), 0.1 mM EDTA, 6 mM β-mercaptoethanol and the protease inhibitors phenylmethylsulphonyl fluoride (1×10^{-5} M) and benzamidine (2×10^{-5} M). Ammonia lysis (pH 9.5) was carried out overnight. Neutralisation was achieved by addition of 5 M lactic acid/ammonia (pH 4.0). The cell debris was removed by centrifugation (9000 RPM for 1 h). SDS-polyacrylamide gel electrophoresis (Laemilli & Favre, 1973) of the crude extract (Figure 2-1) shows a high level of expression, corresponding to 50-80% of the protein present. Protamine sulphate (100 g l^{-1}) was then added (1 ml to each 200 ml of extract, stirred for 30 min) in order to precipitate contaminating nucleic acids. The precipitate was removed by centrifugation (9000 RPM for 1 h) and discarded.

2.2.3. *Ammonium sulphate fractionation of (d_5-Phe)PGK*

300 g of solid $(NH_4)_2SO_4$ (Enzyme grade) was added slowly, with constant stirring, to each litre of extract to give a 50% saturated solution. Stirring was continued for a further 30 min. The material precipitated at 50% saturated $(NH_4)_2SO_4$ was discarded (separation being achieved by centrifugation as

Table 2-1: Composition of growth medium

Yeast nitrogen base	6.7 g l^{-1}
glucose	10.0 g l^{-1}
stock amino acid solution*	20 ml l^{-1}
0.2 % w/w tryptophan	10 ml l^{-1}

* stock amino acid solution

	concentration/g l^{-1}
adenine	1.0
uracil	1.0
histidine	1.0
tyrosine	1.5
phenylalanine	2.5
lysine	1.5
arginine	1.0
methionine	1.0
isoleucine	15.0
valine	7.5
threonine	10.0
serine	17.5
glutamic acid	5.0
aspartic acid	5.0

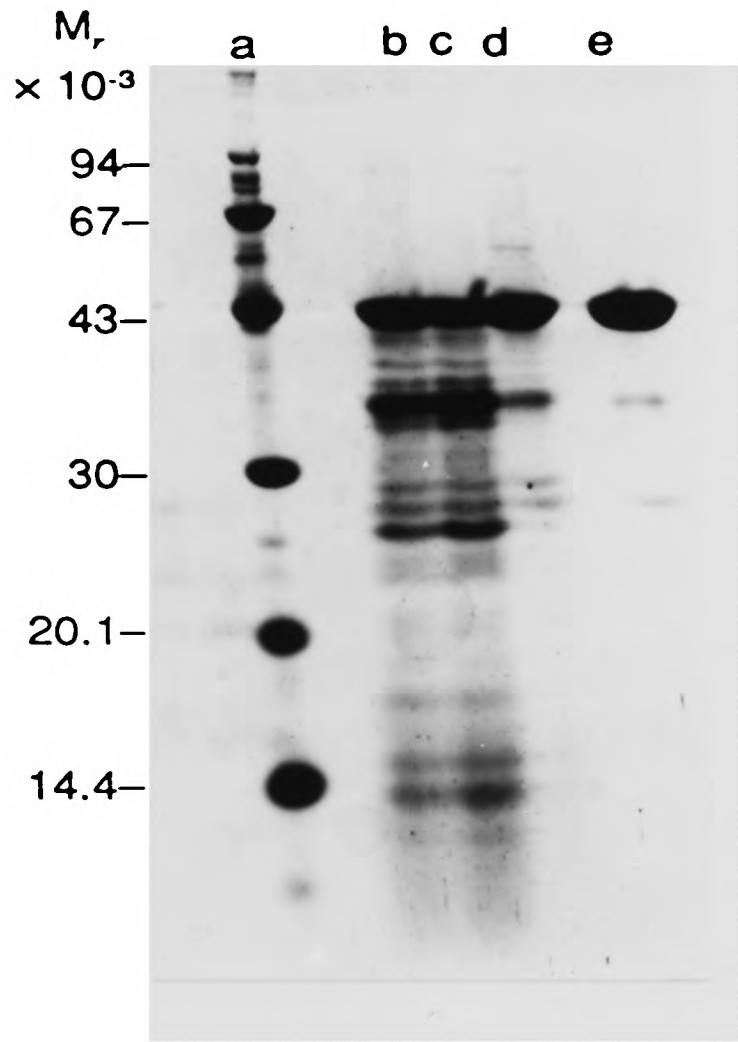

Figure 2-1: SDS-polyacrylamide gel electrophoresis of extracts at various stages of purification. Lane a, molecular mass standards (phosphorylase b, 94 kDa; bovine serum albumin, 67 kDa; ovalbumin, 43 kDa; carbonic anhydrase, 30 kDa; soybean trypsin inhibitor, 20.1 kDa; α-lactalbumin, 14.4 kDa); lane b, crude cell extract; lane c, supernatant following protamine sulphate cut; lane d, supernatant following 50% saturated $(NH_4)_2SO_4$ cut; lane e, resuspended 'acid crash' precipitate following 75% saturated $(NH_4)_2SO_4$ cut. Material precipitated at 75% saturated $(NH_4)_2SO_4$ was treated by gel filtration on Sephacryl S-200 (see Figure 2-2).

before). The supernatant, containing most of the PGK, was made up to 75% saturated $(NH_4)_2SO_4$ as above and stirred for a further 30 min. The resulting precipitate (again separated from the supernatant by centrifugation as above) contained most of the PGK, and was resuspended in as small a volume of extraction buffer (5% saturated $(NH_4)_2SO_4$) as possible. PGK remaining in the supernatant was precipitated in an 'acid crash' step by lowering the pH to 4.5 with 5 M lactic acid (pH ~ 4). The sample was centrifuged (as above) and the resulting pellet resuspended in extraction buffer (5% saturated $(NH_4)_2SO_4$ plus 1 ml of 1 M Tris (pH 7.5) in order to adjust the pH to ~ 7.5).

The material precipitated at 75% saturated $(NH_4)_2SO_4$ was further fractionated by gel filtration on a Sephacryl S-200 column (20 $cm^2 \times 100$ cm). The flow rate used was 50-75 ml h^{-1}. Fractions were pooled on the basis of SDS-polyacrylamide gel electrophoresis, activity and the absorption ratio $A_{280\ nm}/A_{260\ nm}$ (for example see Figure 2-2). Approximately 200 mg of (d_5-Phe)PGK was obtained from each 4 litre culture. The $A_{280\ nm}/A_{260\ nm}$ absorption ratio was 1.5-1.6. A specific activity of 450-550 µmol NADH converted min^{-1} mg^{-1} was obtained when assayed according to the method described below. The enzyme was stored at 4 °C as a pellet in 75% saturated $(NH_4)_2SO_4$.

2.2.4. *PGK assay*

PGK activity was determined at various stages throughout the extraction and purification procedure, using a coupled assay system as previously described (Wilson *et al.*, 1988):

$$\text{3-PG} + \text{Mg.ATP} \overset{\text{PGK}}{\rightleftharpoons} \text{1,3-P}_2\text{G} + \text{Mg.ADP}$$

$$\text{1,3-P}_2\text{G} + \text{NADH} + \text{H}^+ \overset{\text{GAPDH}}{\rightleftharpoons} \text{G-3-P} + \text{NAD}^+ + \text{P}_i$$

where 3-PG is 3-phosphoglycerate, 1,3-P_2G is 1,3-bisphosphoglycerate, GAPDH is glyceraldehyde-3-phosphate dehydrogenase and G-3-P is

Figure 2-2: Analysis by SDS-polyacrylamide gel electrophoresis (A), activity and $A_{280\ nm}/A_{260\ nm}$ absorption ratio (B) of the material precipitated at 75% saturated $(NH_4)_2SO_4$ following gel filtration on Sephacryl S-200. The elution of protein from the gel filtration column was monitored using a LKB Uvicord II spectrometer. Every fourth protein containing fraction was analysed by SDS-PAGE and had the absorption ratio, $A_{280\ nm}/A_{260\ nm}$, measured. These fractions are labelled 1-17. The activity, expressed as the change in absorbance at 340 nm ($\Delta A_{340\ nm}$), was determined for every fifth protein containing fraction using the assay system described in the text. The fractions pooled to give the final sample used for NMR experiments are indicated in (B). Lanes in (A) labelled Std, TCA and AC correspond to molecular mass standards, a trichloroacetic acid precipitate of fraction 10 and the 'acid crash' precipitate respectively.

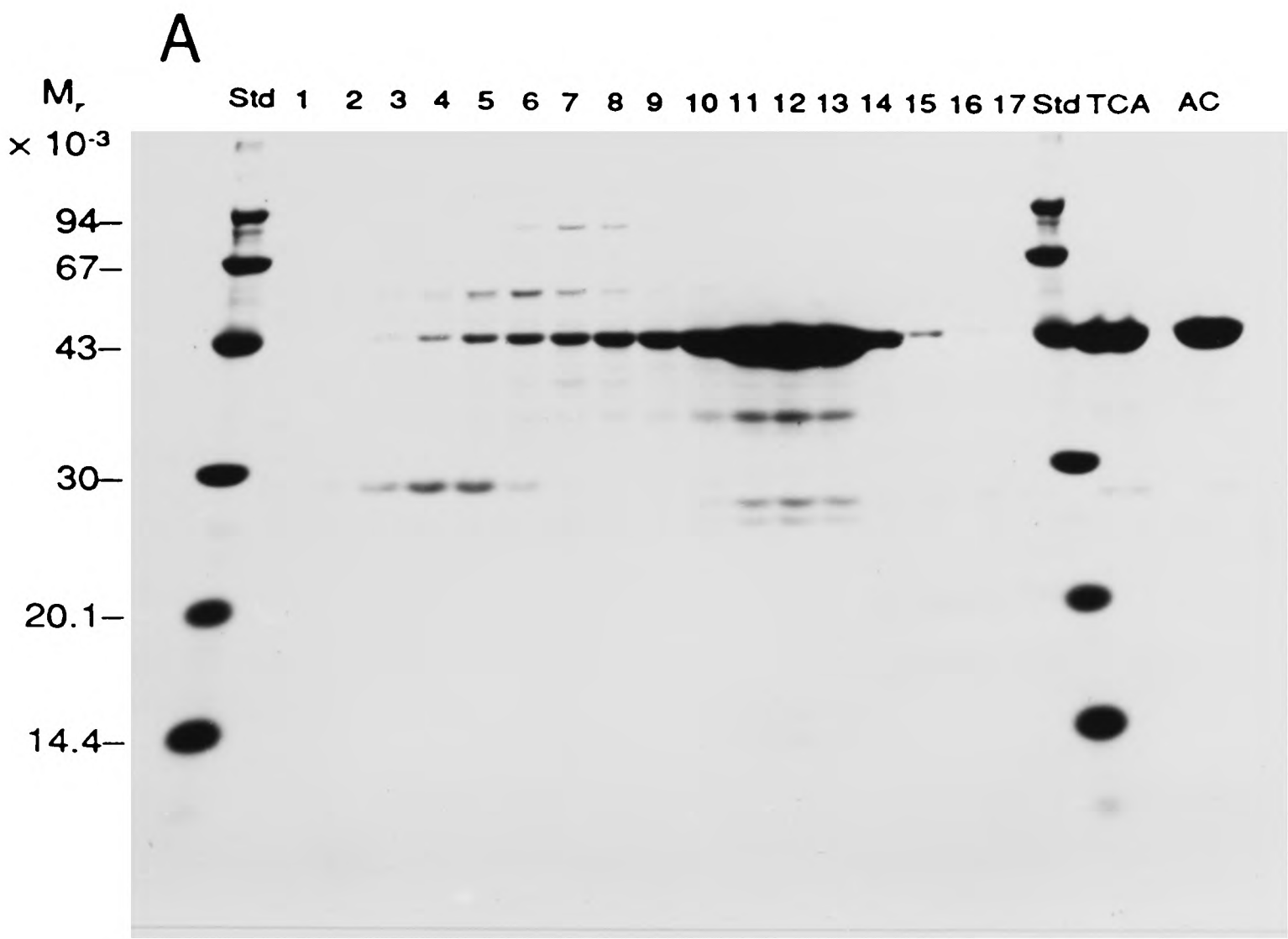
A
M,
× 10-3
94–
67–
43–
30–
20.1–
14.4–
Std 1 2 3 4 5 6 7 8 9 10 11 12 13 14 15 16 17 Std TCA AC

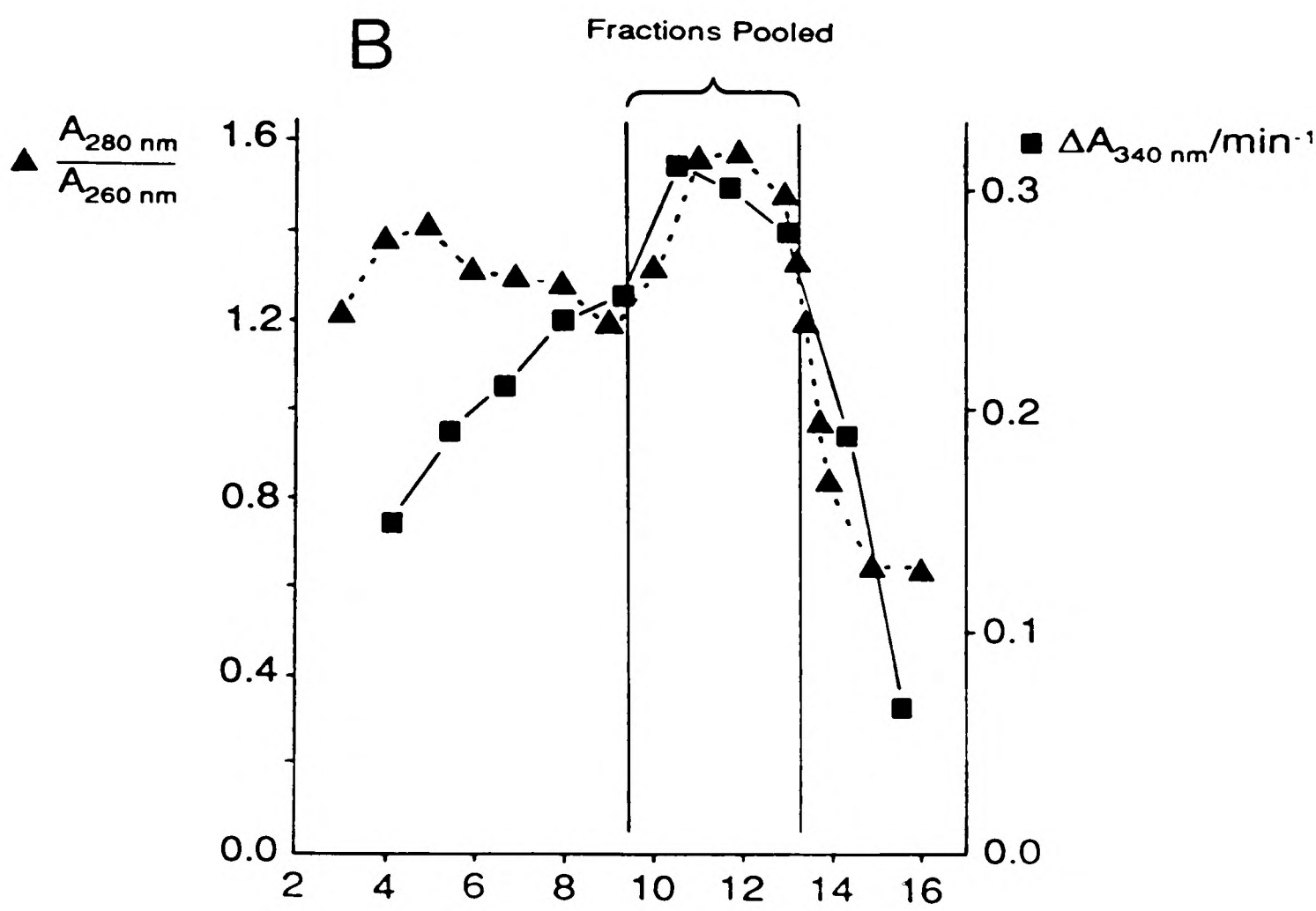
B
Fractions Pooled
A280 nm / A260 nm
ΔA340 nm/min-1
1.6
1.2
0.8
0.4
0.0
0.3
0.2
0.1
0.0
2 4 6 8 10 12 14 16

Figure 2-2

glyceraldehyde-3-phosphate. The concentration of NADH was monitored using a Pye Unicam SP-1800 double beam UV-Vis spectrophotometer. A value of 6.22 mM^{-1} cm^{-1} was used for the absorption coefficient of NADH at 340 nm, with the enzyme activity being expressed as the initial velocity (μmol NADH converted min^{-1}) at 25 °C. Matched quartz cuvettes with a 1 ml capacity and 1 cm path length were used. The final assay mixture contained 0.03 M triethanolamine, 0.05 M KCl, 5 mM $MgCl_2$, 0.2 mM EDTA, 10 mM 3-PG, 4 mM ATP, 0.15 mM NADH and 30 μg ml^{-1} GAPDH, buffered at pH 7.5. The reaction was initiated by addition of 5 μl of PGK sample, the concentration of which was diluted to give an absorbance decay rate of about 0.2 min^{-1}.

The protein concentration was determined using an absorption coefficient of $A^{1\%}_{1cm} = 4.9$ at 278 nm (Krietsch & Bücher, 1970).

2.2.5. *Preparation of NMR samples*

The enzyme/$(NH_4)_2SO_4$ pellet, equivalent to 20-30 mg of protein, was resuspended into extraction buffer (5% saturated $(NH_4)_2SO_4$). This solution was concentrated using Amicon Centricon 30 microconcentrators to a volume of about 200 μl. Sulphate removal and D_2O exchange were performed simultaneously by washing on the Centricon microconcentrator 4-5 times with 2.5 ml of 100 mM sodium d_3-acetate/D_2O (pH 7.3). The final sample was made up to a volume of 450-500 μl with the sodium d_3-acetate/D_2O solution, to give a final concentration of 1-2 mM and a pH of 7.10 ± 0.05. Most samples were used within 24 hours of completing D_2O exchange.

2.2.6. *NMR spectra*

^1H NMR spectra were recorded either on a Bruker AM500 or AM600 spectrometer. One-dimensional (1D) NMR spectra were obtained over 8192 data points; between 320 and 800 accumulations were made, depending on the protein concentration. A pulse angle of 60 ° (5-7 μs) was used, with a

relaxation delay of 0.6 s between pulses. A presaturation pulse for suppression of the residual HDO resonance was applied during the delay. Prior to Fourier transformation, the FIDs were zero-filled to 16384 points and a resolution-enhancement Gaussian multiplication function (Ernst, 1966) was applied (GB = 0.10, LB = -10 Hz). Two-dimensional (2D) NMR experiments (COSY, Aue *et al.*, 1976; NOESY, Jeener *et al.*, 1979) were performed in the phase sensitive mode using the time-proportional phase increment method (Redfield & Kunz, 1975; Bodenhausen *et al.*, 1980; Marion & Wüthrich, 1983). NOESY spectra were recorded with mixing times of 150, 200, 250 and 300 ms with a random variation of ± 20 ms. All experiments were carried out with the transmitter offset placed at the HDO resonance (near the centre of the protein spectrum) using a spectral width of 6024 Hz (500 MHz spectra) or 7042 Hz (600 MHz spectra). Typically 2048 data points were recorded in t_2 for each of 470-512 t_1 values with 96 or 128 transients per FID. A relaxation delay of 1.0 s was used between scans, during which solvent irradiation was carried out. The data were zero-filled to 2048 points in t_1 and multiplied by sine bell window functions in both dimensions or multiplied by a Gaussian function in t_2 (GB2 = 0.3, LB2 = -15 Hz) and a shifted sine bell function in t_1 (SSB1 = 30) before Fourier transformation.

All spectra were recorded at a temperature of 27 °C and a pH of 7.1 unless stated otherwise. The chemical shifts were determined using acetone as an internal reference at 2.214 ppm.

2.2.7. *pH titrations*

pH adjustments of the protein samples were made either with NaOD or DCl (0.4% w/w). The pH values quoted are uncorrected meter readings on a Radiometer PHM 84 Research pH meter, using an Ingold combination electrode inserted directly into a 5 mm NMR tube. [No adjustment was made for isotope effects between H^+ and D^+ as it has been shown that solution

ionisation effects are compensated for by isotope effects at the glass electrode (Glasoe & Long, 1960)].

2.3. Results

2.3.1. *One-dimensional ^1H NMR spectrum of yeast PGK*

The 600 MHz 1D ^1H NMR spectrum of yeast PGK at pH 7.1 is shown in Figure 2-3. This pH gives improved resolution for several resonances of interest when compared with previously reported spectra at pH 5.9 (Wilson *et al.*, 1988). The peak numbering system follows that used in earlier studies (Tanswell *et al.*, 1976; Wilson *et al.*, 1988), with additional resolved resonances being denoted by lower case letters *e.g.* 33a, 33b and 33c. The spectrum of the over-expressed wild-type enzyme was identical to that of PGK obtained conventionally (Fifis & Scopes, 1978) from yeast cells. This confirms that the over-produced enzyme, which represents 50-80% of the total cell protein (Figure 2-1), is correctly folded.

The overall spectrum of yeast PGK can be divided into four simple diagnostic regions, namely the aromatic region (6 ppm - 9 ppm), the predominantly α-CH region around the water resonance (3.5 ppm - 6.0 ppm), the remaining aliphatic region (-0.6 ppm - 3.5 ppm) and the rather broad, overlapping, slow or non-exchangeable amide resonance region (7.0 ppm - 9.6 ppm).

A description of the aromatic region of PGK at pH 5.9 has been given previously, and a number of tentative assignments have been made, mainly to surface histidine residues (Wilson *et al.*, 1988). This region consists of a broad envelope (6.8 ppm - 7.4 ppm) with a number of well dispersed sharper resonances (5.8 ppm - 8.9 ppm) which are labelled in Figure 2-3. The only difference between this region of the spectrum at pH 7.1 and that from the earlier study relate to titratable resonances which have shifted upfield to reveal peaks 5a and 8a-c. These titratable peaks (1, 2a, 2b, 5, 9, 10 and 11)

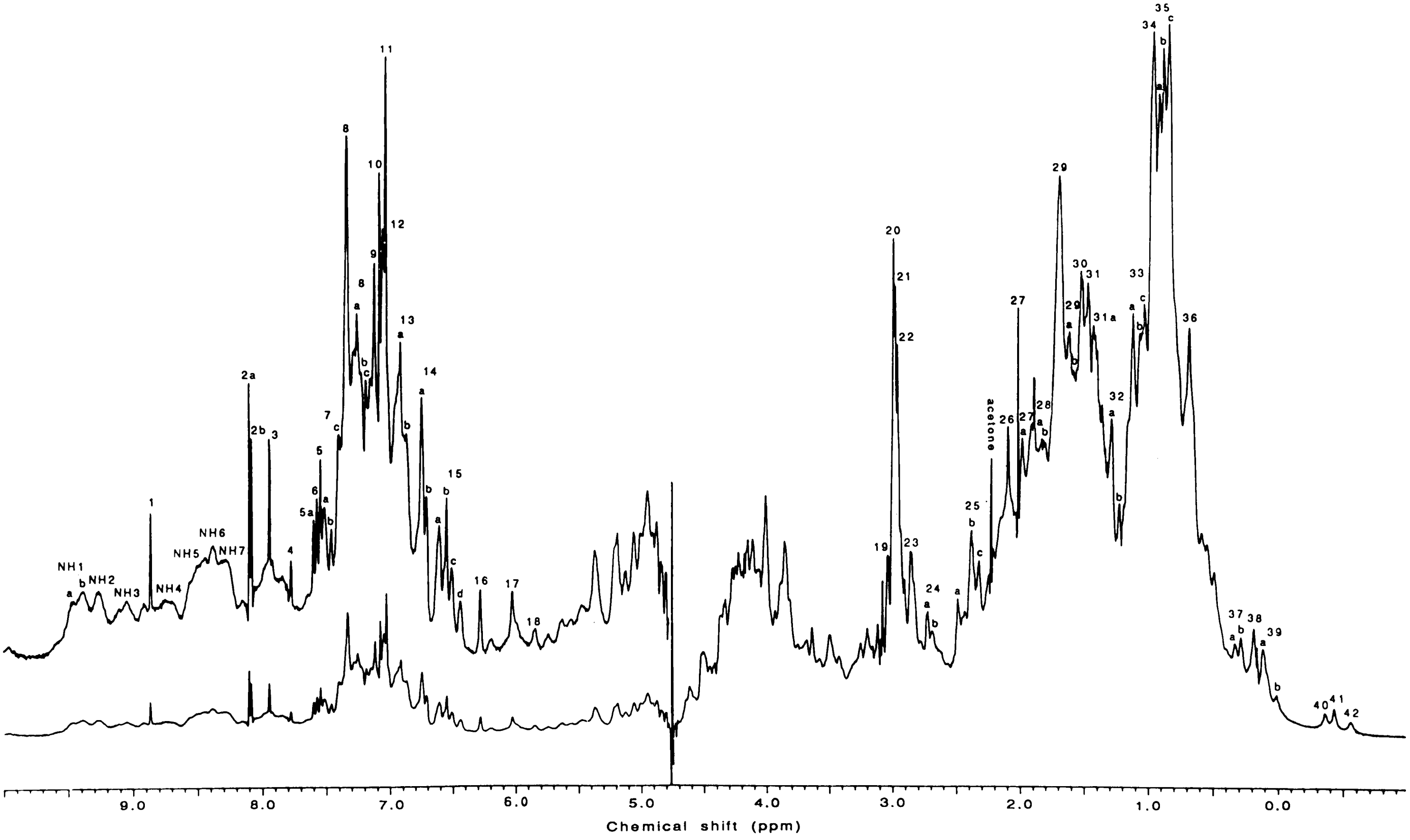

Figure 2-3: 600 MHz ^{1}H NMR spectrum of yeast PGK (1.2 mM, 0.10 M Na d_3-acetate/D_2O, pH 7.1).

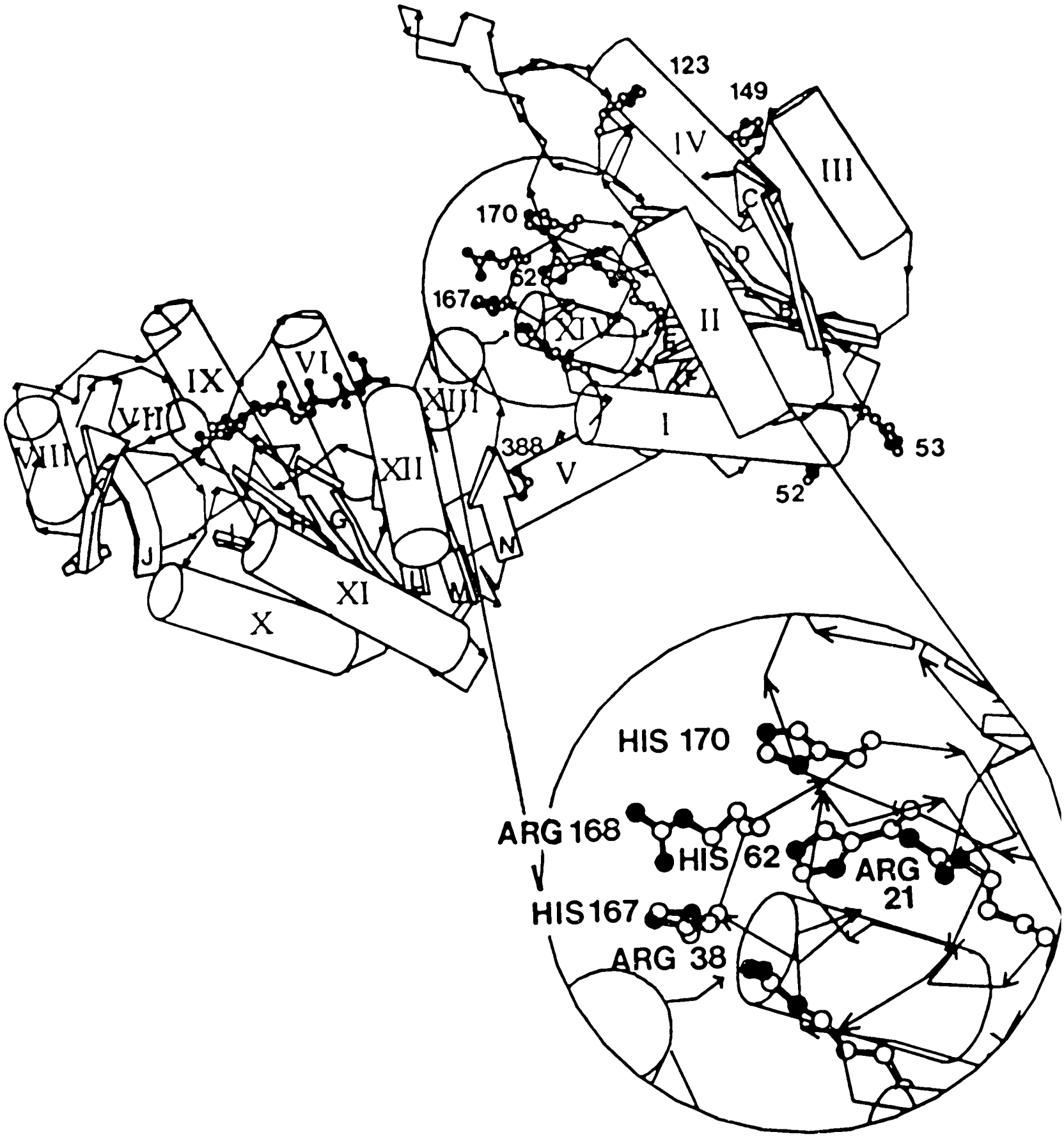

Figure 2-4: A schematic drawing of the crystal structure of yeast PGK (Watson *et al.*, 1982). Helices are denoted by cylinders and β-sheet strands by arrowed laths. The positions of the eight histidine residues (seven in the N-terminal domain and one in the interdomain region) are indicated. The inset highlights the 'basic patch' region of the N-terminal domain, consisting of three arginine and three histidine residues. The drawing was produced using a computer program written by Lesk & Hardman (1982).

were assigned (Scheffler & Cohn, 1986; Wilson *et al.*, 1988) to exposed histidine residues 52, 53, 123 and 149 (Figure 2-4). Resonances 3, 4 and 5a were also assigned in the earlier work, although not specifically, to the three 'basic patch' histidines 62, 167 and 170 (Wilson *et al.*, 1988). In total, the aromatic region contains resonances from eight His, nineteen Phe, seven Tyr and two Trp residues (Watson *et al.*, 1982).

The aliphatic region of the yeast PGK spectrum is also well dispersed (Figure 2-3) and includes a number of relatively broad (but clearly visible) upfield shifted methyl resonances with chemical shifts between -0.6 ppm and 0.6 ppm (peaks 37-42). Other characteristic features of this spectral region include a broad envelope (0.5 ppm - 2.5 ppm), a set of sharp resonances at about 3.0 ppm corresponding to the ε-CH_2 groups of some of the 42 lysine residues in the protein and several other resolvable resonances, which are labelled in Figure 2-3. The only previous assignments in this region were of peaks 26 and 27 to methionine residues (Wilson *et al.*, 1988).

The aliphatic region between 3.5 ppm and 6.0 ppm, contains predominantly α-CH resonances, and those shifted downfield to between 4.5 ppm and 6.0 ppm are commonly indicative of β-structures (Dalgarno *et al.*, 1983).

The fourth region of interest in the PGK spectrum is the set of broad (overlapping) resonances due to slow and non-exchanging amide protons, observable downfield of the aromatic envelope (7.0 ppm - 9.6 ppm). Of these NH peaks only NH6 and a component of NH5 exchange slowly over several days at pH 7.1.

2.3.1.1. One-dimensional spectrum of (d_5-Phe)PGK

It has been previously suggested that some of the relatively well resolved resonances upfield of the aromatic envelope (peaks 13-17) may be due to phenylalanine residues located in the interdomain region of the protein (Wilson *et al.*, 1988). However, from the 1D spectrum alone, it is not possible

to make firm assignments of these peaks to specific spin systems. In order to make such assignments in the aromatic region, PGK was prepared in which the Phe rings were deuterated (see § 2.2).

The aromatic region of the ^{1}H NMR spectra of isotopically normal PGK and (d_5-Phe)PGK are illustrated in Figure 2-5. The difference spectrum (Figure 2-5C) contains only those resonances due to the ring protons of the 19 Phe residues of the enzyme. [Note: yeast does not possess the enzyme phenylalanine hydroxylase (phenylalanine 4-monooxygenase) which catalyses the conversion of phenylalanine to tyrosine (Jones & Fink, 1982)]. From the integrated intensities of peak 16 in Figure 2-5 the incorporation of deuterated Phe is estimated to be about 75%.

Several of the peaks upfield of the aromatic envelope in the spectrum of isotopically normal PGK can now be immediately identified as Phe resonances by their appearance in the difference spectrum (Figure 2-5C). These include a component of peak 14a, and peaks 15a, 15b′, 15c, 15d and 16, as labelled in the spectrum of the isotopically normal PGK. There is also an upfield shifted Phe resonance at 5.36 ppm. The only other clearly resolvable Phe resonance is peak 7a at 7.51 ppm. The remaining Phe resonances between 6.8 and 7.4 ppm are unresolved. The total number of clearly resolved Phe resonances is therefore eight, corresponding to ~ 14% of the expected total.

2.3.2. *Two-dimensional NMR spectroscopy*

2.3.2.1. COSY spectra (aromatic)

2D NMR methods offer a significant improvement in the resolution of selected peaks relative to the 1D spectrum of yeast PGK. The COSY spectrum of the aromatic region of isotopically normal PGK (Figure 2-6) demonstrates this improvement in resolution, with several cross-peaks being observed from resonances within the aromatic envelope. About half of the possible cross-peaks are observed in the spectrum, and these can be assigned to some of

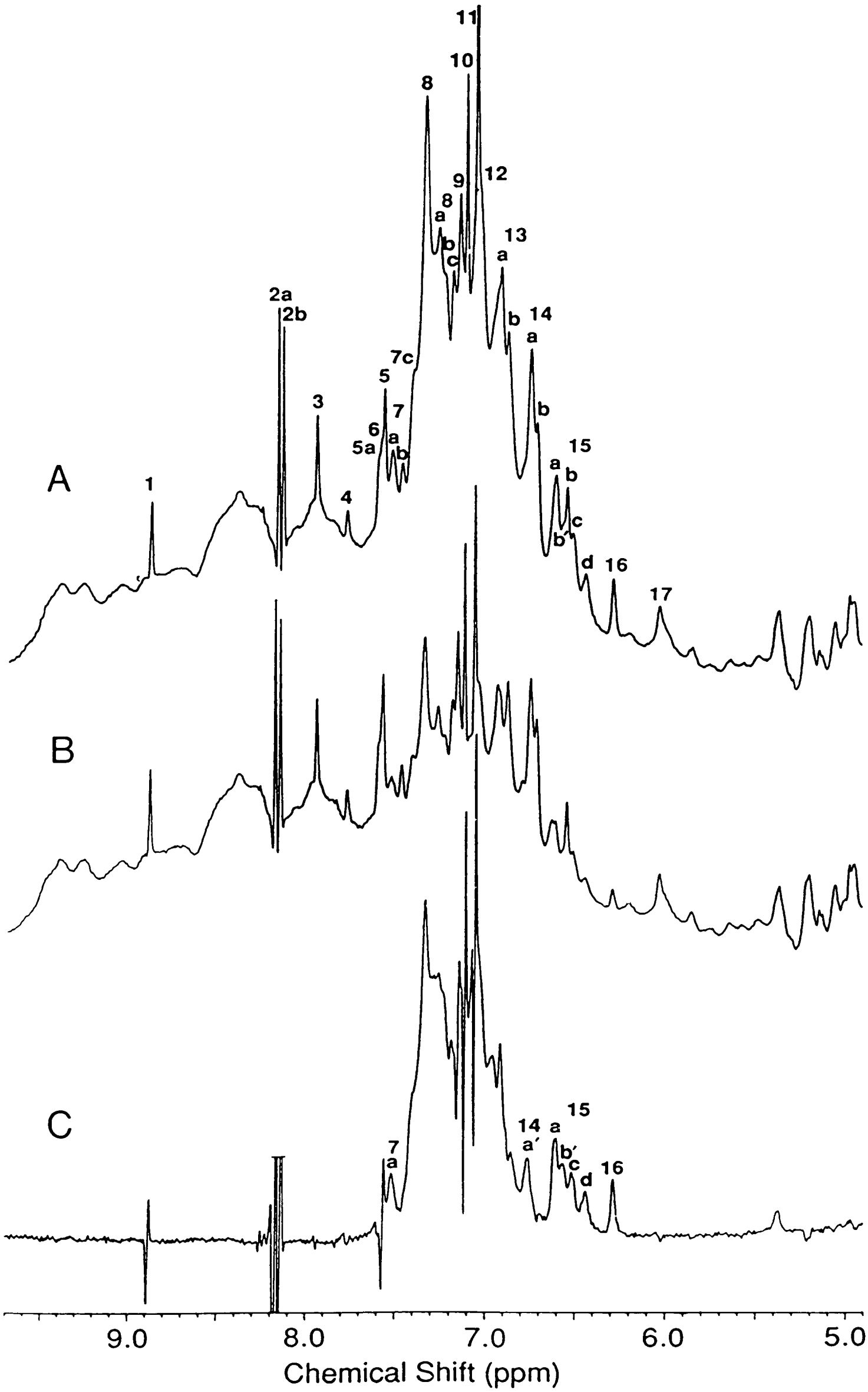

Figure 2-5: Aromatic region of the 500 MHz ^{1}H NMR spectra of (A) isotopically normal yeast PGK and (B) (d_5-Phe)PGK. (C) The difference spectrum (A) - (B). The sharp 'dispersive type' peaks in the difference spectrum result from small differences in the chemical shifts of titratable His resonances 1, 2a, 2b, 5, 9, 10 and 11.

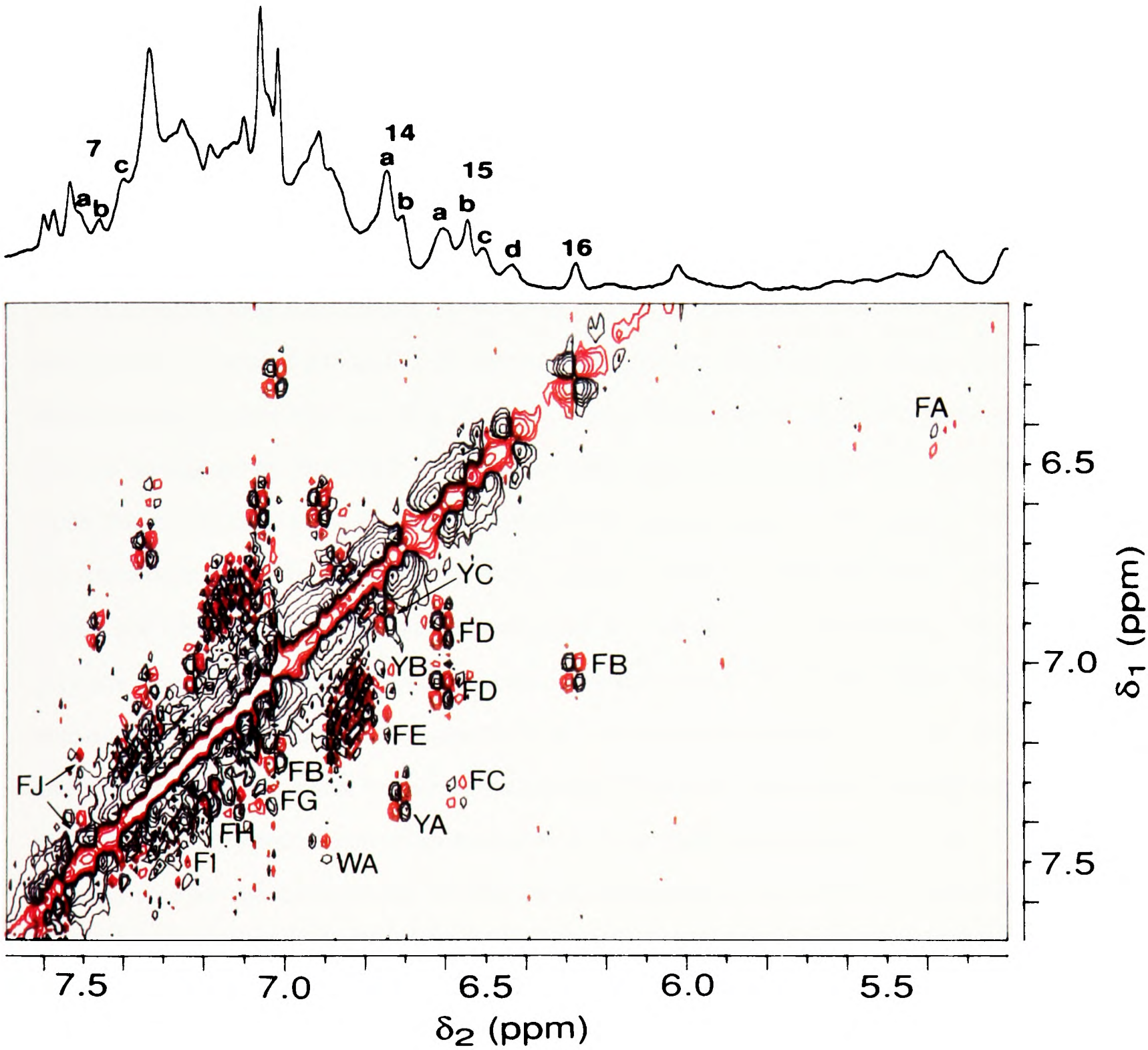

Figure 2-6: Aromatic region of the 500 MHz COSY spectrum of yeast PGK (1.5 mM, 0.10 M Na d_3-acetate/D_2O, pH 7.1, 300 K). The corresponding region of the 1D spectrum is also shown. The cross-peaks are labelled by spin-system. Specific assignments are discussed in the text.

the more mobile aromatic residues of the protein (*i.e.* those with the longest T_2s). Of particular interest are cross-peaks from some of the Phe resonances identified in Figure 2-5. For instance, the most upfield shifted Phe resonance at 5.36 ppm has a weak cross-peak to peak 15d (6.41 ppm) labelled "FA". Peak 16 (6.26 ppm) on the other hand, shows a strong cross-peak to 7.00 ppm, which in turn gives a cross-peak to 7.21 ppm (FB). The latter two Phe resonances lie within the aromatic envelope and are not resolved in the 1D spectrum. Peak 15b′ (6.55 ppm) also gives a cross-peak to a previously unresolved resonance within the aromatic envelope, at 7.32 ppm (FC). Peak 15a (6.59 ppm) has two strong cross-peaks (FD) to resonances at 6.88 ppm (a component of peak 13a) and 7.04 ppm (a component of peak 12). Peak 15a is therefore due to the C3,5-H of a Phe side-chain. Resonance 7a (7.51 ppm) can also be assigned to the C3,5-H of a Phe ring since cross-peaks are observed from this resonance to peak 7c (7.40 ppm) and another peak (7.24 ppm) within the envelope (FJ). In addition to these assignments to Phe residues, cross-peaks are observed which can be assigned to Tyr or Trp side-chains. These include the low intensity cross-peak between peak 7b (7.46 ppm) and a resonance at 6.88 ppm (this resonance is not coupled to peak 15a; see later) and the strong cross-peak between resonance 14b (6.69 ppm) and a component of peak 8 (7.33 ppm). From Figure 2-5 it is clear that neither peaks 7b nor 14b are due to Phe residues. Peak 7b has been assigned to Trp 308 in a previous photo-CIDNP NMR study of the yeast enzyme (Scheffler & Cohn, 1986). If this is the case, the remaining two cross-peaks expected for a Trp spin system are not observed in the COSY spectrum. Possible explanations for this are that they lie within the intensity of the rather broad diagonal or are too broad to be observed. Evidence in support of this assignment has, however, been gained from relayed coherence transfer experiments carried out on the isolated C-terminal domain of yeast PGK (produced by site-directed mutagenesis; see Chapter 8).

Assignment difficulties are encountered in the more crowded regions of the spectrum. Even around peak 14a it is not possible to say which of the three observed cross-peaks (6.725, 7.02 ppm; 6.73, 6.86 ppm; 6.75, 7.13 ppm) is due to the Phe resonance identified in Figure 2-5C. There is also a cluster of cross-peaks around 6.8, 7.1 ppm (close to the position expected for 'random coil' tyrosines; Wüthrich, 1986) and a further grouping close to the diagonal between 7.0-7.3 ppm (probably due to Phe residues).

2.3.2.2. COSY spectrum of (d_5-Phe)PGK

With only 25% of its Phe ring protons potentially observable by ^{1}H NMR, (d_5-Phe)PGK gives a COSY spectrum in which cross-peaks due to Phe residues are either absent or have a greatly reduced intensity relative to the spectrum of isotopically normal PGK (Figure 2-7B). Hence the Phe cross-peaks at 6.59, 6.88 ppm and 6.59, 7.04 ppm (FD), which were strong in the COSY spectrum of the isotopically normal enzyme are observed with a lower relative intensity in the COSY spectrum of (d_5-Phe)PGK, while most of the other cross-peaks which were assigned above to Phe residues are absent. Also absent from this spectrum is the group of cross-peaks close to the diagonal between 7.0-7.3 ppm, indicating that these resonances are in fact those of Phe residues.

In this spectrum we can also clearly observe five cross-peaks which can be assigned to Tyr residues (6.69, 7.33 ppm; 6.73, 6.86 ppm; 6.78, 7.09 ppm; 6.81, 7.13 ppm; 6.86, 7.17 ppm). The weak cross-peak found at 6.88, 7.46 ppm in the COSY spectrum of the isotopically normal enzyme is still present in the spectrum of (d_5-Phe)PGK. A summary of the side-chain specific assignments obtained directly from the spectra of PGK and (d_5-Phe)PGK is given in Table 2-2.

2.3.2.3. COSY spectra (aliphatic)

Most of the aliphatic region of the COSY spectrum of yeast PGK shows

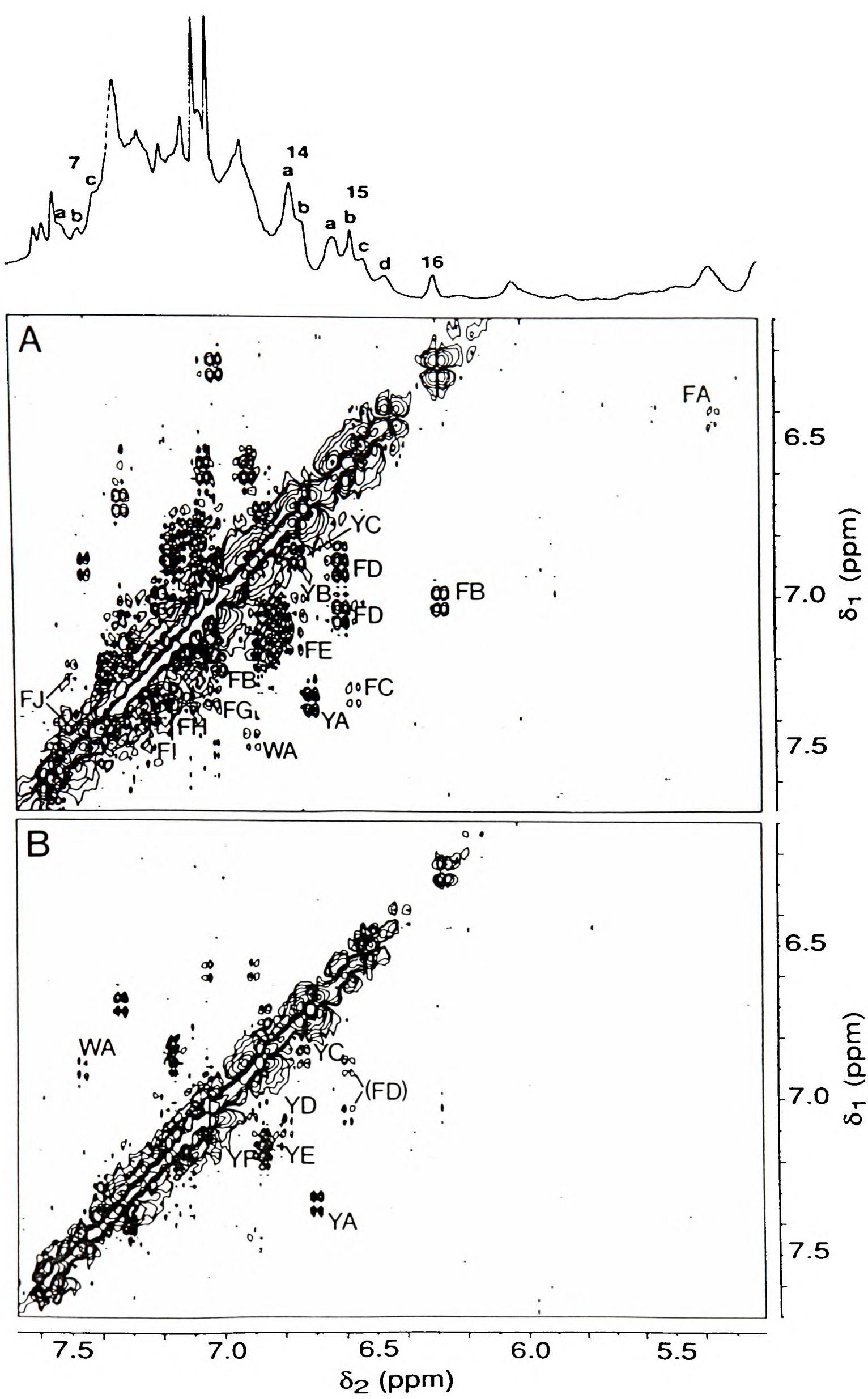

Figure 2-7: Aromatic region of the 500 MHz COSY spectra of (A) isotopically normal PGK and (B) (d_5-Phe)PGK. The corresponding region of the 1D spectrum of the isotopically normal enzyme is also shown.

Table 2-2: Side-chain specific assignments of observable aromatic resonances in the ^1H NMR spectrum of yeast PGK.

pH = 7.1, 0.10 M Na d_3-acetate/D_2O, T = 300 K

Numbers in parentheses correspond to peak labels in the 1D spectrum (Figure 2-3). (s) = strong cross-peaks, (w) = weak cross-peaks

Amino acid type		Chemical shift of ring protons (ppm)			Assignment	Environment
Phe A	(w)	5.36	6.41 (15d)	6.48 (15c)		
Phe B	(s)	6.26 (16)	7.00 (12)	7.21 (8b)	Phe 185	interdomain
Phe C	(w)	6.55 (15b′)	7.32			
Phe D	(s)	6.59 (15a)	6.88	7.04 (12)	Phe 342[a]	surface C[b]
Phe E	(w)	6.75 (14a′)	7.13			
Phe F	(?)	6.81	7.07			
Phe G	(w)	7.03	7.33		Phe 163[a,c]	interdomain
Phe H	(w)	7.11	7.34			
Phe I	(s)	7.17	7.30		Phe 289	surface C
Phe J	(w)	7.24	7.40 (7c)	7.51 (7a)		
Tyr A	(s)	6.69 (14b)	7.33		Tyr 380[d]	surface C
Tyr B	(w)	6.725 (14a)	7.02 (12)		Tyr 48	surface N
Tyr C	(s)	6.73 (14a)	6.86 (13b)		Tyr 193[d]	interdomain
Tyr D	(?)	6.78 (14a′)	7.09		Tyr 74[a,c]	surface N
Tyr E	(w)	6.81	7.13		(Tyr 56)[a,e]	surface N
Tyr F	(s)	6.86	7.17		(Tyr 122)[a,e]	surface N
Trp A	(w)	6.88	7.46 (7b)		Trp 308[d]	surface C

[a] tentative assignment

[b] C = C-terminal domain, N = N-terminal domain

[c] assignment based on titration with the paramagnetic shift probe $[Fe(CN)_6]^{3-}$ (see Chapter 5; § 5.3.3)

[d] assignment based on analysis of the 2D spectra of the isolated C-terminal domain (see Chapter 8)

[e] assignment based on cross-peak intensity/side-chain exposure correlations

considerable peak overlap, with very few resolved cross-peaks. The number of cross-peaks observed is less than the total possible for a protein with a molecular mass of ~ 45000 Da. This can be explained by the increased rotational correlation time (relative to smaller proteins), particularly in the less mobile cores of the two domains, which results in resonance linewidths of the order of, or greater than, the ^1H-^1H scalar coupling. This effect leads to reduced cross-peak intensity since the anti-phase components of the COSY cross-peaks cancel (Neuhaus *et al.*, 1985). Accordingly, the selected set of resonances for which cross-peaks are observed arises from residues situated on the protein surface or in the more mobile regions of the protein (*e.g.* the interdomain region; Wilson *et al.*, 1988).

Relatively few cross-peaks are seen in the methyl region and most of these are weak (Figure 2-8). There are an indeterminate number of overlapping cross-peaks between 0.8-1.0 ppm, 1.0-2.3 ppm corresponding to exposed 'random coil' valine, leucine and isoleucine residues. Cross-peaks observed from upfield shifted methyl resonances 37a (0.31 ppm, 3.13 ppm) and 41 (-0.46 ppm, 3.67 ppm) (Figure 2-9) indicate that these peaks may be assigned to alanine or threonine residues. Peak 41 is assigned to a threonine γ-CH_3 since a cross-peak is also observed between 3.67 ppm and 3.10 ppm (corresponding to the β-CH and α-CH respectively) (Figure 2-9). Observation of an NOE connectivity between -0.46 ppm and 3.10 ppm in the NOESY spectrum (data not shown) supports this assignment. Peak 41 is 1.69 ppm upfield of the 'random coil' chemical shift position for a threonine γ-CH_3 (Wüthrich, 1986) indicating the influence of a nearby aromatic group.

2.3.2.4. NOESY spectra

The NOESY spectrum of the aromatic region of isotopically normal yeast PGK (Figure 2-10) shows several intra- and inter-residue NOE cross-peaks. Three His intra-residue (C2-H/C4-H) NOE connectivities are observed, indicating that peaks 2a (8.16 ppm) and 10 (7.09 ppm) represent a single His,

Figure 2-8: Methyl region of the 500 MHz COSY spectrum of yeast PGK (1.5 mM, 0.10 M Na d_3-acetate/D_2O, pH 7.1, 300 K). The corresponding region of the 1D spectrum is also shown.

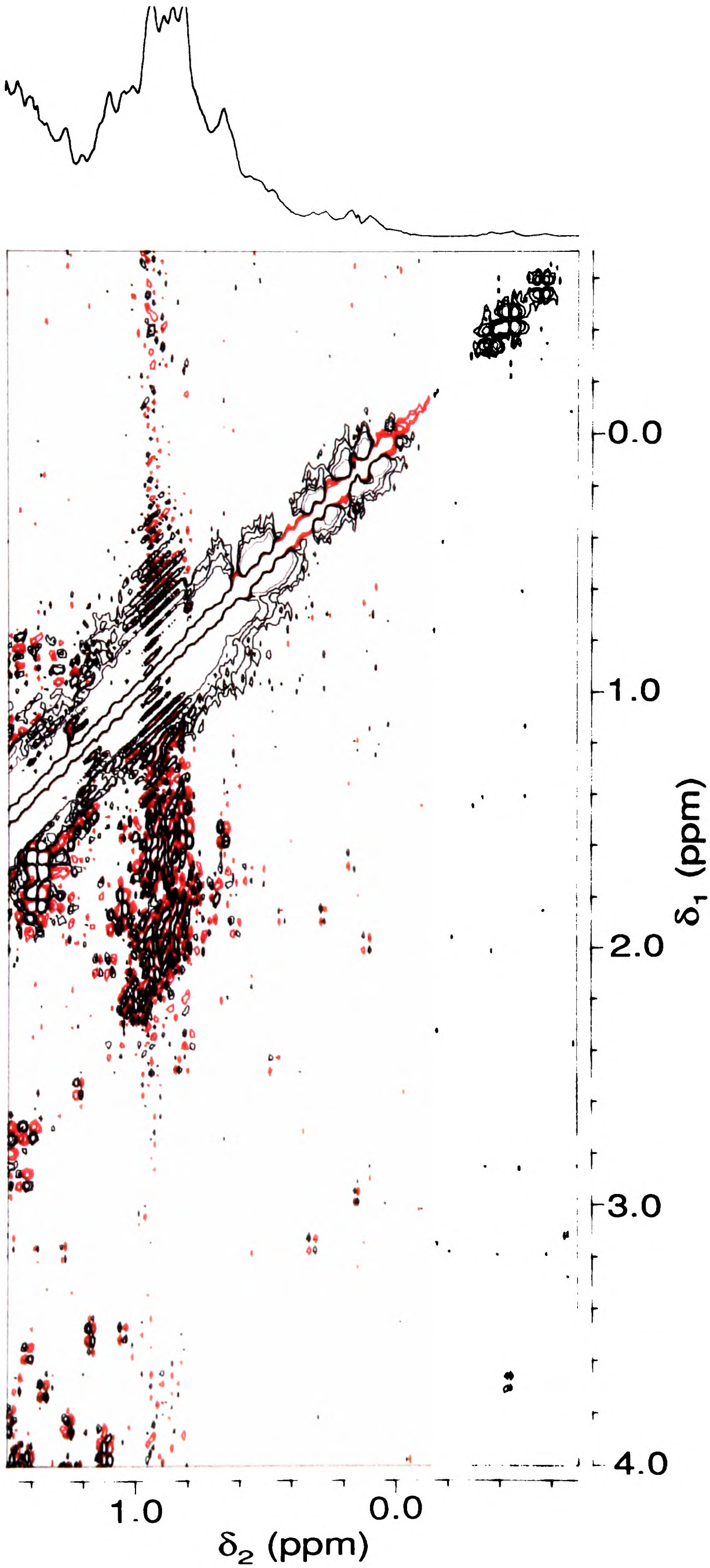

Figure 2-8

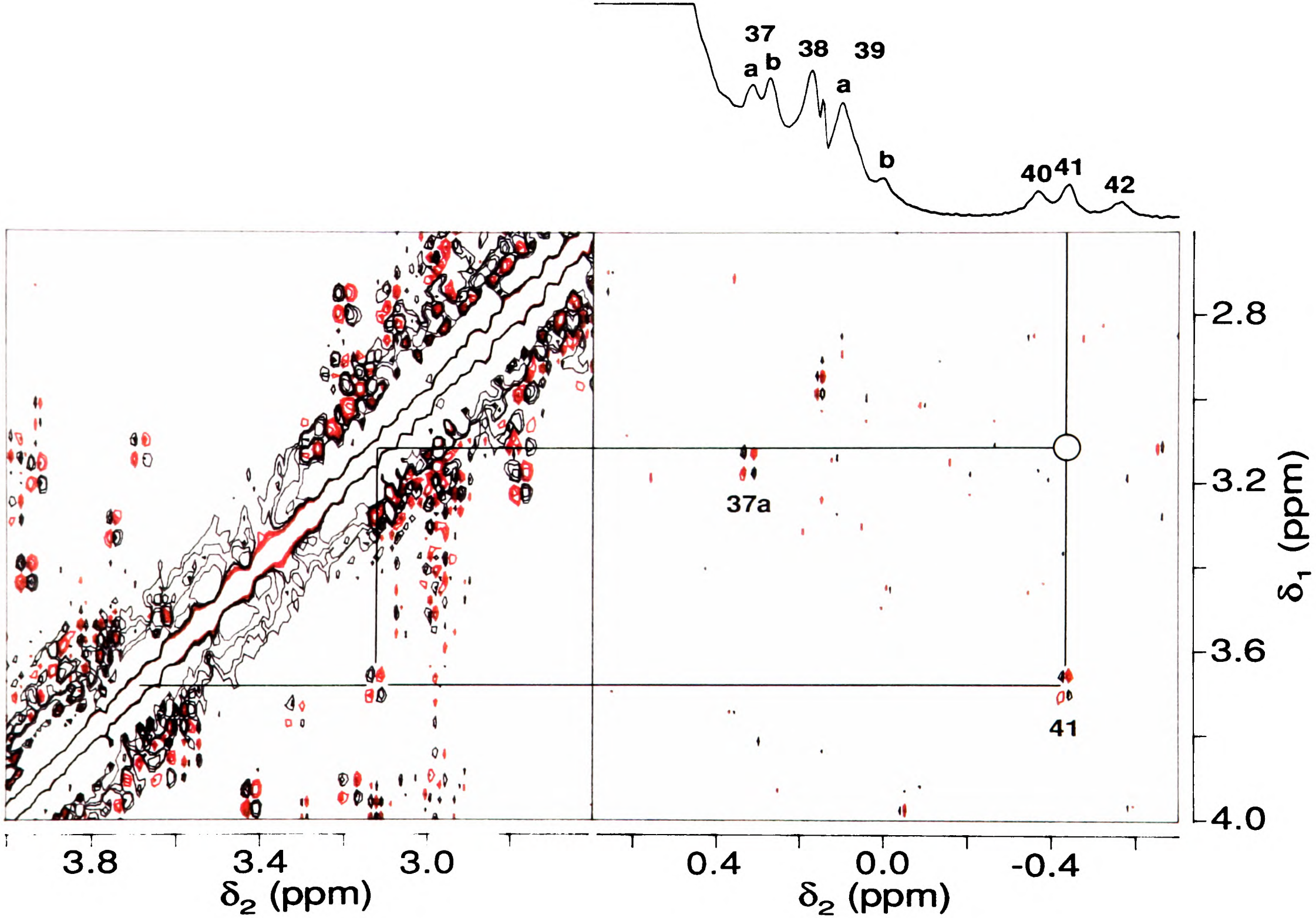

Figure 2-9: Sections of the aliphatic region of the 500 MHz COSY spectrum of yeast PGK showing the spin-system of upfield methyl resonance 41. The circle indicates the position of a cross-peak observed in the NOESY spectrum.

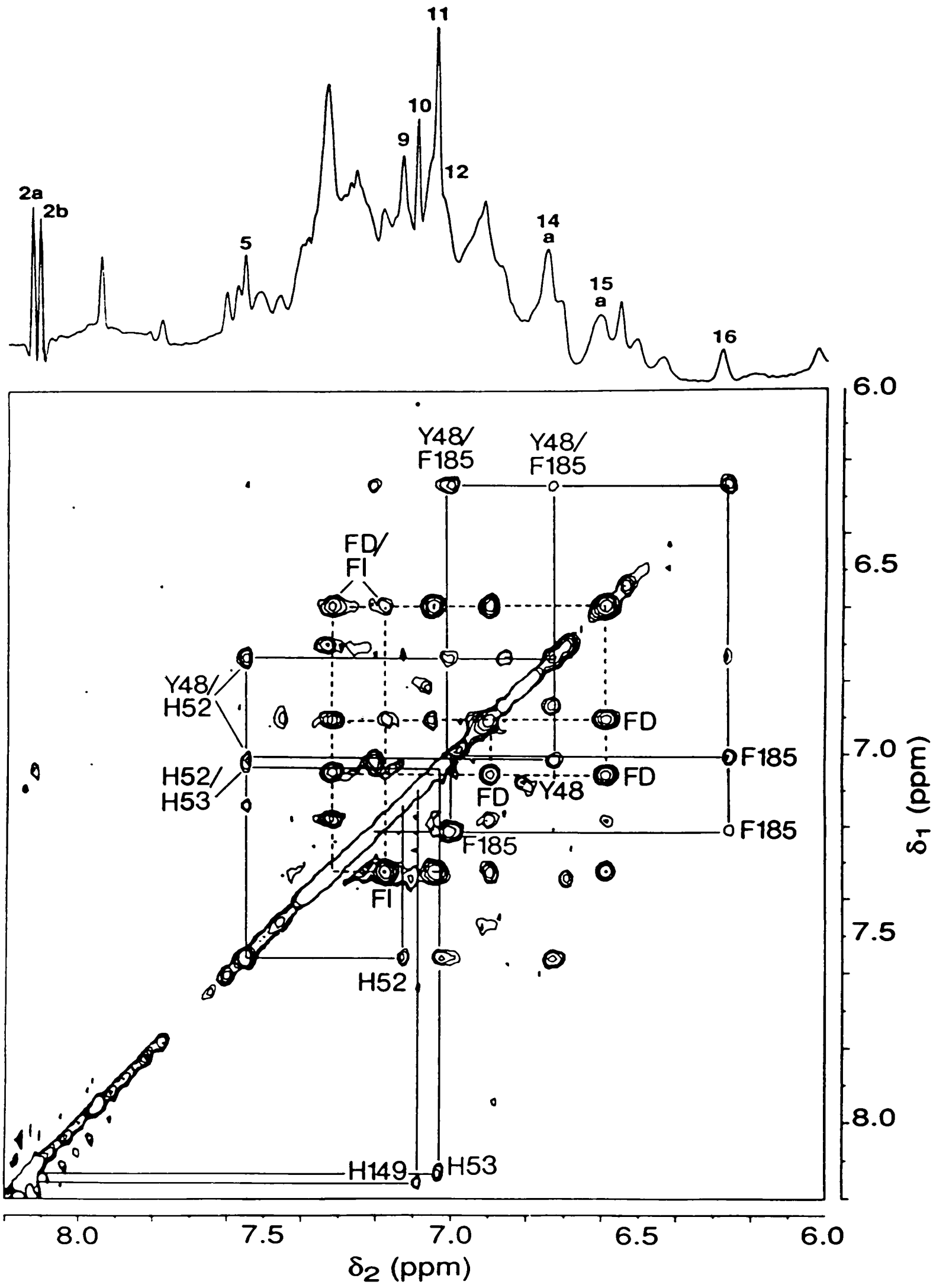

Figure 2-10: Aromatic region of the 500 MHz NOESY spectrum of yeast PGK. Intra-residue NOE cross-peaks for His 52, His 53, His 149, Tyr 48 and Phe 185 (discussed in the text) are indicated below the diagonal and inter-residue NOE cross-peaks are labelled above the diagonal. Intra- and inter-residue NOE connectivities for Phe D and Phe I are similarly labelled and joined by dashed lines.

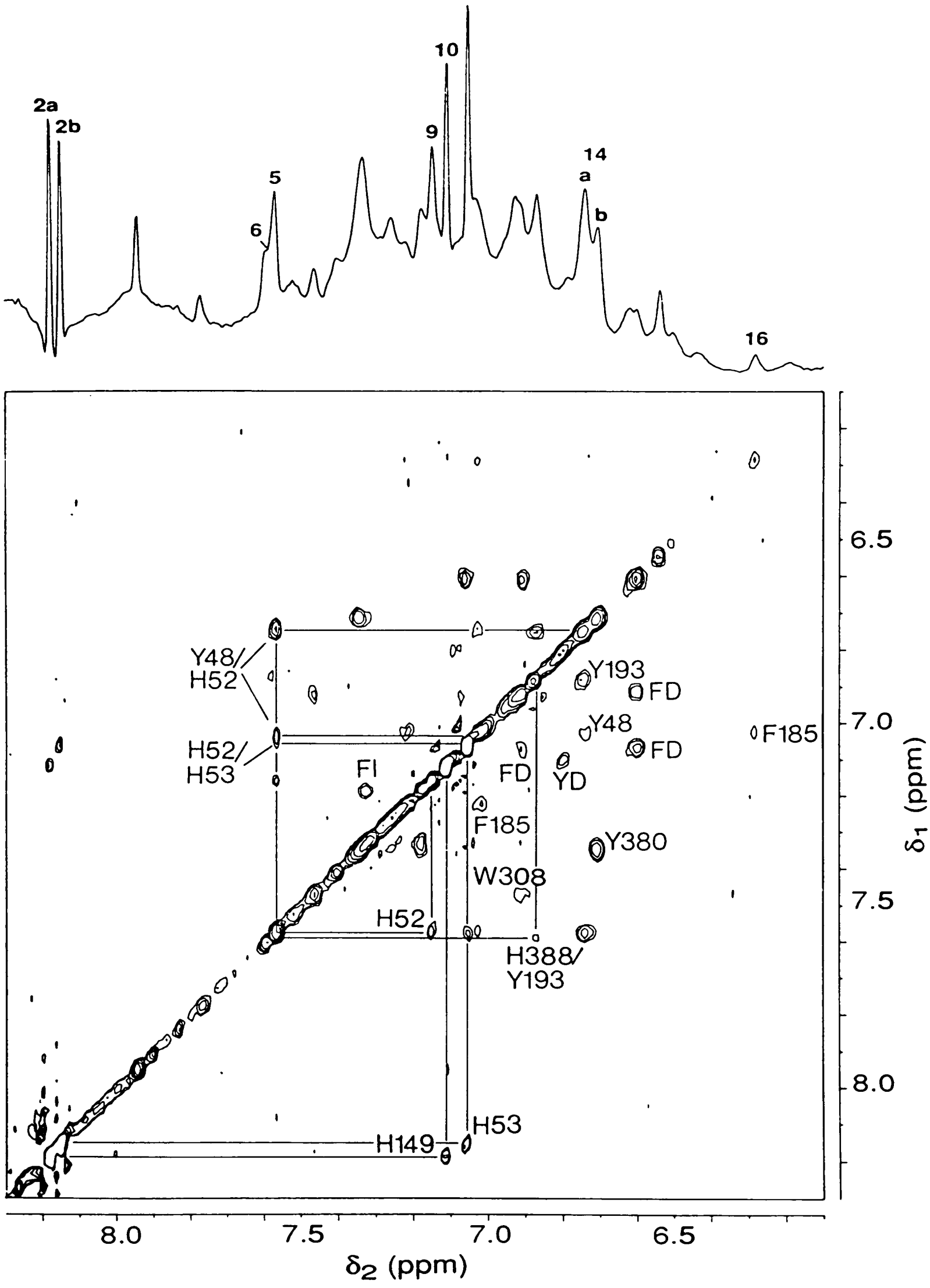

Figure 2-11: Aromatic region of the 600 MHz NOESY spectrum of (d_5-Phe)PGK. Cross-peaks are labelled according to assignments discussed in the text.

2b (8.10 ppm) and 11 (7.03 ppm) represent another and peaks 5 (7.55 ppm) and 9 (7.13 ppm) are due to a third. Peaks 2a and 10 have previously been tentatively assigned to His 149, while 2b and 11 have been assigned to His 53 (Scheffler & Cohn, 1986; these assignments were made in a photo-CIDNP study and are based on an estimation of the relative accessibility of these residues to flavin dyes). Peak 5 was previously assigned to the same His as resonance 1 (His 123) (Wilson *et al.*, 1988). The NOESY data, however, indicate that peak 5 is due to His 52 for the following reasons. As well as the intra-residue NOE cross-peak observed between peaks 5 and 9, a further NOE cross-peak is seen between peaks 5 and 11, *i.e.* the C4-H of His 53 (Figure 2-10). NOE connectivities are also seen from peak 5 to resonances at 7.02 ppm (weak) and 6.725 ppm (strong) (Figure 2-10) which is consistent with the crystallographic finding that His 52 is in contact with Tyr 48 (Watson & Gamblin, 1985). In addition peak 5 is found to be absent (together with peaks 2b, 9 and 11) in the spectrum of a mutant protein in which residues 51-56 have been substituted with the analogous sequence (Bowen *et al.*, 1988) from *T. thermophilus* PGK (Δ51-56; EHHPRY → AGGAS_) (see § 2.3.5 & Figure 2-15).

The NOE cross-peak at 6.725, 7.02 ppm corresponds closely to a weak cross-peak observed in the COSY spectrum of isotopically normal PGK (Figure 2-6). This cross-peak is not seen in the COSY spectrum of (d_5-Phe)PGK (Figure 2-7B) but is observed in the NOESY spectrum (Figure 2-11) of the modified enzyme. Loss of this weak cross-peak in the COSY spectrum of (d_5-Phe)PGK does not necessarily imply that it is due to a Phe residue, especially since it is observed in the NOESY spectrum. The cross-peak observed between resonances at 6.725 ppm and 7.02 ppm in the NOESY spectra of both isotopically normal PGK and (d_5-Phe)PGK has therefore been assigned to Tyr 48.

Further NOE cross-peaks are observed between the resonances of Tyr 48

and peak 16 (6.26 ppm) (Figure 2-10), indicating that Phe B (Table 2-2) is in close proximity to Tyr 48. Examination of the crystal structure (Watson *et al.*, 1982) reveals that Phe 185 is the only Phe in such a position relative to Tyr 48, and that the C4-H of this residue is likely to have an NOE connectivity to the C2,6-H and C3,5-H of the Tyr. Peak 16 is thus assigned to the C4-H of Phe 185. The NOE connectivities that have led to specific assignments for His 52 and His 53, Tyr 48 and Phe 185 are summarised in Figure 2-12. Of these, only the cross-peaks involving resonances of Phe 185 are not observed in the NOESY spectrum of (d_5-Phe)PGK (Figure 2-11).

Further inter-residue NOE cross-peaks are observed between resonances of Phe D and Phe I (Figure 2-10). Experiments detailed in Chapter 8 show that these Phe residues are situated in the C-terminal domain of PGK. A proton-proton distance search of the X-ray crystal structure (Watson *et al.*, 1982), however, failed to find any two Phe rings in the C-terminal domain which are close enough (< 5 Å) to give the observed pattern of NOEs. A question then arises as to the relationship between the structure of the enzyme in the crystalline and solution states. This is considered further in the following section (§ 2.3.3).

In the NOESY spectrum of (d_5-Phe)PGK (Figure 2-11) a weak NOE connectivity is observed between resonance 6 and a resonance assigned to Tyr 193 (Table 2-2). This cross-peak is also found in the NOESY spectrum of isotopically normal PGK when plotted with lower contours than in Figure 2-10. Investigation of the crystal structure (Watson *et al.*, 1982) shows that the closest aromatic group to Tyr 193 is His 388, the shortest inter-proton distance being 3.9 Å. Resonance 6 can therefore be assigned to His 388. This assignment is discussed further in § 2.3.6.

2.3.3. *Effect of nucleotide binding*

In Figure 2-13 it can be seen that a number of resonances are perturbed upon

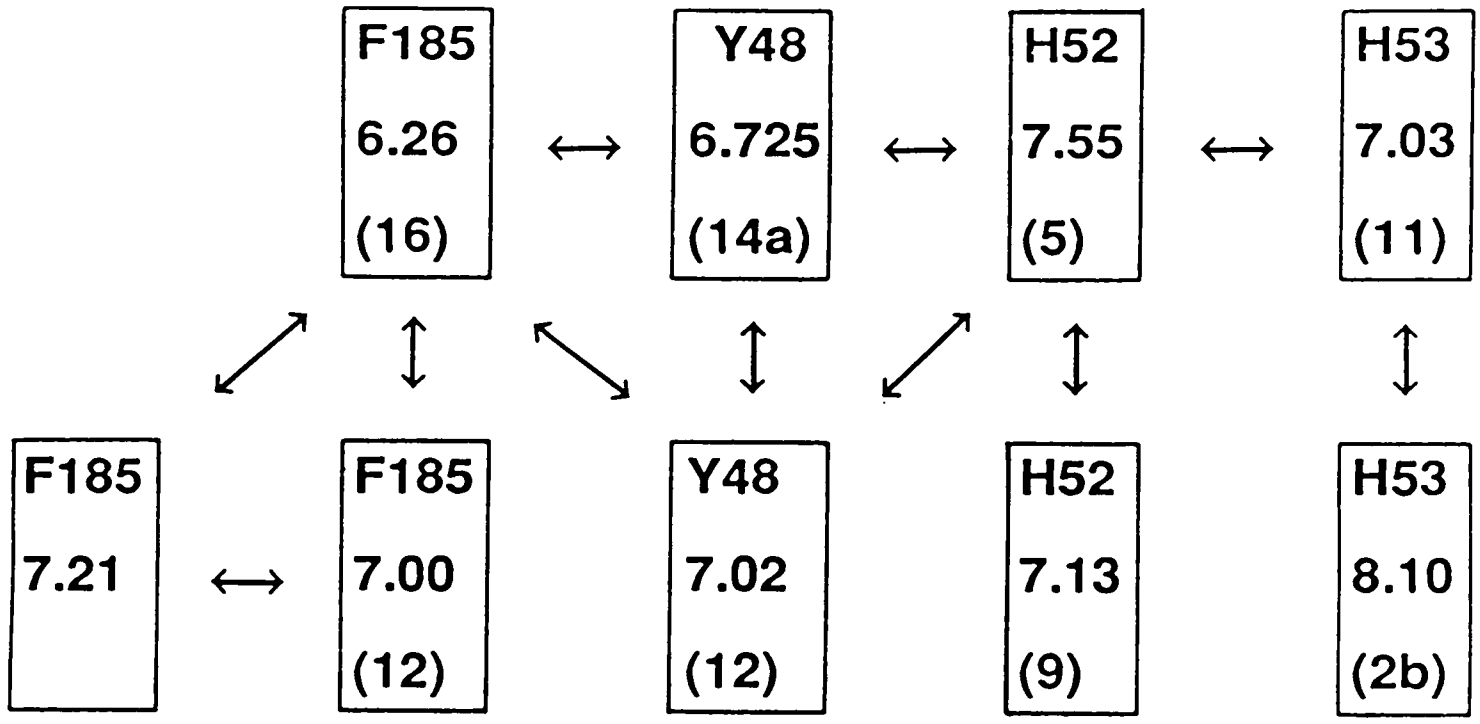

Figure 2-12: Schematic diagram showing NOE connectivities between selected aromatic resonances. The chemical shift (pH 7.1, 0.10 M Na d_3-acetate, 300 K) of each resonance is given in ppm and the peak number in the 1D spectrum (Figure 2-3) is given in parentheses.

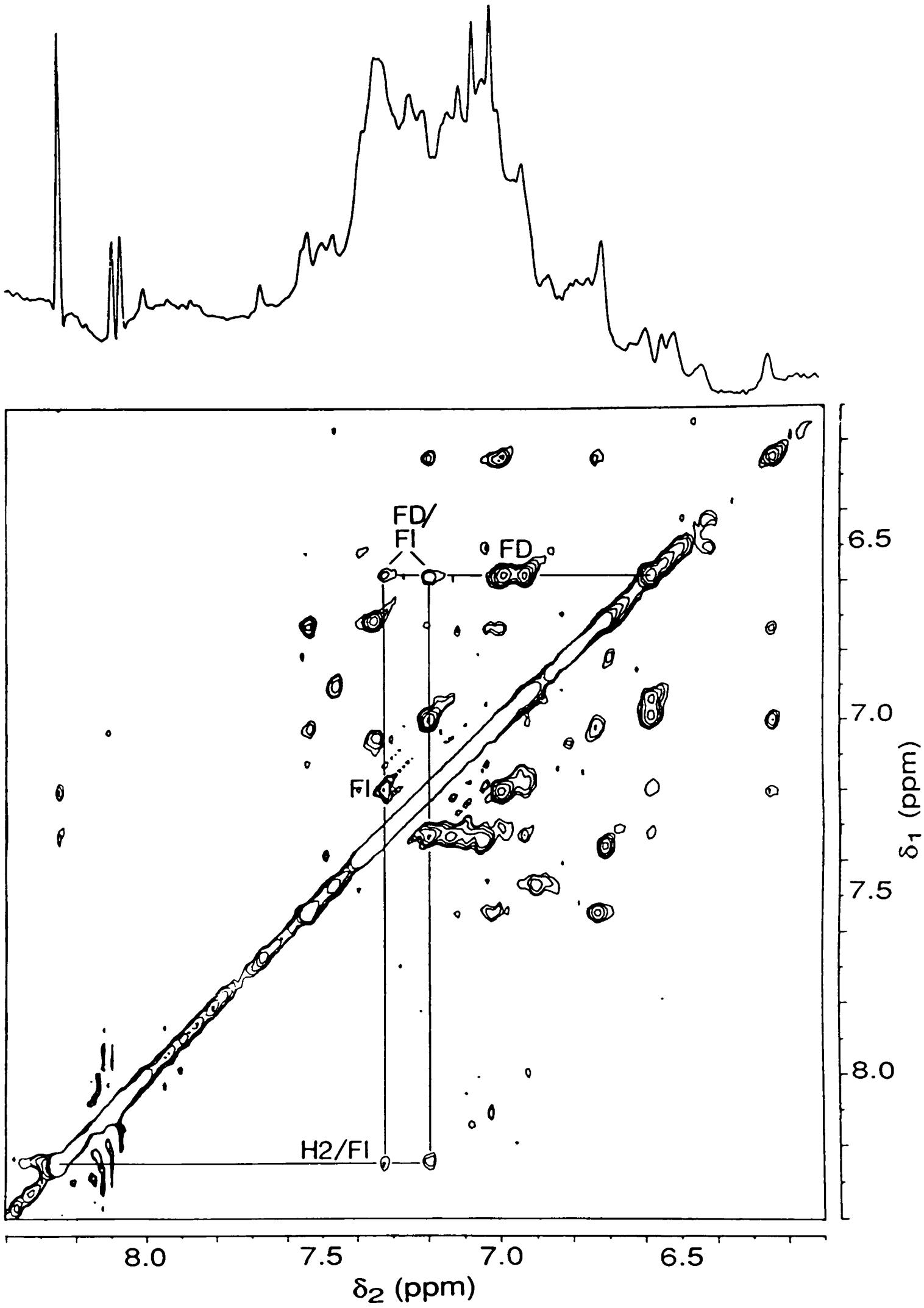

Figure 2-13: Aromatic region of the 600 MHz NOESY spectrum of Mg.ATP.PGK. [Mg.ATP]/[PGK] = 3.0. Inter-molecular NOE connectivities between the C2-H of ATP and Phe I are labelled (H2/FI) as are inter-residue NOEs between Phe I and Phe D. Phe I and Phe D are assigned to Phe 289 and Phe 342 respectively, as discussed in the text.

addition of Mg.ATP to the enzyme. The weak cross-peak seen in the COSY spectrum of free PGK (Figure 2-6) corresponding to Phe C is no longer observed in the COSY spectrum of the Mg.ATP.PGK complex (not shown), indicating possible broadening of this resonance as a result of Mg.ATP binding. The resonances of Phe D are significantly shifted, and at a [Mg.ATP]:[PGK] ratio of ~ 2:1 cross-peaks are found at 6.58, 6.92 ppm and 6.58, 7.01 ppm. Also perturbed is Tyr C, with both aromatic resonances being shifted upfield by ~ 0.03 ppm. The cross-peak assigned to Trp 308 (6.88, 7.46 ppm), however, remains unperturbed by Mg.ATP binding. This would not be expected from the X-ray crystallographic results (Watson *et al.*, 1982) which suggest that the indole ring of Trp 308 moves into a position adjacent to the adenine ring when ATP is bound to the enzyme. This result is discussed in more detail in Chapter 6.

The NOESY spectrum of the Mg.ATP.PGK complex (Figure 2-13) also reveals several inter-molecular NOE connectivities including two between the C2 proton of the adenine ring and Phe I (which has also undergone small changes in chemical shift upon nucleotide binding). In this case, a proton-proton distance search of the crystal structure indicates that Phe I can be assigned to Phe 289 (shortest distances between C2-H of the nucleotide and C2,6-H, C3,5-H and C4-H of Phe 289 are 3.4, 2.1 and 4.4 Å respectively). A problem remains in assigning Phe D, which has NOE connectivities to Phe I (289) in the spectra of both free and nucleotide-bound enzyme. In the crystal structure, the closest Phe side-chain to Phe 289 is that of Phe 342. The shortest inter-proton distance between Phe 289 and Phe 342 is ~ 6 Å, which is too great to give the observed NOEs. Phe 342 is, however, an exposed surface residue and as such would be expected to be quite mobile. It is clear, from the intensity of the observed cross-peaks, that Phe D is a relatively mobile residue (*i.e.* its transverse relaxation time, T_2, is long relative to less exposed side-chains). Thus, it is reasonable to suggest that, in solution,

the average distance between the aromatic rings of Phe 342 and Phe 289 is short enough (< 5 Å) to give the observed pattern of NOEs. Phe D has therefore been tentatively assigned to Phe 342. Note that the inter-residue NOE cross-peaks between Phe 289 and Phe 342 are absent in the NOESY spectrum of (d_5-Phe)PGK (Figure 2-11) although intra-residue NOE cross-peaks due to the ~ 25% isotopically normal Phe 289 and Phe 342 side-chains persist.

Seven additional intermolecular NOEs are observed between the C2-H resonance of ATP and aliphatic resonances between 0.8 ppm and 1.9 ppm. These resonances can be assigned to Leu 311 and Val 339 which, like Phe 289, are in close proximity to the C2-H of the bound nucleotide.

Various other changes are observed throughout the spectrum of the enzyme following Mg.ATP addition. These and the effect of Mn^{2+} addition to the Mg.ATP.PGK complex will be analysed in detail in Chapters 6 and 7.

2.3.4. *Mutant D372N*

The upfield region of the 1D ^{1}H NMR spectrum of a mutant protein in which Asp 372 has been changed to an asparagine residue (D372N; Minard *et al.*, 1989) is compared with that of wild-type PGK in Figure 2-14. Asp 372 is located at the N-terminal end of α-helix XII (Figure 2-4) and is thought to interact with the metal ion when Mg.ATP or Mg.ADP are bound to the protein (Watson & Gamblin, 1985). The observed downfield shift of peak 41 is one of the few effects seen in the spectrum as a result of this mutation, suggesting that it is due to a small local conformational alteration. Peak 41 was identified as being due to a threonine residue in § 2.3.2 (Figure 2-9). The closest threonine γ-CH_3 groups to Asp 372 are those of Thr 373 and Thr 375. A proton-proton distance search of the crystal structure (Watson *et al.*, 1982) shows that the γ-CH_3 protons of Thr 373 are 5.4-6.9 Å from the ring protons of Trp 333 and that the γ-CH_3 protons of Thr 375 are 2.5-6.6 Å from the ring protons of Phe 340. Calculation of the surface accessibility of the γ-CH_3

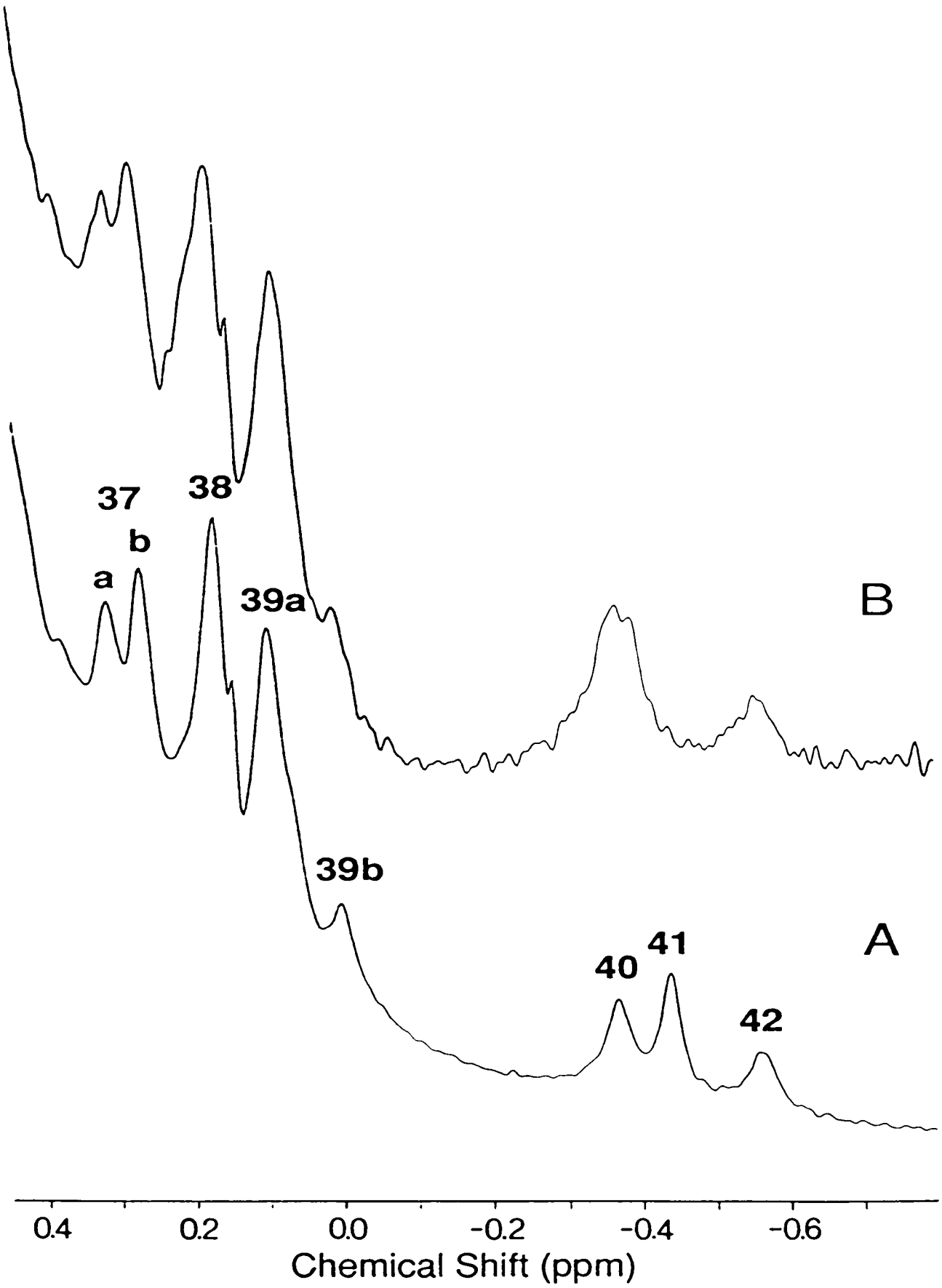

Figure 2-14: Upfield methyl region of the 500 MHz ^{1}H NMR spectra of (A) wild-type PGK and (B) D372N mutant PGK. Resonance 41 has shifted 0.06 ppm downfield as a result of the mutation.

groups of these two threonines from the crystallographic coordinates shows that the γ-CH_3 of Thr 373 is almost totally inaccessible while that of Thr 375 is almost totally exposed on the surface of the protein. Therefore, since peak 41 is due to a relatively exposed threonine in close proximity to an aromatic group, it has been tentatively assigned to Thr 375.

2.3.5. *Δ51-56 mutant PGK*

Consistent with the assignments indicated in Figure 2-12 are changes observed in the aromatic region of the 1D spectrum of the Δ51-56 mutant (Figure 2-15) in which the loop region 51-56 of yeast PGK has been substituted with the analogous sequence from *Thermus thermophilus* PGK (EHHPRY → AGGAS_; D. Bowen & L. Hall, *unpublished data*). In addition to the loss of resonances of His 52 and His 53 (peaks 2b, 5, 9 and 11) we see a 0.12 ppm upfield shift of peak 16 and significant perturbations of components of peaks 12 and 14a. The changes in chemical shift of resonances due to Tyr 48 and Phe 185 indicate a mutual reorientation of these side-chains as a result of the substitution. Unfortunately these changes preclude the assignment of the substituted Tyr 56 in the 1D spectrum. The remainder of the spectrum is similar to that of the wild-type protein, indicating that the overall fold of the two enzymes are closely similar.

2.3.6. *Assignment of His resonances*

Previous tentative assignments of His resonances have been made by correlating observed chemical shift pH dependence (Wilson *et al.*, 1988) and accessibility to flavin dyes (Scheffler & Cohn, 1986) with the X-ray crystal structure of Watson *et al.* (1982). The potential of site-specific mutagenesis for ^1H NMR spectral assignment purposes was demonstrated for His 52 and 53 in the preceding section (Figure 2-15). Comparison of NOESY and X-ray crystallographic data allowed sequence specific assignment of resonances 5 and 9 to His 52, and 2b and 11 to His 53 (Figure 2-12). With the exception of

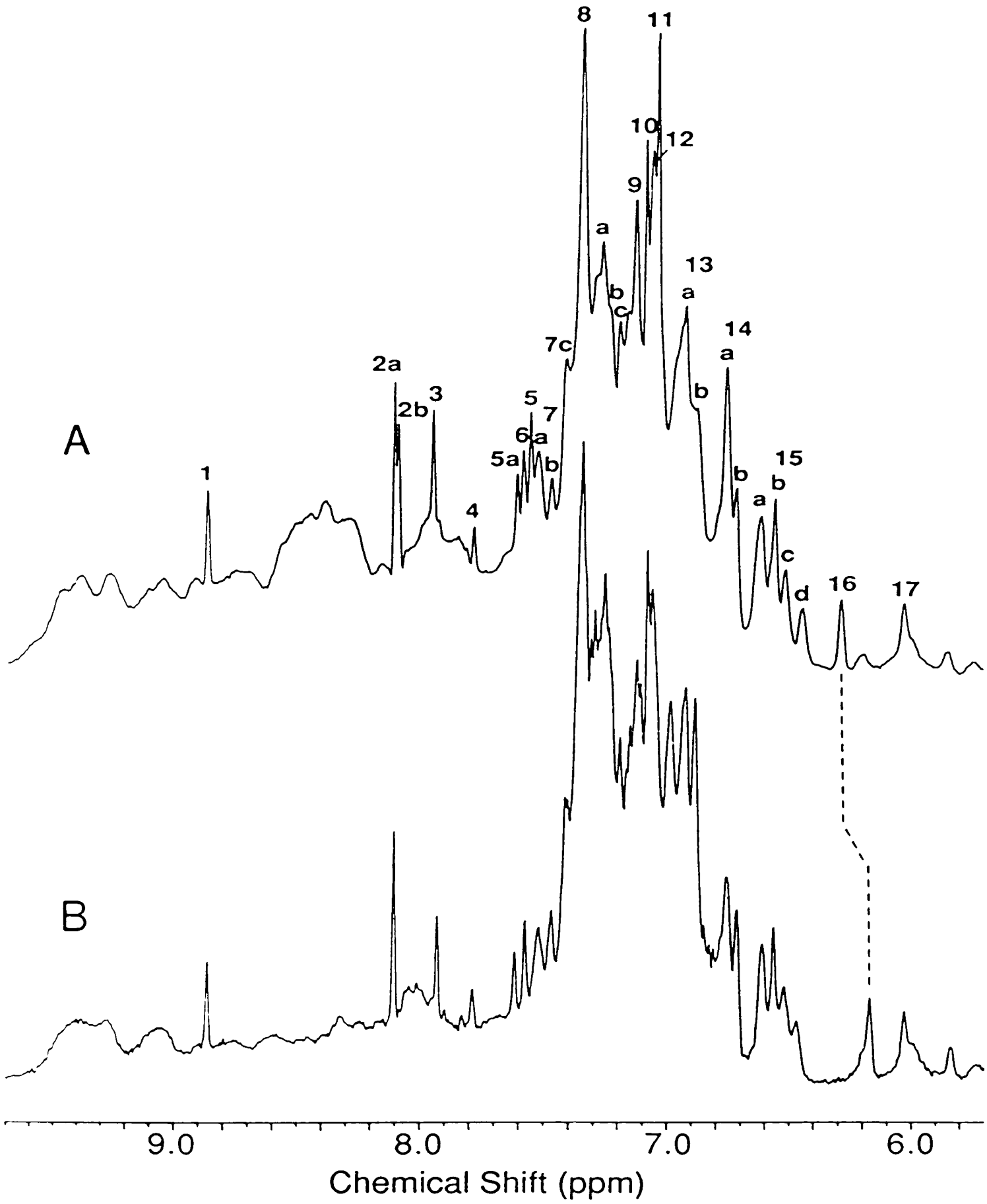

Figure 2-15: Aromatic region of the 600 MHz ^{1}H NMR spectra of (A) wild-type PGK and (B) Δ51-56 mutant PGK. The change in chemical shift of peak 16 as a result of the mutation is indicated.

resonance 5, these assignments are consistent with the non-specific assignments of Wilson *et al.* (1988) and the tentative assignments of Scheffler & Cohn (1986). The use of site-directed mutagenesis and chemical shift pH dependence (combined with crystallographic data) in specifically assigning histidine residues is outlined below.

2.3.6.1. pH dependence

The pH dependence of selected aromatic resonances are shown graphically in Figure 2-16. Resonance 1 has been assigned to His 123 on the basis of its relatively high pK_a (8.3 ± 0.1) and its 'non-random coil' chemical shift (Wilson *et al.*, 1988). The downfield shift of this resonance can be accounted for by the close proximity of the C2-H of His 123 to Tyr 122 and Phe 147 (*i.e.* ring current shift). The elevated pK_a indicates a negatively charged environment, consistent with the proximity of His 123 relative to Asp 143 (Figure 2-17B). No cross-peak has been observed from peak 1 to other resonances in the aromatic region of the NOESY spectrum of yeast PGK, suggesting that the C4-H resonance of His 123 is too broad to be observed. Peak 1 itself is observed to broaden considerably as the pH is increased above 7.2.

Peaks 2a and 2b have pK_a values of about 7. This, together with their narrow line-width, suggests that they are C2-H resonances of histidine groups which are totally exposed to the solvent. The NOESY spectrum of yeast PGK (Figure 2-10) associates peak 2a with peak 10, and peak 2b with peak 11, which is consistent with the observed pH dependence of these resonances (Figure 2-16). The two most exposed histidine residues in the X-ray crystal structure are His 53 and His 149 (Figures 2-4, 2-17A & 2-17B). Evidence from the NOESY spectrum and Δ51-56 mutant (see §§ 2.3.2 & 2.3.5) indicates that peaks 2b and 11 can be assigned to His 53. Peaks 2a and 10 have, therefore, been assigned specifically to His 149. These assignments are also in agreement with

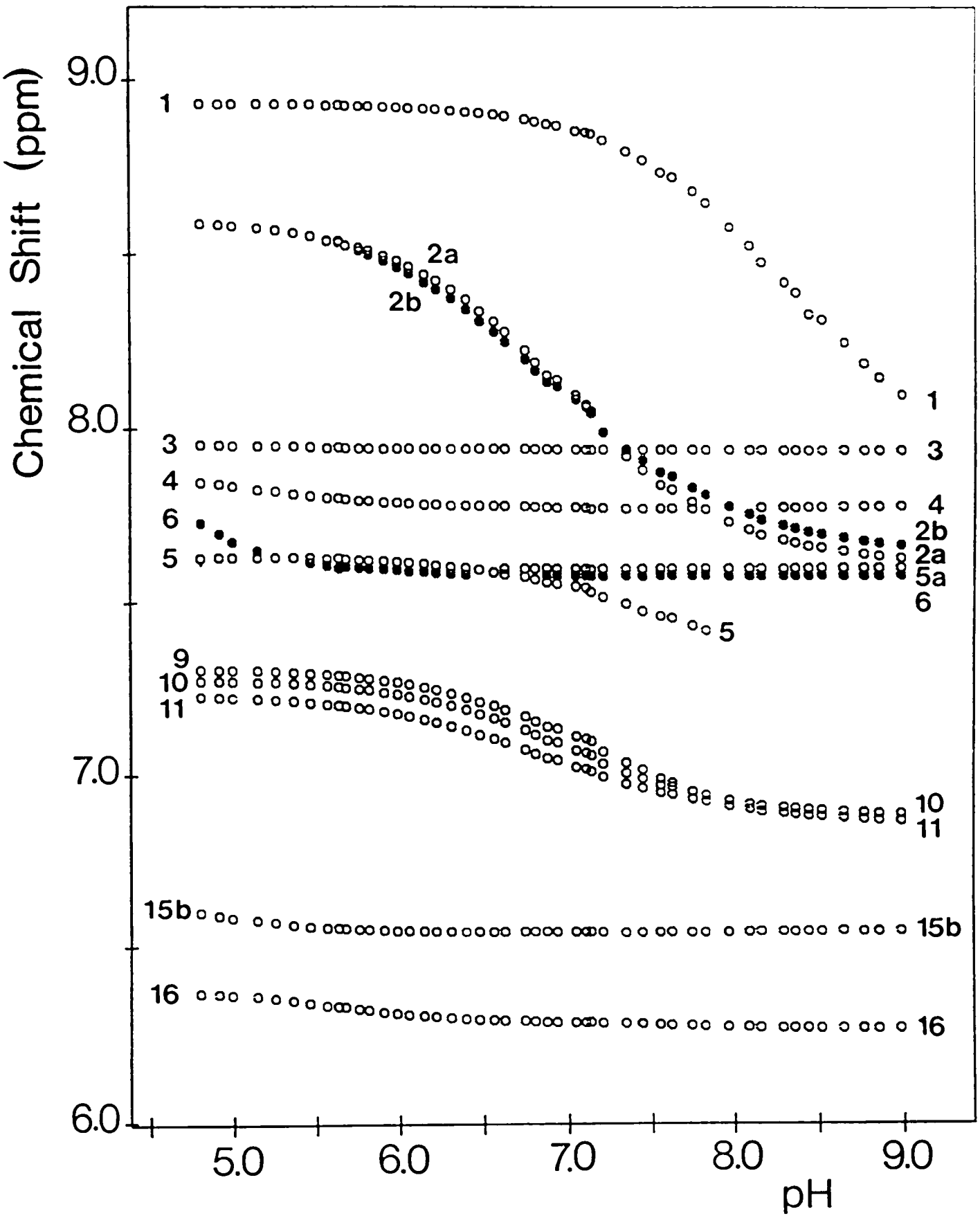

Figure 2-16: The pH dependence of chemical shift for some aromatic resonances of yeast PGK. The numbers correspond to the peak labelling shown in Figure 2-3. The experimental points for peaks 2b and 6 are shaded for clarity.

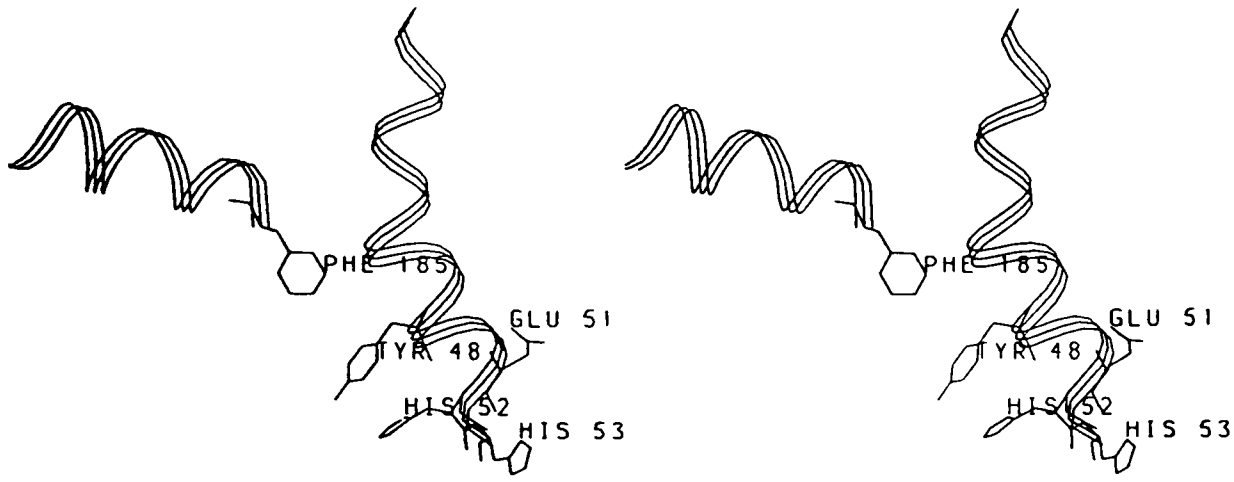

Figure 2-17A: The environments of His 52 and His 53.

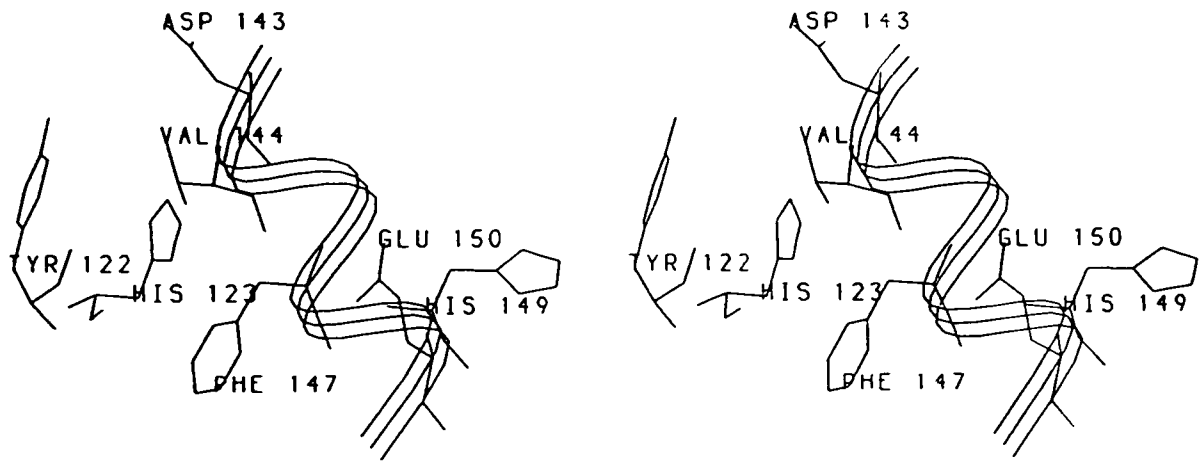

Figure 2-17B: The environments of His 123 and His 149.

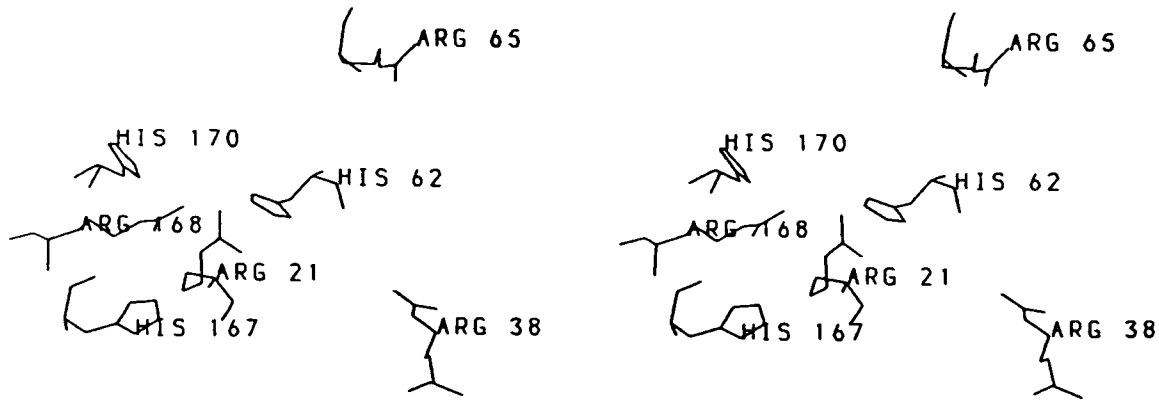

Figure 2-17C: The environments of His 62, His 167 and His 170.

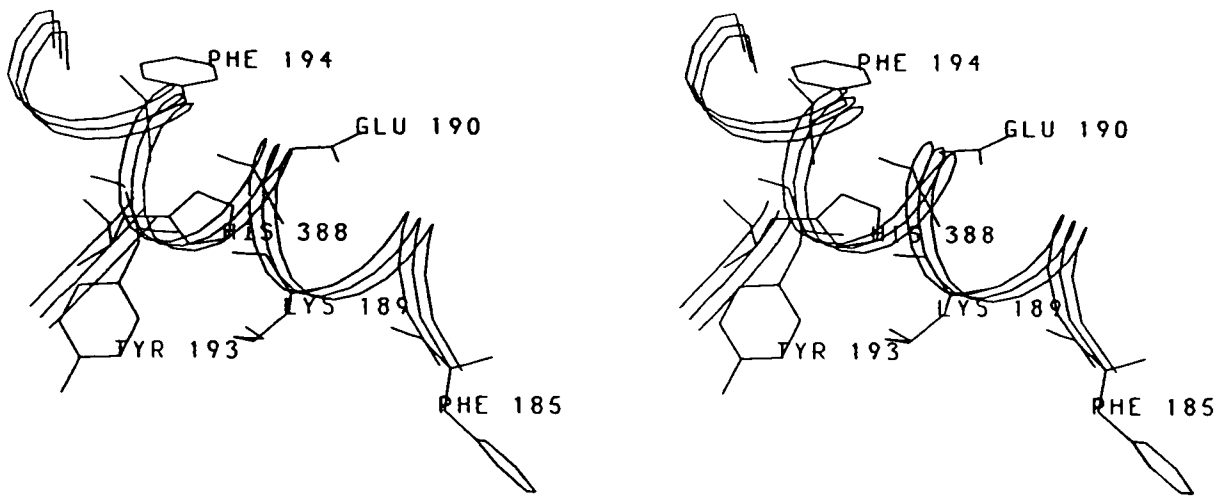

Figure 2-17D: The environment of His 388.

the photo-CIDNP based assignments of Scheffler & Cohn (1986).

Peaks 3, 4 and 5a are independent of pH over the range studied (peak 4 shows a slight pH dependence at pH < 6). Previous studies have associated these peaks with histidines in the vicinity of the phosphoglycerate binding site (Tanswell *et al.*, 1976). Subsequent NMR and crystallographic studies have lead to the non-specific assignment of these three peaks to the 'basic patch' histidines 62, 167 and 170 (Wilson *et al.*, 1988) (Figures 2-4, 2-17C). The NMR observation of low pK_a values for the three 'basic patch' histidines is in accord with the strong positive electrostatic field in which they are situated. It is noted here that the pH dependence of peak 15b is similar to that of peak 4. In the following chapters it will be shown that peaks 3, 4, 5a, a component of peak 13a, and peak 15b are consistently influenced by the addition of substrates and other anions (both paramagnetic and diamagnetic).

Resonance 6 also shifts with a pK_a < 4, indicating interaction with a positively charged group. This resonance was assigned to His 388 (§ 2.3.2) on the basis of an NOE connectivity observed between this peak and Tyr 193. The observed pH dependence of this resonance, however, is inconsistent with the crystallographically observed hydrogen-bond between His 388 and Glu 190 (Watson *et al.*, 1982), indicating a probable difference between the average solution and crystallographic conformations. The low pK_a of His 388 observed in the solution state suggests that this residue probably interacts with the positively charged Lys 189 rather than the acidic Glu 190 (Figure 2-17D).

2.3.6.2. Site-specific mutagenesis

A number of site-specific mutant forms of yeast PGK have been produced in the laboratories of Dr L. Hall and Dr H.C. Watson (Department of Biochemistry, University of Bristol) for studies of the catalytic mechanism and thermostability of the enzyme. NMR spectroscopy has been used to examine the structural integrity and substrate binding properties of these

mutants (see Chapter 4). In favourable cases it is possible to make sequence specific assignments on the basis of the ^{1}H NMR spectra of such mutants. An example, involving assignment of His 52 and His 53 was given earlier (see §§ 2.3.3 & 2.3.5). Mutations in the 'basic patch' region have enabled specific assignments to histidines 62, 167 and 170 as follows.

2.3.6.3. Spectrum of H170D

The mutant protein H170D has the uncharged aromatic residue, His 170, replaced by a smaller aspartic acid residue which has a negatively charged carboxyl group. In the aromatic region of the spectrum of H170D (Figure 2-18), resonance 3 has shifted upfield 0.10 ppm, relative to the wild-type, while resonance 4 has shifted downfield (0.04 ppm) and resonance 5a is absent. Upfield of the aromatic envelope, peak 15b appears to have shifted downfield (0.16 ppm) resulting in an apparent increase in the intensity of peak 14b. There are also changes seen around peak 13, where the spectrum is poorly resolved. This includes the appearance of a new peak at 6.83 ppm which may have shifted upfield from within the intensity of peak 13, or downfield from within the intensity of peak 14a, in the spectrum of the wild-type. The only other changes in the aromatic region of the spectrum of H170D relative to wild-type are small downfield shifts of peaks 8a and 17 (0.02 and 0.01 ppm respectively).

These observations allow the assignment of peak 5a specifically to the C2-H of His 170. The upfield shift of resonance 3 might be thought to indicate that the pK_a of this histidine has been lowered. This is unlikely, however, following the introduction of a negatively charged side-chain to the area. Also, the pK_a of resonance 3 of wild-type PGK has been shown to be less than 3 (Figure 2-16), so any decrease in this value would not be observable by ^{1}H NMR at pH 7.1 (*i.e.* the histidine is already deprotonated beyond detectable limits). The shift is therefore predominantly conformational in origin. The

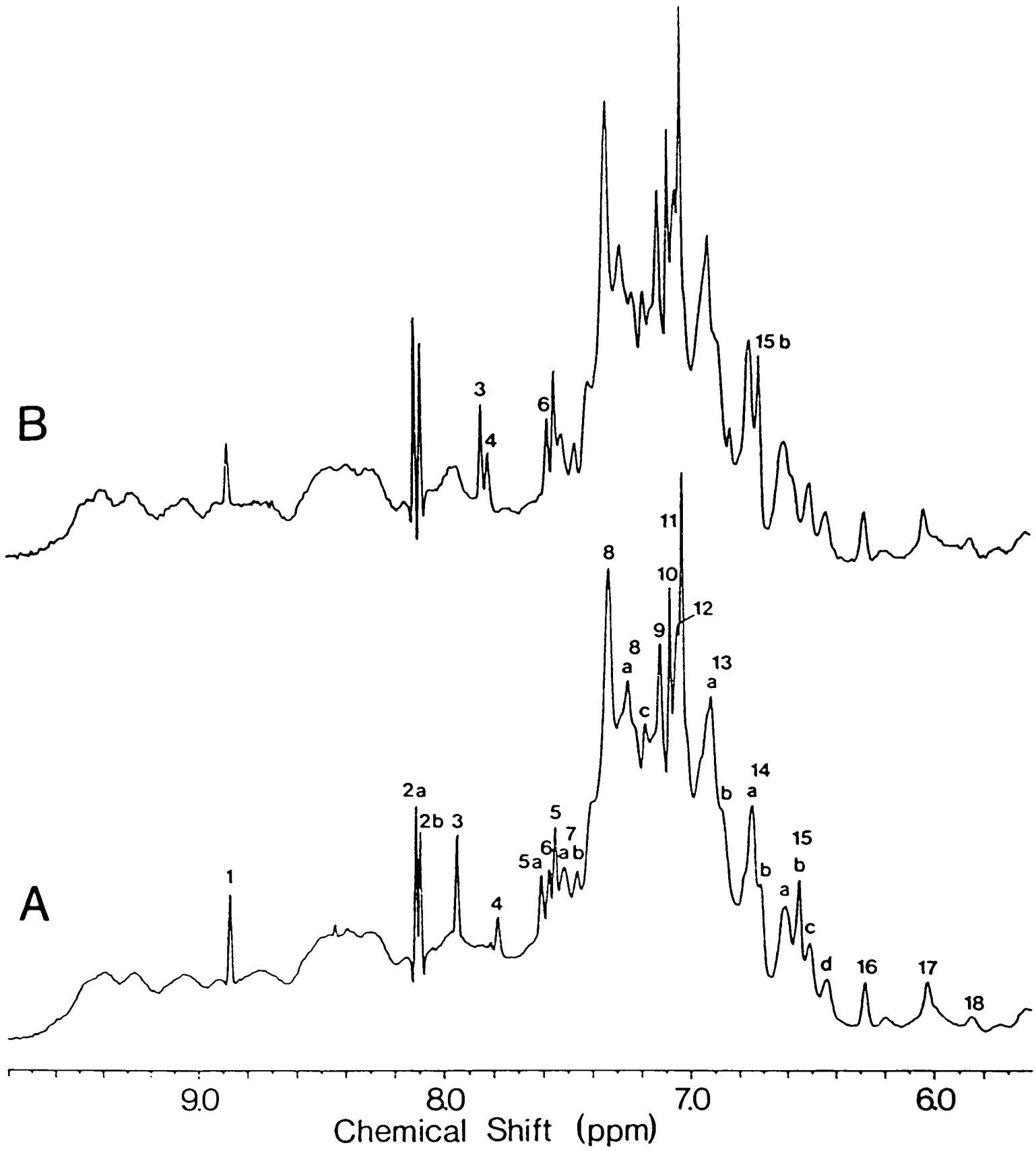

Figure 2-18: Comparison of the aromatic regions of the 500 MHz ^{1}H NMR spectra of wild-type (A) and H170D (B) PGK at pH 7.1.

downfield shifts of resonances 4 and 15b may be due to direct effects of charge redistribution in the area. Evidence presented in Chapter 4, however, suggests that these effects are also conformational. There may also be chemical shift differences due directly to the field effects of the exchanged imidazole ring.

2.3.6.4. Spectrum of H62Q

This mutation involves substitution of 'basic patch' His 62 with glutamine. Comparison of the aromatic region of the spectrum of H62Q with that of wild-type PGK (Figure 2-19) reveals few differences. The most marked difference is the absence of resonance 3 in the spectrum of the mutant enzyme. This peak can now be assigned specifically to His 62. The resonance assigned above to His 170 is seen to have shifted downfield (~ 0.1 ppm). Small shifts of other resonances are best seen in the difference spectrum (Figure 2-20). [Note: the shifts of peaks 1, 2a, 2b, 9, 10 and 11 are attributable to small differences in the pH of the two samples].

Since resonances 4 and 15b are not due to His 62 or His 170, but are perturbed by mutation of either, they can be specifically assigned to His 167. A component of resonance 13a is also seen to be perturbed by substitution at position 62. A resonance in this position is also broadened, together with peaks 3, 4, 5a and 15b, on addition of the paramagnetic relaxation reagents, $[Cr(CN)_6]^{3-}$ and $Mn.ATP^{2-}$ (see Chapters 5 and 7; Figures 5-2, 7-2). This resonance has therefore been tentatively assigned to His 170. The only peak in the difference spectrum that can be assigned to His 62 is resonance 3. The C4-H resonance of this residue is therefore either too broad to be observed or is obscured by the C4-H peaks of histidines 52, 149 and 53 (peaks 9, 10 and 11 respectively).

Assignments to histidine residues, outlined above, are summarised in Table 2-3.

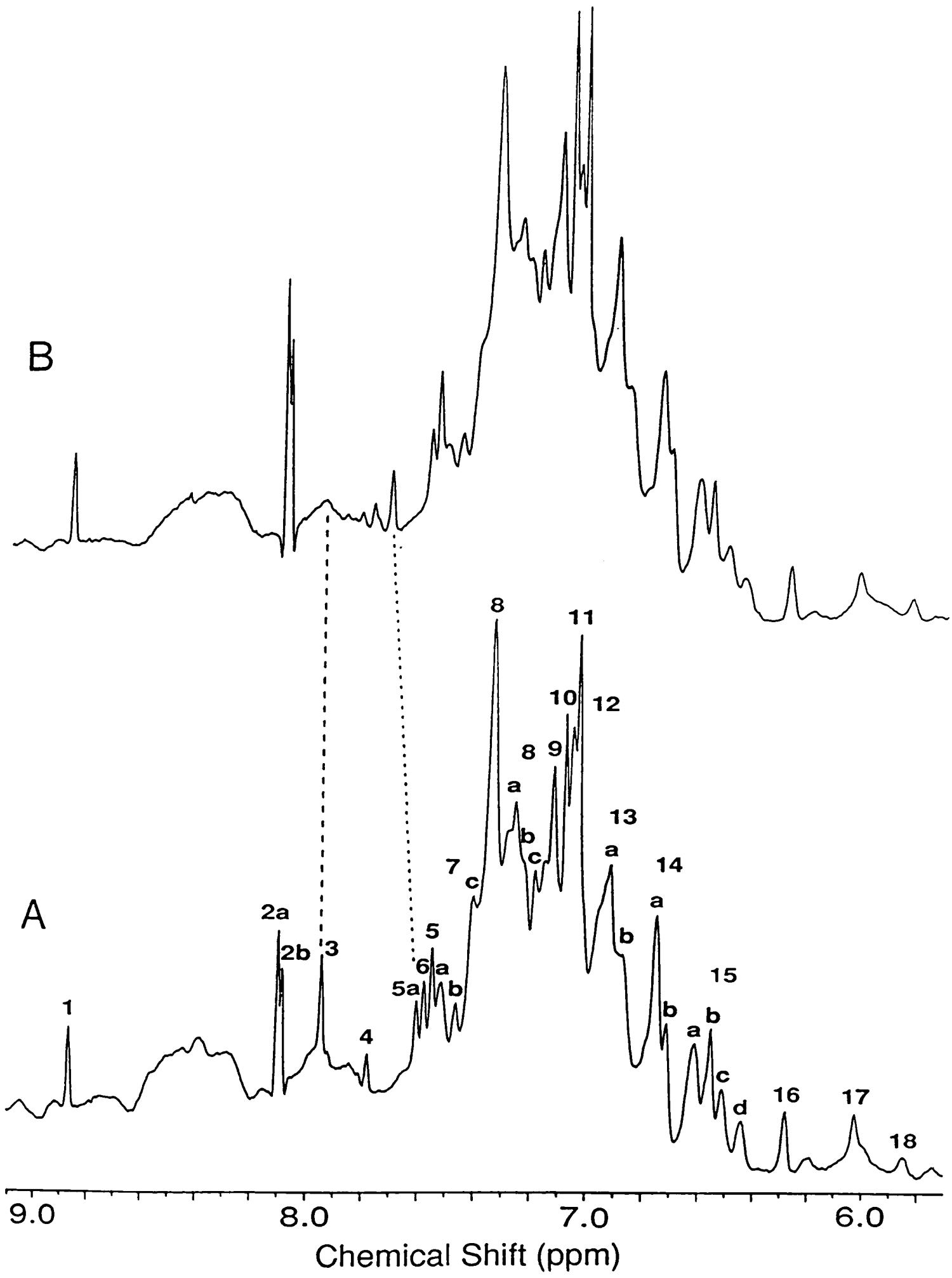

Figure 2-19: Comparison of the aromatic regions of the 500 MHz ^{1}H NMR spectra of wild-type (A) and H62Q (B) PGK at pH 7.1.

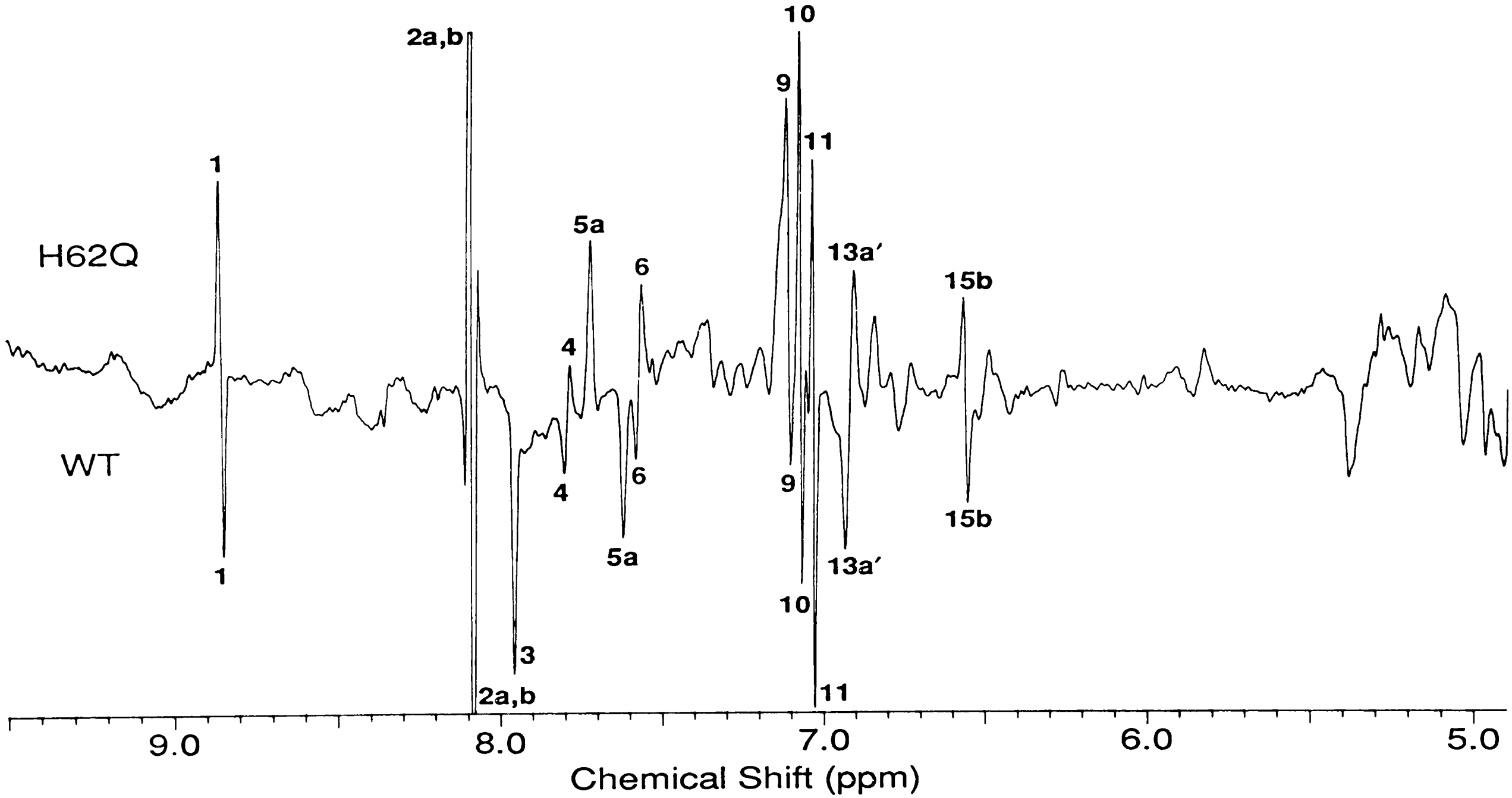

Figure 2-20: Difference spectrum between the aromatic regions of the spectra of wild-type and H62Q PGK.

Table 2-3: Sequence specific assignments to His residues in the ^1H NMR spectrum of yeast PGK.

pH 7.1, 0.10 M Na d_3-acetate/D_2O, T = 300 K

Peak	Chemical shift (ppm)	His assignment
1	8.87	C2-H 123
2a	8.16	C2-H 149
2b	8.10	C2-H 53
3	7.95	C2-H 62
4	7.81	C2-H 167
5a	7.61	C2-H 170
6	7.58	C2-H 388
5	7.55	C2-H[a] 52
9	7.13	C4-H[a] 52
10	7.09	C4-H 149
11	7.03	C4-H 53
13a	6.9	C4-H 170[b]
15b	6.55	C4-H 167

[a] assignments to C2-H and C4-H are tentative

[b] tentative assignment

2.4. Discussion

A selected set of resonances and their cross-peaks are observed in the 2D ^{1}H NMR spectra of yeast PGK. These resonances can be assigned to the more mobile residues of the protein, as discussed by Wilson *et al.* (1988). Using techniques which include specific amino acid deuteration and site-specific mutagenesis, resonances due to 10 out of 19 phenylalanine residues and 6 out of 7 tyrosine residues have been identified. An assignment to Trp 308 (one of two tryptophan residues in the protein) has also been made, based largely on results of experiments carried out with the genetically engineered isolated C-terminal domain (§ 8.3.2). This assignment is also in agreement with the photo-CIDNP results of Scheffler & Cohn (1986). Of the upfield aromatic resonances (14-17) only peak 17 has not been assigned to a specific amino acid type. Some sequence specific assignments have also been made using information contained in the NOESY spectra, and structural information obtained from X-ray crystallographic data (Watson *et al.*, 1982). In this way it has been possible to assign the upfield aromatic resonance 16 to the C4-H of Phe 185 and component of peaks 14a and 13b to Tyr 193 (Table 2-2). These assignments are in line with the suggestion that relatively well resolved resonances of the spectrum may originate from mobile residues in the interdomain region of the protein (Wilson *et al.*, 1988). Phe 185 is located at the N-terminal end of the interdomain α-helix V (Watson *et al.*, 1982), with its C4-H in close proximity to the aromatic ring of Tyr 48 (assigned to another component of peak 14a; Table 2-2). Tyr 193 is situated near the middle of α-helix V. An NOE connectivity observed between Tyr 193 and resonance 6 has led to assignment of the latter to interdomain His 388. The low pK_a of peak 6 suggests that in solution His 388 must be interacting with Lys 189 rather than Glu 190 as observed crystallographically. The above assignment of Tyr 193 is also in agreement with the results of Scheffler & Cohn (1986). The assignment of Tyr 48 to components of peaks 14a and 12 (Table 2-2),

however, does not agree with the previous tentative assignment of a component of peak 8 to this residue (Scheffler & Cohn, 1986). Their assignment relied on an estimation, based on the X-ray crystal structure, of the accessibility in solution of tyrosine residues to flavin dyes. On the basis of the present results it is reasonable to assign the component of peak 8, observed by Scheffler & Cohn, to Tyr 380 (Table 2-2). It is noted here that addition of Mg.ATP to the enzyme resulted in the interaction between this residue and the flavin being blocked (Scheffler & Cohn).

In addition to the above, unambiguous assignments have been made for His 52 and His 53 (Figure 2-12) which enables the assignment of His 149 to peaks 2a and 10, and His 123 to peak 1 by elimination from previous results (Wilson *et al.*, 1988). Specific assignments to the three 'basic patch' histidines 62, 167 and 170 have also been made using site-specific mutant forms of the enzyme.

Figure 2-21 shows the relative positions of assigned side-chains in the protein. It can be seen that resonances have been assigned to surface amino acids in both domains and in the interdomain region. The assigned resonances can now be used as local probes of structure and dynamics in ligand binding studies of the protein.

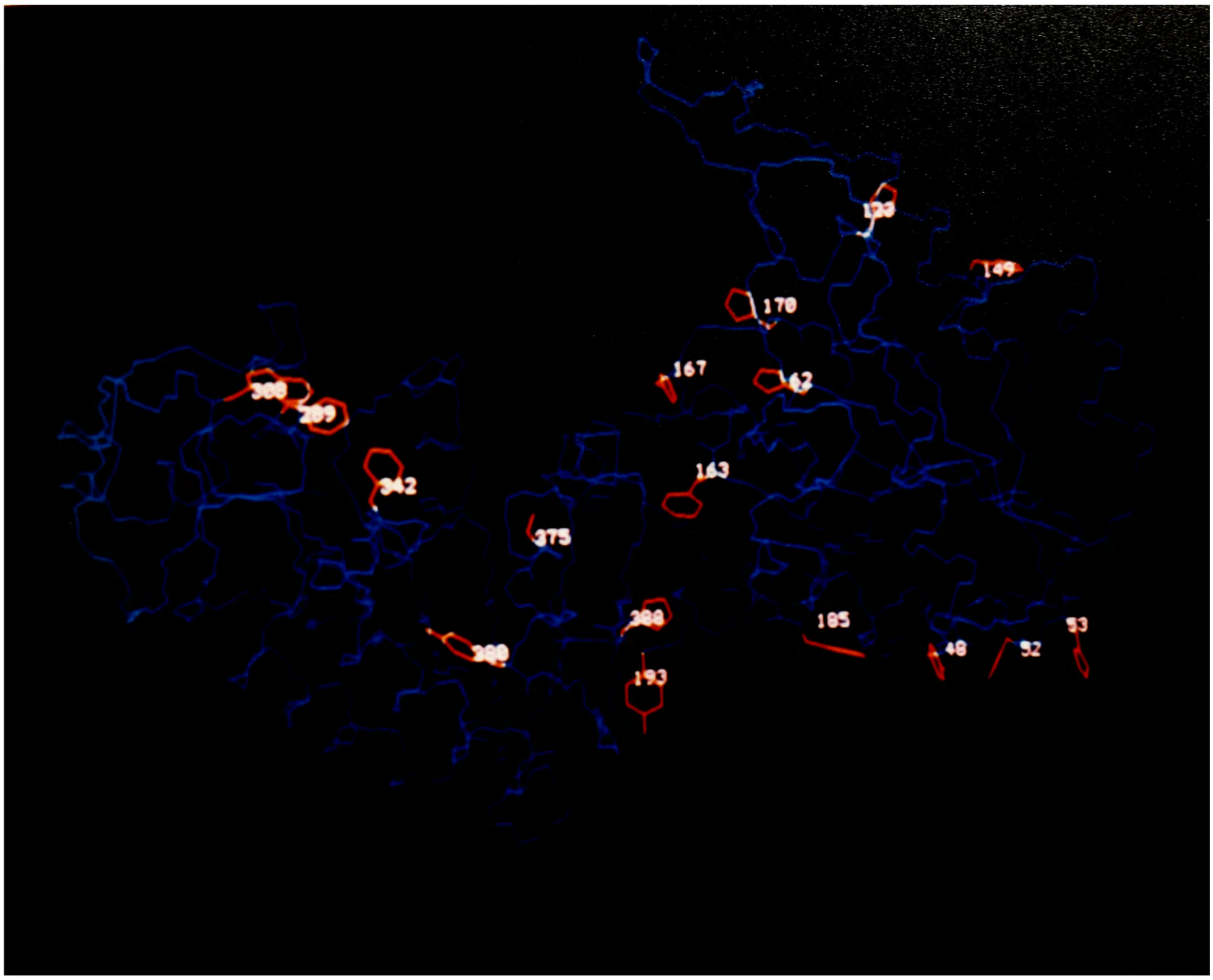

Figure 2-21: Assigned amino acid side-chains (in red) superposed on the main-chain (in blue) of the crystal structure (Watson *et al.*, 1982) of yeast PGK.

2.5. References

Aue, W.P., Bartholdi, E. & Ernst, R.R. (1976) *J. Chem. Phys. 64,* 2229-2246.

Blake, C.C.F. & Rice, D.W. (1981) *Phil. Trans. R. Soc. Lond. A. 293,* 93-104.

Bodenhausen, G., Vold, R.L. & Vold, R.R. (1980) *J. Magn. Reson. 37,* 93-106.

Bowen, D., Littlechild, J.A., Fothergill, J.E., Watson, H.C. & Hall, L. (1988) *Biochem. J. 254,* 509-517.

Campbell, I.D., Dobson, C.M., Williams, R.J.P. & Wright, P.E. (1975) *FEBS Lett. 57,* 96-99.

Clore, G.M. & Gronenborn, A.M. (1987) *Protein Eng. 1,* 275-288.

Cooke, R.M. & Campbell, I.D. (1988) *BioEssays 8,* 52-56.

Dalgarno, D.C., Levine, B.A. & Williams, R.J.P. (1983) *Biosci. Reports 3,* 443-452.

Dobson, M.J., Tuite, M.F., Roberts, N.A., Kingsman, A.J., Kingsman, S.M., Conroy, S.C., Dunbar, B. & Fothergill, L.A. (1982) *Nucleic Acid Res. 10,* 2625-2637.

Ernst, R.R. (1966) *Adv. Magn. Reson. 2,* 1-135.

Ernst, R.R., Bodenhausen, G. & Wokaun, A. (1987) *Principles of Nuclear Magnetic Resonance in One and Two Dimensions,* Clarendon Press, Oxford.

Fifis, T. & Scopes, R.K. (1978) *Biochem. J. 175,* 311-319.

Glasoe, P.K. & Long, F.A. (1960) *J. Phys. Chem. 64,* 188-190.

Ito, H., Fukuda, Y., Murata, K. & Kimaru, A. (1983) *J. Bact. 153,* 163-168.

Jeener, J., Meier, B.H., Bachmann, P. & Ernst, R.R. (1979) *J. Chem. Phys. 71,*

4546-4553.

Jones, E.W. & Fink, G.R. (1982) in *The Molecular Biology of the Yeast Saccharomyces Metabolism and Gene Expression*, pp. 198-207, Cold Spring Harbor Laboratory.

Krietsch, W.K.G. & Bücher, T. (1970) *Eur. J. Biochem. 17*, 568-580.

Laemilli, U.K. & Favre, M. (1973) *J. Mol. Biol. 80*, 575-599.

Lesk, A.K. & Hardman, K.D. (1982) *Science 216*, 539-540.

Marion, D. & Wüthrich, K. (1983) *Biochem. Biophys. Res. Comm. 113*, 967-974.

Minard, P., Bowen, D., Littlechild, J.A., Watson, H.C. & Hall, L. (1989) *in preparation.*

Neuhaus, D., Wagner, G., Vašák, M., Kägi, J.H.R. & Wüthrich, K. (1985) *Eur. J. Biochem. 151*, 257-273.

Oswald, R.E., Bogusky, M.J., Bamberger, M., Smith, R.A.G. & Dobson, C.M. (1989) *Nature (Lond.) 337*, 579-582.

Redfield, A.G. & Kunz, S.D. (1975) *J. Magn. Reson. 19*, 250-254.

Scheffler, J.E. & Cohn, M. (1986) *Biochem. 25*, 3788-3796.

Tanswell, P., Westhead, E.W. & Williams, R.J.P. (1976) *Eur. J. Biochem. 63*, 249-262.

Watson, H.C., Walker, N.P.C., Shaw, P.J., Bryant, T.N., Wendell, P.L., Fothergill, L.A., Perkins, R.E., Conroy, S.C., Dobson, M.J., Tuite, M.F., Kingsman, A.J. & Kingsman, S.M. (1982) *EMBO J. 1*, 1635-1640.

Watson, H.C. & Gamblin, S.J. (1985) *Proc. Int. Symp. Biomol. Struct. Interactions, Suppl. J. Biosci. 8,* 499-506.

Wilson, C.A.B., Hardman, N., Fothergill-Gilmore, L.A., Gamblin, S.J. & Watson, H.C. (1987) *Biochem. J. 241,* 609-614.

Wilson, H.R., Williams, R.J.P., Littlechild, J.A. & Watson, H.C. (1988) *Eur. J. Biochem. 170,* 529-538.

Wüthrich, K. (1986) *NMR of Proteins and Nucleic Acids,* John Wiley & Sons, New York.

Wüthrich, K. (1989) *Acc. Chem. Res. 22,* 36-44.

Chapter 3

NMR ANALYSIS OF 3-PHOSPHOGLYCERATE BINDING TO YEAST PGK

3.1. Introduction

The bilobal nature of the PGK enzyme (Figure 3-1) and the structural characteristics of the active site cleft have led to the suggestion that a conformational change, involving a movement of the domains relative to each other, occurs during the enzymatic reaction (Banks *et al.*, 1979; Blake & Rice, 1981). The proposed 'hinge bending' movement would have the effect of placing the group of basic residues which line the N-terminal domain face of the active site cleft in close proximity to the site of the transferable phosphate group, as determined crystallographically (Watson *et al.*, 1982; see Figure 3-1). Evidence in support of a substrate induced conformational change during catalysis has come from a number of sources, including NMR (Tanswell *et al.*, 1976; Wilson *et al.*, 1988), low angle X-ray scattering (Pickover *et al.*, 1979; Ptitsyn *et al.*, 1986; Sinev *et al.*, 1989) and analytical ultracentrifugation (Roustan *et al.*, 1980) studies. Ptitsyn *et al.* (1986) have pointed out, however, that the reported change in sedimentation constant (Roustan *et al.*, 1980) on adding substrates is "rather strange". More recently Mas and Resplandor (1988) have reported conflicting sedimentation velocity measurements which indicate no difference in the $s_{20,w}$ of yeast PGK in the presence of substrates.

A conformational change on substrate binding, possibly involving 'hinge bending' and consequent domain movement, is generally accepted, although questions have arisen as to the exact mode of substrate binding (particularly the triose substrate) and its relationship to the observed changes in conformational equilibrium.

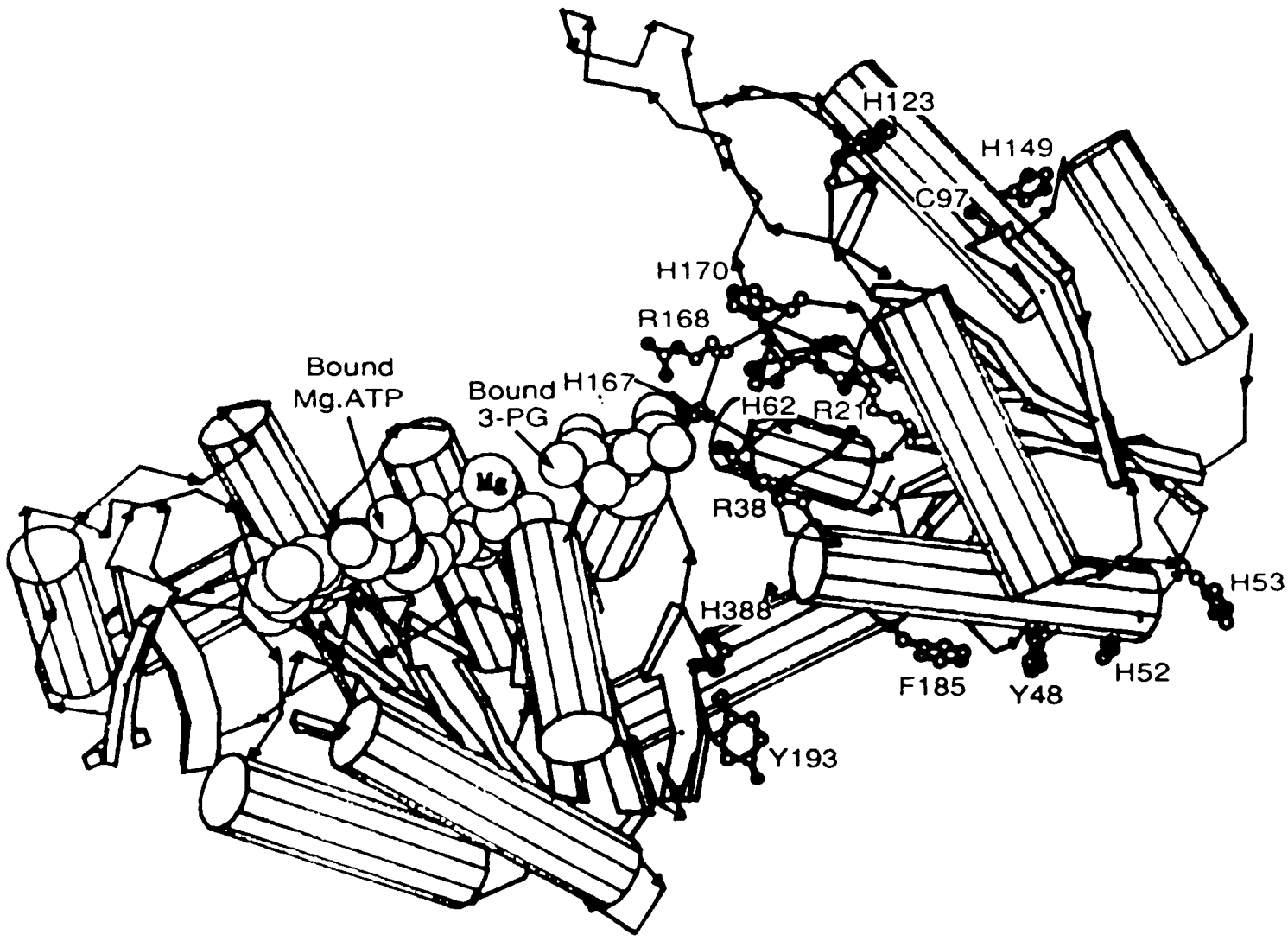

Figure 3-1: A schematic drawing of the crystal structure of yeast PGK (Watson *et al.*, 1982) showing the N-terminal domain to the right and the C-terminal domain to the left. The positions of selected amino acids are indicated. The positions of the crystallographically determined Mg.ATP and 3-PG binding sites are also shown. The drawing was produced using a computer program written by Lesk & Hardman (1982).

Studies with 3-PG analogues have probed the way in which this substrate binds to the enzyme. Orr and Knowles (1974), using a phosphonate analogue (2-hydroxy-4-phosphono-D,L-butanoic acid), demonstrated that a dianionic group on C3 is required for efficient substrate binding. Adams *et al.* (1983) showed that the arsonomethyl analogue of 3-PG (2-hydroxy-4-arsono-D,L-butanoic acid) has a Michaelis constant (K_m) comparable to that of 3-PG, although the catalytic constant was about 1300 times smaller. They speculated that the binding was reasonably tight, despite the fact that not all of the analogue would exist as the trianion, but that the carboxyl group was slightly displaced so that its phosphorylation by ATP was slowed. In a steady-state kinetic study of the inhibition of pig muscle PGK (Tompa *et al.*, 1986) by a variety of 3-PG analogues (D-glycerol-3-phosphate, 2-phosphoglycolate, tartronate, malonate and D-glycerate) it was also concluded that the phosphate of 3-PG was essential for formation of its complex with the enzyme, and that the carboxyl group might strengthen the binding in a synergic manner. The reactivity of thiol groups of the pig muscle protein appeared to be controlled by ligand-induced conformational changes. In the case of two fast-reacting thiols the effect was specifically associated with the presence of a ligand's phosphate group. The above work shows that the phosphate group of 3-PG is involved in specific interactions with the protein.

In a gel filtration study of yeast PGK, Scopes (1978b) identified a single binding site for 3-PG with a dissociation constant of 0.032 mM at high ionic strength (I = 0.15 M) and 0.011 mM at lower ionic strength (I = 0.015 M). A dissociation constant of 0.06 μM was obtained for 1,3-P_2G (I = 0.15 M). Sulphate and phosphate binding were also investigated and found to be mutually competitive, with K_ds of 1.6 mM and 1.1 mM respectively (I = 0.15 M). Sulphate was also found to compete with the binding of all substrates except Mg.ADP.

This result is consistent with Scopes' previous study of the effects of salts

on activity (Scopes, 1978a), which showed that sulphate acts as a competitive inhibitor at high sulphate concentrations. It has also been shown, however, that most anions (especially multivalent anions) cause activation of the enzyme at lower concentrations (the greater the charge the lower the concentration required for activation) and are inhibitory at higher concentrations (Larsson-Raźnikiewicz & Jansson, 1973; Scopes, 1978a; Khamis & Larsson-Raźnikiewicz, 1981). Thus there is evidence for a general anion binding site in the active site region. The activatory effect of sulphate at lower concentrations and the substrate activation phenomena (Larsson-Raźnikiewicz & Schierbeck, 1977) were interpreted in terms of a two-step dissociation of 1,3-P_2G (Scopes, 1978b) *i.e.* the general anion site is the same as, or close to, the 3-PG binding site and at lower concentrations the anion activates the enzyme by acceleration of the dissociation rate of the product, 1,3-P_2G, while at higher concentrations the dominant effect is inhibition through competition with the initial substrate binding. In a subsequent study it was suggested that at least two sulphate binding sites exist, the strongest being a general anion site and the other being the catalytic centre (Khamis & Larsson-Raźnikiewicz, 1981).

Wrobel and Stinson (1978) labelled the single thiol of yeast PGK (Cys 97 situated ~ 25 Å from the crystallographically determined 3-PG site; Watson *et al.*, 1982) with the chromophoric sulfhydryl reagent, 2-chloromercuri-4-nitrophenol, and used the change in absorbance to monitor anion binding. The binding stoichiometry of a number of anions (including substrates) was found to be 1:1 and a linear relationship between the charge of the anion and (-log K_d) for the labelled enzyme.anion complexes was established. It was also found that anions bound to PGK decreased the rate of reaction between the enzyme thiol and 5,5´-dithiobis(2-nitrobenzoic acid). These authors put forward several arguments suggesting that the anion site they were monitoring was not in fact the active site. There is also evidence for a second, low

affinity, 3-PG binding site from product inhibition studies (Schierbeck & Larsson-Raźnikiewicz, 1979). However, since only one site was found in gel filtration studies, Scopes (1978b) suggested that they must be looking at the active site, though indirectly. If this is so then the conformation of the enzyme in solution in the presence of substrates and other anions may differ substantially from that observed in the crystalline state.

Blake and collaborators (Banks *et al.*, 1979; Blake & Rice, 1981) have noted, under certain conditions, significant (but indeterminate) changes throughout the enzyme on binding 3-PG to crystals of horse-muscle PGK (compared to small local changes that accompanied ADP or ATP binding). However, these workers were unable to identify the mode of binding of 3-PG, although they postulated binding between arginine residues 38 and 168 (170 in horse sequence). These two residues, together with Arg 21 and His 62, 167 and 170 (yeast numbering) form the positively charged face of the N-terminal domain, across the cleft from the nucleotide binding site (Figure 3-1). Three histidines were known to be close to the 3-PG site from prior NMR studies (Tanswell *et al.*, 1976). In contrast to the postulated position for the binding site on the horse enzyme, an experimentally based 3-PG site has been defined for crystalline yeast PGK (Watson *et al.*, 1982; Figure 3-1). This binding involves the phosphate and 2′ hydroxyl moieties of the substrate, the conserved triple glycine sequence, 392-394, Thr 391 and Arg 38.

The binding site for 3-PG defined from the study of the yeast enzyme relates to the face of the substrate in contact with the interdomain region. The residues postulated as being involved in 3-PG binding based on the horse structure study relate to the face of the substrate in contact with the N-domain. Both sites have one end in common, that closest to the cleft, which involves the binding of the C3 end of the substrate to Arg 38.

Substrate binding studies of yeast PGK, using 1-anilino-8-naphthalenesulphonate as a fluorescent probe, have given evidence that

conformational changes occur upon 3-PG binding. (Wiksell & Larsson-Raźnikiewicz, 1982).

Results obtained in a recent NMR study of yeast PGK (Wilson *et al.*, 1988) have indicated that, in solution, the molecule fluctuates between many conformational states, with 3-PG first binding to a site in the 'open' form of the structure and that this helps to stabilise an additional set of conformations in which the 'basic patch' histidines (62, 167 and 170), and hence arginines 38 and 168 are brought into closer proximity to both the added ligand and the nucleotide phosphate site.

In the present study, the earlier studies of 3-PG binding to PGK (Tanswell *et al.*, 1976; Wilson *et al.*, 1988) are repeated and extended using 2D techniques. Spectral changes associated with 3-PG binding are characterised in more detail. The assignments made in Chapter 2 make it possible to discuss 3-PG binding in terms of both the conformational and dynamic states of the enzyme.

3.2. Experimental methods

3.2.1. *3-Phosphoglycerate titrations*

3-PG titrations were carried out by adding 1-4 µl aliquots of 50-60 mM 3-PG directly to the protein samples (prepared as described in § 2.2.5) in the NMR tubes and measuring their 1D spectra (as described in § 2.2.6). The pH of the 3-PG solution was initially adjusted to be the same as the enzyme solution (7.10 ± 0.05). The pH of the protein sample was measured both before and after completion of the titration to ensure that any observed effects in the spectrum were not due to changes in pH.

3.2.2. *Determination of dissociation constants*

The change in chemical shifts of resonances 3 (His 62) and 4 (His 167) versus the volume of 3-PG solution (known concentration) added to a known initial volume of enzyme solution was fitted to equation (3-1) (see Appendix 2

for derivation and symbol definition),

$$\Delta\delta_i = \frac{\Delta\delta_{max}}{2}\left[\left(1 + \frac{K_d.R_i}{[S]_i} + R_i \right) - \left\{\left(1 + \frac{K_d.R_i}{[S]_i} + R_i \right)^2 - 4.R_i \right\}^{1/2}\right] \quad \textbf{(3-1)}$$

where,

$$R_i = \frac{[S]_a.V_i}{[E]_0.V_0} \qquad \text{and} \qquad [S]_i = \frac{[S]_a.V_i}{V_0 + V_i.}$$

This was achieved using a non-linear regression routine on a DEC micro-VaxII (NAG routine E04FDF; NAG Library, 1987) to give K_d, $\Delta\delta_{max}$ and $[E]_0$ (dissociation constant, total change in chemical shift and initial enzyme concentration respectively). The calculated 1:1 binding curve was inspected visually by plotting the molar ratio of 3-PG to PGK (R_i) versus the change in chemical shift ($\Delta\delta_i$) superimposed on the experimental points (using Ghost 80 Graphics; Ghost Manual, 1985). The calculated enzyme concentration ($[E]_0$) was also compared with that determined prior to the titration by absorbance at 278 nm (using an absorption coefficient of $A^{1\%}_{1cm}$ = 4.9 at 278 nm (Krietsch & Bücher, 1970) and a molecular mass of 45 kDa).

3.3. Results

3.3.1. *Effect of 3-phosphoglycerate binding on the 1D ^{1}H NMR spectrum of PGK*

A titration of wild-type PGK with 3-PG was monitored using 500 MHz ^{1}H NMR spectroscopy (Figure 3-2). The observed shifts of 'basic patch' histidine resonances 3, 4 and 5a plotted against the molar ratios of 3-PG to enzyme are shown in Figure 3-3. These three peaks, corresponding to histidine residues 62, 167 and 170 respectively, are all shifted downfield: resonance 3 broadens and shifts 0.72 ppm, resonance 4 also broadens and shifts 0.26 ppm, while resonance 5a is only shifted by 0.04 ppm. The large downfield shifts observed

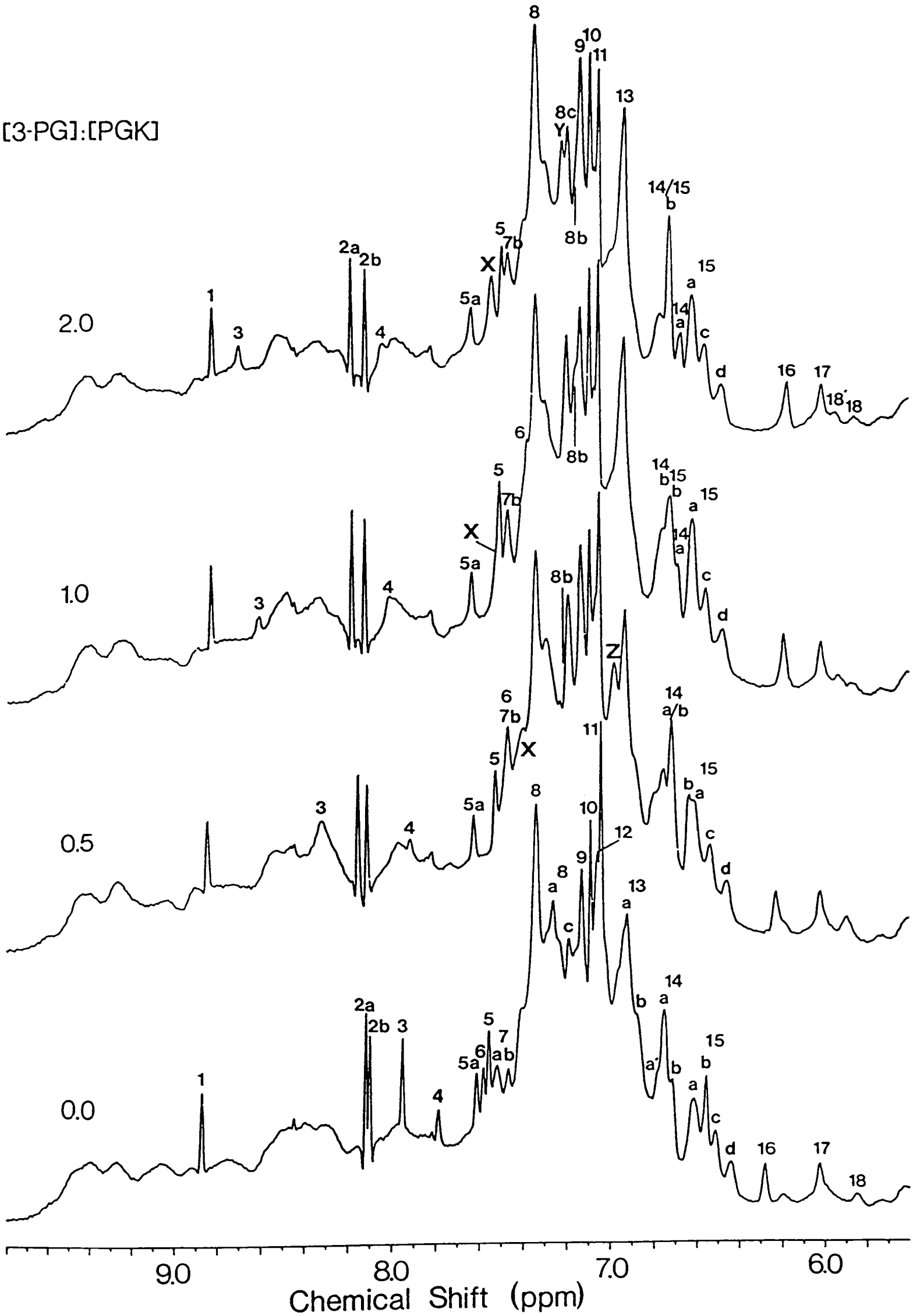

Figure 3-2A: Perturbations of the aromatic region of the 500 MHz ^{1}H NMR spectrum of yeast PGK by 3-PG at the ratios indicated and pH 7.1.

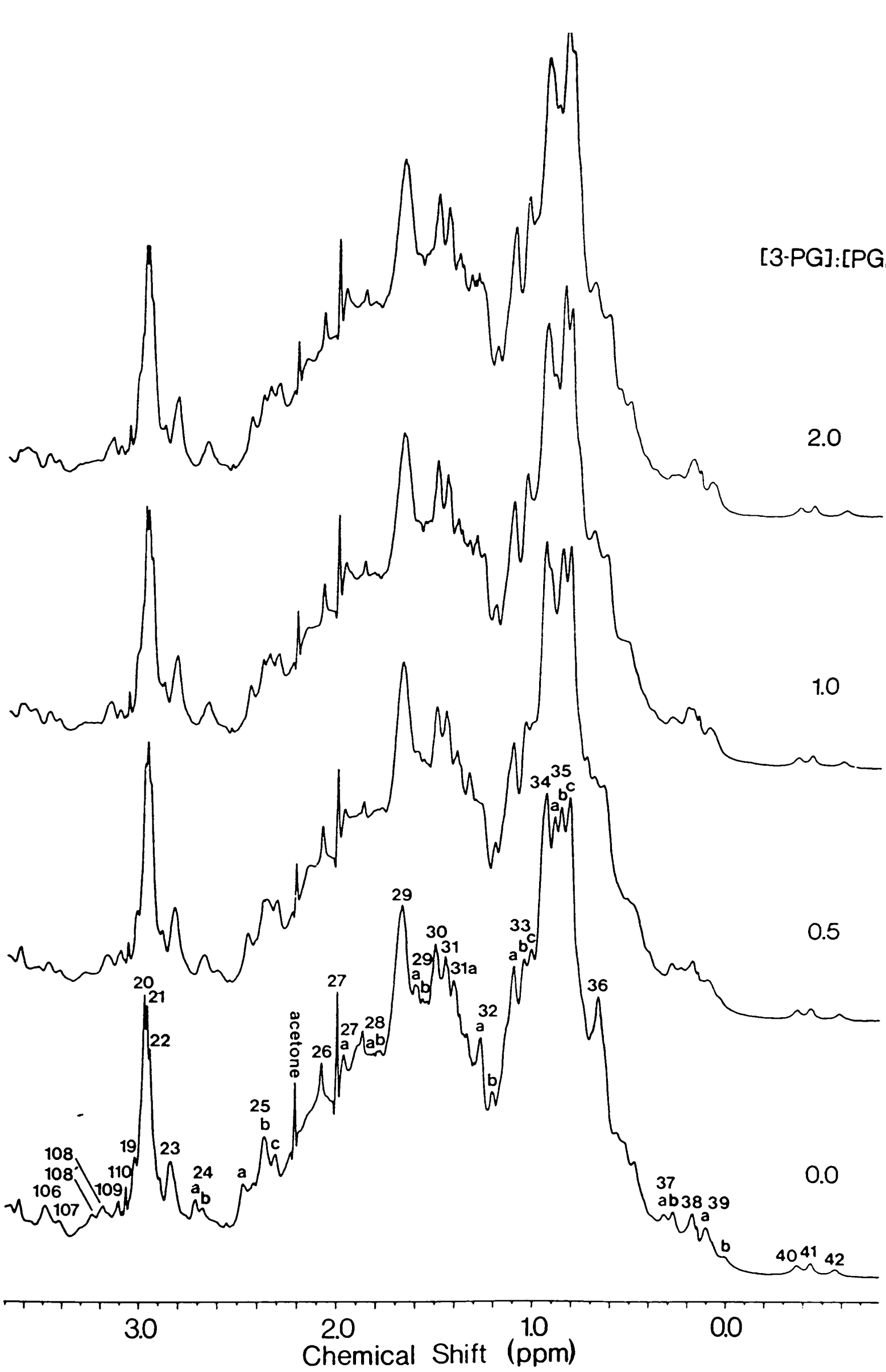

Figure 3-2B: Perturbations of the aliphatic region of the 500 MHz ^{1}H NMR spectrum of yeast PGK by 3-PG at the ratios indicated and pH 7.1.

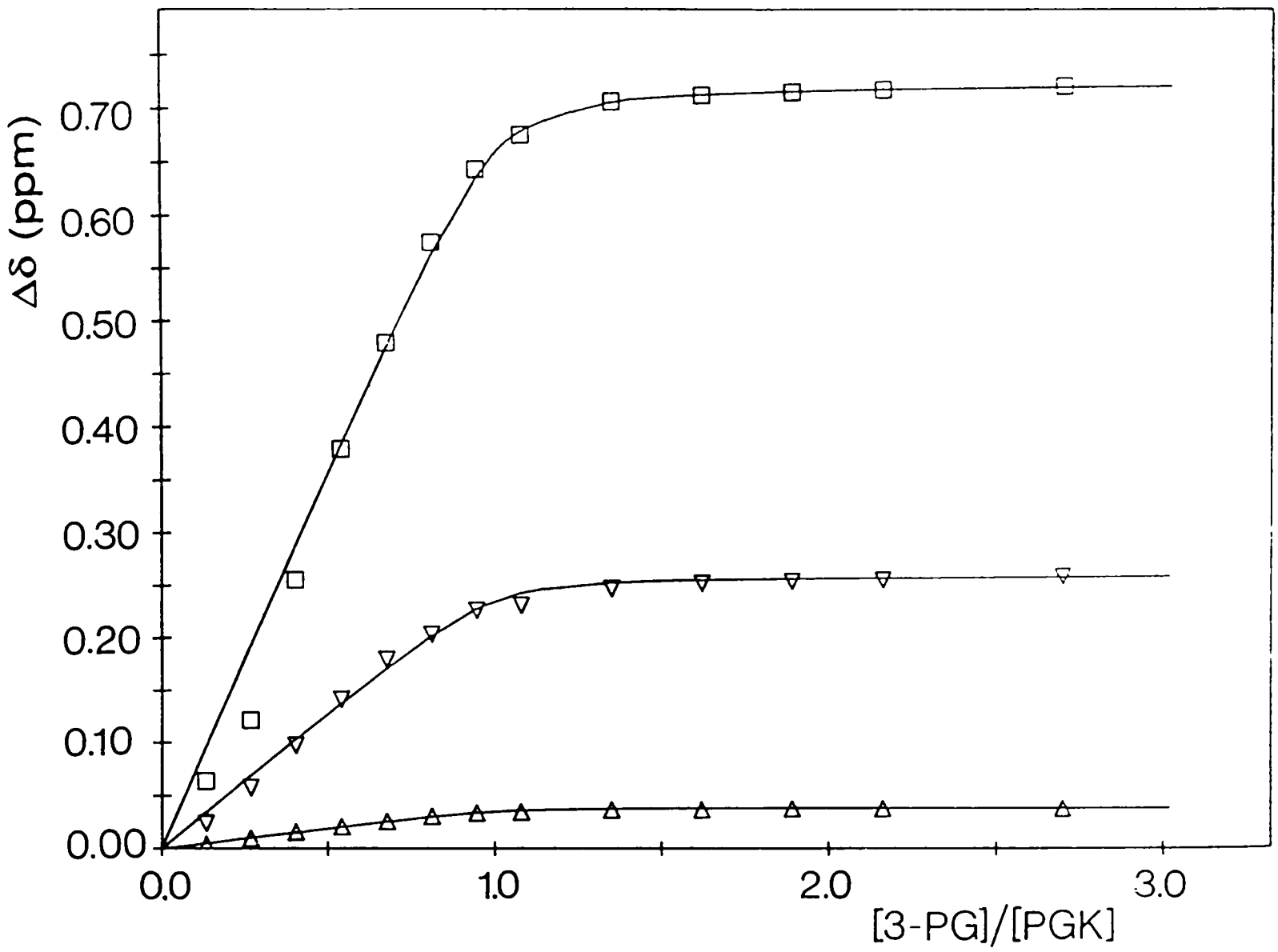

Figure 3-3: The change in the chemical shifts of peaks 3 (□; His 62), 4 (∇; His 167) and 5a (Δ; His 170) plotted as a function of the 3-PG:enzyme molar ratio. The continuous lines represent theoretical binding curves corresponding to a dissociation constant of 0.011 mM (see § 3.3.3).

for resonances 3 and 4 on binding 3-PG to PGK suggests that the pK_a values of His 62 and His 167 have been increased by interaction with the phosphate and/or carboxyl groups of the substrate, leading to their partial protonation (about 75% and 25% respectively if the shifts are due solely to protonation effects; Markley, 1975). This is consistent with shifts observed using model phosphate and amine compounds to analyse phosphate/amine interactions (Wilson & Williams, 1987; Wilson, 1986). A decrease in the pK_a of the triose phosphate on binding to PGK has been demonstrated previously using ^{31}P NMR (Wilson *et al.*, 1988; Ray & Nageswara Rao, 1988), indicating that this group may be involved in a salt bridge with one or more amino acids of the protein. From the relative magnitude of the total shifts (*i.e.* at saturating amounts of 3-PG) of resonances 3, 4 and 5a in the ^{1}H NMR spectrum it can be seen that 3-PG interacts with His 62 > 167 >> 170.

Other aromatic resonances affected by the addition of 3-PG are listed in Table 3-1, and are seen to include a number of the upfield shifted peaks (13-18), some of which have been assigned to aromatic residues in the interdomain region of the protein (Phe 185, Tyr 193, His 388). Some (but not all) of the perturbed peaks were also observed to broaden on addition of Mn^{2+} or Gd^{3+} to the Mg.ATP.Enzyme complex (Tanswell *et al.*, 1976; Wilson *et al.*, 1988; see also Chapter 7).

The use of difference spectroscopy (Figure 3-4) has also enabled the observation of downfield shifts of peaks 8a, 13a′ (original chemical shift 6.90 ppm corresponding to His 170), and peaks labelled X and Y (original chemical shifts ~ 7.33 ppm and ~ 7.03 ppm respectively), within the aromatic envelope. The peak labelled X is shifted to a position downfield of the aromatic envelope (7.54 ppm), while the resonance labelled Y in Figures 3-2A and 3-4 is shifted to a position 0.025 ppm downfield of resonance 8c. Resonances 6 and 8b shift upfield approximately 0.23 ppm and 0.09 ppm, with resonance 8b contributing to the apparent increase in intensity of resonance 9.

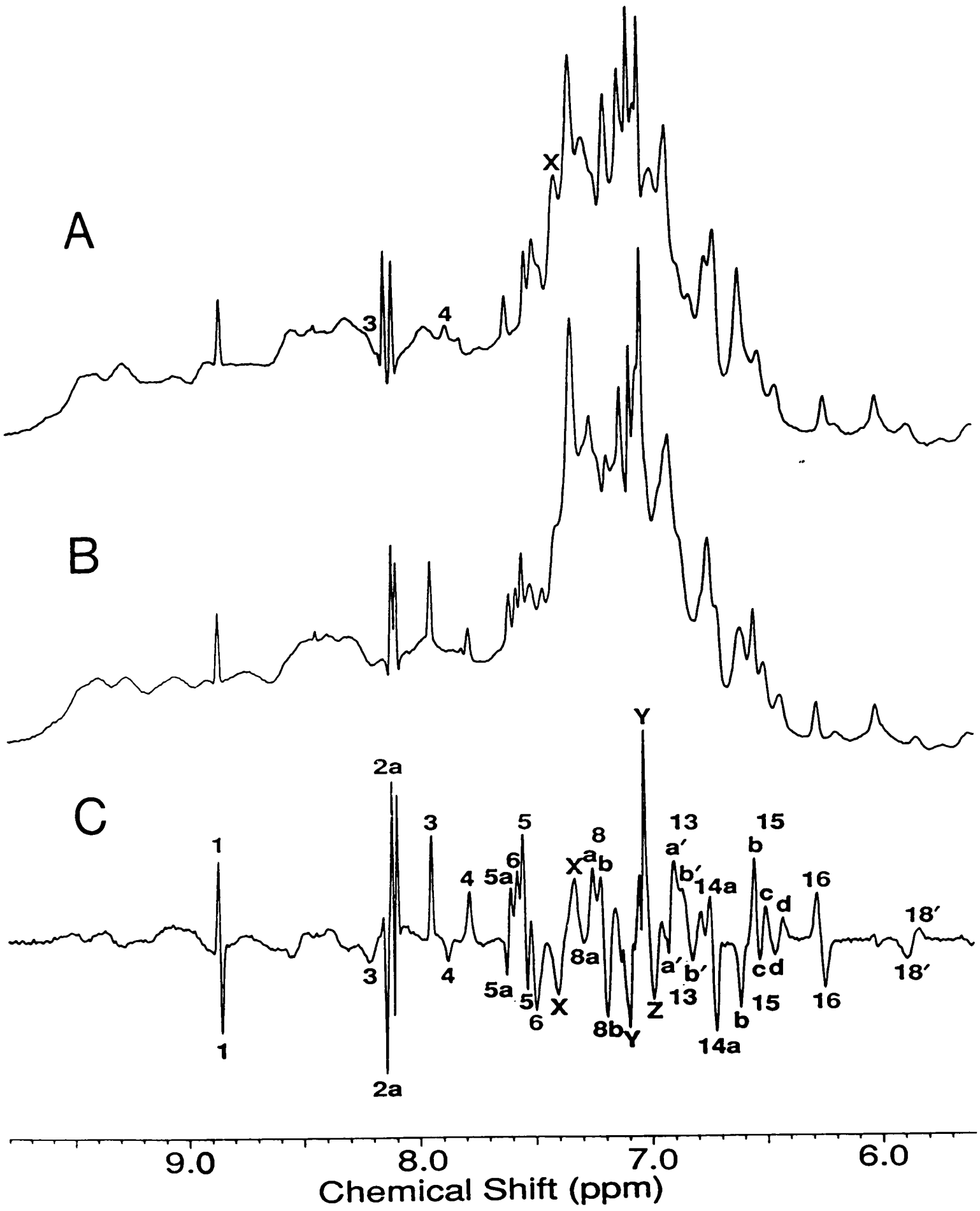

Figure 3-4: Comparison of the aromatic regions of the 500 MHz ^{1}H NMR spectra of yeast PGK at [3-PG]:[PGK] ratios of 0.33:1 (A) and 0:1 (B). (C) represents the difference spectrum (B) - (A).

Table 3-1: Effects of 3-phosphoglycerate binding on resonances of the ^1H NMR spectrum of yeast PGK

Numbers are observed shifts in ppm, negative shifts are upfield. (B) = broadening, (I) = apparent increase in intensity, (Sp) = peak split, (-) = upfield shift of indeterminant magnitude, (+) = downfield shift of indeterminant magnitude, – = no observable effect, ? = possible effect, * = broadened by Mn^{2+} in Mg.ATP.PGK complex.

Aromatic		Aliphatic	
Resonance	Effect	Resonance	Effect
1	-0.05	108′	(B)
2a	+0.06	108	-0.03
2b	+0.01	109	(+)
* 3	+0.72 (B)	23	-0.02
* 4	+0.26 (B)	24a	-0.03
* 5a	+0.04	25a	-0.03
6	-0.23	25b	(Sp)
5	-0.06	29a	(B)
* 7a	(-)	31a	(B)
7b	–	32a	(+)(B)
7c	?	33a	(+)
8	?	33c	(B)
* 8a	+0.04 (B)	35a	(-)
8b	-0.09	35c	?
* 8c	–	36	(+)
9	–	37a	(+)
10	–	37b	(B)(Sp)
11	–	39a	(B)(Sp)
* 12	see text	39b	(+)
* 13a′	(+)	42	-0.05
* 13b′	(-)		
* 14a	-0.08		
14b	?		
* 15a	(I)		
* 15b	+0.16 (B)		
15c	+0.04		
15d	+0.04		
16	-0.10		
17	-0.01		
18′	+0.09		

Another component of peak 12 (~ 7.0 ppm), labelled Z in Figures 3-2A and 3-4, shifts upfield into peak 13. A component of peak 13b (13b′) is observed to shift upfield and becomes confused with the downfield shoulder of peak 14a (14a′). A component of peak 14a itself, is shifted upfield 0.08 ppm. Resonance 16 (Phe 185), which has an NOE connectivity with a component of peak 14a (Tyr 48; § 2.3.2), is also shifted upfield (-0.10 ppm) following addition of 3-PG. In the absence of NOE data it is not possible to determine whether the upfield shifted component of peak 14a is due to Tyr 48 or Tyr 193 (but see § 3.3.2).

Also shifted are resonances 1 and 2a which have been assigned to histidines 123 and 149 respectively, and peak 5 which has been assigned to His 52. Both His 123 and His 149 are remote from the crystallographically defined triose binding site (Watson *et al.*, 1982; Figure 3-1), but are in the vicinity of Cys 97 (the thiol group whose reactivity is affected by anion binding; Wrobel & Stinson, 1978). His 52 is also remote from the 3-PG binding site, being part of the loop connecting α-helix I and β-strand B (Watson *et al.*, 1982; Figure 3-1). These two elements of secondary structure are associated with the 'basic patch' region via Arg 38 and His 62 respectively.

Several of the broad, overlapping resonances due to non-exchanging amide protons are also affected by triose addition (Figure 3-2A). The most significant effect is the loss of NH3 (9.05 ppm). Any loss or broadening of these NH resonances is likely to be due to proton exchange resulting from a conformational change in the protein. In the absence of substrate, peak NH3 persists in D_2O solution for six weeks at 4 °C.

A number of effects are also observed in the aliphatic region of the spectrum (Figure 3-2B, Table 3-1). Resonance 108′ is broadened, while 108 moves upfield by ~ 0.03 ppm. Peak 23 shifts downfield by ~ 0.02 ppm, while resonances 24a and 25a both move upfield by ~ 0.03 ppm. Peak 25b splits into at least three components. Broadening is also observed at resonances 29a, 31a

(downfield component), 32a and 33c. Peaks 33a is shifted downfield, while peak 35a is shifted upfield. Further effects, due to conformational changes, in the upfield methyl region include downfield shifts of peaks 36, 37a and 39b, splitting of peaks 37b and 39a and upfield movement (-0.05 ppm) of resonance 42. Peaks 38, 40 and 41 are unaffected by addition of 3-PG. Although the above effects involve unassigned resonances they are generally indicative of minor rearrangement of aliphatic groups with respect to aromatic groups of the protein on binding 3-PG and can be used in comparative work with site-specific mutant PGKs (see Chapter 4).

3.3.2. *Effect of 3-phosphoglycerate binding on the 2D ^{1}H NMR spectrum of PGK*

From the above analysis of the effect of 3-PG binding on the 1D ^{1}H NMR spectrum of PGK it can be seen that binding is associated with a well defined conformational change which is characterised by the various shifts and broadenings observed in the spectrum. In order to establish more clearly which aromatic resonances are being perturbed, and specifically which regions of the protein are being affected by triose substrate binding, a 2D NOESY spectrum of the 3-PG.PGK complex was obtained and compared with that obtained for the free enzyme (Figure 3-5).

On addition of 3-PG both the C2,6-H and C3,5-H resonances of Phe 185 shift upfield (by ~ 0.09 ppm and 0.08 ppm respectively), together with the C4-H resonance (peak 16) as observed in the 1D spectrum. The C2,6-H and C3,5-H resonances of Phe 185 therefore appear to correspond to peaks 8b and Z, respectively, which were observed to shift upfield in the 1D spectrum (§ 3.3.1). NOE connectivities observed between peak 16 and a component of peak 14a, corresponding to Tyr 48, in the NOESY spectrum of the free protein are also observed in the NOESY spectrum of the 3-PG.PGK complex. An additional weak NOE cross-peak is observed from the upfield resonance of

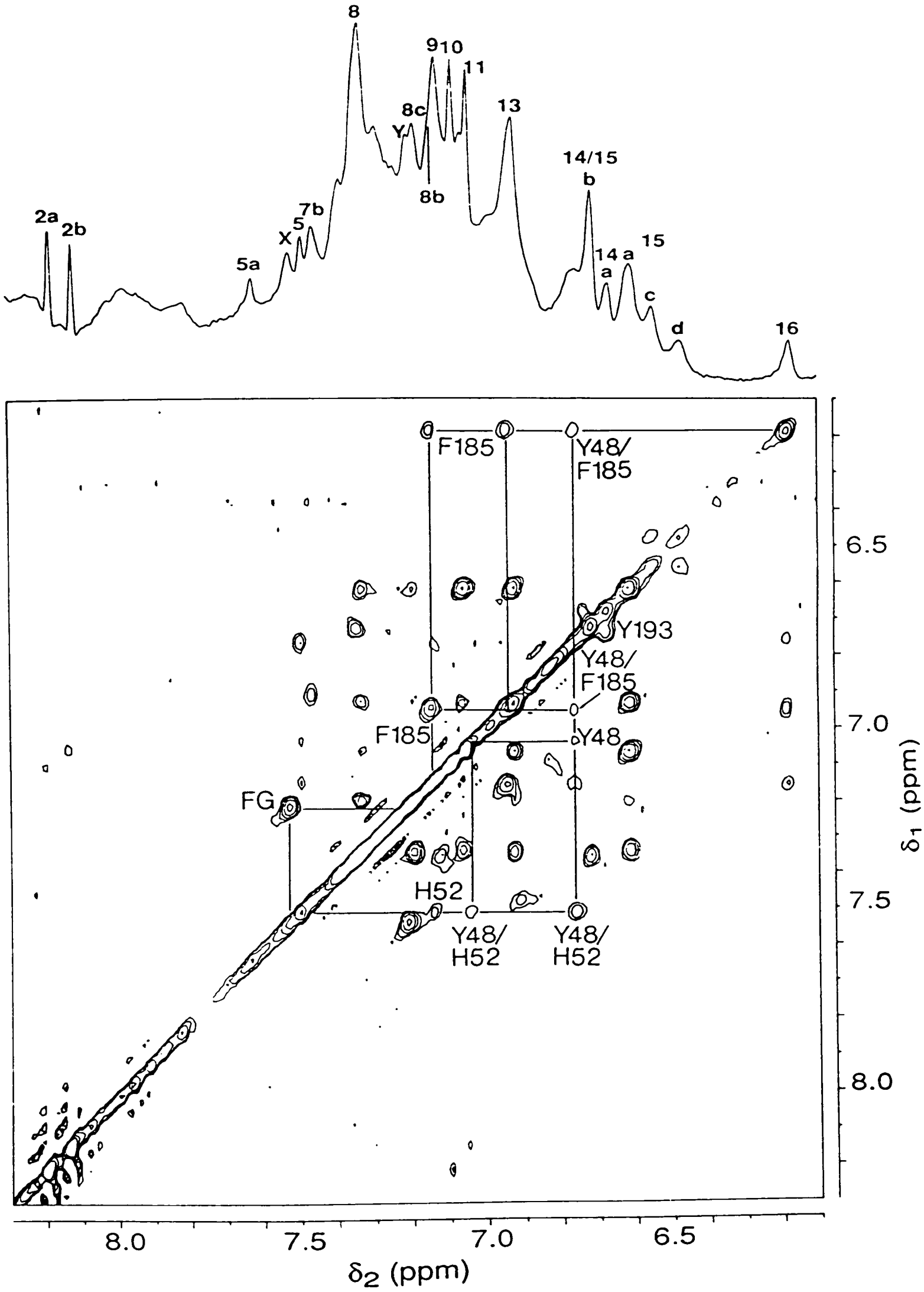

Figure 3-5A: The aromatic region of the 600 MHz NOESY spectrum of 3-PG.PGK. [3-PG]/[PGK] = 1.5.

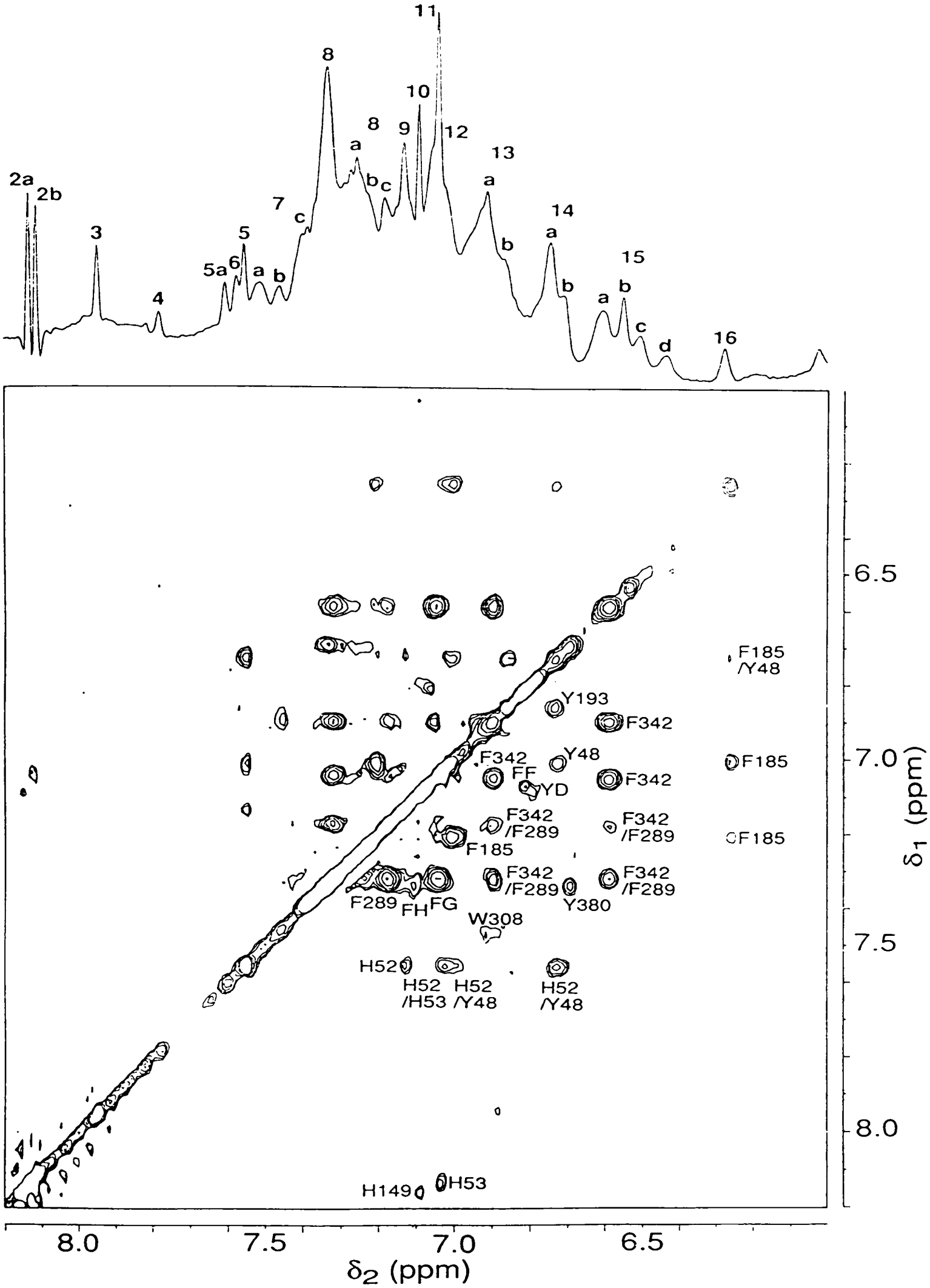

Figure 3-5B: The aromatic region of the 500 MHz NOESY spectrum of free PGK for comparison with Figure 3-5A.

Tyr 48 (6.75 ppm) to the C3,5-H resonance of Phe 185, which was not seen in the NOESY spectrum of the free protein, while the NOE observed between the downfield resonance of Tyr 48 and peak 16 in the spectrum of the free protein is absent from the NOESY spectrum of the substrate.enzyme complex. Inter-residue NOE cross-peaks between His 52 (peak 5) and both resonances of Tyr 48 in the spectrum of free PGK remain on addition of 3-PG, although peak 5 has shifted upfield by ~ 0.06 ppm. The NOE cross-peak observed between peak 5 (His 52) and peak 11 (His 53) in the spectrum of substrate free PGK is, however, absent. These changes in chemical shift and dipolar couplings can be interpreted as being due to a change in the mutual orientations of Phe 185, Tyr 48, His 52 and His 53 as a result of 3-PG binding at (or near to) the 'basic patch' of the N-terminal domain, more than 20 Å away on the opposite side of the protein.

The NOESY spectrum of the 3-PG.PGK complex also shows that the upfield shifts of components of peaks 14a and 13b (13b′), observed in the 1D spectrum (Table 3-1), are in fact due to a change in the environment of Tyr 193. The weak NOE observed between His 388 and Tyr 193 in the spectrum of the free protein (§ 2.3.2) is absent from the NOESY spectrum in the presence of the triose substrate. This, together with the considerable upfield shift observed for peak 6 (His 388) in the 1D spectrum (Table 3-1), suggests that a mutual reorientation of Tyr 193 and His 388 also occurs as a result of 3-PG binding. Tyr 193 and His 388 are situated in the interdomain region of the protein (Figure 3-1).

Another significant difference between the NOESY spectrum of the enzyme in the presence and absence of 3-PG is the appearance of a strong cross-peak at 7.52, 7.20 ppm on addition of the substrate. These resonances correspond to the peaks labelled X and Y, respectively, in the 1D spectrum. These peaks were observed to shift downfield from ~ 7.03 ppm and ~ 7.33 ppm, using difference spectroscopy (Figure 3-4). A cross-peak at this position was

identified in Chapter 2 (§ 2.3.2) as belonging to a Phe side-chain (Phe G; Table 2-2). Evidence is presented in Chapter 5 which suggests that Phe G may be assigned to Phe 163 (§ 5.3.3). Again, these chemical shift changes are indicative of a conformational change as a result of 3-PG binding.

It is also noted that inter- and intra-residue cross-peaks assigned in Chapter 2 (§ 2.3.2) to residues within the C-terminal domain (Phe 289, Trp 308, Phe 342 and Tyr 380) are virtually unaffected by 3-PG binding.

3.3.3. *Dissociation constant for 3-phosphoglycerate binding*

The dissociation constant for 3-PG binding to yeast PGK was determined by following the chemical shifts of resonances 3 (His 62) and 4 (His 167) as a function of 3-PG concentration (see § 3.2.2). The data (Figure 3-3) were analysed assuming 1:1 binding, with the experimental shift values being fitted to theoretical binding curves as discussed in § 3.2.2. The dissociation constant was calculated to be 0.011 ± 0.005 mM (I = 0.10 M, pH = 7.1, T = 300 K), from two titrations of over-expressed wild-type enzyme. A value of 0.036 ± 0.006 mM was obtained using enzyme purchased from Boehringer Mannheim GmbH. Both of these values compare well with previously reported dissociation constants (Wrobel & Stinson, 1978; Scopes, 1978) confirming the validity of the method.

3.4. Discussion

Earlier 3-PG binding studies using wild-type PGK (Tanswell *et al.*, 1976; Wilson *et al.*, 1988) have been repeated and analysed in greater detail. With the firm assignments to the 'basic patch' histidine residues (§ 2.3.6) it is now possible to say that 3-PG interacts with His 62 > His 167 >> His 170. It might, therefore, be expected that His 170 has little influence on 3-PG binding. This is in agreement both with its position relative to the bound sugar substrate, as observed crystallographically (Watson *et al.*, 1982; Figure 3-1), and with the fact that His 170 is a non-conserved residue (Osinga *et al.*,

1985; Swinkels *et al.*, 1988). The large downfield shift of resonance 3 (Table 3-1) suggests that, for part of the time at least, the phosphate of 3-PG is hydrogen-bonded to His 62. The smaller downfield shift observed for His 167 (peaks 4 and 15b; Table 3-1) could also be due to hydrogen-bond formation, although it is not large enough to rule out a possibly significant contribution due to conformational changes. Simultaneous interaction of the phosphate of 3-PG with His 62 and the carboxyl group with His 167 would seem possible, however, as judged from the X-ray structure, provided a minor conformational change in the 'basic patch' region takes place on going from solution to the crystalline state (Walker *et al.*, 1989; Watson & Gamblin, 1985). Further evidence for formation of cross-linking hydrogen-bonds between the phosphate and carboxyl oxygens of the triose substrate and the imidazole groups of His 62 and His 167 comes from the concomitant increase in the linewidths of resonances 3 and 4 on binding 3-PG to PGK, suggesting that the motion of these histidine side-chains becomes restricted.

A number of small substrate induced conformational effects, both close to and remote from the 3-PG binding site, were also observed. These effects saturate at the same ratio of [3-PG]:[PGK] as the shifts of the 'basic patch' histidines discussed above (Figure 3-3), indicating that they are the result of 3-PG binding to a single site on the molecule (*i.e.* the active site). The effects extend to considerable parts of the N-terminal domain, as indicated by perturbations that occur at remote histidines 52, 123 and 149. Resonances of Phe 185, Tyr 193 and His 388, associated with the 'hinge' region of the molecule (Watson *et al.*, 1982; Figure 3-1), are also affected. The observed shifts have been interpreted as being due to changes in the mutual orientations of Tyr 193 and His 388, and of Phe 185 and Tyr 48, as a result of 3-PG binding. The upfield shift observed for resonance 5 can similarly be attributed to reorientation of His 52 with respect to Tyr 48.

Tyr 48 is situated in the C-terminal half of α-helix 1 (residues 37-51),

which is associated with the crystallographically determined 3-PG binding site via Arg 38 (Watson *et al.*, 1982; Walker *et al.*, 1989; see Figure 3-1). It is therefore possible that the above conformational effect involves movement of α-helix I with respect to the interdomain α-helix V (residues 185-199). It is noted that α-helix I contains a totally conserved (see Appendix 1) proline residue at position 44 which may allow the helix to 'bend'. Another possible mechanism for the communication of triose induced conformational changes is mutual reorientation of the two interdomain helices V and XIII (residues 393-401). In this model (similar to that proposed by Blake *et al.*, 1986) the interaction of 3-PG with the amino end of helix XIII (Watson *et al.*, 1982) would result in a relative reorientation of the two helices and therefore change the relative orientations of Phe 185 (at the N-terminal end of helix V) and Tyr 48, and of Tyr 193 (near the middle of helix V) and His 388. It is most probable that 3-PG binding induces movement of all three helices (I, V and XIII) since the three are interacting.

The 3-PG induced changes in the conformation of the interdomain region do not appear to be transmitted, to any significant extent, to the C-terminal domain (as judged by the invariance of the chemical shifts of resonances due to Phe 289, Trp 308, Phe 342 and Tyr 380).

From the NMR results presented in this chapter it is not possible to say whether the changes in protein conformation which are observed on formation of the 3-PG.PGK binary complex lead to a catalytically competent active site. However, experiments using a non-reactive, isopolar and isosteric nucleotide analogue, adenosine 5′-(β,γ-difluoromethylene)triphosphate (APP(CF_2)P; Blackburn *et al.*, 1984; supplied by Dr G.M. Blackburn, Department of Chemistry, University of Sheffield) and the triose substrate show that similar effects occur on formation of the ternary complex. The effects of nucleotide binding at the catalytic, hydrophobic site are increased as 3-PG binds to the 'basic patch' region. As will be discussed in Chapter 6, this result indicates

that 3-PG displaces the nucleotide from the 'basic patch'.

The dissociation constant for the binary substrate.enzyme complex, determined by following the chemical shifts of His 62 and His 167 as a function of the [3-PG]:[PGK] ratio, was found to be in good agreement with K_d determinations by other methods (Wrobel & Stinson, 1978; Scopes, 1978). This is therefore a good method for comparison of the 3-PG binding properties of site-specific mutant forms of the protein with the wild-type (see Chapter 4).

3.5. References

Adams, S.R., Sparkes, M.J. & Dixon, H.B.F. (1983) *Biochem. J. 213,* 211-215.

Banks, R.D., Blake, C.C.F., Evans, P.R., Haser, R., Rice, D.W., Hardy, G.W., Merrett, M. & Phillips, A.W. (1979) *Nature (Lond.) 279,* 773-777.

Blackburn, G.M., Kent, D.E. & Kolkmann, F. (1984) *J. Chem. Soc. Perkin Trans. I,* 1119-1125.

Blake, C.C.F. & Rice, D.W. (1981) *Phil. Trans. R. Soc. Lond. A. 293,* 93-104.

Blake, C.C.F., Rice, D.W. & Cohen, F.E. (1986) *Int. J. Pep. Protein Res. 27,* 443-448.

Ghost Manual (1985) *The GHOST 80 Users Manual,* 2nd edn, UKAEA.

Khamis, M.M. & Larsson-Raźnikiewicz, M. (1981) *Biochim. Biophys. Acta 657,* 190-194.

Krietsch, W.K.G. & Bücher,T. (1970) *Eur. J. Biochem. 17,* 568-580.

Larsson-Raźnikiewicz, M. & Jansson, J.R. (1973) *FEBS Lett. 29,* 345-347.

Larsson-Raźnikiewicz, M. & Schierbeck, B. (1977) *Biochem. Soc. Trans. 5,* 770-771.

Lesk, A.K. & Hardman, K.D. (1982) *Science 216,* 539-540.

Markley, J. (1975) *Acc. Chem. Res. 8,* 70-80.

Mas, M.T. & Resplandor, Z.E. (1988) *Proteins 4,* 56-62.

NAG Library (1987) *The NAG Fortran Library Manual-Mark 12,* Numerical Algorithms Group.

Orr, G.A. & Knowles, J.R. (1974) *Biochem. J. 141,* 721-723.

Osinga, K.A., Swinkels, B.W., Gibson, W.C., Borst, P., Veeneman, G.H., van Boom, J.H., Michels, P.A.M. & Opperdoes, F.R. (1985) *EMBO J. 4,* 3811-3817.

Pickover, C.A., McKay, D.B., Engelman, D.M. & Steitz, T.A. (1979) *J. Biol. Chem. 254,* 11323-11329.

Ptitsyn, O.B., Pavlov, M.Y., Sinev, M.A. & Timchenko, A.A. (1986) in *Multidomain Proteins,* (Patthy, L. & Friedrich, P. eds) pp. 9-25, Akadémiai Kiadó, Budapest.

Ray, B.D. & Nageswara Rao, B.D. (1988) *Biochem. 27,* 5574-5578.

Roustan, C., Fattoum, A., Jeanneau, R. & Pradel, L.-A. (1980) *Biochem. 19,* 5168-5175.

Schierbeck, B. & Larsson-Raźnikiewicz, M. (1979) *Biochim. Biophys. Acta, 568,* 195-204.

Scopes, R.K. (1978a) *Eur. J. Biochem. 85,* 503-516.

Scopes, R.K. (1978b) *Eur. J. Biochem. 91,* 119-129.

Sinev, M.A., Razgulyaev, O.I., Vas, M., Timchenko, A.A. & Ptitsyn, O.B. (1989) *Eur. J. Biochem. 180,* 61-66.

Swinkels, B.W., Evers, R. & Borst, P. (1988) *EMBO J. 7,* 1159-1165.

Tanswell, P., Westhead, E.W. & Williams, R.J.P. (1976) *Eur. J. Biochem. 63,* 249-262.

Tompa, P., Hong, P.T. & Vas, M. (1986) *Eur. J. Biochem. 154,* 643-649.

Walker, P.A., Littlechild, J.A., Hall, L. & Watson, H.C. (1989) *Eur. J. Biochem.*, in press.

Watson, H.C. & Gamblin, S.J. (1985) *Proc. Int. Symp. Biomol. Struct. Interactions, Suppl. J. Biosci. 8,* 499-506.

Watson, H.C., Walker, N.P.C., Shaw, P.J., Bryant, T.N., Wendell, P.L., Fothergill, L.A., Perkins, R.E., Conroy, S.C., Dobson, M.J., Tuite, M.F., Kingsman, A.J. & Kingsman, S.M. (1982) *EMBO J. 1,* 1635-1640.

Wiksell, E. & Larsson-Raźikiewicz, M. (1982) *J. Biol. Chem. 257,* 12672-12677.

Wilson, H.R. (1986) D.Phil. Thesis, University of Oxford.

Wilson, H.R. & Williams, R.J.P. (1987) *J. Chem. Soc., Faraday Trans. 1 83,* 1885-1892.

Wilson, H.R., Williams, R.J.P., Littlechild, J.A. & Watson, H.C. (1988) *Eur. J. Biochem. 170,* 529-538.

Wrobel, J.A. & Stinson, R.A. (1978) *Eur. J. Biochem. 85,* 345-350.

Chapter 4

NMR ANALYSIS OF 3-PHOSPHOGLYCERATE BINDING TO SITE-SPECIFIC MUTANTS OF YEAST PGK

4.1. Introduction

In the preceding chapter it was established that the triose substrate, 3-PG, interacts directly with the 'basic patch' region of PGK and forms a hydrogen-bond, for part of the time at least, with His 62. The presence of a hydrogen-bond between the carboxyl group of 3-PG and His 167 was also postulated. Binding of 3-PG was observed to cause specific conformational changes which were characterised by various chemical shift changes and broadening effects in the ^{1}H NMR spectrum.

Crystallographic studies of horse-muscle PGK have led to the suggestion that Arg 38 and Arg 168 are directly involved in binding 3-PG (Banks *et al.*, 1979; Blake & Rice, 1981). In yeast PGK the only 'basic patch' residue identified as forming a hydrogen-bond in the crystallographically determined 3-PG binding site is Arg 38 (Watson *et al.*, 1982). A possible transition-state stabilisation role has been proposed for Arg 168 of the yeast enzyme (Watson & Gamblin, 1985). Chemical modification studies suggest that two essential arginyl residues situated at or near the 3-PG site are important for binding of this substrate (Philips *et al.*, 1978).

In order to investigate the role of the 'basic patch' residues in both substrate binding and catalysis a program of site-specific mutagenesis has been initiated in the laboratories of Drs L. Hall and H.C. Watson (Department of Biochemistry, University of Bristol). 'Basic patch' mutants prepared and analysed thus far include changes at His 62, Arg 168 and His 170. His 62, which is conserved in all known PGK sequences (see Appendix 1), has been changed to a glutamine residue (H62Q). Arg 168, which is also totally

conserved (Appendix 1), has been replaced with a lysine (R168K) and a methionine residue (R168M) (Walker *et al.*, 1989). In mutant R168K the length of the side-chain has been shortened, resulting in about a 1 Å displacement of the positive charge, whereas in the Arg 168 to methionine mutant the side-chain has been shortened by about 2 Å and the charge eliminated. In other site-directed mutagenesis experiments residue 170, which in the crystal structure is in close proximity to Arg 168 (Figure 4-1), has been changed from histidine to aspartate (H170D) thus introducing a negatively charged group into the 'basic patch' region.

In this chapter NMR is used to examine the structural integrity of these single-site mutant forms of yeast PGK. Techniques described in Chapter 3 are used to examine the effect that these mutations have on the binding of 3-PG to the enzyme. The results are discussed in terms of both the conformation and the catalytic properties of the modified and native enzymes.

4.2. Experimental methods

4.2.1. *Site-specific mutants*

Mutant yeast PGK enzymes were supplied by Drs L. Hall and H.C. Watson (Department of Biochemistry, University of Bristol).

Oligonucleotide-directed site-specific mutagenesis was based on the double-priming procedure of Zoller & Smith (1982), modified as in Minard *et al.* (1989). Preparation, extraction and purification of the over-expressed mutant proteins was carried out essentially as described for (d_5-Phe)PGK in Chapter 2 (Minard *et al.*, 1989; Walker *et al.*, 1989). Remaining traces of nucleic acids (indicated by a $A_{280\ nm}/A_{260\ nm}$ ratio < 1.5) were removed by passage over a Mono Q FPLC column run in MES buffer, pH 6.5 (Walker *et al.*, 1989).

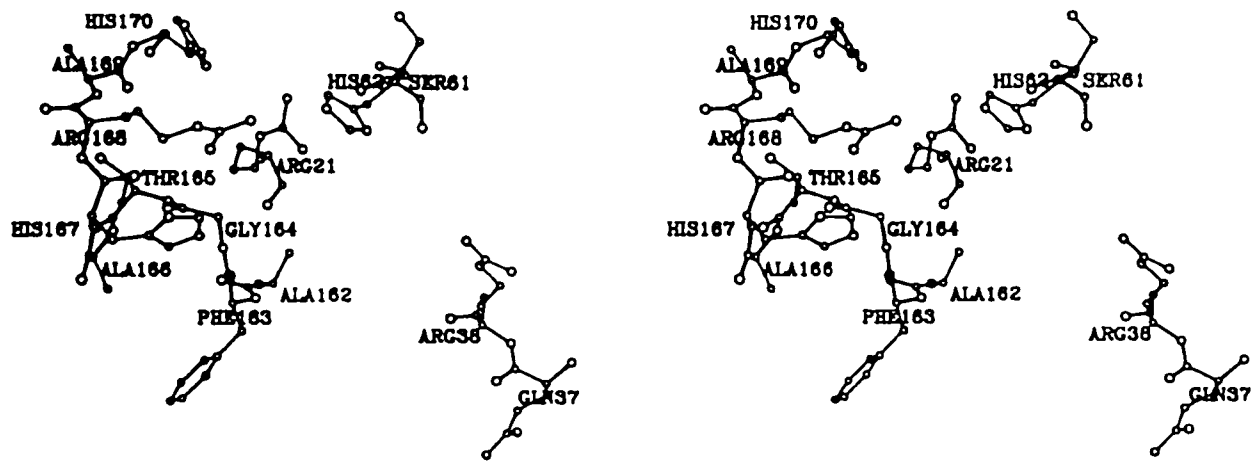

Figure 4-1: A stereo drawing of the 'basic patch' region of the N-terminal domain of yeast PGK. The coordinates used are those of Watson *et al.* (1982), available from the Brookhaven Protein Data Bank.

4.3. Results

4.3.1. *^{1}H NMR spectra of mutant PGKs*

In order to investigate the role of particular 'basic patch' amino acids (Figure 4-1) in both substrate binding and catalysis, a number of site-specific mutant forms of yeast PGK have been produced. These include mutants in which His 62 and His 170 have been changed to glutamine (H62Q) and aspartate (H170D) respectively. These mutants were used to specifically assign the 'basic patch' histidine resonances in Chapter 2. Other mutants investigated include replacement of the totally conserved arginine residue 168 with either lysine (R168K) or methionine (R168M) (Walker *et al.*, 1989). The 1D ^{1}H NMR spectrum of yeast PGK, described in § 2.3.1, provides a 'fingerprint' for the folding of the molecule in solution. Comparison of the spectra obtained from the mutant enzymes with that of the wild-type PGK allows their conformational state, in solution, to be assessed. Spectral comparisons for each mutant are outlined below.

4.3.1.1. Spectrum of H62Q

This mutant protein has His 62 replaced by a glutamine residue. The aromatic region of the spectrum of H62Q is compared with that of wild-type PGK in Figure 4-2A and differences are summarised in Table 4-1. As discussed in Chapter 2, effects in the aromatic region of the ^{1}H NMR spectrum include the disappearance of resonance 3, due to the loss of His 62, and shifts of resonances assigned to 'basic patch' histidines 167 (peaks 4 and 15b) and 170 (peaks 5a and 13a). A small shift of resonance 6, assigned to the interdomain His 388, is also observed. There are no obvious differences between the NH regions of the spectra of H62Q and the wild-type enzymes.

In the aliphatic region of the spectrum of H62Q (Figure 4-2B, Table 4-2) there are no effects which can be directly attributed to the introduced glutamine residue or to the loss of the substituted histidine. In the methyl

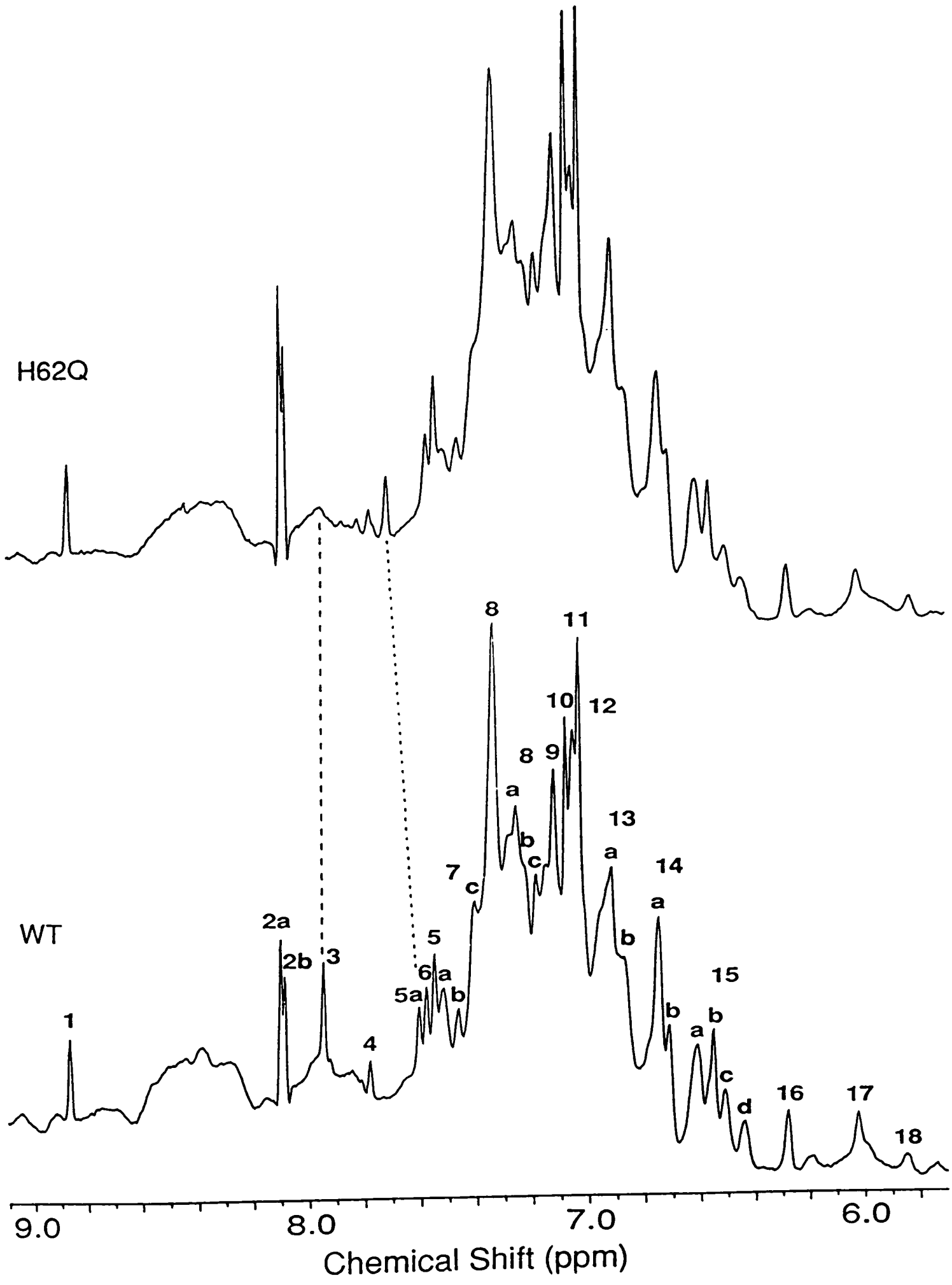

Figure 4-2A: Comparison of the aromatic regions of the 600 MHz ^{1}H NMR spectra of wild-type yeast PGK (lower) and site-specific mutant H62Q (upper).

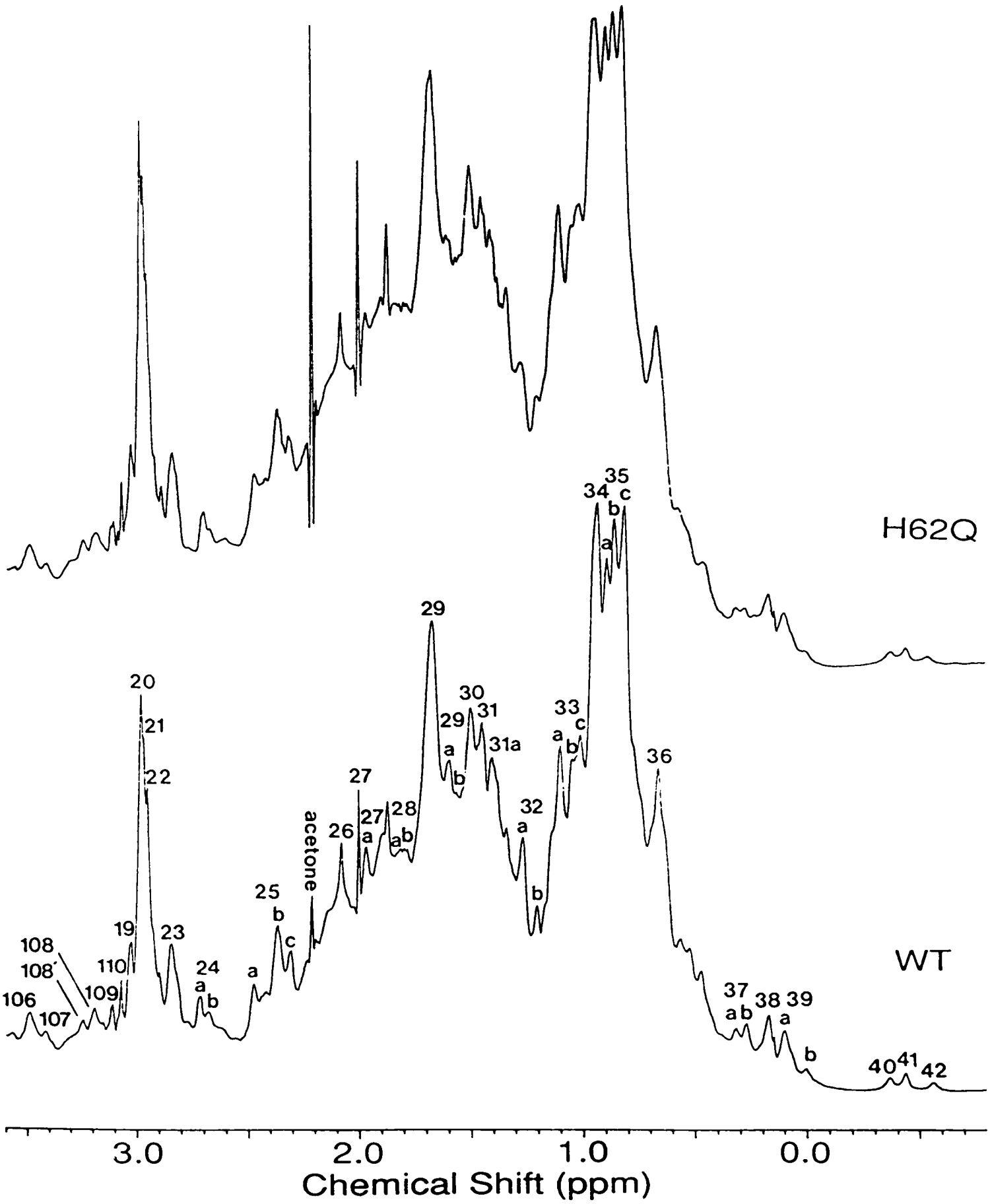

Figure 4-2B: Comparison of the aliphatic regions of the 600 MHz ^{1}H NMR spectra of wild-type yeast PGK (lower) and site-specific mutant H62Q (upper).

Table 4-1: Differences between the aromatic regions of the spectra of mutant and wild-type PGKs

pH = 7.1, 0.10 M Na d_3-acetate/D_2O, T = 300 K

Numbers represent chemical shift differences (δ_{Mutant} - δ_{WT})

– = no observable effect

(I) = apparent increase in intensity

Resonance	Wild-type chemical shift (ppm)	Effect of mutation			
		H62Q	H170D	R168K	R168M
3	7.94	absent	-0.10	–	–
4	7.77	-0.01	+0.04	+0.09	+0.09
5a	7.60	+0.11	absent	+0.02	+0.07
6	7.58	-0.01	–	-0.01	-0.01
7c	7.40	–	–	+0.01	+0.01
8a	7.33	–	+0.02	–	–
13a	6.92	-0.01	?	?	?
14a	6.74	–	–	(I)	(I)
14b	6.70	–	(I)	–	–
15b	6.54	+0.01	+0.16	+0.20	+0.20
15c	6.50	–	–	+0.01	+0.01
17	6.03	–	+0.01	+0.01	+0.02

Table 4-2: Differences between the aliphatic regions of the spectra of mutant and wild-type PGKs

pH = 7.1, 0.10 M Na d_3-acetate/D_2O, T = 300K

Numbers represent chemical shift differences (δ_{Mutant} - δ_{WT})

– = no observable effect

(B) = apparent broadening

Resonance	Wild-type chemical shift (ppm)	Effect of mutation			
		H62Q	H170D	R168K	R168M
32a	1.28	+0.06	(B)	(B)	–
32b	1.21	(B)	(B)	–	–
33c	1.02	–	–	+0.005	+0.01
35a	0.90	–	(B)	(B)	(B)
36[a]	0.67	–	+0.03	+0.10	+0.09
37a	0.32	–	-0.01	+0.05	?
37b	0.28	-0.04	-0.02	–	–
42	-0.56	+0.03	–	–	–

[a] major component

region a component of peak 32a (~ 1.28 ppm) appears to have shifted downfield (+ 0.06 ppm). Peak 37b has also been perturbed with a component being shifted upfield to give a 'new' resonance at 0.24 ppm (between peaks 37b and 38). Peak 42 has shifted downfield ~ 0.03 ppm.

4.3.1.2. Spectrum of H170D

In this mutant, His 170 has been replaced by a negatively charged aspartic acid residue. This substitution allowed the assignment of resonance 5a to His 170 (§ 2.3.6) and was also found to perturb the resonances of the nearby 'basic patch' histidines 62 (peak 3) and 167 (peaks 4 and 15b) (Figure 4-3A, Table 4-1). As with H62Q, substitution of His 170 had no detectable effect on the NH region of the spectrum.

In the aliphatic region of the spectrum of H170D (Figure 4-3B, Table 4-2) there are no effects which are directly attributable to the introduced aspartic acid residue or to the loss of the substituted histidine. Of the upfield shifted methyl peaks only 37a and 37b are perturbed, being shifted further upfield by 0.01 ppm and 0.02 ppm respectively. The remainder of the upfield shifted methyl resonances (38-42) are unaffected by the mutation.

4.3.1.3. Spectrum of R168K

This mutation involves substitution of a positively charged residue, Arg 168, with one of similar size and character, a lysine. Peak 4 (His 167), in the aromatic region of the spectrum of R168K, has shifted downfield by 0.09 ppm while peak 5a (His 170) has moved 0.02 ppm downfield, relative to the spectrum of the wild-type enzyme (Figure 4-4A, Table 4-1). The position of resonance 3 has remained unchanged from that in the wild-type spectrum. The apparent increase in intensity of peak 14a, relative to wild-type (see Table 4-1), arises from a downfield shift of peak 15b (His 167). There are no clear differences between the NH regions of the spectrum of R168M and that of the wild-type protein (Figure 4-4A).

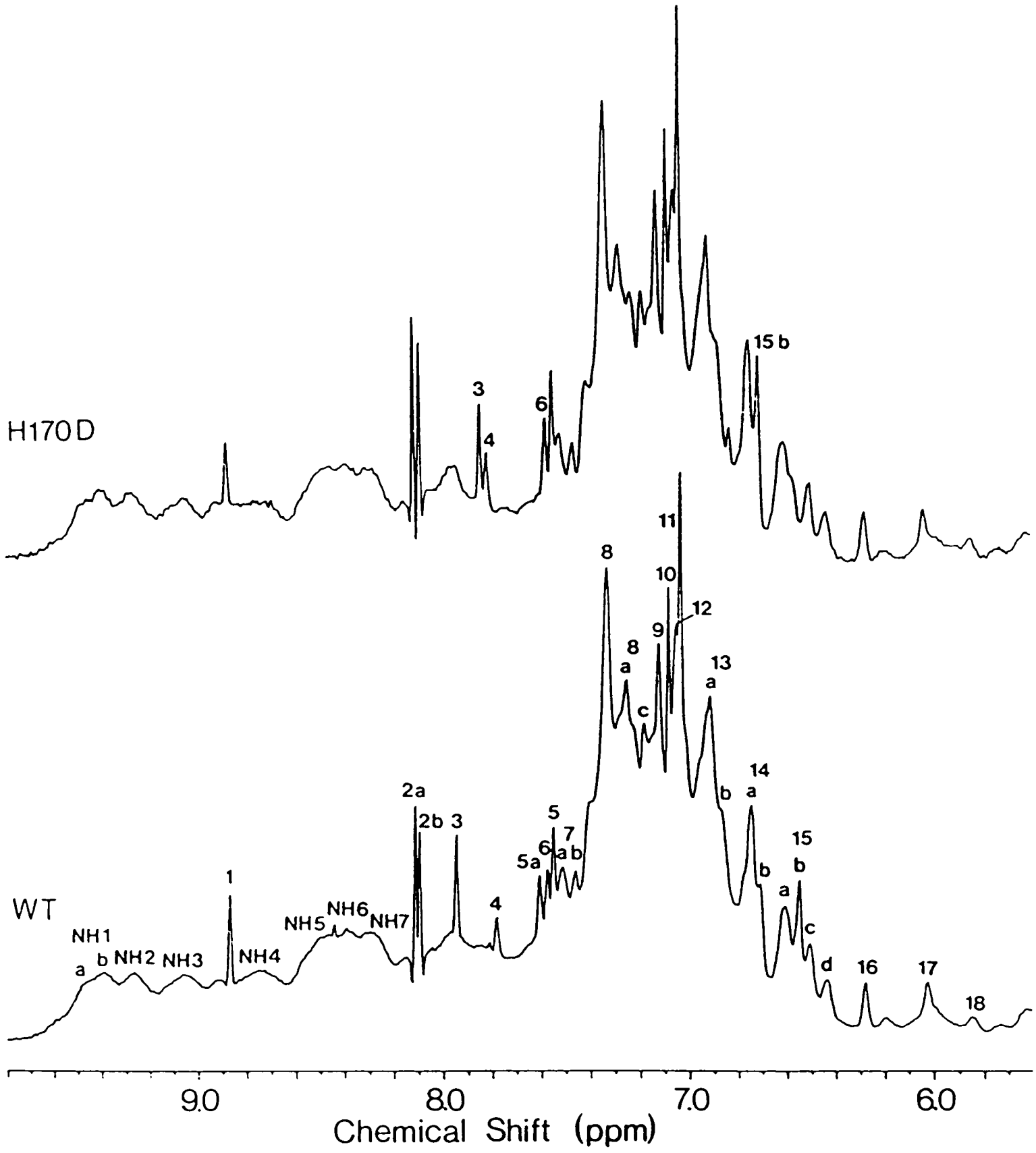

Figure 4-3A: Comparison of the aromatic regions of the 500 MHz ^{1}H NMR spectra of wild-type yeast PGK (lower) and site-specific mutant H170D (upper).

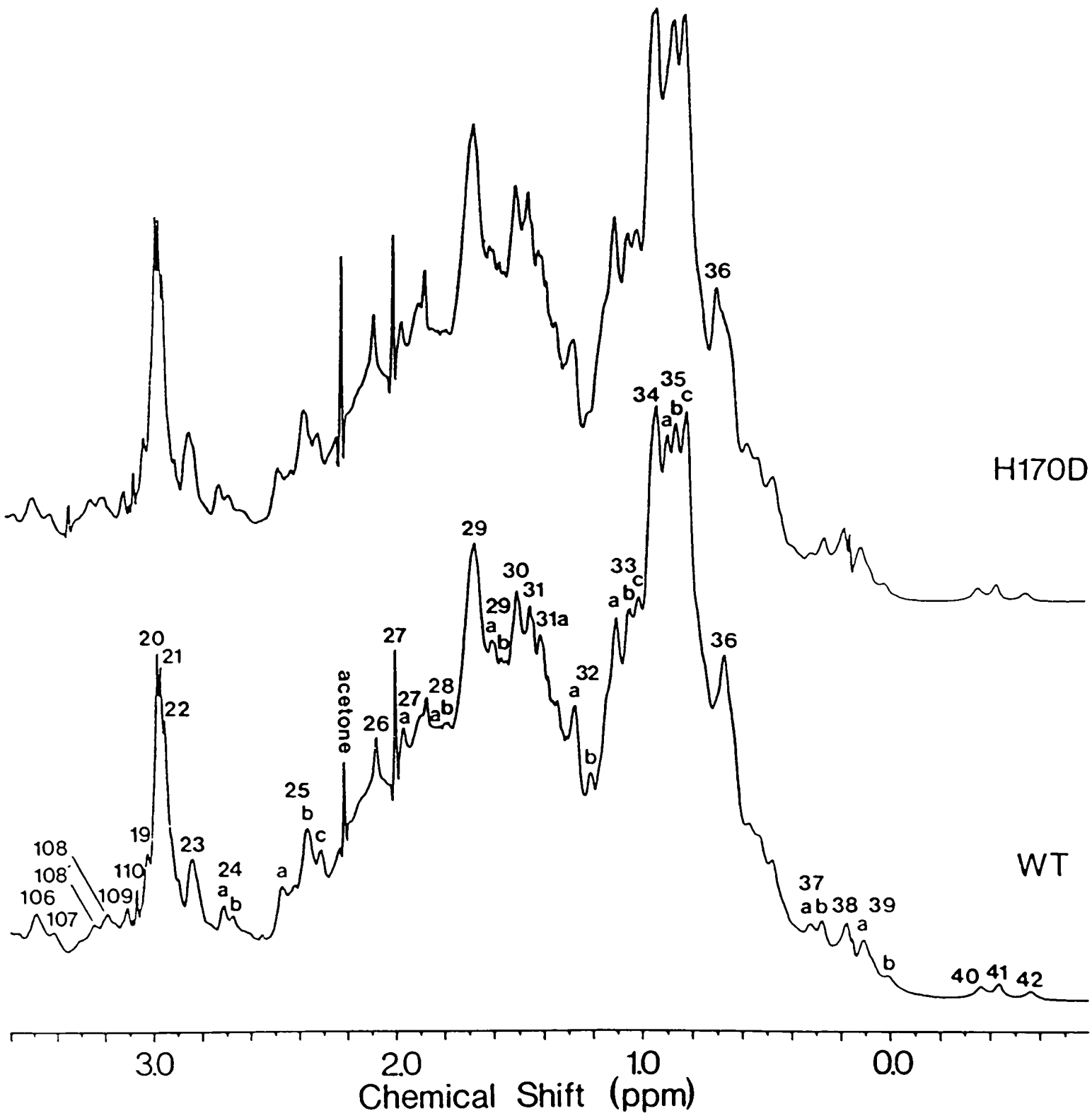

Figure 4-3B: Comparison of the aliphatic regions of the 500 MHz ^{1}H NMR spectra of wild-type yeast PGK (lower) and site-specific mutant H170D (upper).

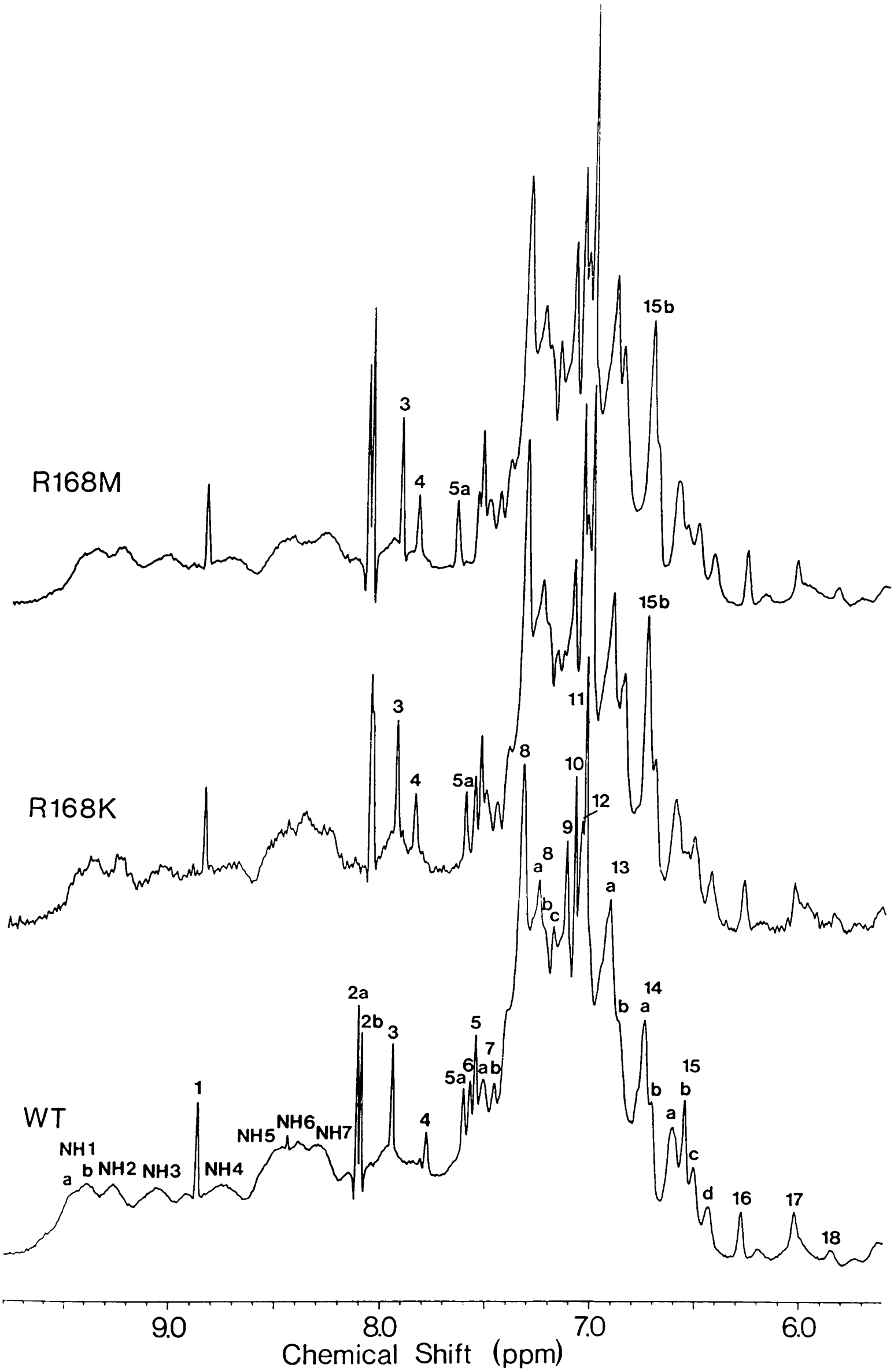

Figure 4-4A: Comparison of the aromatic regions of the 500 MHz ^{1}H NMR spectra of wild-type yeast PGK (lower) and site-specific mutants R168K (middle) and R168M (upper).

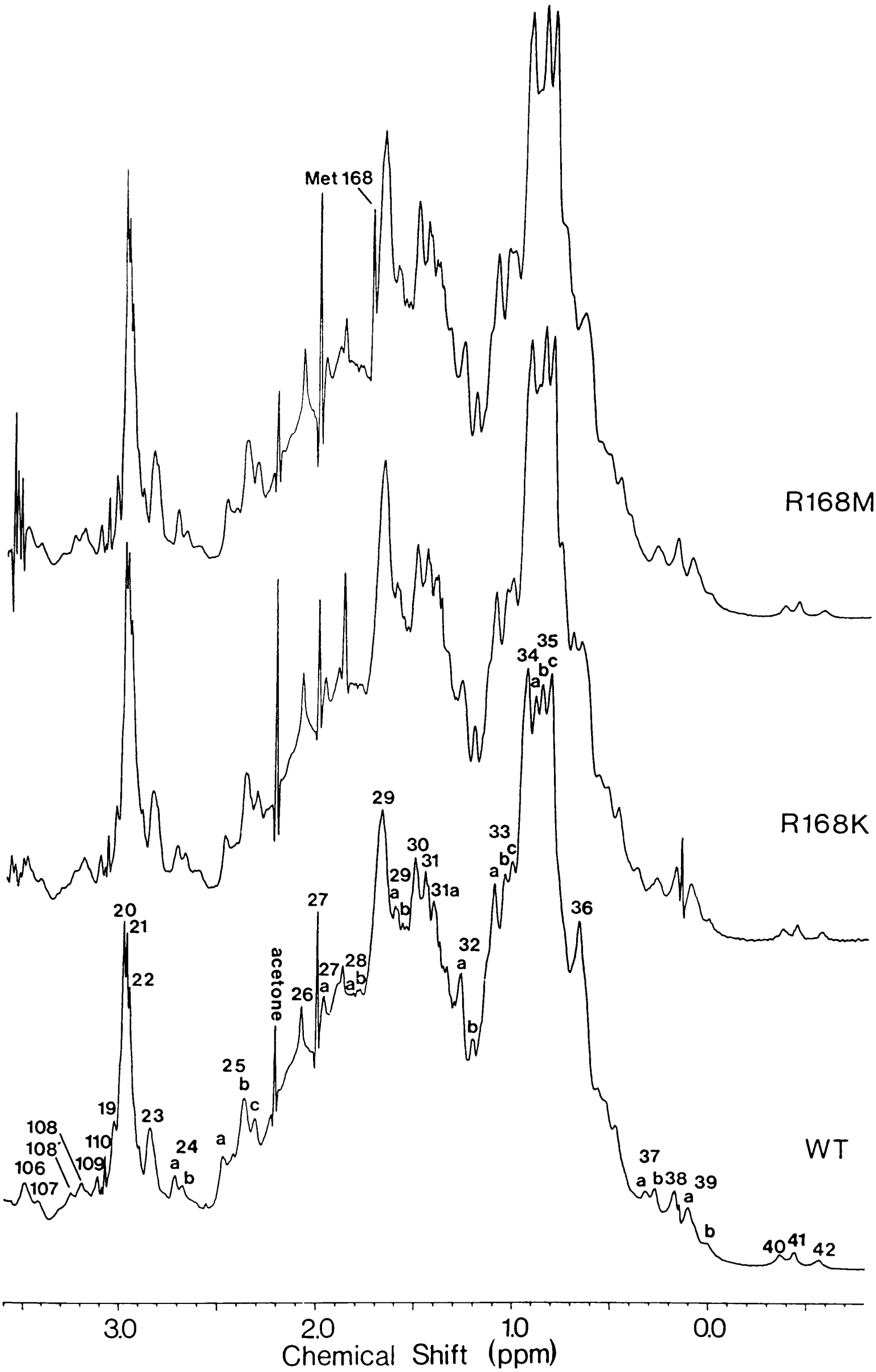

Figure 4-4B: Comparison of the aliphatic regions of the 500 MHz ^{1}H NMR spectra of wild-type yeast PGK (lower) and site-specific mutants R168K (middle) and R168M (upper).

Examination of the aliphatic spectrum of R168K (Figure 4-4B) reveals no changes which can be directly attributed to Lys 168 or to the replaced arginine side-chain. Indirect effects of the mutation are given in Table 4-2. As with the previous mutants, the number of observable differences between the mutant and wild-type aliphatic regions are few, with the most upfield shifted methyl resonances (38-42) remaining unaffected.

4.3.1.4. Spectrum of R168M

The differences between the aromatic region of the spectrum of R168M and the spectrum of wild-type PGK are summarised in Table 4-1 (see also Figure 4-4A). The replacement of Arg 168 by Met causes a greater downfield shift (3.5 times) of resonance 5a (His 170) than that observed with mutant R168K. Other effects on the aromatic resonances of R168M, however, are similar to those observed for mutant R168K. Resonance 3 (His 62) has not shifted, relative to the spectrum of the wild-type, while peaks 4 and 15b (His 167) have moved downfield by 0.09 ppm and 0.20 ppm respectively (Table 4-1).

The only effect in the amide region of the spectrum of R168M (Figure 4-4A) is broadening of NH6 (8.38 ppm). This can be attributed to proton exchange, since this sample remained in D_2O (4 °C) for about 36 hours before the spectrum was obtained. The same effect is observed for the wild-type protein.

The effects of mutation in the aliphatic region of the spectrum of R168M are summarised in Table 4-2 (see also Figure 4-4B). All the effects are seen to be similar to those observed for mutant R168K. As with R168K, no observed change can be directly assigned to the substituted Arg 168. A marked difference, however, is an additional peak at 1.72 ppm in the spectrum of R168M (Figure 4-4B), which can be assigned to the methyl protons of the introduced methionine side-chain. This resonance is ~ 0.4 ppm upfield of the 'random coil' chemical shift of the ε-CH_3 resonance of a methionine (Wüthrich, 1986), and is therefore consistent with the positioning of this group between the imidazole rings of His 167 and His 170, as would be inferred from the

crystal structure (Figure 4-1).

4.3.2. *NOEs observed for wild-type and R168M PGK*

To assess further the structural effect of the single-site mutations on various regions of the PGK molecule a comparison has been made of the 1D NOEs observed for the wild-type protein and mutant R168M. The effects observed by preirradiating peaks 1, 3 and 4 were chosen for comparison, since these histidine C2-H resonances correspond to groups both remote from (His 123) and close to (His 62 and His 167) the site of mutation (Figure 4-5). The chemical shifts of these resonances, downfield of the main aromatic envelope, allows for more selective irradiation than is possible in other regions of the spectrum.

In the wild-type spectrum several NOEs are observed from these three resonances to resonances in the aliphatic region (Table 4-3). Inspection of the crystal structure (Watson *et al.*, 1982) indicates that the resonance observed at 0.65 ppm is due to the methyl protons of Val 144 which is close to His 123 (see Figure 2-17B). The identity of the resonances at 1.26 ppm and 1.46 ppm is less clear. In the crystal structure of the protein there are no methyl or methylene groups within 5 Å of the C2 protons of **both** His 62 and His 167 which could account for the NOEs observed from peaks 3 and 4 to the resonance at 1.26 ppm. It therefore seems probable that the structure of the protein in solution differs in some way from that of the X-ray crystal structure (Watson *et al.*, 1982). This is in accordance with the domain flexibility in the PGK molecule observed in previous NMR studies (Wilson *et al.*, 1988). For part of the time at least, His 62 and His 167 are within an NOE observable distance (*i.e.* < 5 Å) of a single methyl or methylene group (with a chemical shift of 1.26 ppm). Possible candidates for the resonances at 1.26 ppm and 1.46 ppm include the methyl and methylene protons of Leu 63, Ile 124, Ala 166 and Ala 395.

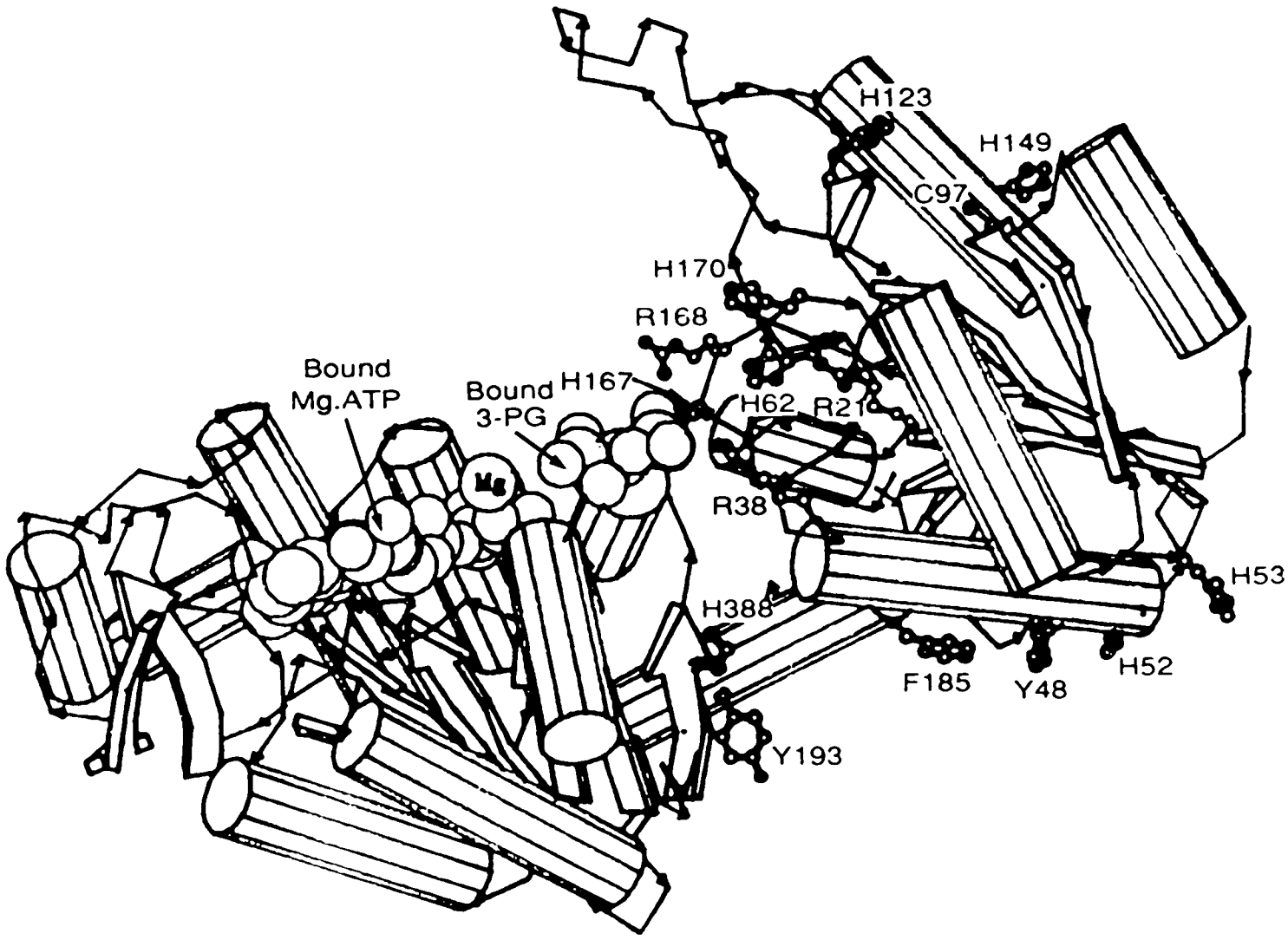

Figure 4-5: A schematic drawing of the crystal structure of yeast PGK (Watson *et al.*, 1982) showing the N-terminal domain to the right and the C-terminal domain to the left. The positions of selected amino acids are indicated. The positions of the crystallographically determined Mg.ATP and 3-PG binding sites are also shown. The drawing was produced using a computer program written by Lesk & Hardman (1982).

Table 4-3: NOEs observed in the aliphatic region following irradiation of downfield histidine resonances

The duration of the preirradiation pulse used was 150 ms. Resonances 1, 3, 4 and 5a have been assigned to histidines 123, 62, 167 and 170 respectively. Chemical shifts are in ppm.

	Wild-type		R168M	
Irradiated resonance	Irradiated chemical shift	Observed chemical shift	Irradiated chemical shift	Observed chemical shift
1	8.86	0.65[a]	8.86	0.65
3	7.94	1.26[a], 1.46	7.94	1.19, 1.46
4	7.77	1.26[a]	7.86	1.19, 1.72
5a	7.60	–	7.67	1.72

[a] NOE connectivities also observed in the 2D NOESY spectrum of yeast PGK.

In the spectrum of R168M peak 5a (His 170) has shifted downfield relative to that of the wild-type (Figure 4-4A), thereby making selective irradiation of this resonance possible. An NOE is observed at 1.72 ppm (the peak assigned in § 4.3.1 to Met 168) following irradiation of either resonance 4 or 5a (Table 4-3), confirming the previous assignment of these resonances to histidine residues 167 and 170 respectively (§ 2.3.6). Distances in the crystal structure from the C2 of His 167 and His 170 to the ε-N of Arg 168 are both ~ 3.5 Å. Observation of these NOEs also indicates that the orientation of the side-chain of Met 168 in mutant R168M (and in particular the position of its ε-CH_3), relative to His 167 and His 170, must be similar to that of Arg 168 in the native protein.

Further NOEs are observed in the spectrum of R168M from peak 1 (His 123) to a resonance at 0.65 ppm, from peak 3 (His 62) to resonances at 1.46 ppm and 1.19 ppm and from peak 4 (His 167) to a resonance at 1.19 ppm (Table 4-3). Similar NOEs were described above for the wild-type spectrum. It is probable that the resonance at 1.26 ppm (discussed above) in the wild-type spectrum has undergone an upfield shift on mutation to give the peak at 1.19 ppm in the spectrum of the mutant protein. This change in chemical shift occurs without a large change in the intensity of the NOEs to His 62 and His 167 *i.e.* the average distances between the protons giving rise to this resonance and the C2-H of His 62 (resonance 3) and His 167 (resonance 4) have not been drastically altered.

4.3.3. *Effect of pH on the mutants R168K and R168M*

The chemical shifts of the aromatic resonances (peaks 1-18) of mutants R168K and R168M were measured as a function of pH over the range pH 4.9-7.3. The titration curves obtained for R168M are compared with those of the native protein in Figure 4-6. It is clear that the titration curves and hence the pK_a values of resonances 1, 2a, 2b, 5, 9, 10 and 11 of the mutant protein are identical to those of the wild-type enzyme. It can, therefore, be

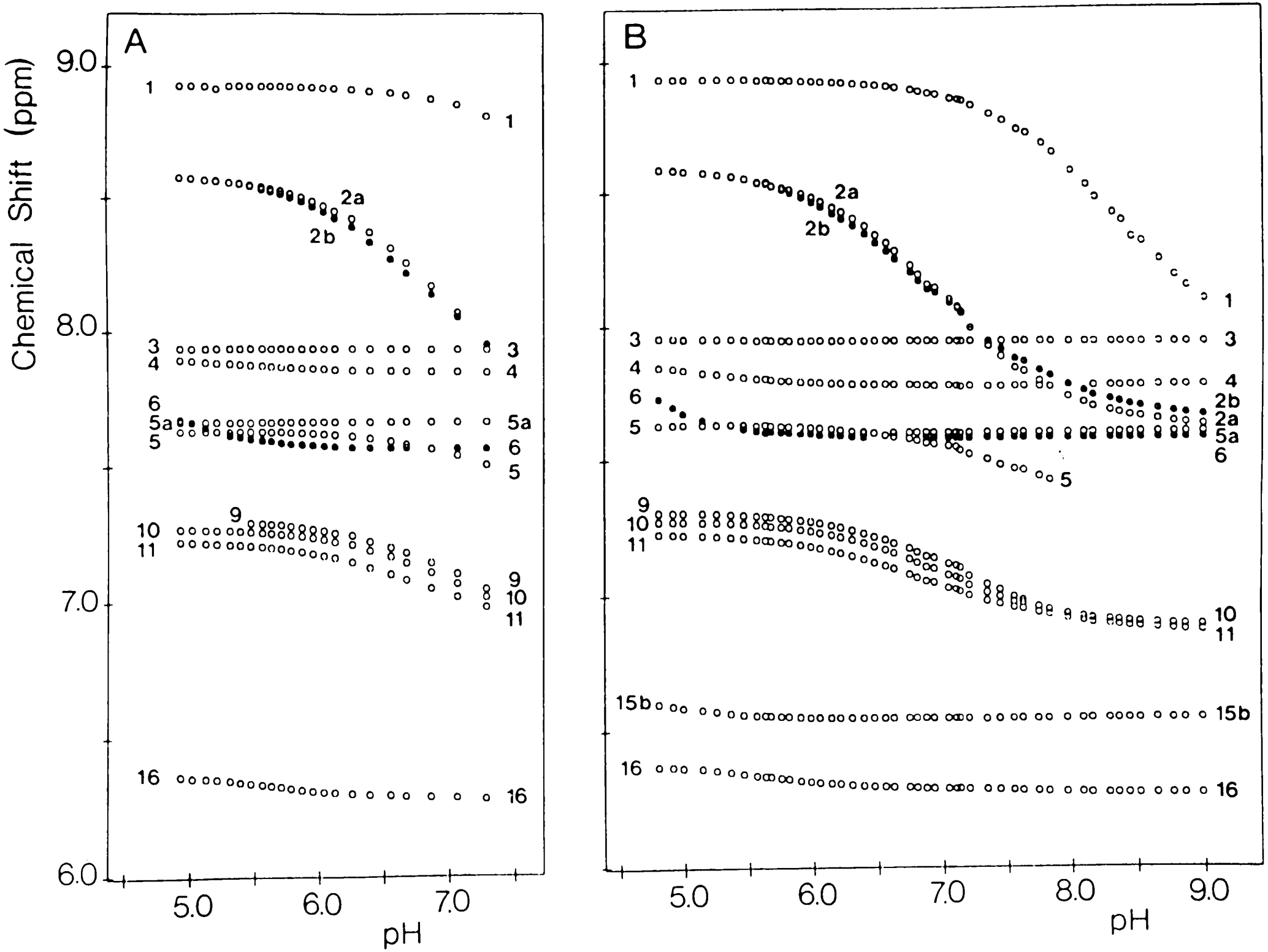

Figure 4-6: pH dependence of chemical shift for some aromatic resonances of mutant R168M (A) and of wild-type (B) PGK. The experimental points obtained for peaks 2b and 6 are shaded for clarity.

concluded that the environments of the surface histidine residues 52, 53, 123 and 149 have been unaffected by the mutation. Similar results were obtained for mutant R168K and can be inferred for H62Q and H170D since the chemical shifts of these peaks at pH 7.1 are the same as those observed for the wild-type protein.

The downfield shifts observed for resonances 4 (His 167), 5a (His 170) and 15b (His 167) following substitution of Arg 168, resonances 4 and 15b following substitution of His 170, and resonance 5a following substitution of His 62, could arise either from partial protonation of these residues or from small changes in side-chain orientations in the 'basic patch' region of the protein. The former can be eliminated as a cause for the observed shifts of these resonances in mutants R168K and R168M since the pH titration profiles of these peaks (3, 4, 5a and 15b) are precisely parallel to those determined for the wild-type protein *i.e.* the pK_a of His 167 is unaffected and the pK_a values of His 62 and His 170 remain less than 3 on substitution of Arg 168 with either lysine or methionine. These results indicate that the shifts observed for His 167 and His 170 in these mutants are due solely to local conformational effects.

4.3.4. *Structural integrity of the mutant PGKs*

The overall conformations of mutants H62Q, H170D, R168K and R168M are very similar to the wild-type as is evident from the invariance of most of the upfield shifted methyl peaks (-0.6 ppm - 0.6 ppm), the aromatic peaks (5.8 ppm - 7.6 ppm), the downfield amide resonances (7.9 ppm - 9.6 ppm) and the general dispersion throughout the ^{1}H NMR spectrum (Figures 4-2 - 4-4). This result is as expected since single amino acid substitutions on the surface of a protein are unlikely to cause conformational effects at internal residues. Also, the environments of titratable surface histidine residues 52, 53, 123 and 149, remote from the site of substitution, are unchanged as shown by their

invariant chemical shifts and pK_as (Figure 4-6). The same NOEs are observed in the spectrum of mutant R168M as in the wild-type spectrum (Table 4-3), both from peaks 1 (His 123, remote from the point of mutation), and from peaks 3 and 4 (His 62 and His 167 respectively, close to the point of mutation), providing further evidence for the occurrence of only minor conformational changes between mutant and wild-type enzymes. It is therefore reasonable to assume that the small number of spectral changes which are observed are due to local effects in the vicinity of the substitution. The use of Mn^{2+} or Gd^{3+} as relaxation probes when Mg.ATP^{2-} is bound to the wild-type enzyme (Tanswell *et al.*, 1976; Wilson *et al.*, 1988; see also Chapter 7) has shown that most of the protons giving rise to resonances affected by mutation are close together in space. In addition all the resonances affected by mutations are perturbed by binding of the triose substrate, 3-PG (§ 3.3.1).

The upfield shift of resonance 3 (His 62) following substitution of His 170 with an aspartic acid residue was attributed to a conformational change (§ 2.3.6). A repositioning of the imidazole group of His 62 would follow if the carboxyl group of the mutant residue were to interact with the guanidinium group of Arg 21, as might be expected from inspection of the wild-type crystal structure (Figure 4-1). A possible source of susceptibility anisotropy in this region of the protein is the carbonyl group of His 62 itself (Figure 4-1) which is within 4 Å of the C2-H. A relatively minor reorientation of Arg 21, to form a charge interaction with Asp 170, would affect the position of the imidazole ring and would, therefore, easily account for the observed upfield shift (-0.10 ppm) of the C2-H resonance of His 62 (Perkins, 1982). There may also be a contribution to the observed shift as a direct result of the removal of the aromatic side-chain of His 170 since the shortest distance between His 62 and His 170 in the crystal structure (Figure 4-1) is ~ 5 Å.

The downfield shifts of resonances 4 (His 167) and 5a (His 170) following

substitution of Arg 168 with either lysine or methionine have also been shown to be conformational in origin, since the pK_as of these residues have not moved into the pH range studied (§ 4.3.3). It is clear that the magnitude of the implied conformational change is not large, as the NOE data for R168M indicates that the position of Met 168 in this mutant, relative to His 167 and His 170, is similar to that of Arg 168 in the wild-type protein (§ 4.3.2). It seems likely, therefore, that the imidazole groups of residues 167 and 170 move slightly in the two mutant enzymes in order to accomodate the water molecule(s) which must occupy the space taken up in the wild-type enzyme by the additional side-chain atoms. In Figure 4-1 it can be seen that the imidazole ring of His 167 is in close proximity to a number of carbonyl groups (in particular its own and that of Gly 164, with C2 to carbonyl distances of ~ 3.5 Å). As with His 62 in H170D it would appear that the changes in chemical shifts of His 167 and His 170 in mutants R168K and R168M, relative to the wild-type protein, result from minor rearrangement of these residues with respect to neighbouring carbonyl groups.

Given the above results, it is reasonable to assume that the downfield shifts of peaks 5a (His 170) and 15b (His 167) following substitution of His 62 (Table 4-1), and peaks 4 (His 167) and 15b (His 167) following substitution of His 170 (Table 4-1), are also due to conformational effects.

There are a number of other differences between the effects of substitution of His 62, Arg 168 and His 170, apart from those related to histidines 62, 167 and 170. These effects are again indicative of small, but differing, local conformational changes resulting from substitution of these 'basic patch' amino acids. It can therefore be concluded with some confidence that, with the exception of minor variations close to the site of mutation, the mutant proteins have folded correctly to give the same average solution structure as native PGK.

4.3.5. *3-Phosphoglycerate binding to mutant PGKs*

3-PG titrations, similar to that described for wild-type PGK in the preceding chapter (§ 3.2.1), were carried out on the mutant forms of the enzyme (H62Q, H170D, R168K and R168M). A description of the spectral changes observed and determination of dissociation constants for each mutant are outlined below.

4.3.5.1. H62Q + 3-phosphoglycerate

The effect of 3-PG addition on the spectrum of H62Q is very similar to that observed for wild-type PGK (Figure 4-7; Table 4-4; *c.f.* § 3.3.1). This indicates that the conformational changes induced by triose substrate binding to mutant H62Q and to wild-type enzyme are similar in both cases.

Since resonance 3 is absent in the spectrum of H62Q (§ 4.3.1), the dissociation constant for 3-PG was calculated by fitting the observed changes in chemical shifts of resonances 4 and 15b (Figure 4-8), corresponding to His 167. The shifts of these two resonances saturate with a K_d of 0.029 ± 0.009 mM, which is only a factor of 3 greater than that obtained for the over-expressed wild-type enzyme (Table 4-5; § 3.3.3). The K_m for this substrate has increased by about a factor of 2 over that for the wild-type enzyme (P.A. Walker, personal communication).

4.3.5.2. H170D + 3-phosphoglycerate

In the spectrum of mutant H170D, almost all the shifts observed upon addition of 3-PG to the wild-type protein, including the conformational effects on the upfield shifted methyl resonances, were observed (Figure 4-9; see Table 4-4 for changes in the aromtic region). The obvious exception to this is resonance 5a which is absent from the mutant's spectrum. The magnitude of the observed shifts for fully bound complexes, however, were all between 0.4 and 0.6 times those observed for wild-type PGK (Table 4-4). The line-width effects observed in the spectrum of the wild-type protein, including those in

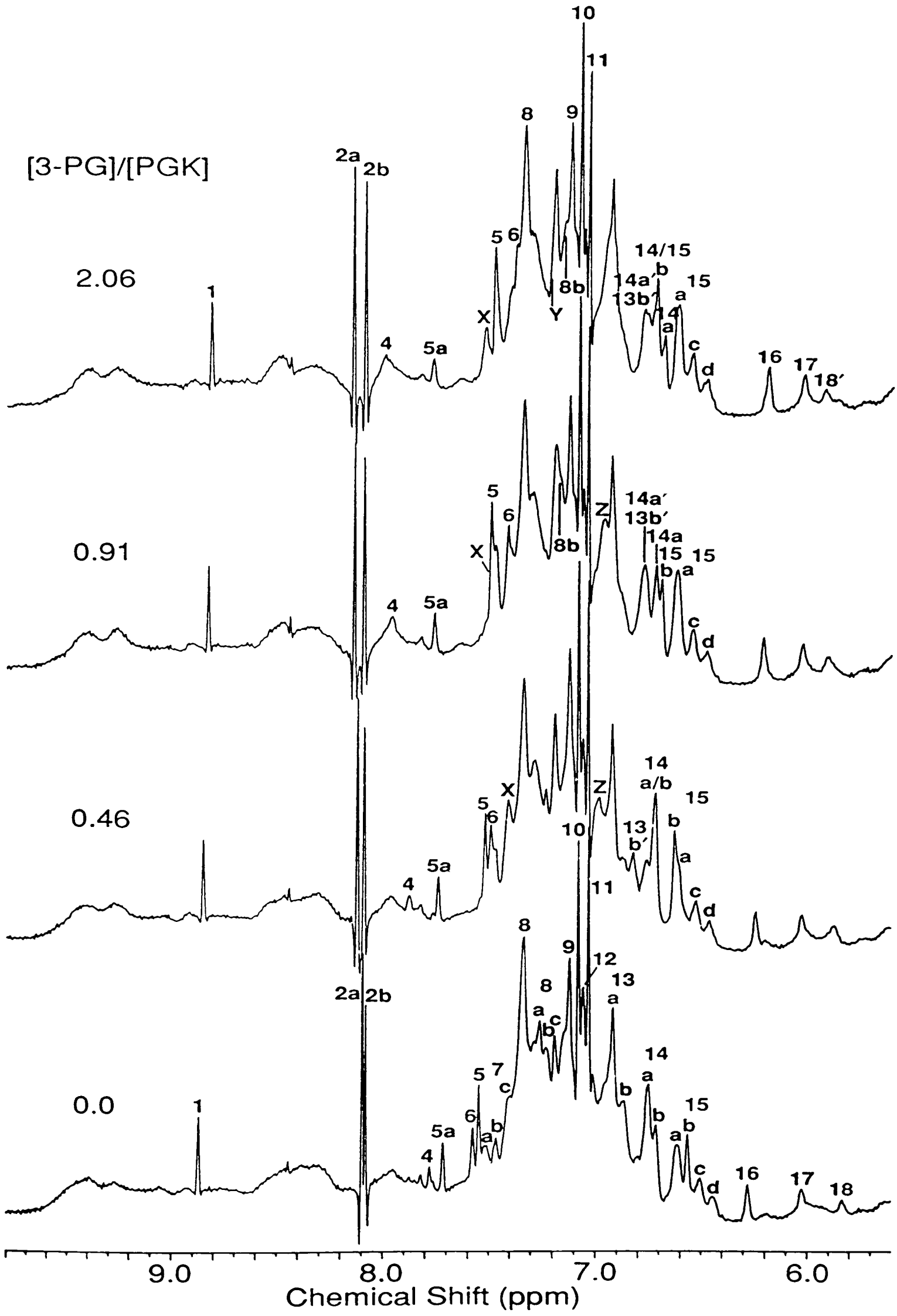

Figure 4-7A: Perturbations of the aromatic region of the 500 MHz ^{1}H NMR spectrum of H62Q PGK by 3-PG, at the ratios indicated and pH 7.1.

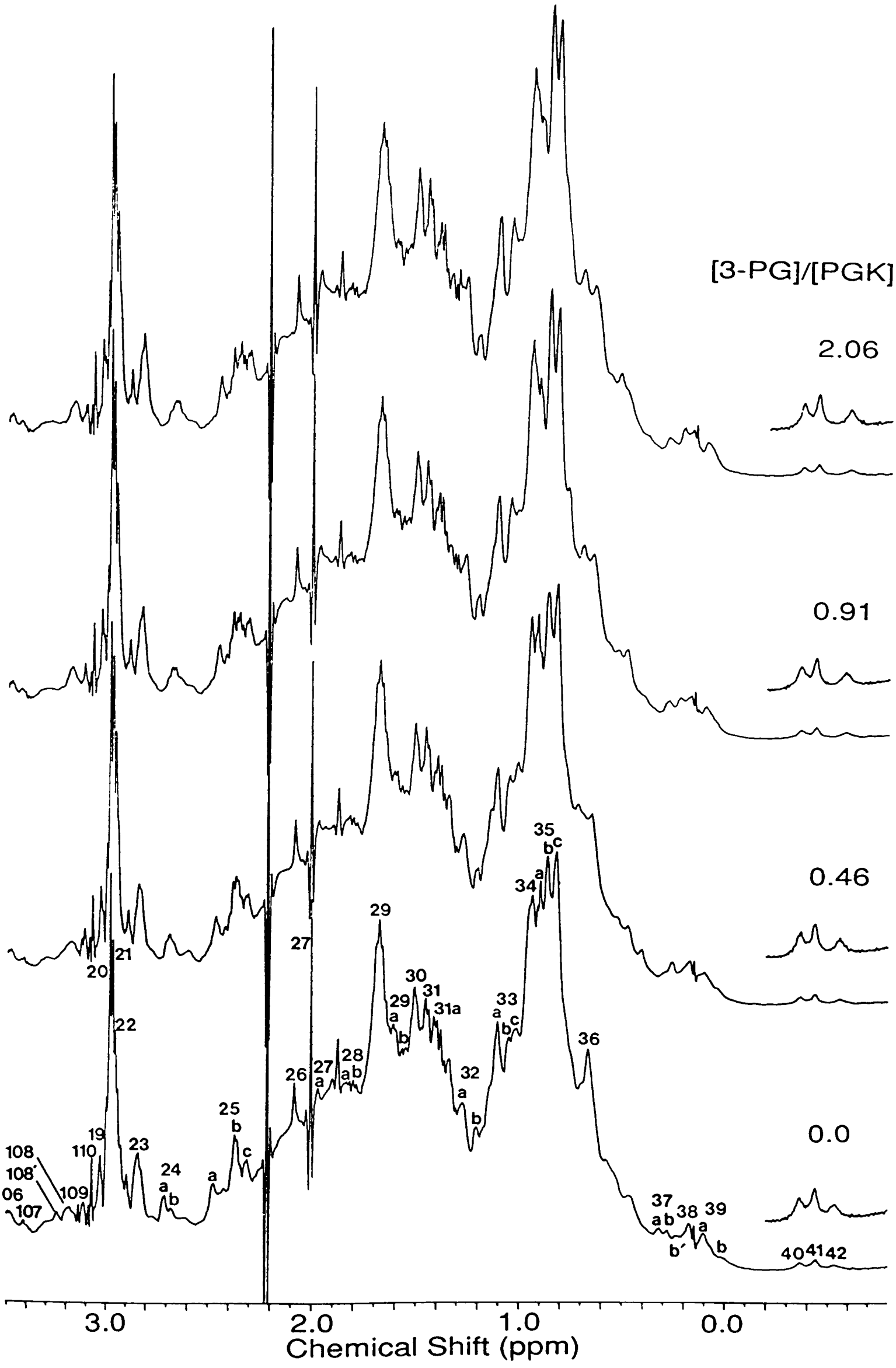

Figure 4-7B: Perturbations of the aliphatic region of the 500 MHz ^{1}H NMR spectrum of H62Q PGK by 3-PG, at the ratios indicated and pH 7.1.

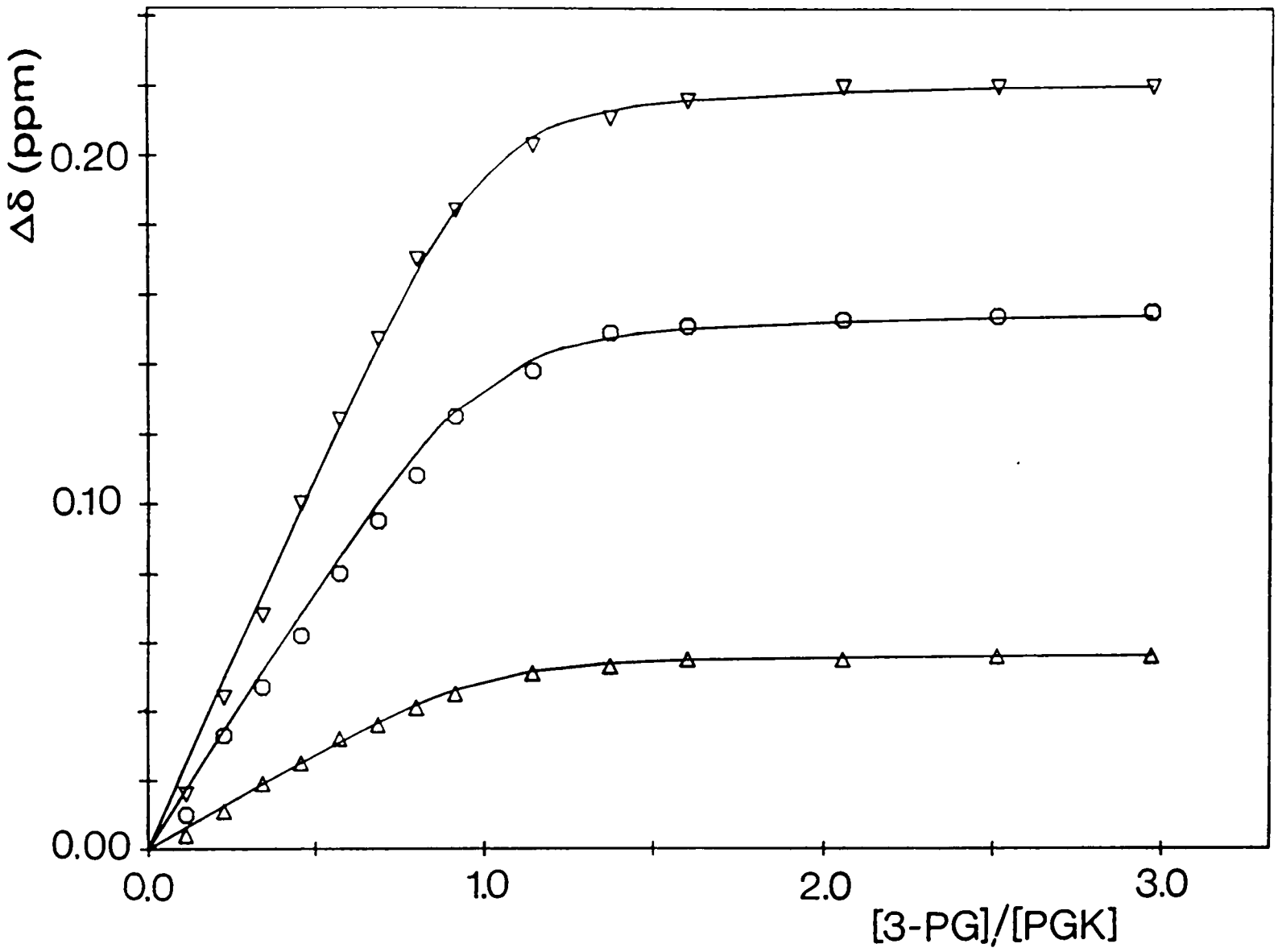

Figure 4-8: The change in the chemical shifts of peaks 4 (∇; His 167), 5a (Δ; His 170) and 15b (○; His 167) plotted as a function of the 3-PG:H62Q molar ratio. The continuous lines represent theoretical binding curves corresponding to a dissociation constant of 0.029 mM.

Table 4-4: Effects of 3-phosphoglycerate binding on aromatic resonances of wild-type and mutant PGKs

Numbers are observed shifts in ppm, negative shifts are upfield. (B) = broadening, (I) = apparent increase in intensity, (-) = upfield shift of indeterminate magnitude, (+) = downfield shift of indeterminate magnitude, – = no observable effect, ? = possible effect, * = broadened by Mn^{2+} in Mg.ATP.PGK complex

	Resonance	WT	H62Q	H170D	R168K	R168M
	1	-0.05	-0.05	-0.03	-0.01	-0.01
	2a	+0.06	+0.06	+0.03	+0.01	–
	2b	+0.01	+0.01	–	–	–
*	3	+0.72(B)	absent	+0.36(B)	+0.06(B)	+0.04(B)
*	4	+0.26(B)	+0.22	+0.15(B)	+0.07(B)	+0.05(B)
*	5a	+0.04	+0.06	absent	+0.05	+0.01
	6	-0.23	-0.2	-0.1	–	–
	5	-0.06	-0.07	-0.03	–	-0.01
*	7a	(-)	(-)	-0.01	-0.02	-0.02
	7b	–	–	–	–	–
	7c	?	?	?	-0.01	?
	8	?	?	?	?	?
*	8a	+0.04(B)	+0.04 (B)	+0.01(B)	(+)	–
	8b	-0.09	(-)	-0.02 (B)	?	–
*	8c	–	–	–	+0.01	–
	9	–	–	–	–	–
	10	–	–	–	–	–
	11	–	–	–	–	–
*	12	see text	see text	see text	–	–
*	13a′	(+)	(+)	(+)	+0.04	+0.03
*	13b′	(-)	(-)	?	?	?
*	14a	-0.08	-0.07	-0.04	-0.01	–
	14b	?	?	?	–	–
*	15a	(I)	(I)	?	–	–
*	15b	+0.16(B)	+0.16 (B)	+0.07(B)	?	?
	15c	+0.04	+0.04	+0.01	–	-0.01
	15d	+0.04	+0.04	+0.02	–	–
	16	-0.10	-0.09	-0.05	-0.01	-0.01
	17	-0.01	–	-0.01	-0.01	-0.01
	18′	+0.09	+0.09	+0.04	?	?

Table 4-5: Dissociation constants for 3-phosphoglycerate with wild-type and mutant PGKs

K_d values were determined from the shifts of resonances 3 and 4 in titrations of the enzymes with 3-phosphoglycerate, in 0.10 M Na d_3-acetate (pH = 7.1, T = 300 K). Resonances 3 and 4 have been assigned to histidines 62 and 167 respectively.

PGK	$\Delta\delta_3$ (ppm)	$\Delta\delta_4$ (ppm)	K_d (mM)	V_{max}/K_m (EU mg^{-1} mM^{-1})
Wild-type	+0.72	+0.26	0.011 ± 0.005	640[a]
H62Q	–	+0.22	0.029 ± 0.009	817[b]
H170D	+0.36	+0.15	0.040 ± 0.010	592[c]
R168K	+0.06	+0.07	0.025 ± 0.010	96[a]
R168M	+0.04	+0.05	0.16 ± 0.04	15[a]

[a] Calculated from Walker *et al.*, 1989

[b] Personal communication, P.A. Walker, J.A. Littlechild & H.C. Watson (University of Bristol)

[c] From Fairbrother *et al.*, 1989

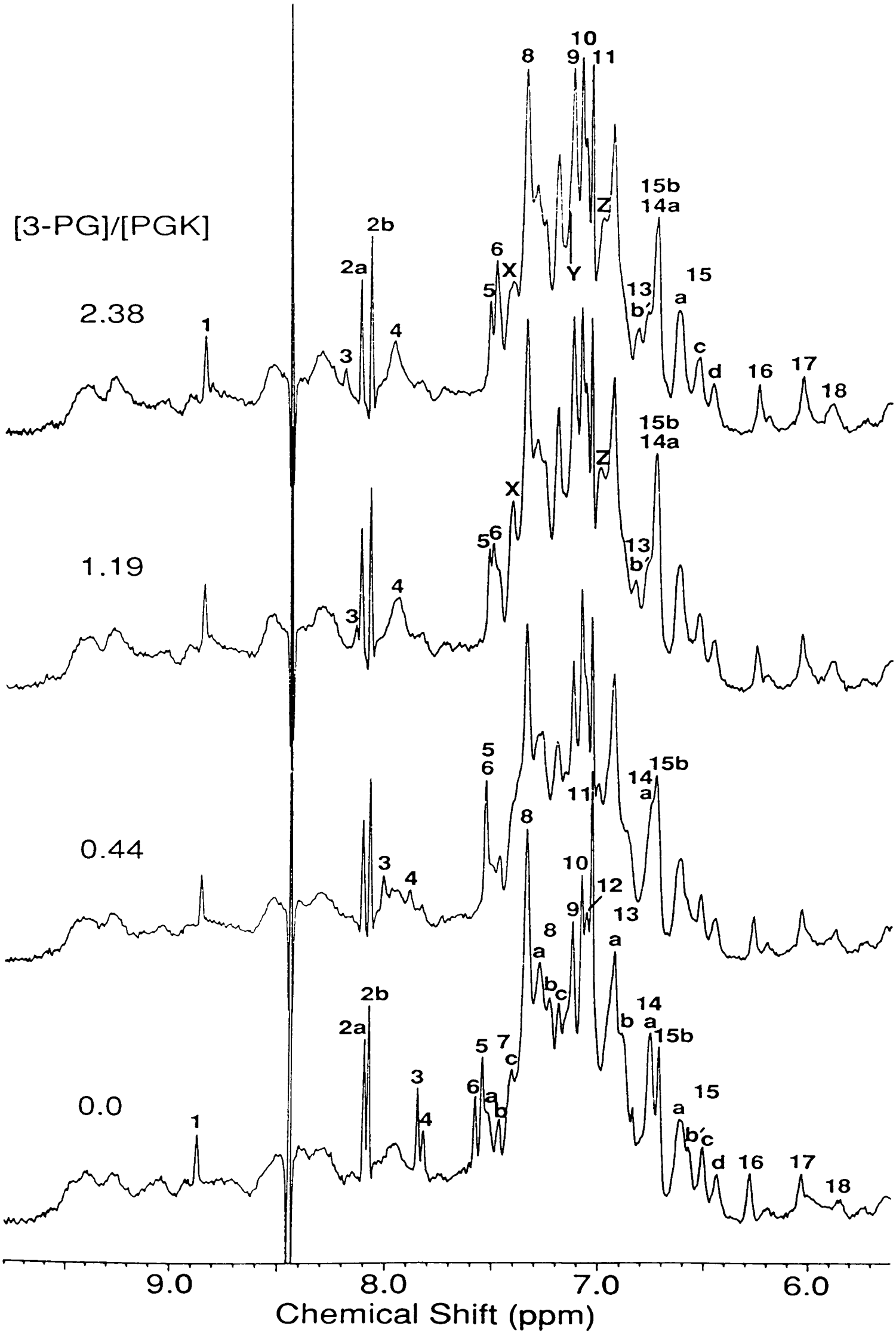

Figure 4-9A: Perturbations of the aromatic region of the 500 MHz ^{1}H NMR spectrum of H170D PGK by 3-PG, at the ratios indicated and pH 7.1.

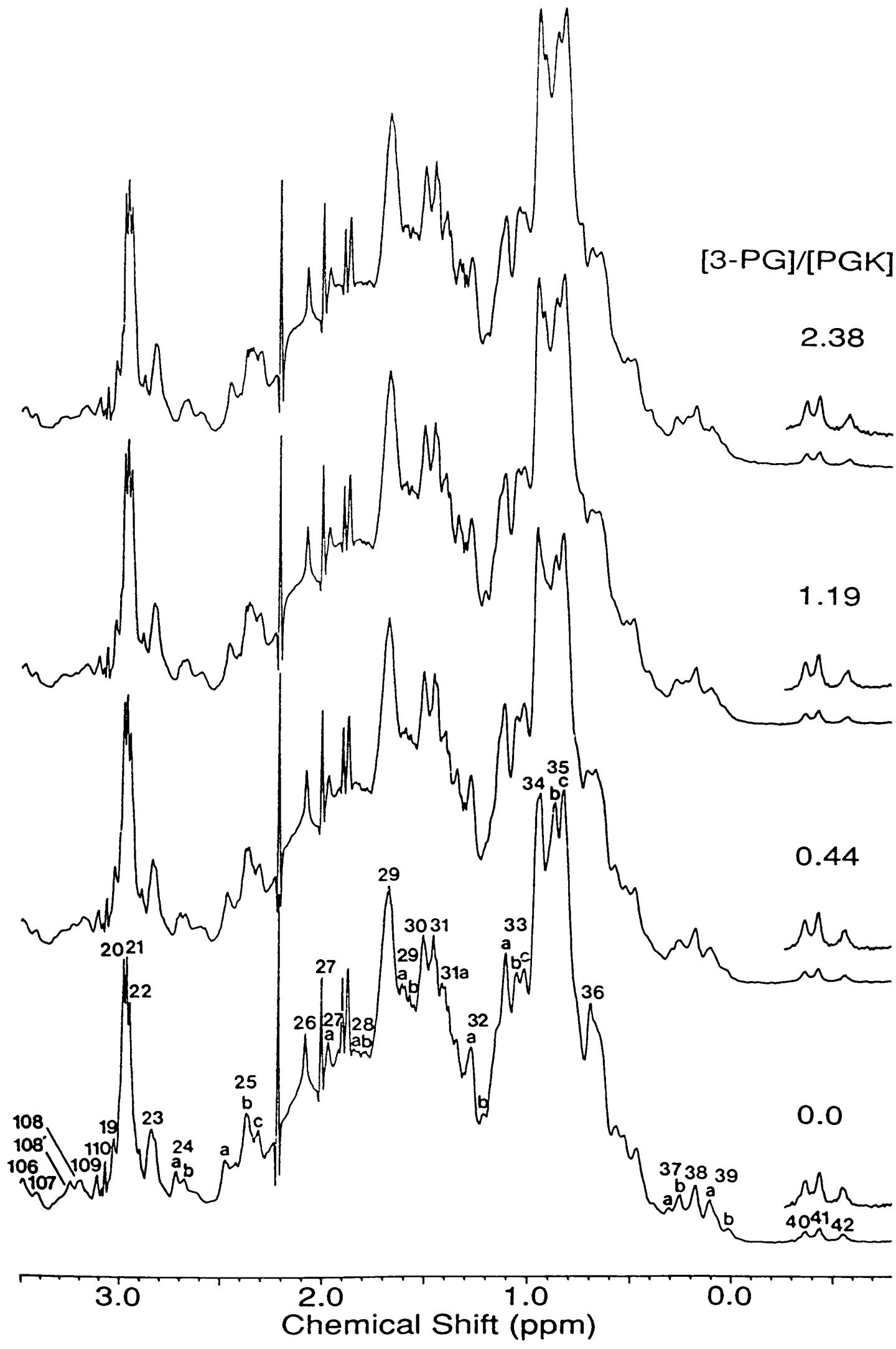

Figure 4-9B: Perturbations of the aliphatic region of the 500 MHz ^{1}H NMR spectrum of H170D PGK by 3-PG, at the ratios indicated and pH 7.1.

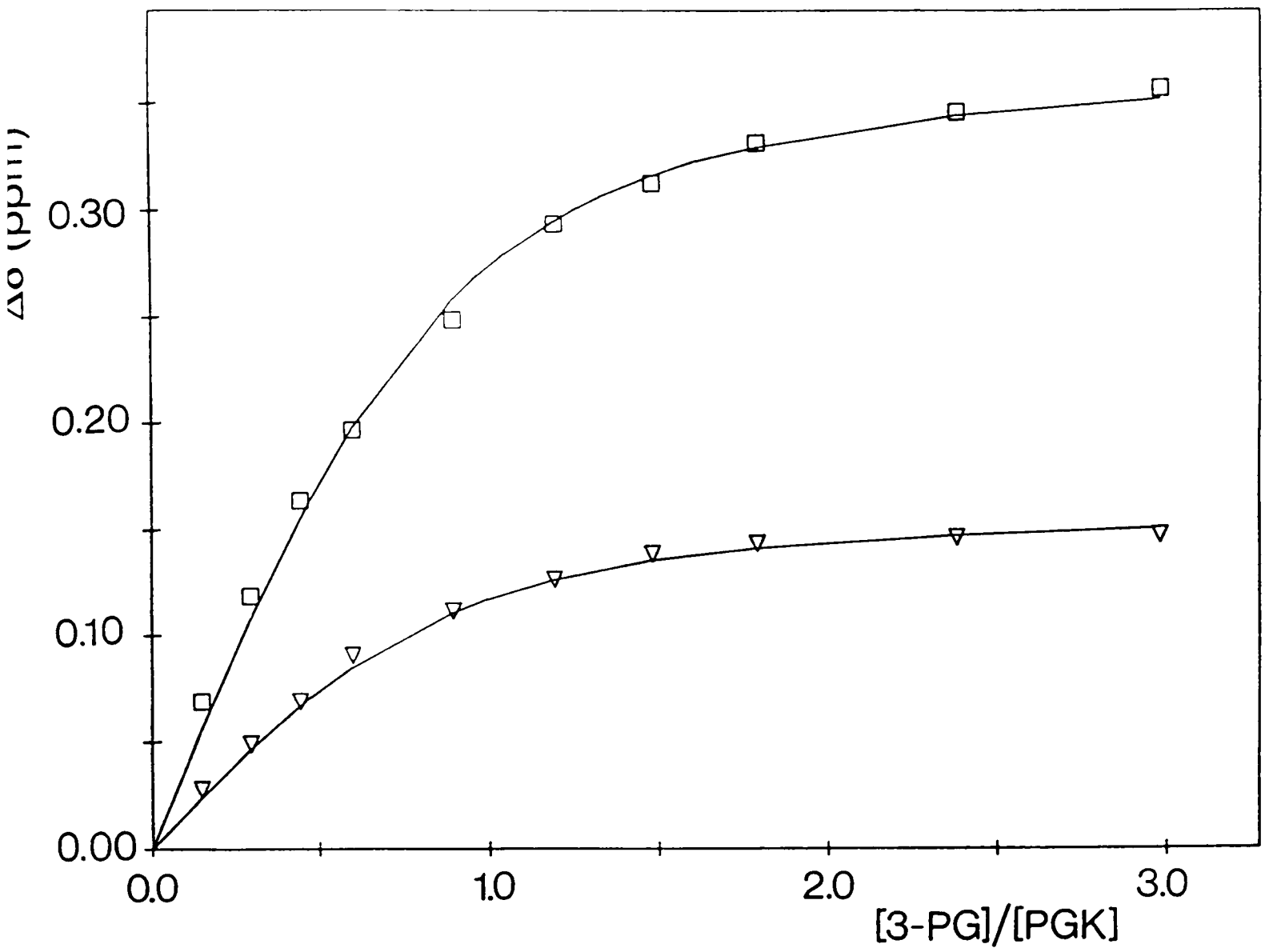

Figure 4-10: The change in the chemical shifts of peaks 3 (□; His 62) and 4 (▽; His 167) plotted as a function of the 3-PG:H170D molar ratio. The continuous lines represent theoretical binding curves corresponding to a dissociation constant of 0.040 mM.

the NH region, are also seen in this mutant.

A dissociation constant of 0.040 ± 0.010 mM is obtained from a plot of resonances 3 (His 62) and 4 (His 167) against the molar ratio of 3-PG to protein (Figure 4-10). The slightly decreased binding of the substrate to mutant H170D PGK (K_d = 0.040 mM compared to K_d = 0.011 mM for over-expressed wild-type; Table 4-5) would be expected following substitution of the imidazole group of residue 170 by a carboxyl group, as this change reduces the overall positive charge in the area defined by histidines 62, 167 and 170, and arginines 21, 38 and 168 by at least one unit. As already noted (§ 4.3.4), the substitution results in a minor conformational change at His 62 which may also affect substrate binding. The specific activity of mutant H170D is, surprisingly, unchanged from that of wild-type PGK (Fairbrother *et al.*, 1989) despite its slightly lower affinity for 3-PG and the reduced interaction of this substrate with the 'basic patch' histidines, 62 and 167.

4.3.5.3. R168K + 3-phosphoglycerate

Addition of 3-PG to R168K has very little effect on the ^{1}H NMR spectrum of this mutant (Figure 4-11). Significantly smaller shifts, relative to wild-type, H62Q and H170D, are recorded for histidine resonances 3 and 4 (Figure 4-12; Table 4-4), although broadening of these resonances is still observed.

None of the conformational effects observed in the amide region of the wild-type following addition of 3-PG are observed for this mutant. The only effects upfield of 0.5 ppm are a small downfield shift of peak 41 (Thr 375; +0.01 ppm) which was not observed using wild-type enzyme, and splitting of a peak at 0.37 ppm (thought to correspond to peak 37a in the wild-type spectrum) into two components, which shift 0.02 ppm downfield and 0.01 ppm upfield, respectively. The conformational effects at peaks 37b, 39a, 39b and 42 recorded upon addition of 3-PG to the native enzyme (and H62Q and H170D) are not observed with this mutant.

The dissociation constant for 3-PG binding to mutant R168K, determined

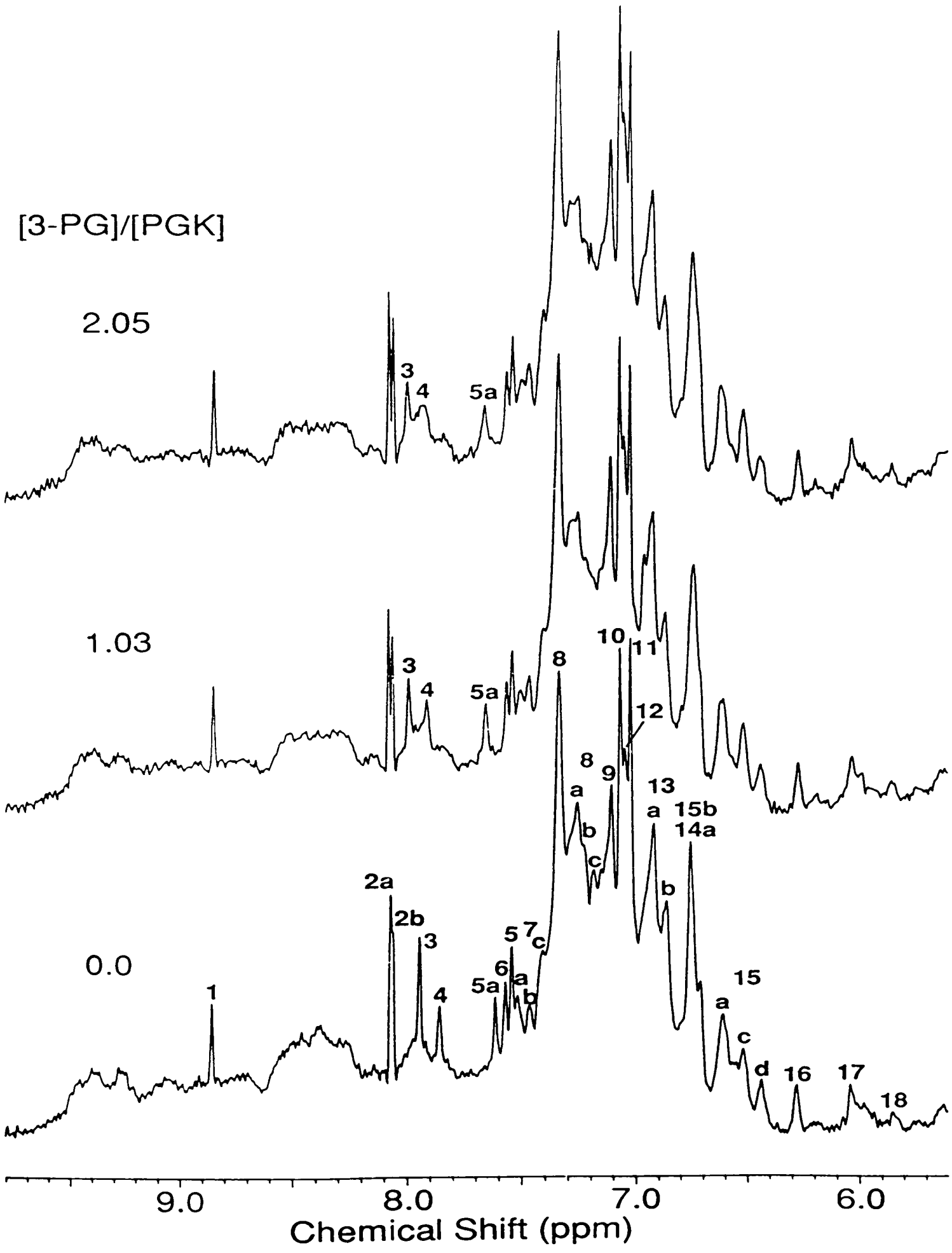

Figure 4-11A: Perturbations of the aromatic region of the 500 MHz ^{1}H NMR spectrum of R168K PGK by 3-PG, at the ratios indicated and pH 7.1.

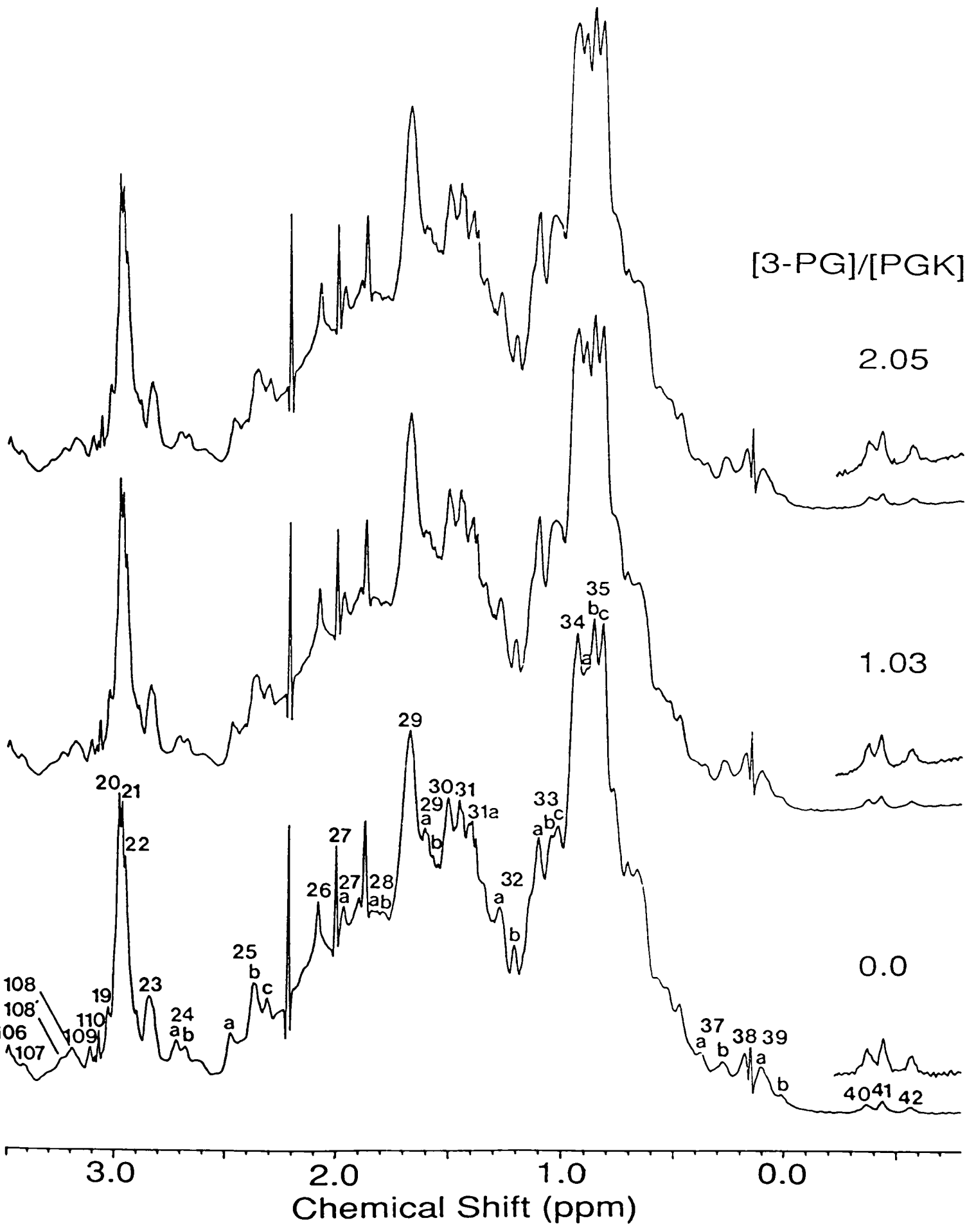

Figure 4-11B: Perturbations of the aliphatic region of the 500 MHz ^{1}H NMR spectrum of R168K PGK by 3-PG, at the ratios indicated and pH 7.1.

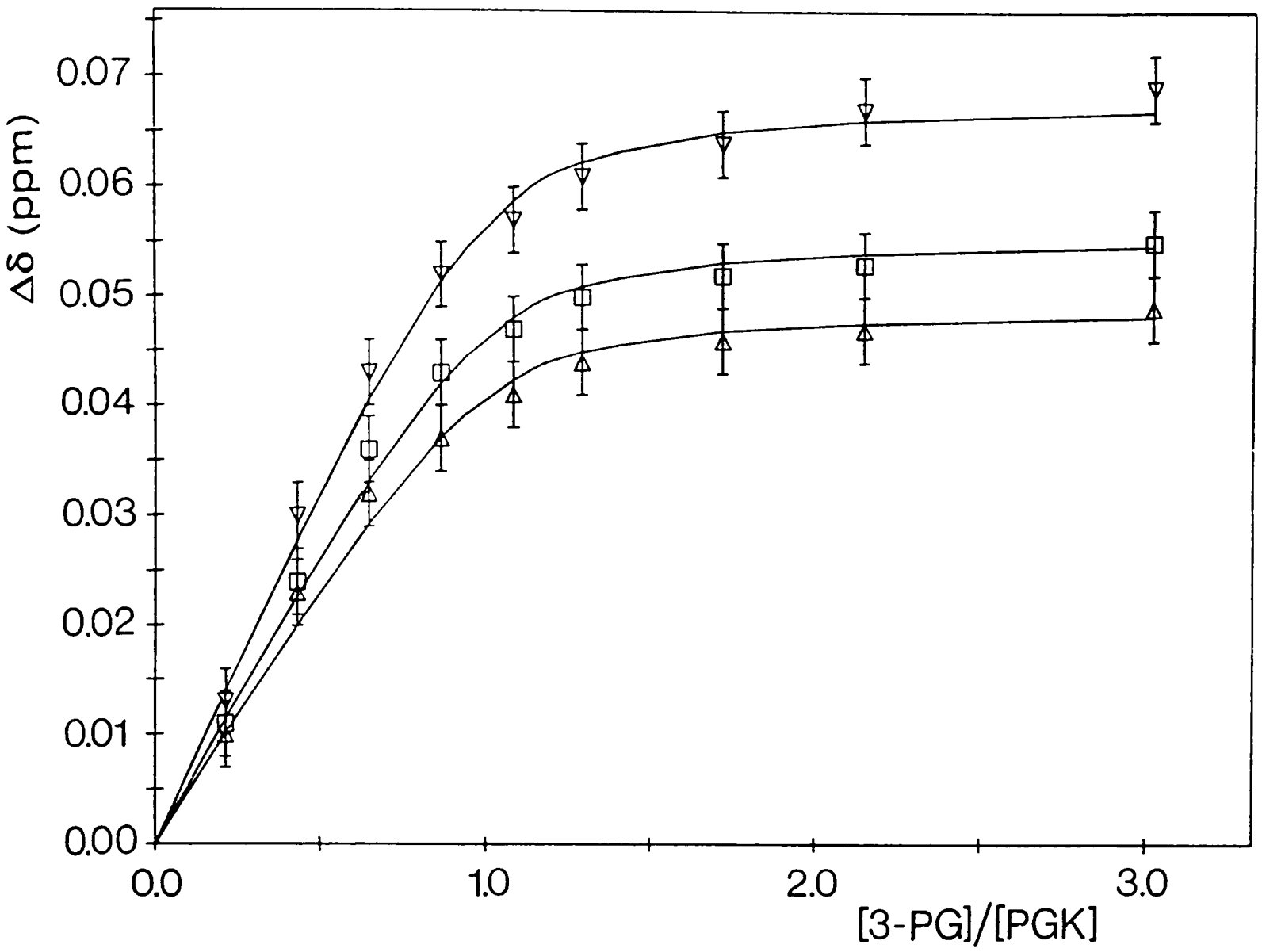

Figure 4-12: The change in chemical shifts of peaks 3 (□; His 62), 4 (∇; His 167) and 5a (Δ; His 170) plotted as a function of 3-PG:R168K molar ratio. The continuous lines represent theoretical binding curves corresponding to a dissociation constant of 0.025 mM.

from the shifts of resonances 3 and 4 (Figure 4-12; Table 4-5), is similar to that of wild-type PGK. The small increase (K_d = 0.025 mM compared to 0.011 mM for over-expressed wild-type PGK) is comparable to the observed 2.7 times increase in the K_m of 3-PG for this mutant (Walker *et al.*, 1989). It is apparent from these results that substitution of Arg 168 with lysine does not greatly affect the proteins affinity for binding 3-PG, but does prevent some of the 3-PG induced conformational changes observed on formation of the binary complex with the wild-type enzyme.

4.3.5.4. R168M + 3-phosphoglycerate

As found with R168K, addition of 3-PG to mutant R168M has very little effect on its spectrum (Figure 4-13). The magnitude of the downfield shifts of the 'basic patch' histidine resonances 3, 4 and 5a (Figure 4-14; Table 4-5) are less than those observed for R168K. In the aliphatic region of the spectrum the peak at 1.72 ppm, due to the introduced methionine residue, broadens on addition of 3-PG, indicating that its mobility is reduced on binding the substrate. All the other effects observed, however, are similar to those seen for the mutant R168K. As for mutant R168K, the many conformational effects found with the wild-type enzyme are noticeable by their absence.

A value of 0.16 ± 0.04 mM was obtained for the dissociation constant of 3-PG from mutant R168M (Figure 4-14; Table 4-5), which is about an order of magnitude greater than that found for wild-type or mutant R168K enzymes, and can be compared to the eight fold increase in the K_m of 3-PG for mutant R168M (Walker *et al.*, 1989).

4.4. Discussion

4.4.1. *Substrate free mutant proteins*

The overall NMR spectra of the mutant proteins were found to be almost unaffected by substitutions made within the 'basic patch' region of the

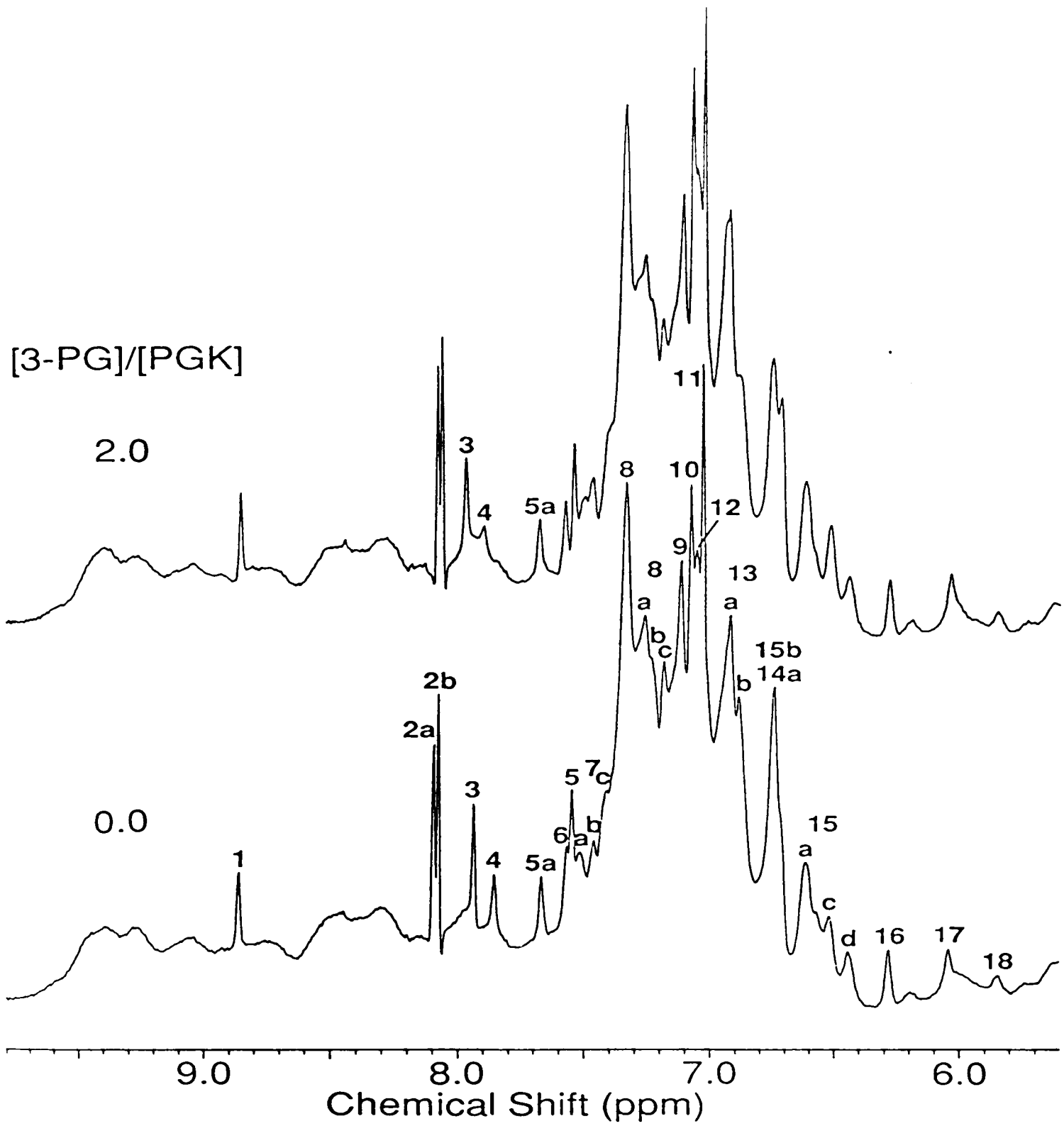

Figure 4-13A: Perturbations of the aromatic region of the 500 MHz ^{1}H NMR spectrum of R168M PGK by 3-PG, at the ratios indicated and pH 7.1.

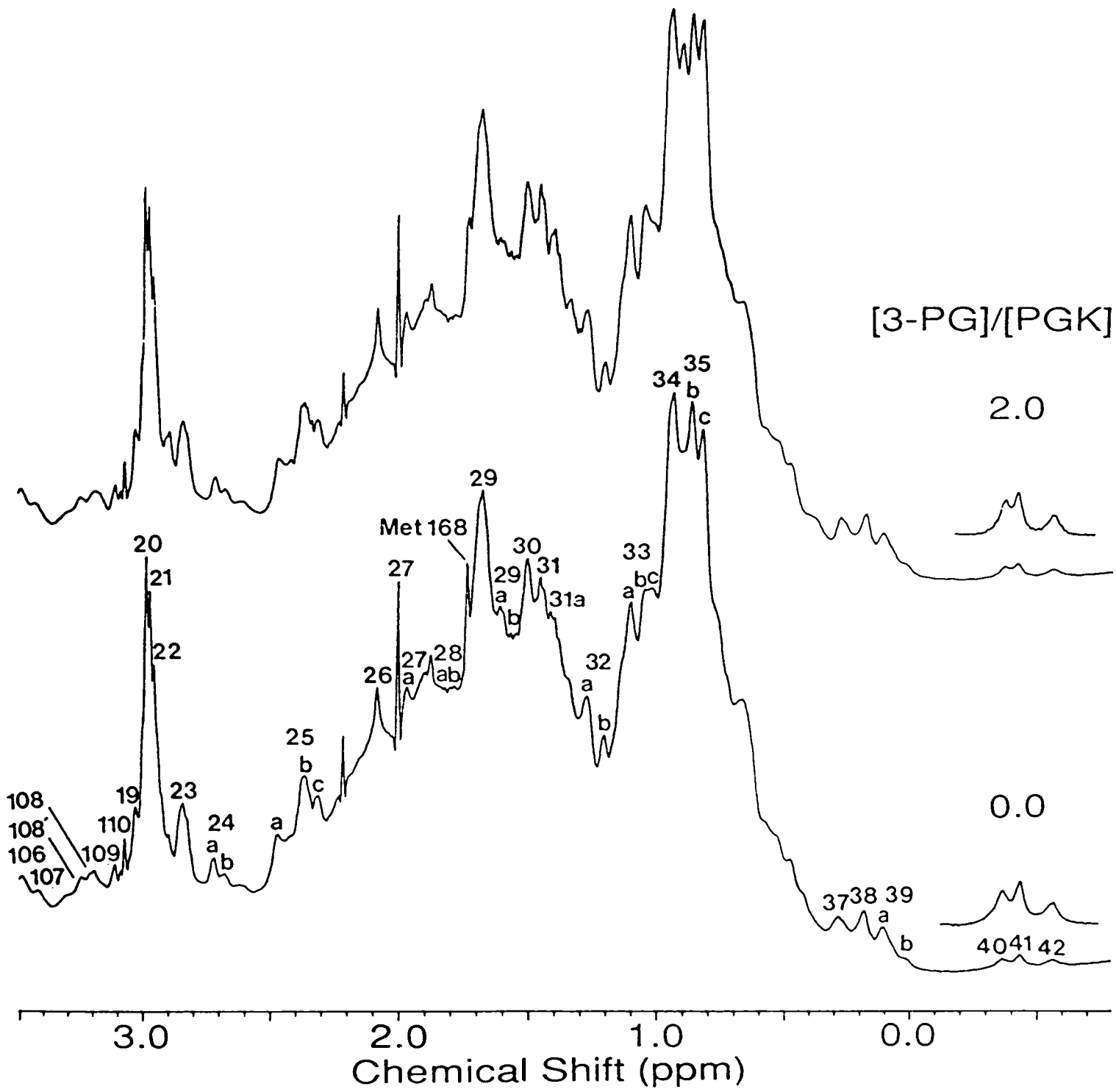

Figure 4-13B: Perturbations of the aliphatic region of the 500 MHz ^{1}H NMR spectrum of R168M PGK by 3-PG, at the ratios indicated and pH 7.1.

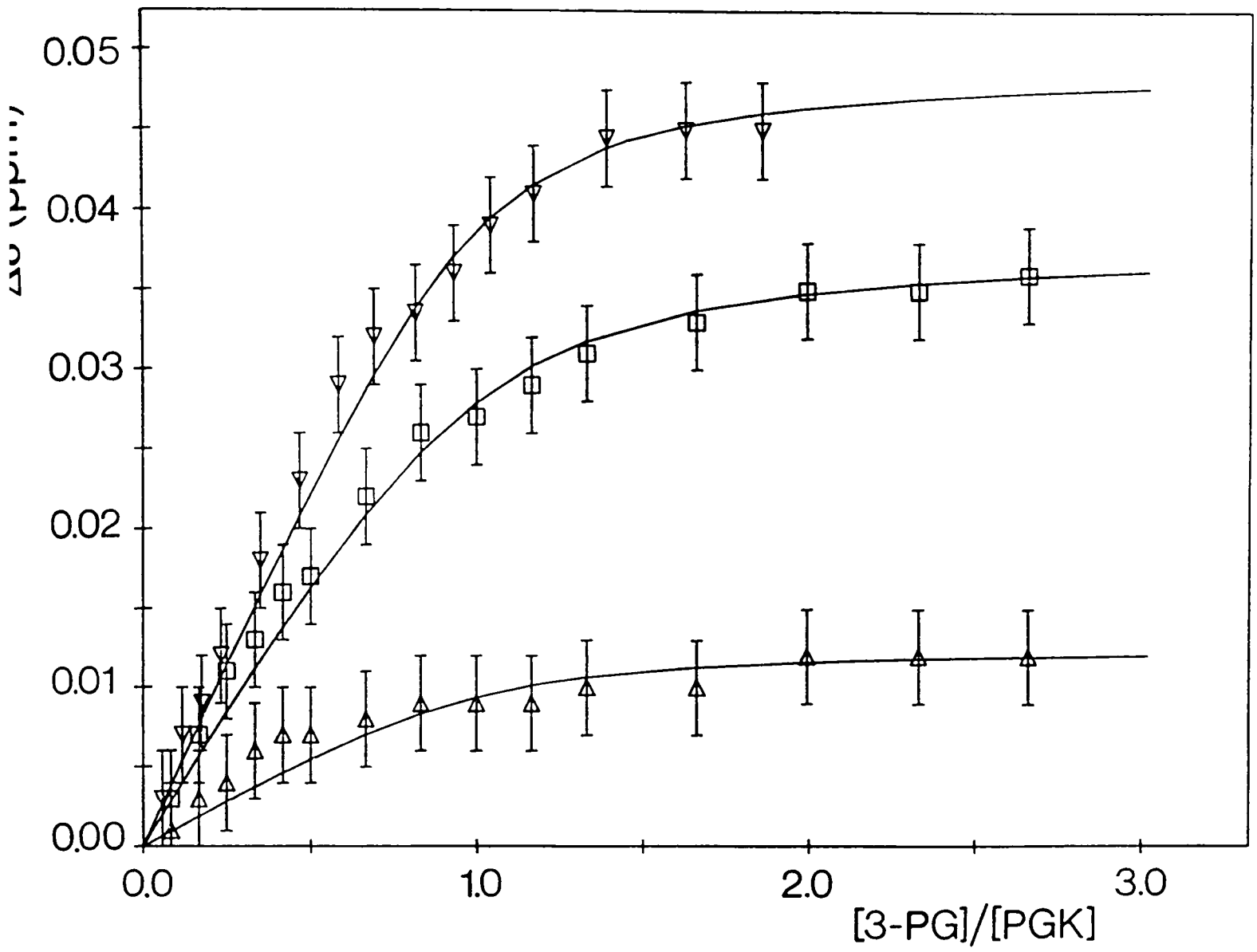

Figure 4-14: The change in the chemical shifts of peaks 3 (□; His 62), 4 (∇; His 167) and 5a (Δ; His 170) plotted as a function of 3-PG:R168M molar ratio. The continuous lines represent theoretical binding curves corresponding to a dissociation constant of 0.16 mM.

molecule, indicating that the mutants have the same gross fold in solution as wild-type PGK. However, small discernable effects due to minor reorientations of residues close to the sites of mutation were seen.

In order to understand any structural changes in solution additional (NOE) experiments have been carried out with the wild-type protein (Table 4-3). The results indicate that the average structure in solution of the interdomain region of free wild-type PGK is in some way different to that observed crystallographically. These results are also consistent with the suggestion that interdomain His 388 is in a different environment in solution compared to the crystalline state (§ 2.3.5). There is no evidence for structural differences within either domain and it has therefore been assumed that the individual domains have the same overall conformations in the crystal and solution states. This assumption is in agreement with the solution X-ray results of Ptitsyn *et al.* (1986). The assumption cannot be applied to the conformation of surface side-chains, however, as illustrated by Phe 342 (§ 2.3.3).

Nuclear Overhauser effects observed in the spectrum of R168M showed that the methionine side-chain is located in a similar position to the arginine it replaces. These NOEs also confirmed the assignment of resonances 3, 4 and 5a to histidines 62, 167 and 170 respectively. Observation of an NOE from peak 1 (His 123) to a resonance at 0.65 ppm in the spectrum of R168M confirmed that the conformation in this region of the N-terminal domain, remote from position 168, has remained unaffected by the mutation. Likewise, the NOEs seen from resonances 3 and 4 to the same peaks as observed for wild-type protein showed that the conformational effects which result in changes in the chemical shifts of residues close to the site of mutation are small in magnitude. The observed shifts of the 'basic patch' histidine resonances in the spectra of R168K and R168M cannot be attributed to protonation of these residues since their pK_a values remain outside the range of pH studied. Also,

the magnitude of the observed shifts in the lysine and methionine mutants are similar. The shifts of the 'basic patch' histidine resonances have therefore been attributed to minor adjustments in the conformations of these side-chains. The mutations of His 62 to a glutamine, and His 170 to an aspartic acid have also been found to produce effects due only to small conformational changes in the vicinity of the mutations, in addition to differences due directly to the local field effects of the substituted side-chains.

4.4.2. *Substrate bound mutant proteins*

The 3-PG binding studies described in Chapter 3 have been extended to include the four 'basic patch' mutant forms of yeast PGK.

The mutant H62Q appears to bind the substrate, 3-PG, in a similar fashion to wild-type PGK as indicated by the very similar spectral perturbations observed following addition of 3-PG to both proteins (Table 4-4). These include the relayed conformational changes in the interdomain region (Phe 185, Tyr 193 and His 388) and remote regions of the N-terminal domain (His 52, His 123 and His 149). The affinity for 3-PG binding, however, is slightly decreased as a result of the substitution.

In Chapter 3 it was shown that His 62 probably forms a hydrogen-bond with the bound substrate. The observed reduction in affinity, however, is too small to suggest the loss of a full hydrogen-bond (Fersht *et al.*, 1985). It is possible, of course, that the side-chain of Gln 62 will have a similar interaction with the bound substrate as the histidine it has replaced. While His 62 is a totally conserved residue (Appendix 1), the fact that the only observed natural mutation of 'basic patch' His 167 is to a Gln (in PGK from *Penicillium chrysogenum*; van Solingen *et al.*, 1988) supports this argument.

Addition of 3-PG to mutant H170D resulted in spectral changes analogous to, but of smaller magnitude than, those observed for the wild-type enzyme. The increase in the dissociation constant for 3-PG binding to mutant H170D

relative to wild-type PGK (Table 4-5) can be explained by the reduction in the charge of the 'basic patch' when the negatively charged aspartate side-chain is substituted for the neutral His 170. Slight changes in the conformations of the remaining 'basic patch' histidine residues, which may result in a reduction in the interaction between these residues and the triose substrate, have also been noted in this mutant.

On substitution of Arg 168 with either lysine (R168K) or methionine (R168M) the effects of 3-PG addition on the resonances of surface histidines 52, 123 and 149 and on the upfield shifted methyl resonances of the spectra are markedly reduced. Changes observed at these resonances result from alterations of the relative orientations of these groups with respect to nearby aromatic and/or carbonyl groups. It can therefore be concluded that mutations at position 168 tend to prevent the 3-PG induced changes in conformational equilibrium, observed on formation of the binary complex between this substrate and the native enzyme. A small movement of the positive charge at position 168 (~ 1 Å on going from Arg 168 to Lys 168), however, has only a small effect on the binding strength of 3-PG, while neutralisation of the charge (as in R168M) significantly lowers the enzyme's affinity for this substrate as is shown in Table 4-5. The smaller shifts (relative to the wild-type protein) observed for resonances of His 62 and His 167 following addition of 3-PG to both 168 mutants indicates that the time averaged interactions between these side-chains and the triose substrate have been altered.

4.4.3. *Effect of mutations on catalysis*

Kinetic studies on mutant H62Q show that both the K_m for 3-PG and the V_{max} have increased relative to the wild-type enzyme (from 0.75 mM to 1.20 mM and from 499 EU mg^{-1} to 980 EU mg^{-1} respectively; P.A. Walker, personal communication). The increased K_m is consistent with the observed small increase in K_d for 3-PG. The NMR observations of 3-PG binding suggest that

this substrate binds to mutant H62Q in a similar way to wild-type PGK and is therefore, presumably, correctly positioned for phosphoryl transfer from Mg.ATP. To explain the increased turnover of this enzyme relative to wild-type PGK it is neccessary to assume that binding of 1,3-P_2G has also been perturbed by about a factor of 2. Since dissociation of this substrate is the rate determining step in the catalytic reaction (Scopes, 1978), increasing its dissociation constant by a factor of ~ 2 would increase the rate by a similar factor, assuming that the rate of phosphoryl transfer remains unaltered.

From the mutations at positions 168 and 170 it can be seen that alterations of the charge in the sequence 168-170 reduce binding of 3-PG. The indications are that the anionic groups of this substrate lie closer to Arg 168 than to His 170. This is reflected not only in the K_d values determined using NMR spectroscopy but also in the K_m values from kinetic studies (Walker *et al.*, 1989). Kinetic data also show (see Table 4-5) that the mutation of His 170 to aspartate has little or no effect on the catalytic efficiency of the enzyme. In other words the introduction of a negative charge at position 170 in the sequence of yeast PGK does not reduce the binding of 3-PG enough to significantly influence catalysis. This is as might be expected, given that this residue is not totally conserved (Osinga *et al.*, 1985; Swinkels *et al.*, 1988) and does not appear to interact directly with the substrate (§ 3.3.1).

Kinetic studies of mutants R168K and R168M (Walker *et al.*, 1989) have shown that the catalytic efficiency of these enzymes has been reduced by about 7-fold and 40-fold respectively, relative to wild-type PGK (Table 4-5). The most prominent feature of the present NMR results which has to be correlated with the observed loss of activity of these mutants is the absence of extensive conformational changes seen on binding 3-PG to the wild-type enzyme. Possible explanations are that the substitutions at position 168 have altered the mobility of the binding-site in such a way that the optimum

conformation for catalysis cannot be attained or that the relative orientation of 3-PG binding to the enzyme has been changed. The results therefore indicate that Arg 168 is important for binding of 3-PG (and presumably 1,3-P_2G) and for correctly orientating it for phosphoryl transfer.

4.5. References

Banks, R.D., Blake, C.C.F., Evans, P.R., Haser, R., Rice, D.W., Hardy, G.W., Merrett, M. & Phillips, A.W. (1979) *Nature (Lond.) 279,* 773-777.

Blake, C.C.F. & Rice, D.W. (1981) *Phil. Trans. R. Soc. Lond. A. 293,* 93-104.

Fairbrother, W.J., Walker, P.A., Minard, P., Littlechild, J.A., Watson, H.C. & Williams, R.J.P. (1989) *Eur. J. Biochem.*, in press.

Fersht, A.R., Shi, J.P., Knill-Jones, J., Lowe, D.M., Wilkinson, A.J., Blow, D.M., Carter, P., Waye, M.M.Y. & Winter, G. (1985) *Nature (Lond.) 314,* 235-238.

Lesk, A.K. & Hardman, K.D. (1982) *Science 216,* 539-540.

Minard, P., Bowen, D., Littlechild, J.A., Watson, H.C. & Hall, L. (1989) *in preparation.*

Osinga, K.A., Swinkels, B.W., Gibson, W.C., Borst, P., Veeneman, G.H., van Boom, J.H., Michels, P.A.M. & Opperdoes, F.R. (1985) *EMBO J. 4,* 3811-3817.

Perkins, S.J. (1982) in *Biological Magnetic Resonance,* vol. 4 (Berliner, L.J. & Reubens, J. eds) pp. 192-336, Plenum Press, New York.

Philips, M., Roustan, C., Fattoum, A. & Pradel, L.-A. (1978) *Biochim. Biophys. Acta 523,* 368-376.

Ptitsyn, O.B., Pavlov, M.Y., Sinev, M.A. & Timchenko, A.A. (1986) in *Multidomain Proteins,* (Patthy, L. & Friedrich, P. eds) pp. 9-25, Akadémiai Kiadó, Budapest.

Swinkels, B.W., Evers, R. & Borst, P. (1988) *EMBO J. 7,* 1159-1165.

Tanswell, P., Westhead, E.W. & Williams, R.J.P. (1976) *Eur. J. Biochem. 63,* 249-262.

van Solingen, P., Muurling, H., Koekman, B. & van den Berg, J. (1988) *Nucleic Acid Res. 16,* 11823.

Walker, P.A., Littlechild, J.A., Hall, L. & Watson, H.C. (1989) *Eur. J. Biochem.* in press.

Watson, H.C. & Gamblin, S.J. (1985) *Proc. Int. Symp. Biomol. Struct. Interactions, Suppl. J. Biosci. 8,* 499-506.

Watson, H.C., Walker, N.P.C., Shaw, P.J., Bryant, T.N., Wendell, P.L., Fothergill, L.A., Perkins, R.E., Conroy, S.C., Dobson, M.J., Tuite, M.F., Kingsman, A.J. & Kingsman, S.M. (1982) *EMBO J. 1,* 1635-1640.

Wilson, H.R., Williams, R.J.P., Littlechild, J.A. & Watson, H.C. (1988) *Eur. J. Biochem. 170,* 529-538.

Wüthrich, K. (1986) *NMR of Proteins and Nucleic Acids,* John Wiley & Sons, New York.

Zoller, M.J. & Smith, M. (1982) *Nucleic Acid Res. 10,* 6487-6500.

Chapter 5

INTERACTION OF PARAMAGNETIC ANIONS WITH YEAST PGK

5.1. Introduction

Binding of the triose substrate, 3-PG, to PGK is largely due to electrostatic interactions of the trianion with the positively charged 'basic patch' region of the N-terminal domain (Chapters 3 and 4). Kinetic studies of the effects of a variety of salts on the enzymes activity, have shown that anions (especially multivalent anions) can cause activation of the enzyme, but inhibit at higher concentrations (Larsson-Raźnikiewicz & Jansson, 1973; Scopes, 1978a; Khamis & Larsson-Raźnikiewicz, 1981). In a subsequent gel filtration study Scopes (1978b) has shown sulphate and phosphate to bind at a "site adjacent to or at the area where phosphate transfer takes place in the catalytic reaction". The ionic strength was found to have a substantial effect on the dissociation constants of sulphate and phosphate, a lesser effect on ATP, and a relatively small effect on ADP and 3-PG (Scopes, 1978b). Khamis & Larsson-Raźnikiewicz (1981) suggested the existence of at least two sulphate binding sites, one which was defined as a general anion binding site, and a second, being the catalytic centre. The former seems to have higher affinity for sulphate than the latter. Competition between primary sulphate binding and 3-PG binding has also been demonstrated in recent ^{1}H NMR studies of the enzyme (H.C. Graham, personal communication).

In order to define the site(s) of general anion binding to the protein, the paramagnetic relaxation probe, $[Cr(CN)_6]^{3-}$, and shift probe, $[Fe(CN)_6]^{3-}$, have been used. The spectral perturbations caused by paramagnetic ions have been reviewed in detail by Dwek (1973), James (1975), Burton *et al.* (1979) and Jardetzky & Roberts (1981), and are outlined in Appendix 3.

The $[Cr(CN)_6]^{3-}$ complex (high-spin $3d^3$ ion, S = 3/2) is an isotropic dipolar relaxation probe and the nuclear dipole-dipole contribution to the transverse relaxation time, T_2, is given by

$$\frac{1}{T_{2,M}} = f(\tau_c)\ \frac{1}{r^6} \qquad \textbf{(5-1)}$$

where $1/T_{2,M}$ is the transverse relaxation rate in the presence of the probe, r is the distance between the nucleus and the paramagnetic ion and τ_c is the correlation time for the dipolar relaxation. Relative values of r can be obtained for two nuclei, i and j, by taking the ratio

$$\frac{(1/T_{2,M})_i}{(1/T_{2,M})_j} = \frac{r_j^6}{r_i^6}. \qquad \textbf{(5-2)}$$

Since low-spin Fe(III) has a short electron-spin relaxation time, $[Fe(CN)_6]^{3-}$ (low-spin $3d^5$ ion, S = 1/2) acts as a shift probe. In this case the ratio of the dipolar (pseudo-contact) shifts, assuming axial symmetry, is

$$\frac{(\Delta\omega_M)_i}{(\Delta\omega_M)_j} = \left(\frac{3\cos^2\theta_i - 1}{r_i^3} \right)_{av} \Big/ \left(\frac{3\cos^2\theta_j - 1}{r_j^3} \right)_{av} \qquad \textbf{(5-3)}$$

where $\Delta\omega_M$ is the shift from the corresponding position in the diamagnetic complex, r is the distance between the nucleus and the paramagnetic ion and θ is the angle between the vector r and the principal symmetry axis of the complex.

The paramagnetic shifts induced by $[Fe(CN)_6]^{3-}$ on resonances of amines, however, have been shown to result from a predominantly contact interaction (*i.e.* delocalisation of unpaired electron spin density at the resonating nucleus) (Huang & Moore, 1983). The contact (Fermi) shift is given by

$$\frac{\Delta\omega_M}{\omega_I} = -\left(\frac{A}{\hbar} \right) \frac{g\beta S(S+1)}{3kT\gamma_I} \qquad \textbf{(5-4)}$$

where $A/\hbar$ is the hyperfine coupling constant in rad s^{-1}, g is the Landé g-factor, γ_I is the magnetogyric ratio of the hydrogen nuclei in rad s^{-1} G^{-1}, β is the Bohr magneton, S is the total electron spin and ω_I is the irradiating frequency. Equation (5-4) is only valid for systems with isotropic g-values and can, therefore, not be used in the case of $[Fe(CN)_6]^{3-}$ ($|g_x| = 2.35$, $|g_y| = 2.10$, $|g_z| = 0.915$; Bleaney & O'Brien, 1956). Paramagnetic shifts induced by $[Fe(CN)_6]^{3-}$ can, however, be used in a qualitative way to define the binding site(s) of this anion (see for example Eley *et al.*, 1982).

Diamagnetic $[Co(CN)_6]^{3-}$ was also added to the protein in a preliminary experiment, in order to distinguish between direct conformational effects and paramagnetic induced effects. This anion has also been shown to activate the enzyme at low concentrations and inhibit at higher concentrations (Wilson *et al.*, 1988; H.C. Graham, personal communication; see Figure 5-1). This result is consistent with those of Scopes (1978a) and suggests that the hexacyanide anions also bind at, or near to, the active site of the enzyme. $[Co(CN)_6]^{3-}$ binding has also been demonstrated to compete directly with binding of the triose substrate, 3-PG (H.C. Graham, personal communication).

5.2. Experimental methods

5.2.1. *Metal hexacyanide titrations*

The potassium salts of $[Cr(CN)_6]^{3-}$ (2 mM), $[Co(CN)_6]^{3-}$ (60 mM) and $[Fe(CN)_6]^{3-}$ (60 mM) were titrated (1-4 µl aliquots) into solutions of wild-type PGK (~ 1 mM prepared as described in § 2.2.5) with the 1D ^1H NMR spectra being recorded following each addition. As for 3-PG titrations (§ 3.2.1) the pH of the inorganic probe solutions were adjusted to be the same as the protein solutions (7.10 ± 0.005). The pH of the protein sample was measured both before and after completion of the titration, with any variation being taken into account in analysis of the spectra.

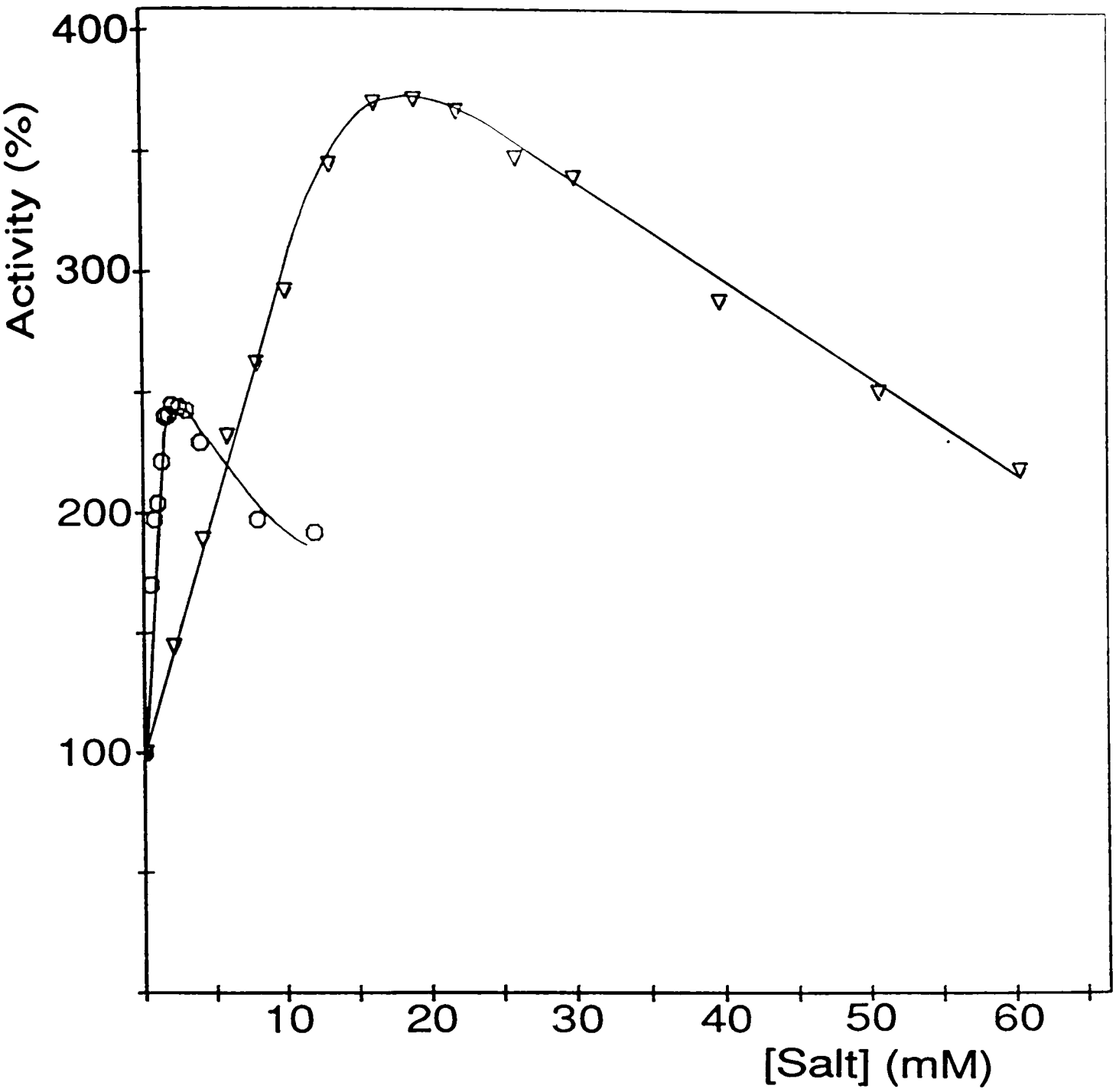

Figure 5-1: The effects of $(NH_4)_2SO_4$ (▽) and $K_3[Co(CN)_6]$ (○) on the activity of yeast PGK. In each case [3-PG] = 0.5 mM, [ATP] = 0.5 mM and $[MgCl_2]$ = 1.5 mM, T = 25°C. Data supplied by H.C. Graham.

5.3. Results

5.3.1. *Titration with $[Cr(CN)_6]^{3-}$*

Small aliquots of a solution of $K_3[Cr(CN)_6]$ were added to a solution of PGK to give molar ratios of paramagnetic anion:enzyme ranging from 0.003:1 to 0.08:1, with 500 MHz ^1H NMR spectra being recorded after each addition.

The effects on the aromatic region of the spectrum at a $[[Cr(CN)_6]^{3-}]$:[PGK] ratio of 0.012:1 are illustrated in Figure 5-2. From the paramagnetic difference spectrum (Figure 5-2C) it can be seen that the only aromatic resonances significantly broadened in the presence of the relaxation probe at this ratio are those assigned to the 'basic patch' histidines 62, 167 and 170. A plot of the reciprocal change in peak height as a function of the molar ratio of PGK:$[Cr(CN)_6]^{3-}$ ($1/\Delta p$ versus [PGK]/$[[Cr(CN)_6]^{3-}]$; Figure 5-3) enables an estimation of the relative distances of the 'basic patch' histidine protons from the paramagnetic probe. The ratios of the slopes in Figure 5-3 yield the broadening ratios $(R_i)_{T2} = (1/T_{2,M})_3/(1/T_{2,M})_i$, using resonance 3 as a reference, and hence the distance ratios $(R_i)_{T2}^{1/6} = r_i/r_3$ (Table 5-1; see Appendix 3 for details).

A computer program was written to determine coordinates of bound $[Cr(CN)_6]^{3-}$ to satisfy the calculated distance ratios. The 'basic patch' histidine coordinates used were those from the X-ray crystallographic structure (Watson *et al.*, 1982). The site of $[Cr(CN)_6]^{3-}$ binding to PGK thus determined is shown in Figure 5-4, and the average calculated distances from the histidine nuclei to the paramagnetic ion, $\langle r_i \rangle$, are given in Table 5-1. The coordinates of the bound anion were also calculated using a program written by Dr M.J. Sutcliffe (Inorganic Chemistry Laboratory, University of Oxford) which fitted the experimentally determined slopes by calculation of error functions using simultaneous scaling of all theoretical values. This approach gives all slopes equal weighting and eliminates possible errors due to

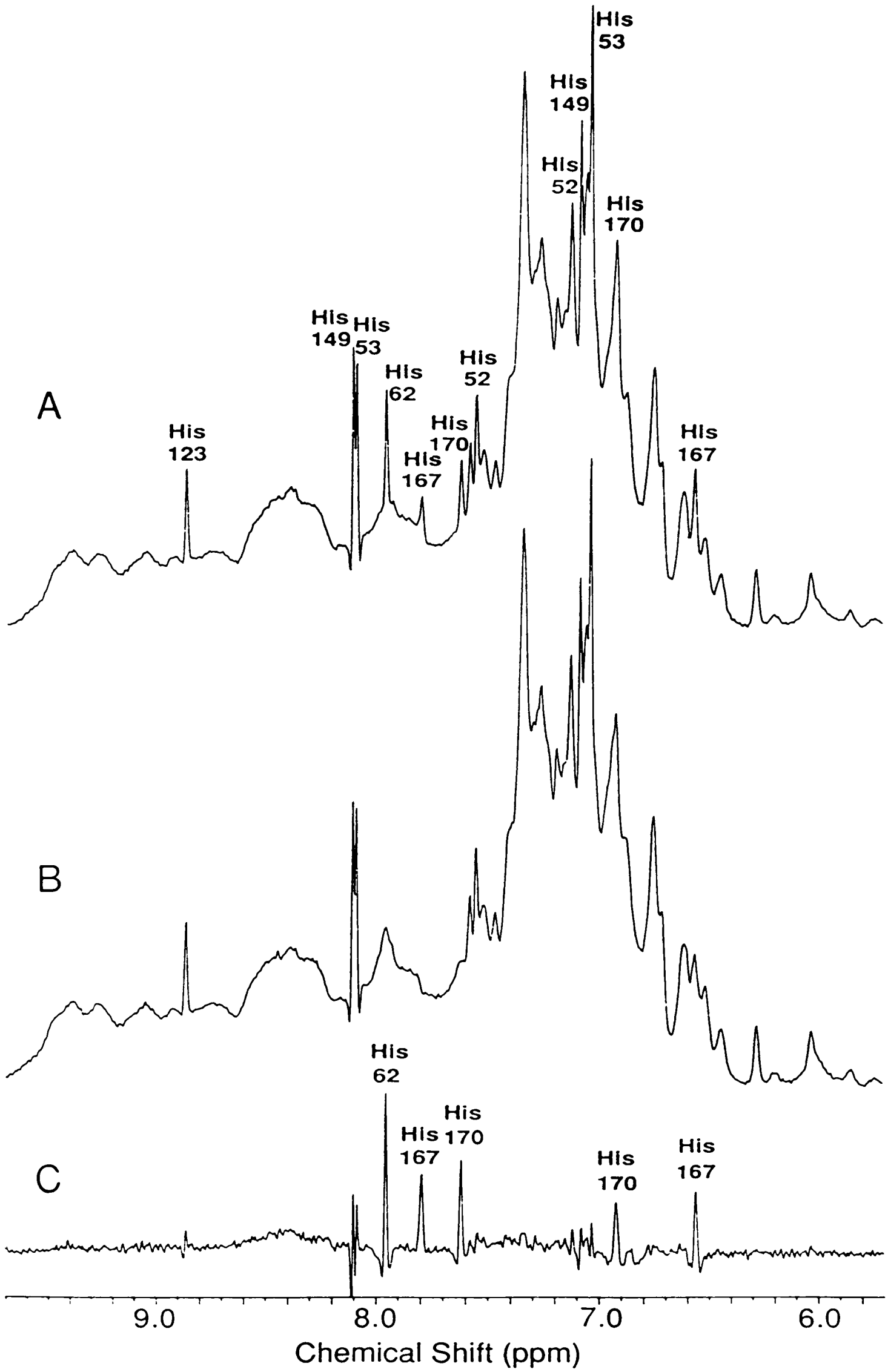

Figure 5-2: Perturbation of the aromatic region of the 500 MHz ^{1}H NMR spectrum of yeast PGK by $[Cr(CN)_6]^{3-}$. (A) Spectrum in the absence of $[Cr(CN)_6]^{3-}$. (B) Spectrum in the presence of a 0.012:1 molar ratio of $[Cr(CN)_6]^{3-}$:protein. (C) The difference spectrum (A) - (B).

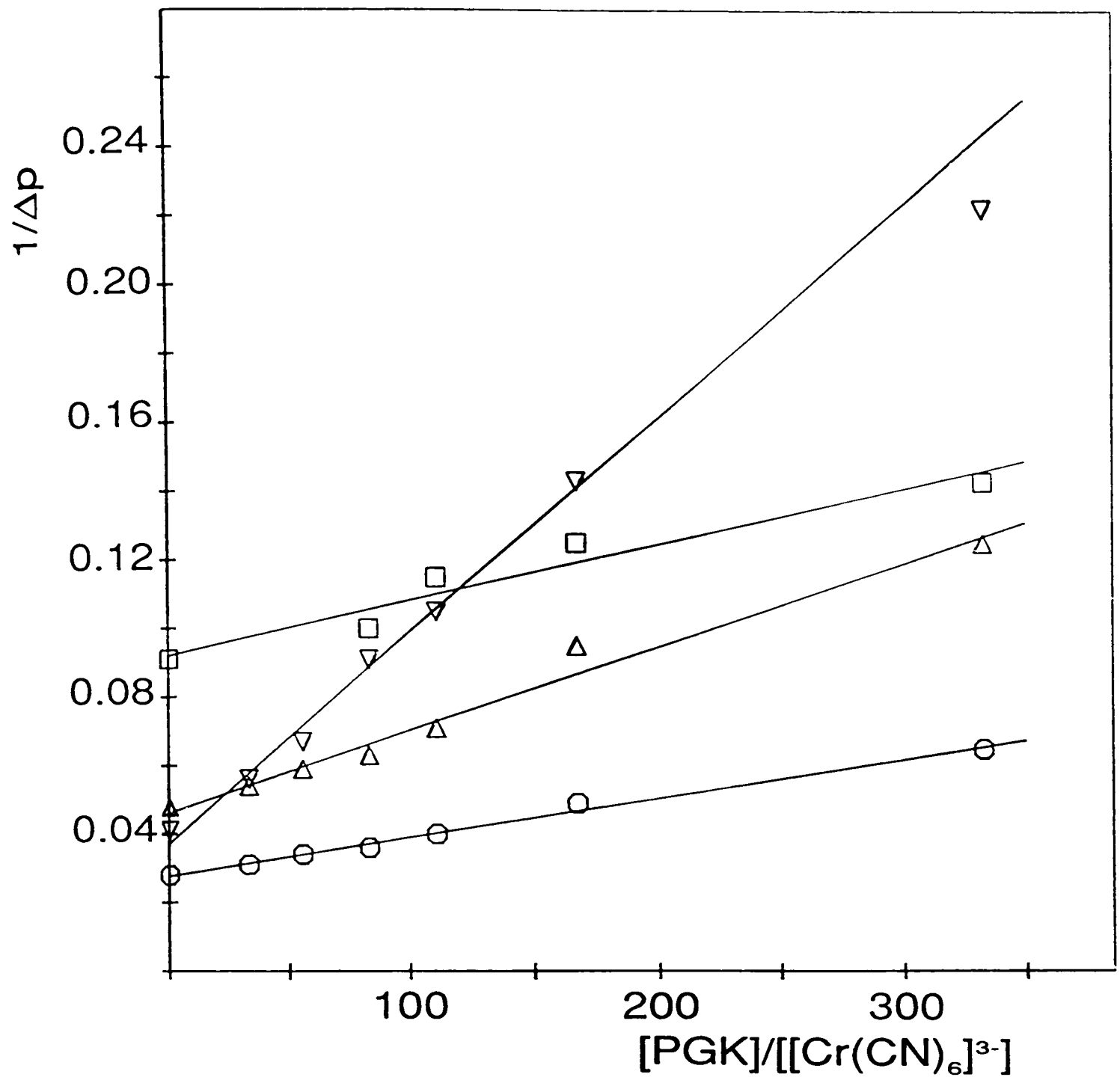

Figure 5-3: Plot of the change in peak height (Δp) of 'basic patch' histidine resonances 3 (○; His 62), 4 (□; His 167), 5a (△; His 170) and 15b (▽; His 167) as a function of PGK:$[Cr(CN)_6]^{3-}$ concentration ratio.

Table 5-1: Relative broadenings of the 'basic patch' histidine resonances resulting from $[Cr(CN)_6]^{3-}$ binding.

Slopes were determined from Figure 5-3.

Parameter	Resonance			
	3 (His 62)	4 (His 167)	5a (His 170)	15b (His 167)
slope × 10^4	1.15 ± 0.10	1.61 ± 0.20	2.43 ± 0.10	6.11 ± 0.35
broadening ratio $(R_i)_{T2}$	1	1.40 ± 0.30	2.11 ± 0.30	5.31 ± 0.70
distance ratio $(R_i)_{T2}^{1/6} = r_i/r_3$	1	1.06 ± 0.04	1.13 ± 0.03	1.32 ± 0.03
average calculated distance $\langle r_i \rangle$/Å	7.3	7.8	8.3	9.7

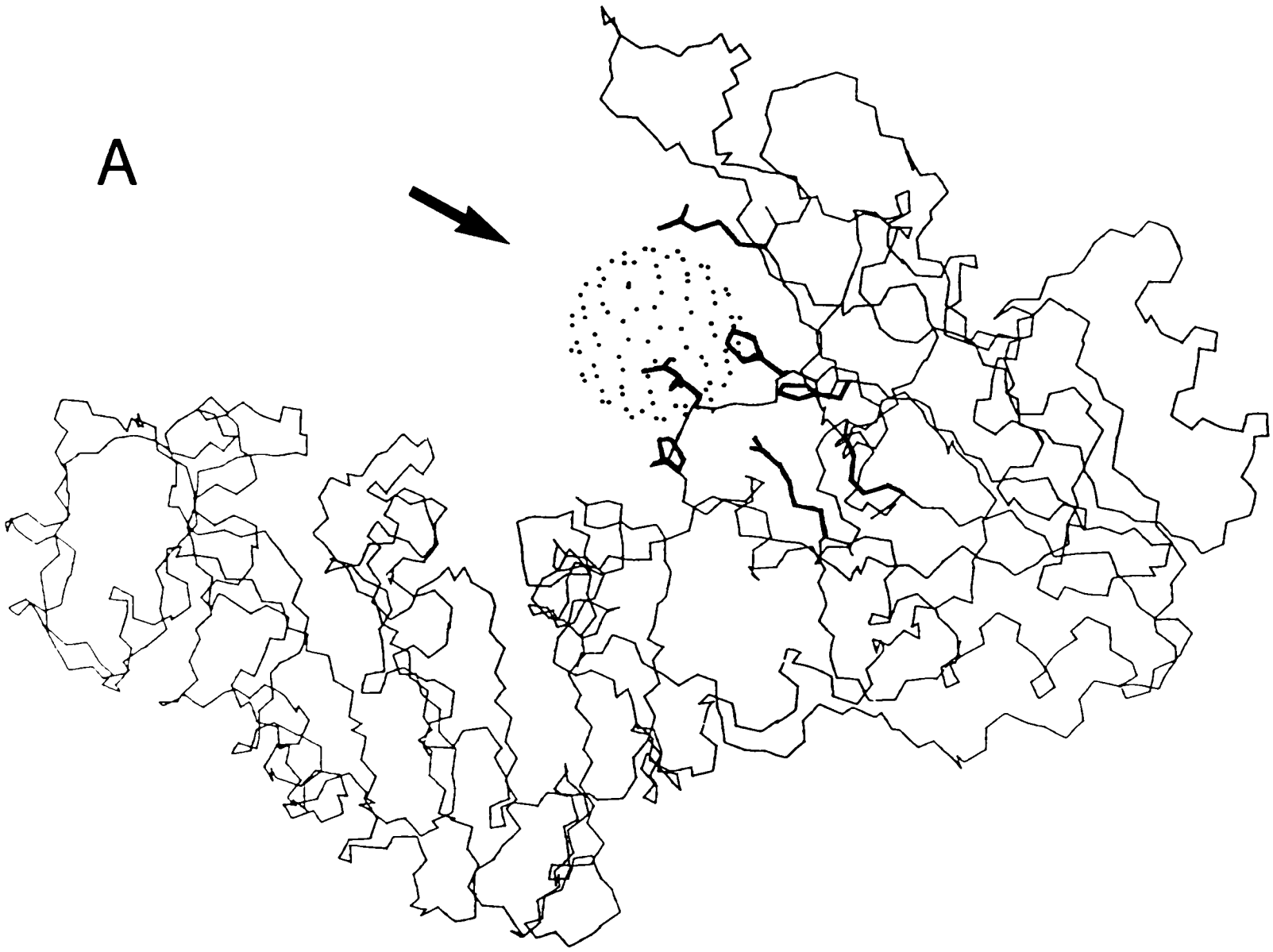

Figure 5-4: Average position of $[Cr(CN)_6]^{3-}$ binding to yeast PGK as calculated from the relative broadenings of the resonances of His 62, His 167 and His 170. The average coordinates, with standard deviations in parentheses, are $\langle x \rangle$ = 18.16 (0.15), $\langle y \rangle$ = -2.39 (0.54), $\langle z \rangle$ = 6.78 (0.50). (A) The position of the anion superposed on the main chain atoms of yeast PGK. The 'basic patch' residues are highlighted in red. (B) A stereo drawing of the binding site from the direction of the arrow in (A). The protein coordinates used are those of Watson *et al.* (1982), available from the Brookhaven Protein Data Bank.

inaccuracies in the chosen reference slope. The coordinates thus calculated were found to be in good agreement with those obtained using the ratio method.

It appears from Figure 5-4B that the $[Cr(CN)_6]^{3-}$ ion interacts most closely with the positively charged side-chains of Arg 65 and Arg 168. The latter was shown in Chapter 4 to be important for binding of the triose substrate, 3-PG. This model for $[Cr(CN)_6]^{3-}$ binding, however, has assumed a rigid protein conformation identical to that determined crystallographically. It has already been established (§ 4.3.2) that the conformation of the 'basic patch' region in solution is in some way different from that of the X-ray crystal structure. Also, the resonances of His 62, His 167 and His 170 undergo small diamagnetic shifts on binding the structural homologue $[Co(CN)_6]^{3-}$ (§ 5.3.2) which are indicative of some conformational rearrangement in the 'basic patch' region on binding the hexacyanide anions. Such changes may result in closer interactions between Arg 38 and the trianion.

A selected set of resonances are also observed to broaden in the aliphatic region of the spectrum on addition of small amounts of $[Cr(CN)_6]^{3-}$ (Figure 5-5). The broadening effect is very much dependent on the distance of the bound paramagnetic ion from the broadened residue (*i.e.* there is an r^{-6} relationship). This is illustrated in Figure 5-6, where the broadening ratio, relative to resonance 3, is plotted against the distance from the paramagnetic ion, assuming a distance of 7.3 Å from the C2-H of His 62 (Table 5-1). If an upper limit of $r_i \approx 12.5$ Å ($(R_i)_{T2} \approx 25$) is assumed to result in observable broadening then the residues listed in Table 5-2 may be expected to give rise to the resonances observed in the paramagnetic difference spectrum (Figure 5-5C), again assuming $[Cr(CN)_6]^{3-}$ binding as in Figure 5-4. The most significant broadening effects in the aliphatic region are of peaks 22a, 32a, 35a, 35c and 37a. A component of peak 32a (1.26 ppm) has NOE connectivities to peaks 3 (His 62) and 4 (His 167) (§ 4.3.2) and would

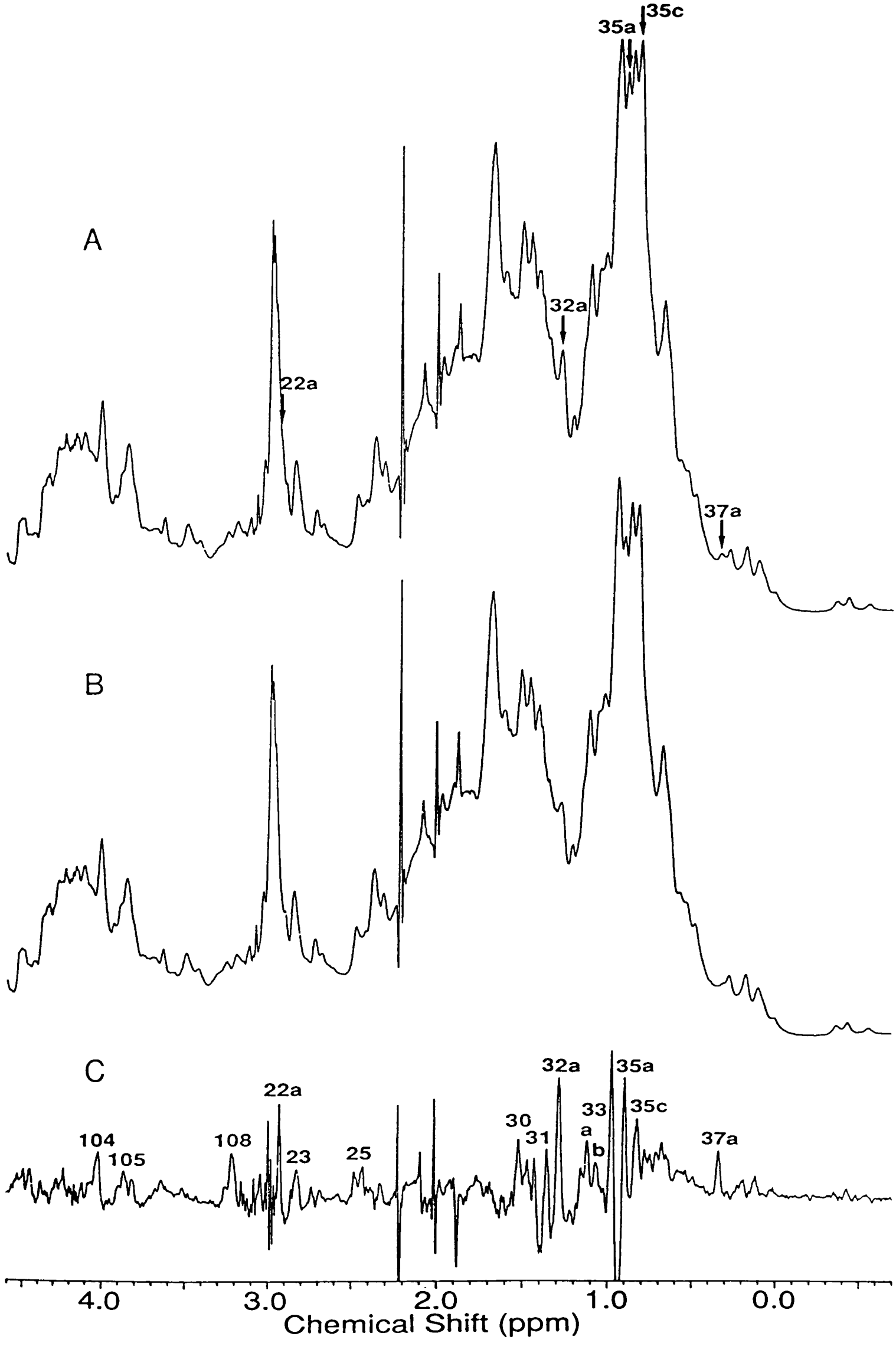

Figure 5-5: Perturbation of the aliphatic region of the 500 MHz ^{1}H NMR spectrum of yeast PGK by $[Cr(CN)_6]^{3-}$. (A) Spectrum in the absence of $[Cr(CN)_6]^{3-}$. (B) Spectrum in the presence of a 0.030:1 molar ratio of $[Cr(CN)_6]^{3-}$:protein. (C) The difference spectrum (A) - (B).

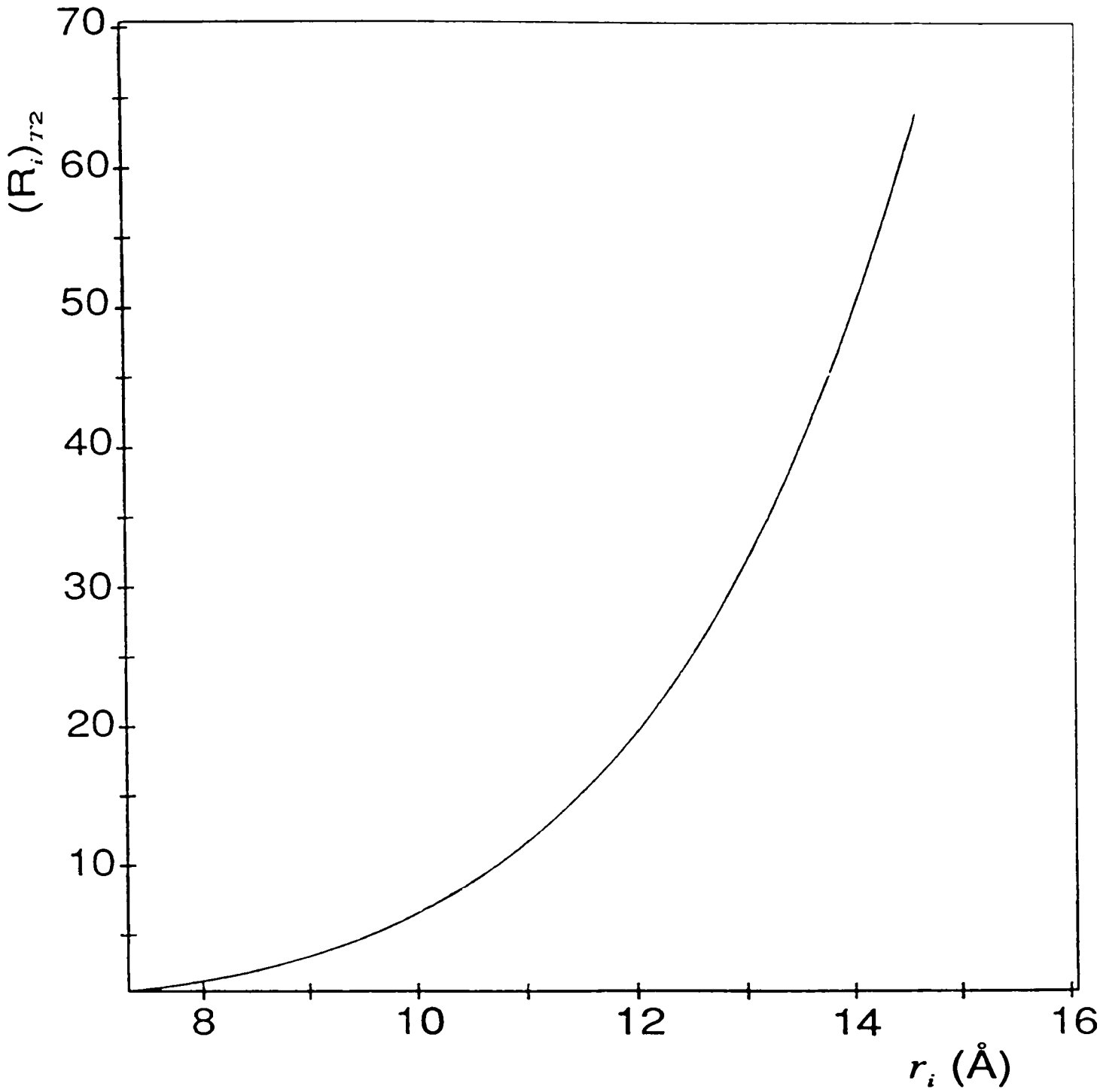

Figure 5-6: Theoretical broadening ratio ($(R_i)_{T2} = r_i/r_3$) plotted as a function of distance (r_i) from the paramagnetic anion, $[Cr(CN)_6]^{3-}$. A distance of 7.3 Å has been assumed from the C2-H of His 62 to the paramagnetic centre (r_3).

Table 5-2: Aliphatic groups less than 12.5 Å from bound $[Cr(CN)_6]^{3-}$ as calculated using the coordinates from Figure 5-4.

Residue	Proton(s)	r_i/Å
Asn 25	α	11.8
	β	10.0
Leu 28	δ_2	12.5
His 62	β	12.1
Leu 63	α	9.0
	β	10.9
	δ_1	12.5
Gly 64	α	9.3
Arg 65	α	7.9
	β	6.9
	γ	7.8
	δ	8.7
Pro 66	γ	12.4
	δ	10.2
Asn 67	α	11.4
	β	11.6
Asn 119	β	11.0
Ile 124	γ_1	11.8
	δ_1	11.8
Glu 125	α	11.3
	β	11.2
	γ	12.2
Gly 128	α	12.1
Gly 164	α	11.1
His 167	β	12.4
Arg 168	β	11.2
	γ	10.4
	δ	9.3
His 170	β	11.8
Gly 371	α	11.9
Gly 392	α	10.8
Gly 393	α	12.2
Gly 394	α	10.8
Ala 395	α	11.3
	β	10.7

therefore be expected to broaden in the presence of $[Cr(CN)_6]^{3-}$. The broadening data are therefore consistent with the NOE data. It is not possible, however, to assign peak 32a on the basis of the crystal structure. Peak 37a has been assigned to the β-CH_3 of an alanine or the γ-CH_3 of a threonine (§ 2.3.2; Figure 2-9). From Table 5-2 it can be seen that the only alanine or threonine side-chain within 12.5 Å of the proposed $[Cr(CN)_6]^{3-}$ binding site is Ala 395. Peak 22a is probably due to the δ-CH_2s of either Arg 65 or Arg 168, while peaks 35a and 35c may be due to the methyl protons of Leu 28, Leu 63 and/or Ile 124. The remaining intensity in the paramagnetic difference spectrum can be accounted for by the residues listed in Table 5-2, indicating that the proposed single site for $[Cr(CN)_6]^{3-}$ binding is qualitatively correct. For instance, the broadening observed around 4 ppm (peaks 104 and 105) may be attributed to Gly 64 with contributions from glycines 128, 164, 371, 392, 393 and 394. The broadening observed at peak 108 (~ 3.2 ppm) may be accounted for by the β-CH_2s of His 62, His 167 and His 170, and the δ-CH_2s of Arg 65 and Arg 168. Broadening of peaks 23 (~ 2.8 ppm) and 25 (~ 2.4 ppm) is probably due to the proximity of the β-CH_2s of Asn 25, Asn 67 and Asn 119 to the bound paramagnetic centre.

At higher concentrations of $[Cr(CN)_6]^{3-}$ additional peaks are observed to broaden. These include the upfield shifted methyl resonance 41 which has been tentatively assigned to Thr 375 (§ 2.3.4). Observation of this broadening is consistent with the position of Thr 375 in the crystal structure (Figure 5-4), ~ 17.2 Å from the proposed $[Cr(CN)_6]^{3-}$ binding site.

5.3.2. *Titration with $[Co(CN)_6]^{3-}$*

A titration of PGK at 300 K and pH 7.1 with $K_3[Co(CN)_6]$ was carried out as described in § 5.2.1. The effect on the aromatic region of the ^1H NMR spectrum is illustrated in Figure 5-7. The resulting shifts of the 'basic patch' histidine resonances are plotted against the $[[Co(CN)_6]^{3-}]$:[PGK] ratios in Figure 5-8. Small effects were also noted at peaks 7a, 7c, 8, 8b, 8c, 14a′,

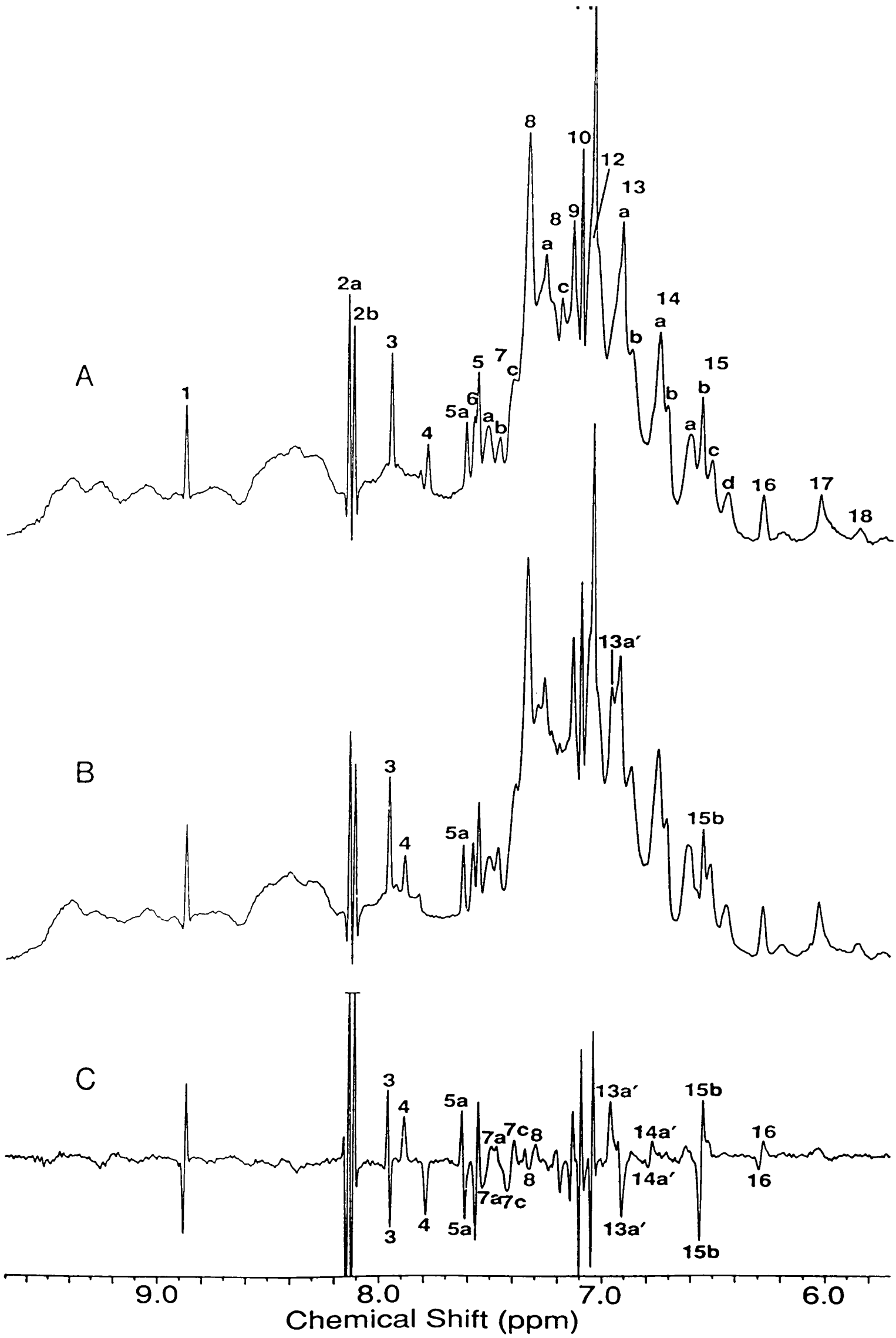

Figure 5-7: Perturbation of the aromatic region of the 500 MHz ^{1}H NMR spectrum of yeast PGK by $[Co(CN)_6]^{3-}$. (A) Spectrum in the absence of $[Co(CN)_6]^{3-}$. (B) Spectrum in the presence of a 2.2:1 molar ratio of $[Co(CN)_6]^{3-}$:protein. (C) The difference spectrum (B) - (A).

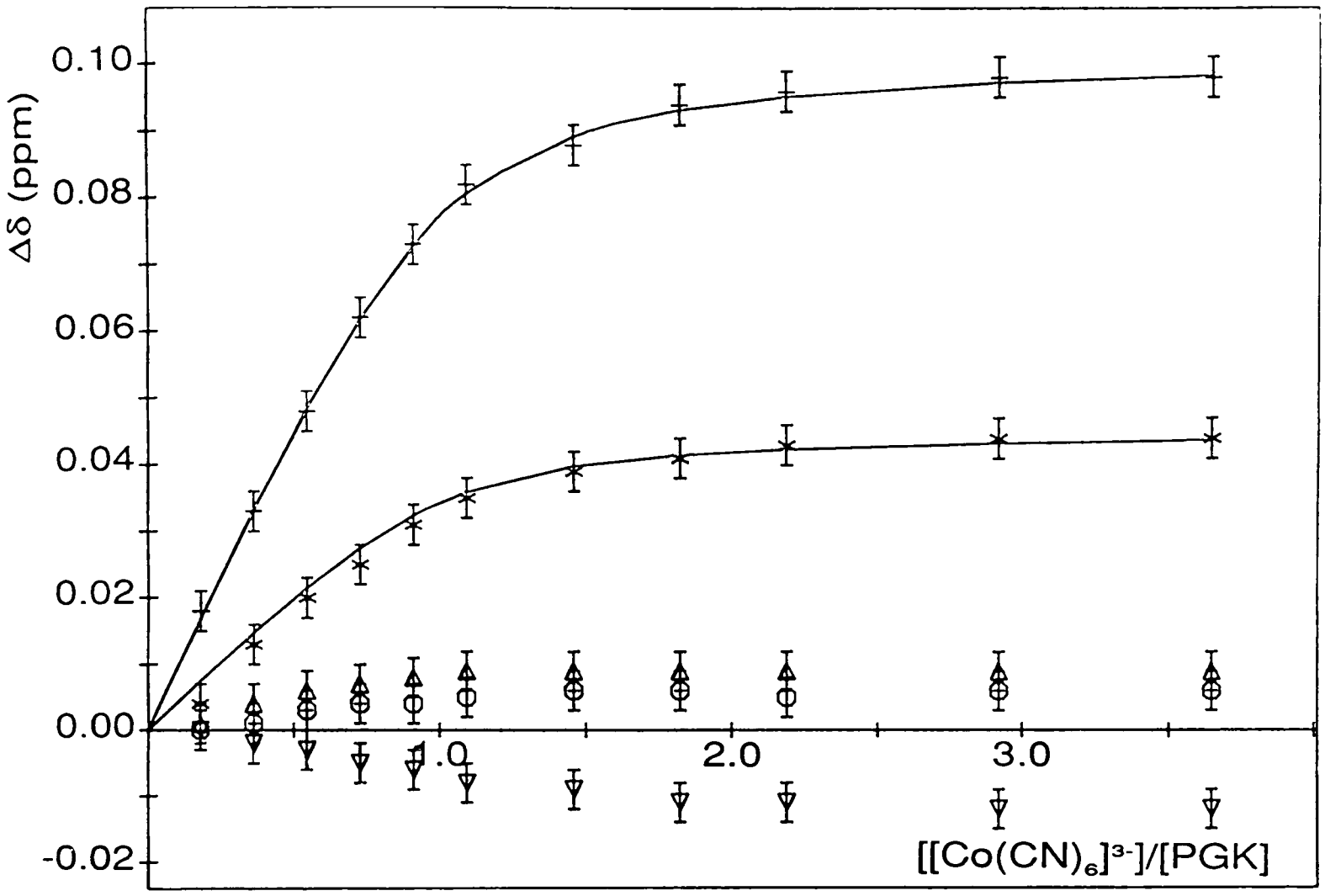

Figure 5-8: The change in the chemical shifts of peaks 3 (○; His 62), 4 (+; His 167), 5a (Δ; His 170), 13a′ (∗; His 170) and 15b (∇; His 167) plotted as a function of the $[Co(CN)_6]^{3-}$:enzyme molar ratio. The continuous lines represent theoretical binding curves corresponding to a dissociation constant of 0.065 mM.

15a, 15c, 15d, 16 and 17 (Figure 5-7C) . [Note that the small upfield shifts of titratable histidine peaks 1, 2a, 2b, 5, 9, 10 and 11 are attributed to a slight increase in the pH of the solution on addition of $[Co(CN)_6]^{3-}$]. With the exception of resonances 4 and 13a′ (His 167 and His 170 respectively) all total shifts were < 0.02 ppm.

Small effects are also observed in the aliphatic region of the spectrum. Most of the peaks which are perturbed by addition of diamagnetic $[Co(CN)_6]^{3-}$ were found to be broadened by the relaxation probe $[Cr(CN)_6]^{3-}$, indicating that these perturbations are due to small conformational rearrangements in the vicinity of the anion binding site. All the observed effects, in both the aromatic and aliphatic regions of the spectrum, saturated at similar molar ratios of $[Co(CN)_6]^{3-}$ to PGK (up to a 3.6 fold excess of the anion over the protein was used) indicating that there is only one significant general anion binding site on the protein. At higher molar ratios of anion to protein (~ 10:1) there is, however, evidence to suggest that other weak binding sites exist (Wilson *et al.*, 1988; see § 5.3.3).

5.3.2.1. Dissociation constant for $[Co(CN)_6]^{3-}$ binding

The dissociation constant for $[Co(CN)_6]^{3-}$ binding to PGK can be determined in the same way as for 3-PG binding (§§ 3.2.2 & 3.3.3). The shifts of resonances 4 and 13a′ have been plotted against the molar ratio of $[Co(CN)_6]^{3-}$:PGK in Figure 5-8, and the data used to evaluate the dissociation constant of the trianion assuming that there is a single anion binding site. The K_d for $[Co(CN)_6]^{3-}$ and PGK was thus calculated to be 0.065 ± 0.010 mM (I = 0.10 M, pH = 7.1, T = 300 K).

5.3.3. *Titration with $[Fe(CN)_6]^{3-}$*

The addition of $[Fe(CN)_6]^{3-}$ was carried out in the same way as the diamagnetic blank. The effects on the spectrum are illustrated in Figures 5-9 and 5-10. The major shifts observed in the aromatic region of the spectrum are

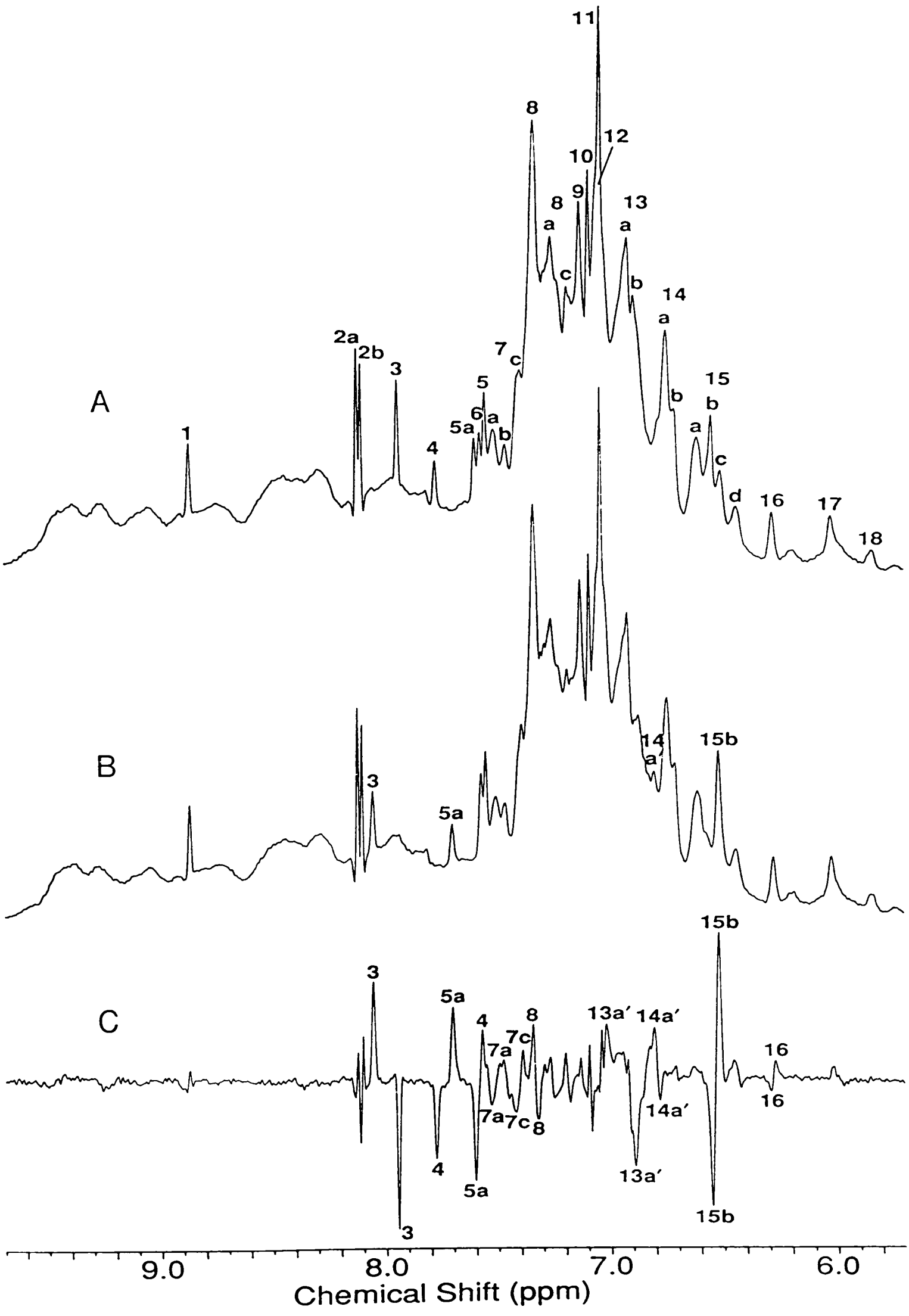

Figure 5-9: Perturbation of the aromatic region of the 500 MHz ^{1}H NMR spectrum of yeast PGK by $[Fe(CN)_6]^{3-}$. (A) Spectrum in the absence of $[Fe(CN)_6]^{3-}$. (B) Spectrum in the presence of a 0.86:1 molar ratio of $[Fe(CN)_6]^{3-}$:protein. (C) The difference spectrum (B) - (A).

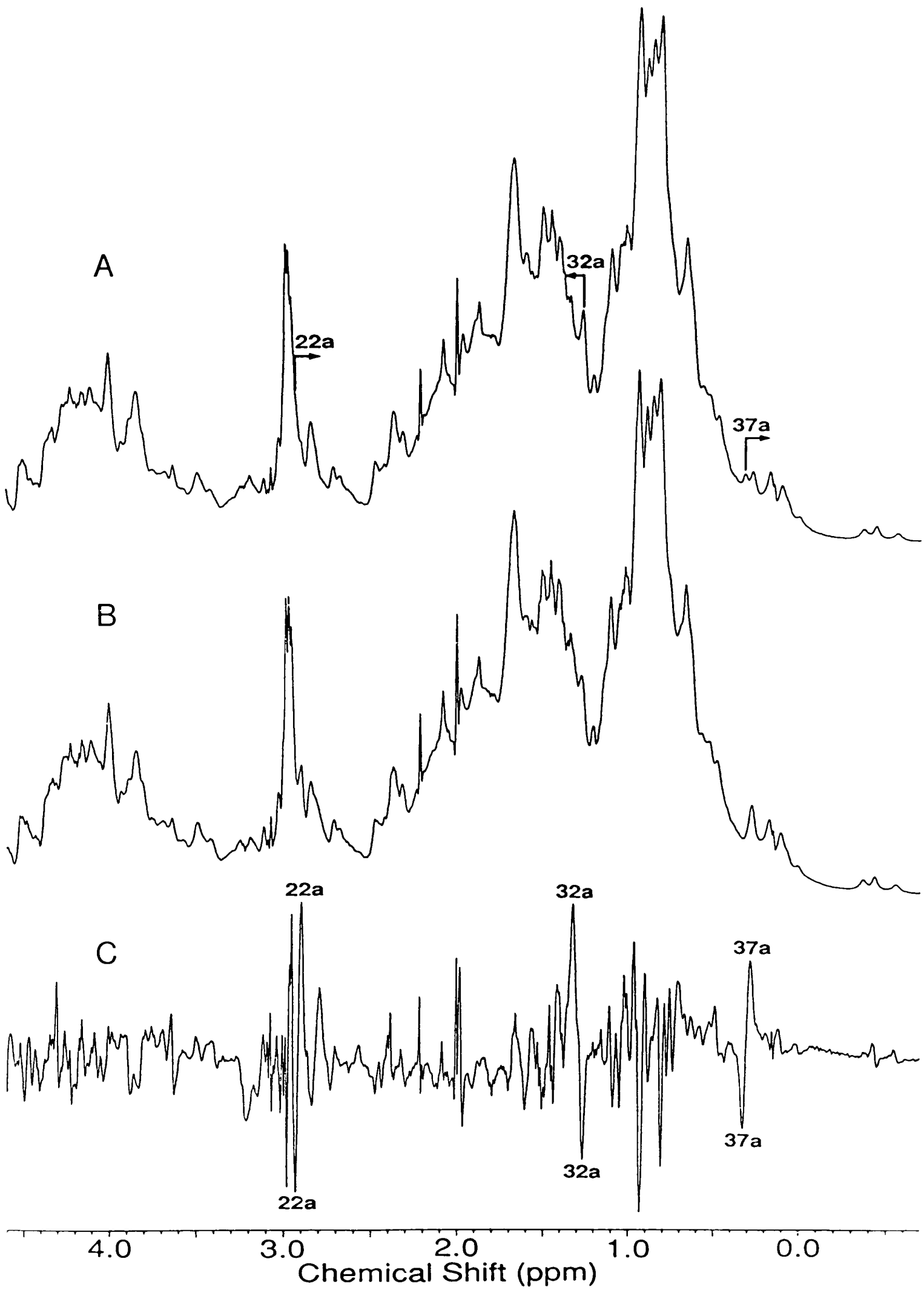

Figure 5-10: Perturbation of the aliphatic region of the 500 MHz ^{1}H NMR spectrum of yeast PGK by $[Fe(CN)_6]^{3-}$. (A) Spectrum in the absence of $[Fe(CN)_6]^{3-}$. (B) Spectrum in the presence of a 0.86:1 molar ratio of $[Fe(CN)_6]^{3-}$:protein. (C) The difference spectrum (B) - (A).

compared with those induced by $[Co(CN)_6]^{3-}$ binding in Table 5-3 and plotted against the $[[Fe(CN)_6]^{3-}]$:[PGK] ratios in Figure 5-11.

It is noted that the shifts of the 'basic patch' histidine resonances 3, 5a, 13a′ and 15b are substantially greater than those induced by the diamagnetic blank, $[Co(CN)_6]^{3-}$, and are thus predominantly paramagnetic in origin. The $[Fe(CN)_6]^{3-}$ induced shift of resonance 4 is also large, but in the opposite direction to that induced by the diamagnetic blank, and is therefore entirely of paramagnetic origin. These observations are consistent with the $[Cr(CN)_6]^{3-}$ broadening data.

In addition to the above effects on the 'basic patch' histidine resonances downfield shifts are observed for a downfield component of peak 14a (+0.05 ppm; original chemical shift 6.78 ppm) and a component of peak 8 (+0.02 ppm; original chemical shift 7.33 ppm) (Figure 5-9C). These shifts are both in the opposite direction to the small upfield shifts observed for these peaks on addition of $[Co(CN)_6]^{3-}$ (Figure 5-7C) and must also be due to a paramagnetic influence. The component of peak 14a (14a′) may be due to either a tyrosine (Tyr D) or a phenylalanine (Phe E) side-chain (see Table 2-2). The component of peak 8 corresponds to Phe G (Table 2-2) which was also observed to shift upfield following 3-PG binding (§§ 3.3.1 & 3.3.2) to the enzyme. The closest (non-histidine) aromatic side-chains to the proposed metal hexacyanide binding site (Figure 5-4) are Tyr 74 ($\langle r_{C3,5\text{-}H} \rangle \sim 12.7$ Å) and Phe 163 ($\langle r_{C2,6\text{-}H} \rangle \sim 14.7$ Å). These inter-nuclei distances are within the possible range for which a paramagnetic dipolar shift may be expected. [Note there is an r^{-3} dependence for a shift probe compared to an r^{-6} dependence for a relaxation probe]. Other shifted resonances include 7a, 7c, 8b, 8c, 15a, 15c, 15d, 16 and 17. These shifts are all small in magnitude, and each resonance is similarly effected by diamagnetic $[Co(CN)_6]^{3-}$. The effect of $[Fe(CN)_6]^{3-}$ on these peaks is therefore indicative of a small conformational change in the protein.

Table 5-3: Total shifts of selected aromatic resonances following addition of $[Co(CN)_6]^{3-}$ and $[Fe(CN)_6]^{3-}$.

Numbers are observed shifts in ppm, negative shifts are upfield. Values in parentheses are paramagnetic induced shifts

i.e. $\Delta\delta([Fe(CN)_6]^{3-}) - \Delta\delta([Co(CN)_6]^{3-})$

Resonance	Chemical Shift (ppm)	Residue	Anion		Shift Ratios
			$[Co(CN)_6]^{3-}$	$[Fe(CN)_6]^{3-}$	
3	7.95	His 62	+0.006	+0.172 (+0.17)	1
4	7.80	His 167	+0.098	-0.31 (-0.41)	-2.41
5a	7.61	His 170	+0.009	+0.156 (+0.15)	0.88
8	7.33	?	-0.03	+0.02 (+0.05)	0.29
13a′	6.91	His 170	+0.044	+0.19 (+0.15)	0.88
14a′	6.78	?	-0.017	+0.045 (+0.06)	0.35
15b	6.55	His 167	-0.012	-0.050 (-0.04)	-0.24

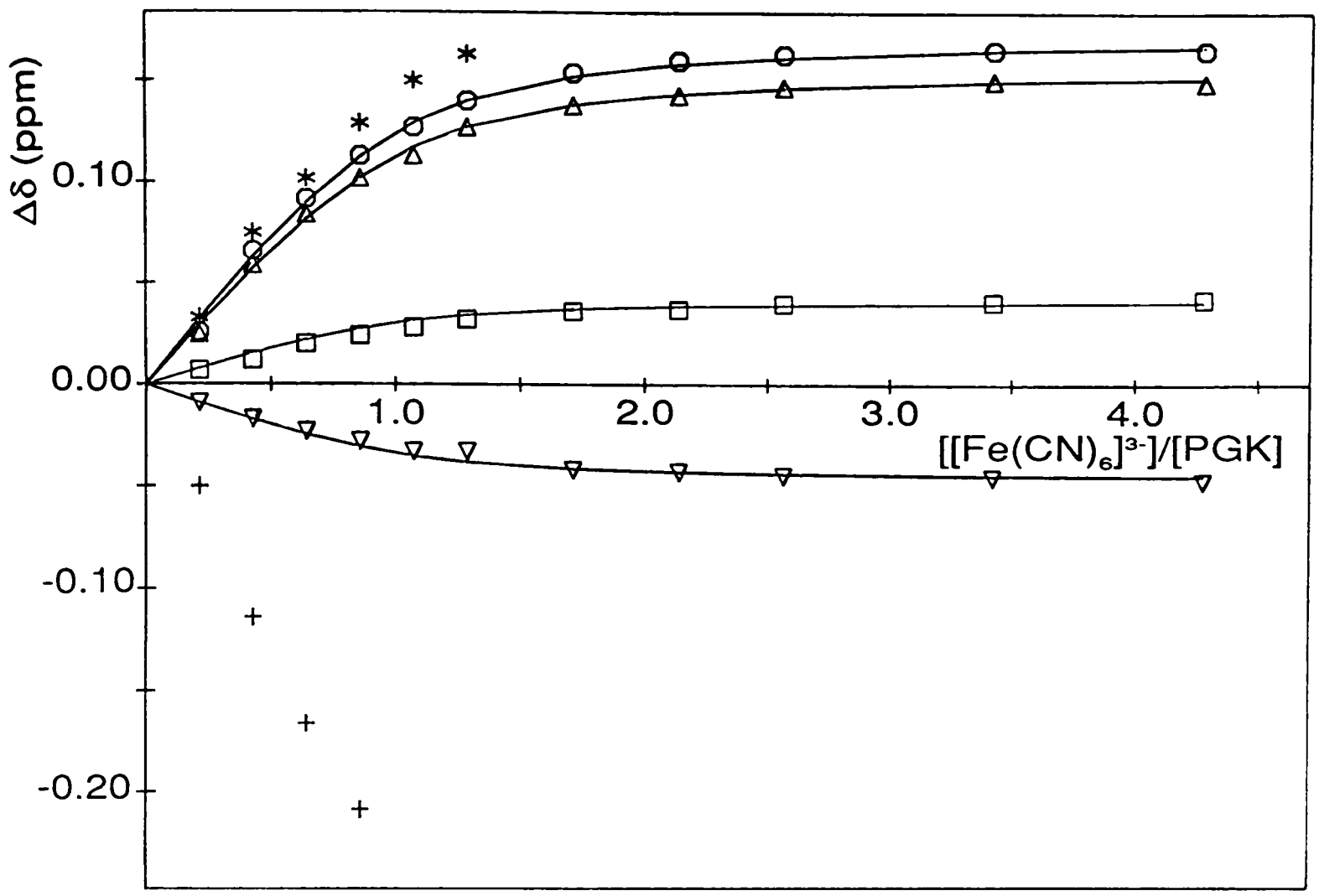

Figure 5-11: The change in the chemical shifts of peaks 3 (○; His 62), 4 (+; His 167), 5a (Δ; His 170), 13a′ (∗; His 170), 14a′ (□) and 15b (∇; His 167) plotted as a function of the $[Fe(CN)_6]^{3-}$:enzyme molar ratio. The continuous lines represent theoretical binding curves corresponding to a dissociation constant of 0.080 mM.

The paramagnetic shifts given in Table 5-3 cannot be rationalised solely in terms of the theoretical dipolar shift equation (assuming axial or rhombic symmetry, see Appendix 3) using the binding coordinates deduced from $[Cr(CN)_6]^{3-}$ relaxation data (Figure 5-4). The most plausible explanation for the observed deviation from theoretical dipolar shifts is that there is (for His 62 and His 167 at least) a significant contact contribution to the observed shifts. This is consistent with the results of Huang & Moore (1983) who found the shifts induced by $[Fe(CN)_6]^{3-}$ on resonances of simple amines to be caused predominantly by contact interactions. Given that $[Fe(CN)_6]^{3-}$ is magnetically anisotropic, with $|g_x| = 2.35$, $|g_y| = 2.10$ and $|g_z| = 0.915$ (Bleaney & O'Brien, 1956), it is reasonable to assume that a proportion of the shifts are also dipolar in origin. There are, however, insufficient data to test this.

Perturbations in the aliphatic region of the spectrum are illustrated in Figure 5-10. The most significant paramagnetic shifts are of resonances 22a (upfield), 32a (downfield) and 37a (upfield), which are consistent with the $[Cr(CN)_6]^{3-}$ relaxation data (§ 5.3.1).

5.3.3.1. Dissociation constant for $[Fe(CN)_6]^{3-}$ binding

The dissociation constant for $[Fe(CN)_6]^{3-}$ binding to PGK was determined as for $[Co(CN)_6]^{3-}$, except the larger shifts of resonances 3 and 5a were used (Figure 5-11). The dissociation constant for $[Fe(CN)_6]^{3-}$ binding to the primary anion site was thus calculated to be 0.080 ± 0.005 mM (I = 0.10 M, pH = 7.1, T = 300 K). This value is very similar to that determined for the diamagnetic blank, $[Co(CN)_6]^{3-}$ (§ 5.3.2), as would be expected given the close homology between the two anions.

5.3.3.2. Secondary binding

From Figures 5-8 and 5-11 it is apparent that there is a general, relatively strong ($\log K \approx 4.1$ for the metal hexacyanide trianions), anion binding site involving residues from the so called 'basic patch' region of the protein. This

site can be specifically located using $[Cr(CN)_6]^{3-}$ broadening data (Figure 5-4). However, as the concentration of $[Fe(CN)_6]^{3-}$ approaches that required for saturation of this binding site a second group of resonances is seen to be shifted. Figure 5-12 shows the difference between spectra with $[[Fe(CN)_6]^{3-}]$:[PGK] ratios of 4.3:1 and 3.4:1. There are significant shifts between 2.8-3.0 ppm and 1.5-1.7 ppm which are not consistent with binding at the primary anion site (*i.e.* shifts due to binding in the 'basic patch' region have effectively reached saturation at a lower ratio of $[[Fe(CN)_6]^{3-}]$:[PGK]; see Figure 5-11). These shifts are not observed at less than equimolar ratios of paramagnetic probe:protein, indicating that they are due to binding at a lower affinity site(s). The upfield shifts observed in the difference spectrum are consistent with the paramagnetic anion binding to surface lysine side-chains of the protein. The smaller perturbations observed between 0.4-1.0 ppm are possibly due to dipolar shifts of methyl groups close to these lysine side-chains.

Since there are 42 lysine residues in yeast PGK and more than 200 methyl groups it is not possible to locate the site(s) of secondary binding. It is possible to speculate, however, that one such site may involve the totally conserved lysines 213 and 217 (Appendix 1) which interact with the phosphate chain of the bound nucleotide substrates (Watson *et al.*, 1982). This would be close to the crystallographically determined selenate binding site (Walker *et al.*, 1989). A secondary anion site within the active site region may provide an alternative explanation for the observed anion activatory/inhibitory effect, other than the single site hypothesis of Scopes (1978b), in agreement with the suggestion of Khamis & Larsson-Raźnikiewicz (1981).

5.4. Discussion

The use of anionic paramagnetic probes has provided direct evidence for binding of anions in the 'basic patch' region of the N-terminal domain.

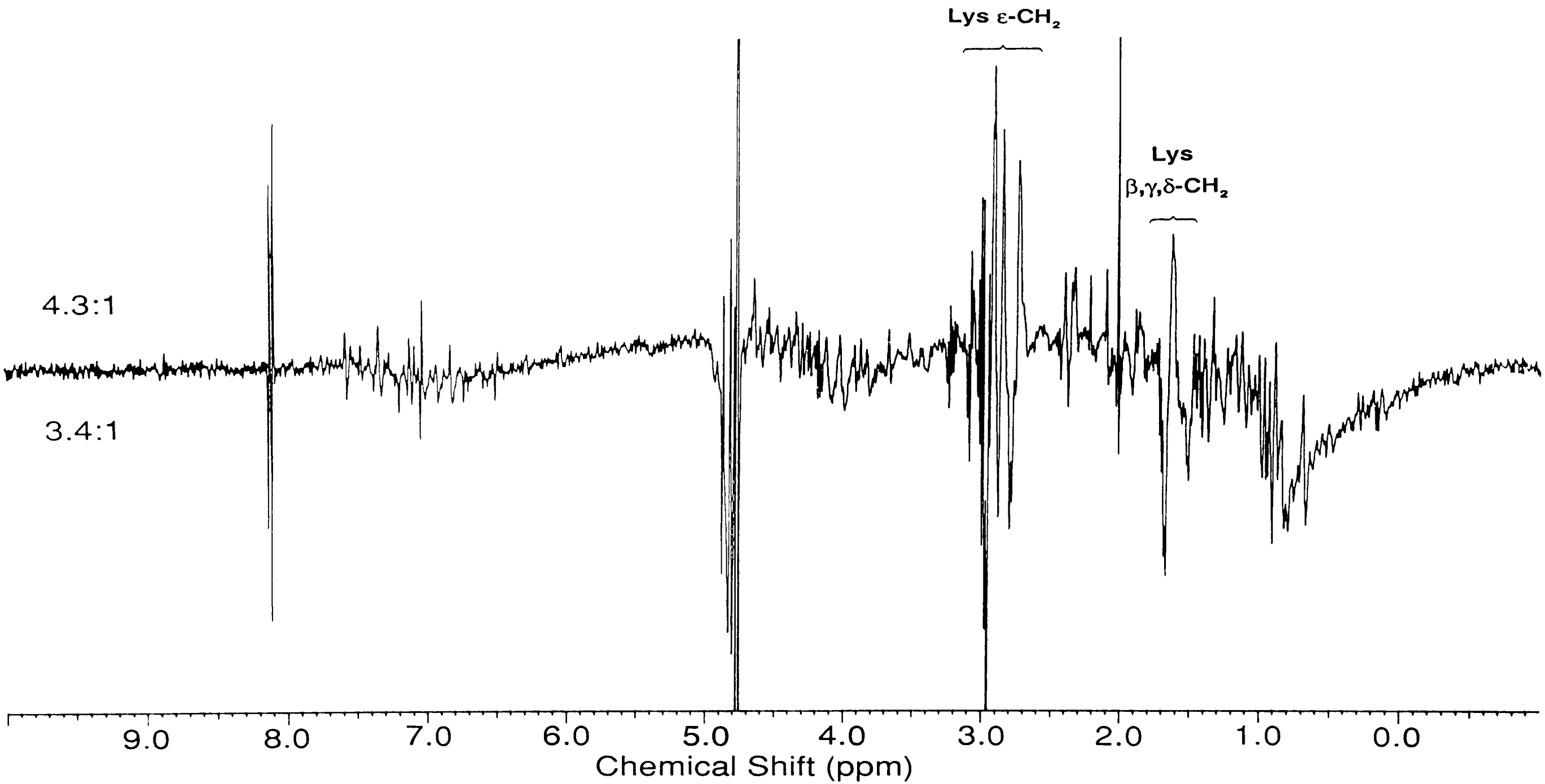

Figure 5-12: Difference spectrum between PGK solutions with molar ratios of $[Fe(CN)_6]^{3-}$:enzyme of 4.3:1 and 3.4:1. The most significant shifts observed, between 1.5-1.7 ppm and 2.8-3.0 ppm are consistent with the perturbation of lysine residues.

Relaxation data from titrations with $[Cr(CN)_6]^{3-}$ have been used to locate this primary anion binding site in the crystal structure of the protein (Figure 5-4). The anion appears to interact very closely with the positively charged guanidinium groups of Arg 65 and Arg 168. Care must be taken in interpretation of this calculated anion binding site, however, since it relies on the assumption that the solution and crystal structures are identical. This has been shown not to be the case in the 'basic patch' region, where both His 62 and His 167 have NOE connectivities with a methyl or methylene group, which cannot be accounted for using the crystallographic data (§ 4.3.2). Also, no account has been made of mobility within the 'basic patch' region and the effect of anion binding on the average conformation. Despite these assumptions, the proposed anion binding site is qualitatively correct and is supported by shift data obtained from titrations with $[Fe(CN)_6]^{3-}$. While it was not possible to calculate a binding site on the basis of these data, the likely possibility that the observed shifts of His 62 and His 167 have a contact contribution is strong evidence for the anion to be binding close in space to these residues.

The primary, general, anion binding site therefore shares at least two residues which have been shown to interact with the bound triose substrate, 3-PG, namely His 62 and Arg 168. This is consistent with $[Co(CN)_6]^{3-}$ binding being directly competitive with 3-PG binding (H.C. Graham, personal communication). The dissociation constant for the metal hexacyanide trianions are also of the same order of magnitude as for the triose substrate.

Evidence has also been gained of a weaker secondary anion binding site(s) involving the side-chains of surface lysine residues. This is consistent with earlier observations made at higher molar ratios of the inorganic probes:PGK (Wilson *et al.*, 1982). While the primary anion binding site, as determined from the $[Cr(CN)_6]^{3-}$ broadening data, is not the same as the crystallographically determined selenate binding site (Walker *et al.*, 1989),

the secondary site may be. It is also noted that difference Fourier maps of horse-muscle PGK in sulphate and tartrate revealed the presence of two bound sulphate ions, one near Lys 217 (219 in horse sequence) and the other near Arg 168 (170 in horse sequence) (Blake & Rice, 1981). This observation is consistent with the present results. It seems likely that the primary anion site is responsible for the observed activatory effect of anions at low concentrations (Larsson-Raźnikiewicz & Jansson, 1973; Scopes, 1978a, Khamis & Larsson-Raźnikiewicz, 1981) while the secondary anion binding site leads to inhibition, but only at higher anion concentrations.

5.5. References

Blake, C.C.F. & Rice, D.W. (1981) *Phil. Trans. R. Soc. Lond. A. 293,* 93-104.

Bleaney, B. & O'Brien, M.C.M. (1956) *Proc. Phys. Soc. B. 69,* 1216-1230.

Burton, D.R., Forsen, S., Karlstrom, G. & Dwek, R.A. (1979) *Prog. Nucl. Magn. Reson. Spectrosc. 13,* 1-45.

Dwek, R.A. (1973) *NMR in Biochemistry,* Clarendon Press, Oxford.

Eley, C.G.S., Moore, G.R., Williams, G. & Williams, R.J.P. (1982) *Eur. J. Biochem. 124,* 295-303.

Huang, Z.-X. & Moore, G.R. (1983) *J. Magn. Reson. 52,* 505-510.

James, T.L. (1975) *NMR in Biochemistry,* Academic Press, New York.

Jardetzky, O. & Roberts, G.C.K. (1981) *NMR in Molecular Biology,* Academic Press, New York.

Khamis, M.M. & Larsson-Raźnikiewicz, M. (1981) *Biochim. Biophys. Acta 657,* 190-194.

Larsson-Raźnikiewicz, M. & Jansson, J.R. (1973) *FEBS Lett. 29,* 345-347.

Scopes, R.K. (1978a) *Eur. J. Biochem. 85,* 503-516.

Scopes, R.K. (1978b) *Eur. J. Biochem. 91,* 119-129.

Walker, P.A., Littlechild, J.A., Hall, L. & Watson, H.C. (1989) *Eur. J. Biochem.,* in press.

Watson, H.C., Walker, N.P.C., Shaw, P.J., Bryant, T.N., Wendell, P.L., Fothergill, L.A., Perkins, R.E., Conroy, S.C., Dobson, M.J., Tuite, M.F., Kingsman, A.J. & Kingsman, S.M. (1982) *EMBO J. 1,* 1635-1640.

Wilson, H.R., Williams, R.J.P., Littlechild, J.A. & Watson, H.C. (1988) *Eur. J. Biochem. 170,* 529-538.

Chapter 6

NMR ANALYSIS OF ADENOSINE 5′-TRIPHOSPHATE BINDING TO YEAST PGK

6.1. Introduction

The catalytic mode of Mg.ATP binding to PGK has been described by X-ray crystallography (Banks *et al.*, 1979; Blake & Rice, 1981; Watson *et al.*, 1982; Watson & Gamblin, 1985) and is illustrated schematically in Figure 6-1. The adenine group binds in a hydrophobic depression on the surface of the C-terminal domain with its N6 nitrogen forming a hydrogen-bond with the main chain carbonyl of totally conserved Leu 311 (Appendix 1). The adenine pocket is lined by conserved glycines 210, 211, 234, 235, 236 and 338, and the aliphatic side-chains of Leu 311 and Val 339. The ribose ring is located in a shallow depression between totally conserved residues, Gly 338 and Pro 336, with the 2′-OH forming a hydrogen-bond with the side-chain of Glu 341, and in yeast PGK, the 3′-OH forming a hydrogen-bond with the side-chain of Asp 372. The α- and β-phosphates are in contact with a section of the main chain containing totally conserved Gly 335. Two lysine residues (213 and 217, again totally conserved) are situated within hydrogen-bonding distance of the α- and β-phosphoryl groups. In the yeast structure the γ-phosphate appears to cross from the main chain to the amino end of α-helix XII where it makes hydrogen-bonds with the main chain nitrogens of totally conserved Asp 372 and Gly 371. The metal ion (Mg^{2+}) was judged to interact with the γ-phosphate and the carboxyl group of Asp 372 of the yeast enzyme (Watson & Gamblin, 1985).

The predominantly hydrophobic nature of the nucleotide binding site has been demonstrated spectrophotometrically using the AMP analogue 2-(dansylamino)ethyl monophosphate (Roustan *et al.*, 1973) and

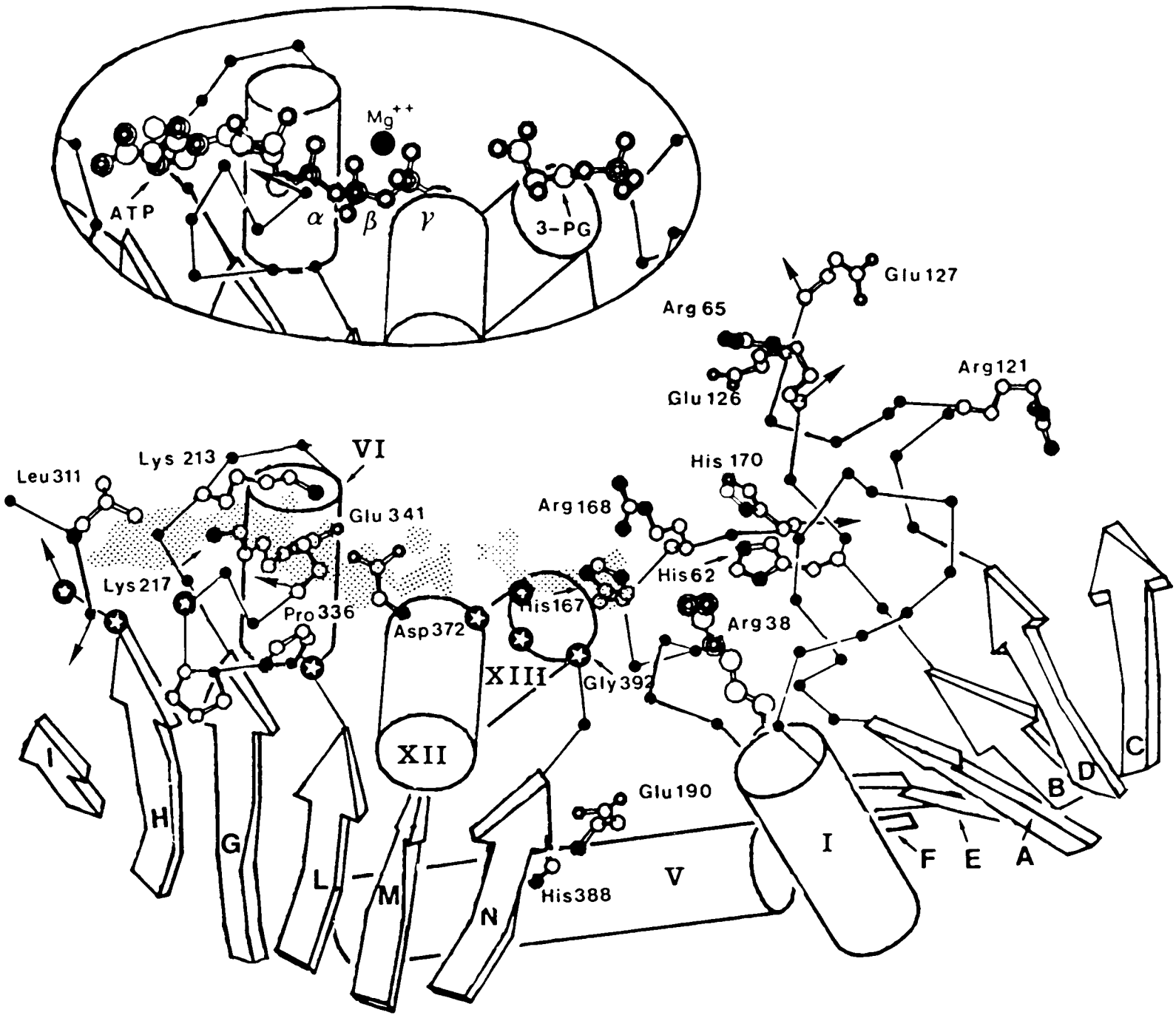

Figure 6-1: A schematic drawing of the active-site cleft of yeast PGK showing the binding site for Mg.ATP as determined by soaking crystals of the enzyme in solutions containing nucleotide substrates. The figure also includes the crystallographically determined 3-PG binding site (after Wilson *et al.*, 1988).

fluorimetrically with 1-anilino-8-naphthalenesulphonate (Wiksell & Larsson-Raźnikiewicz, 1982). Studies of the specificity of nucleotide substrates as phosphoryl donors to 3-PG (Krietsch & Bücher, 1970; Roustan *et al.*, 1973) show that purine analogues are better substrates than pyrimidine analogues.

The strength of Mg.ATP binding has been calculated from gel filtration studies (K_d = 0.11 ± 0.04 mM, I = 0.15 M; Scopes, 1978), thiol reactivity studies (K_d = 0.15 ± 0.03 mM, I = 0.10 M; Tompa *et al.*, 1986) and 270 MHz ^{1}H NMR studies (K_d = 0.15 ± 0.07 mM, I = 0.10 M; Tanswell *et al.*, 1974). Thiol reactivity studies with pig muscle PGK (Tompa *et al.*, 1986) have also quantified the interaction between adenosine and the enzyme (K_d = 1.05 ± 0.20 mM, I = 0.10 M). Adenine, which is a competitive inhibitor of the enzyme with respect to Mg.ATP, was found not to induce the same conformational changes observed for Mg.AMP, Mg.ADP and Mg.ATP binding (Tompa *et al.*, 1986).

Interaction of Mg.ATP at a secondary binding site has been found by equilibrium dialysis and gel filtration studies (Larsson-Raźnikiewicz, 1973; Tanswell *et al.*, 1974; Scopes, 1978). The existence of a second, low affinity, site was confirmed by product inhibition studies and a regulatory role was suggested (Schierbeck & Larsson-Raźnikiewicz, 1979). Evidence for ATP binding to the enzyme at two sites, with one site binding Mg^{2+} much more weakly than the other, has also been gained from a ^{31}P NMR study (Nageswara Rao *et al.*, 1978). Subsequent ^{31}P NMR studies suggest that ATP binds about 7-fold weaker and Mg.ATP about 75-fold weaker at the secondary enzyme site compared to binding at the catalytic site, assuming an independent binding model (Ray & Nageswara Rao, 1988). This, together with spectrophotometric results which indicate that the hydrophobic interaction between the enzyme and the adenine ring occurs only at the primary catalytic site (Roustan *et al.*, 1973), suggests that binding at the secondary site is predominantly electrostatic and presumably involves the phosphate groups of

the substrate. The position of the second site, whether near the active site and interdomain region or elsewhere on the protein surface, is unknown. The fact that at high concentrations Mg.ATP appears to be competitive with 3-PG (Schierbeck & Larsson-Raźnikiewicz, 1979), however, indicates that the secondary site may be the general anion site described in Chapter 5.

Nucleotide binding to PGK has also been analysed using ^{1}H NMR techniques (Tanswell *et al.*, 1976; Scheffler & Cohn, 1986; Wilson *et al.*, 1988). Conformational changes were monitored on binding ATP and ADP both with and without Mg^{2+}, with only a single nucleotide binding site being detected. Experiments using Gd(III) as a paramagnetic relaxation probe have led to the conclusion that, in solution, the binding of nucleotide substrates to PGK alters the average conformation about the interdomain region of the molecule (Wilson *et al.*, 1988). A more detailed analysis of the paramagnetic probe studies is given in the following chapter.

In this chapter 1D and 2D ^{1}H NMR techniques are used to analyse ATP binding in more detail than was possible in the previous studies and to investigate the effect of Mg^{2+} on the mode of binding.

6.2. Experimental methods

6.2.1. *ATP titrations*

ATP titrations were carried out in an analogous way to the 3-PG titrations (§ 3.2.1) by adding 1-4 µl aliquots of 50-60 mM solutions of ATP, containing the required molar ratio of $MgCl_2$, directly to the protein samples (prepared as described in § 2.2.5) in the NMR tubes and measuring their 1D ^{1}H NMR spectra (as described in § 2.2.6). The protein-free nucleotide concentration was determined spectrophotometrically using an absorption coefficient of $A_{260\ nm} = 15.4 \times 10^3\ M^{-1}\ cm^{-1}$. The pH of each ATP solution was initially adjusted to be the same as the enzyme solutions (7.10 ± 0.05). The pH of each

protein sample was measured before and after the titration to ensure that any observed effects were not due to pH changes.

6.3. Results

6.3.1. *Effect of ATP^{4-} binding on the 1D ^1H NMR spectrum of PGK*

A titration of wild-type PGK with ATP at pH 7.1 was monitored using 500 MHz ^1H NMR spectroscopy (Figure 6-2). The difference spectrum corresponding to an [ATP]:[PGK] ratio of 2.15:1 is given in Figure 6-3. The observed shifts of 'basic patch' histidine resonances 3, 4 and 5a are plotted against the molar ratio of ATP to enzyme in Figure 6-4. These three peaks, corresponding to histidine residues 62, 167 and 170 respectively, are initially shifted downfield. The 'basic patch' histidines are situated between 14-19 Å from the γ-phosphate of ATP in the crystallographically determined nucleotide binding site (Watson *et al.*, 1982; Figure 6-1). At a ratio of about 1:1, however, peak 4 (His 167) begins to broaden and shift upfield. Peak 15b, the C4-H resonance of His 167, also initially shifts slightly downfield (+0.006 ppm) and then upfield (-0.01 ppm) at [ATP]:[PGK] ratios greater than 1:1. This result clearly demonstrates the existence of a secondary nucleotide binding site, and that ATP perturbs the 'basic patch' region (*i.e.* the general anion binding site) from both its primary and secondary sites.

Other aromatic resonances affected by the addition of ATP to the protein solution are listed in Table 6-1. [Note that the downfield shifts of histidine resonances 2a, 2b, 9, 10 and 11 can be attributed to a small increase in the pH of the protein solution]. Perturbations observed by difference spectroscopy (Figure 6-3) for peaks 8 (broadening) and 13b (downfield shift and broadening) have been reported previously (Tanswell *et al.*, 1976; Wilson *et al.*, 1988) and were shown to be adenosine specific effects. As such they are likely to originate from ATP binding at the crystallographically observed hydrophobic catalytic site (Watson *et al.*, 1982). From 2D NMR experiments

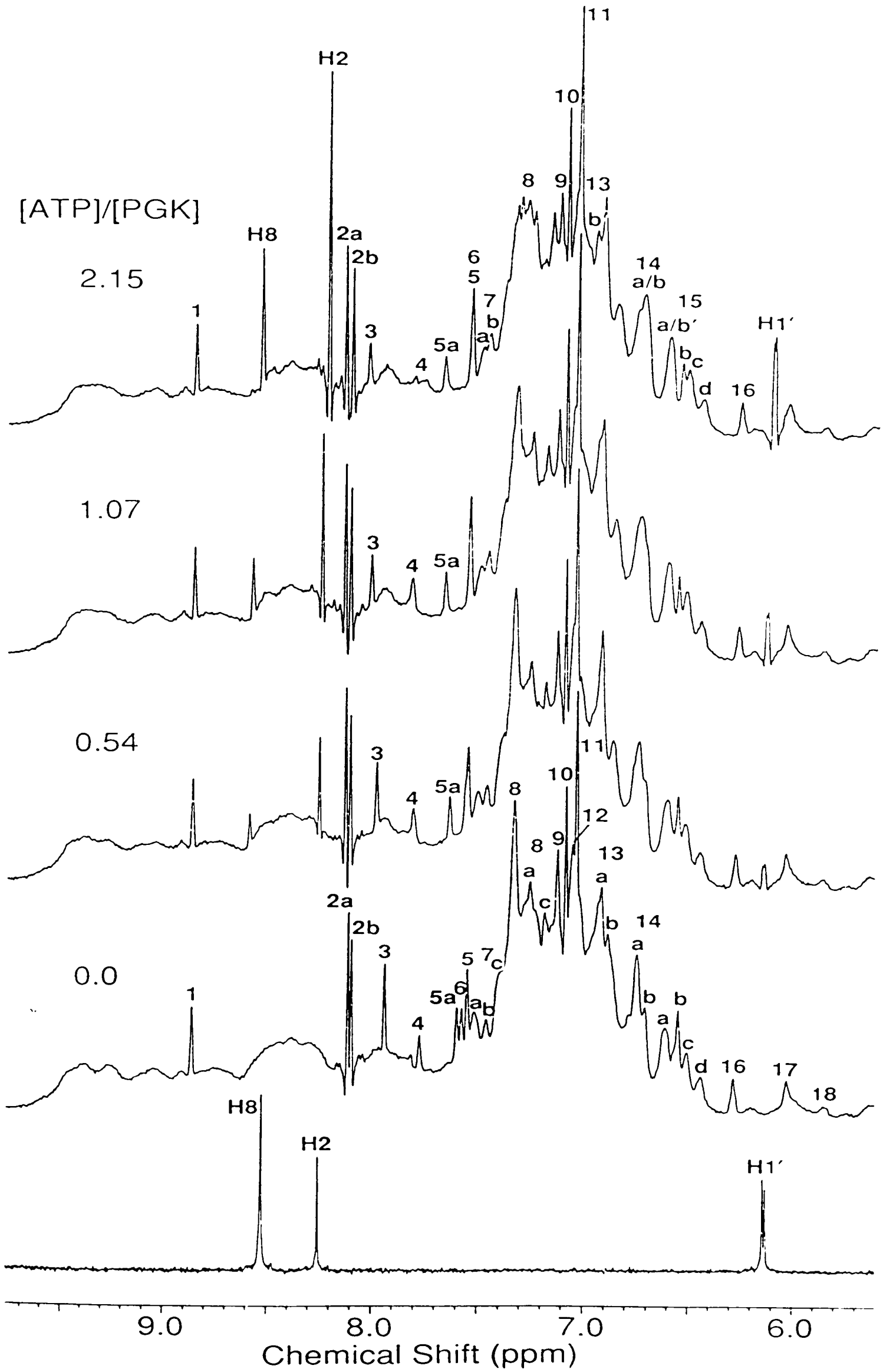

Figure 6-2A: Perturbations of the aromatic region of the 500 MHz ^{1}H NMR spectrum of yeast PGK by ATP at the ratios indicated and pH 7.1. The bottom spectrum is that obtained from a 1 mM solution of ATP (pH 7.07).

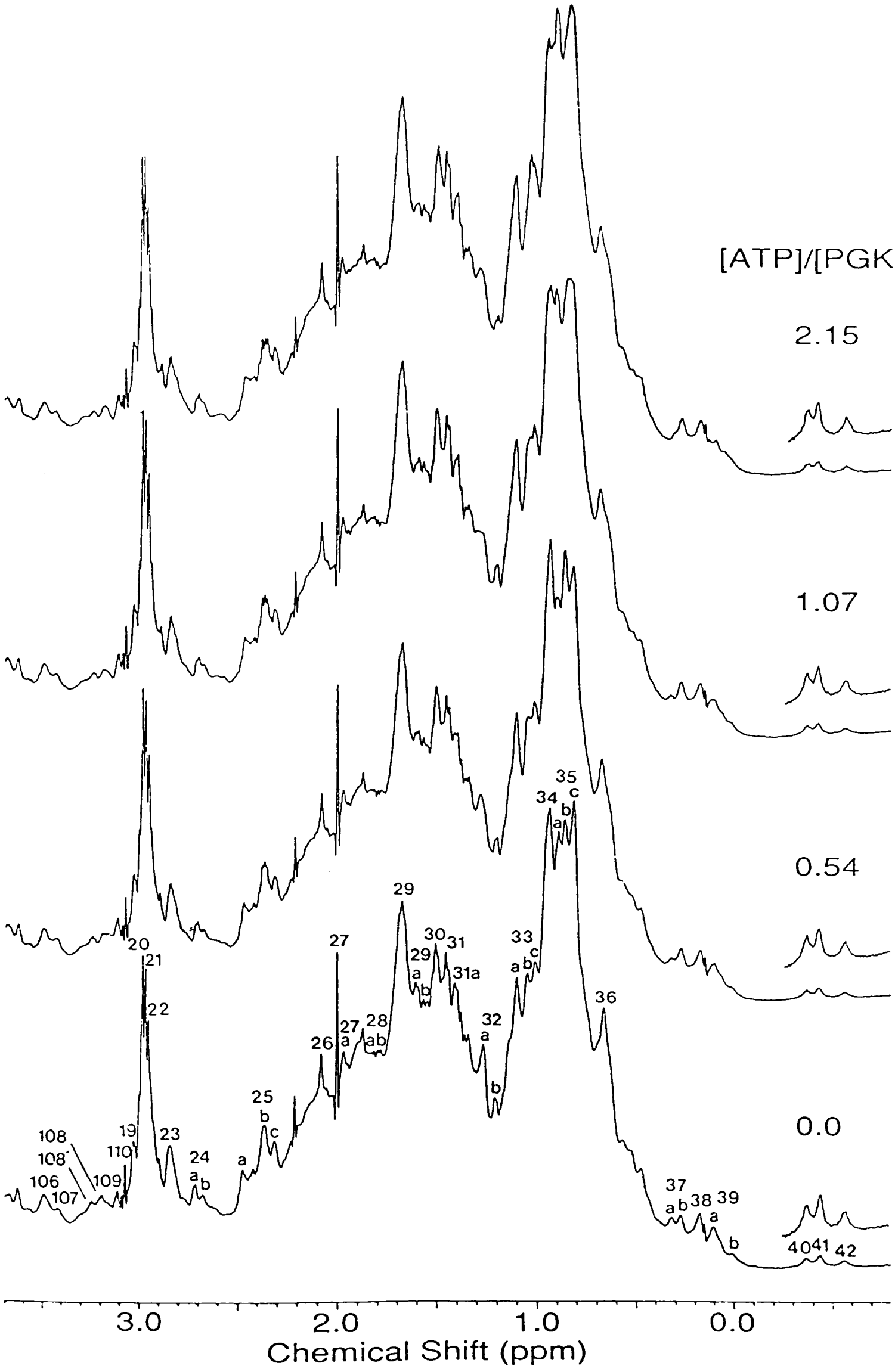

Figure 6-2B: Perturbations of the aliphatic region of the 500 MHz ^{1}H NMR spectrum of yeast PGK by ATP at the ratios indicated and pH 7.1.

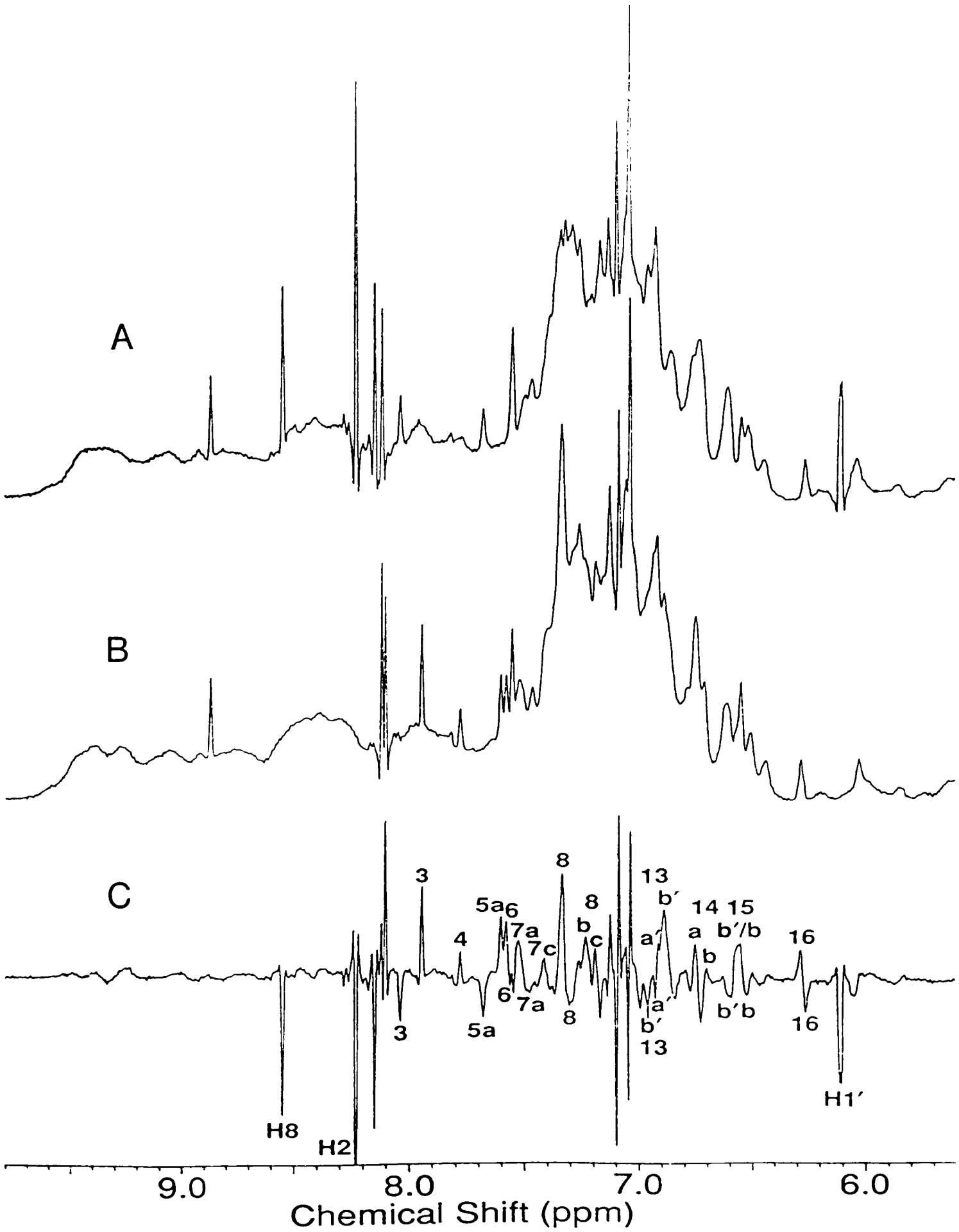

Figure 6-3A: Perturbation of the aromatic region of the 500 MHz ^{1}H NMR spectrum of yeast PGK by ATP. (A) Spectrum in the presence of a 2.15:1 molar ratio of ATP:protein. (B) Spectrum in the absence of ATP (C) The difference spectrum (B) - (A).

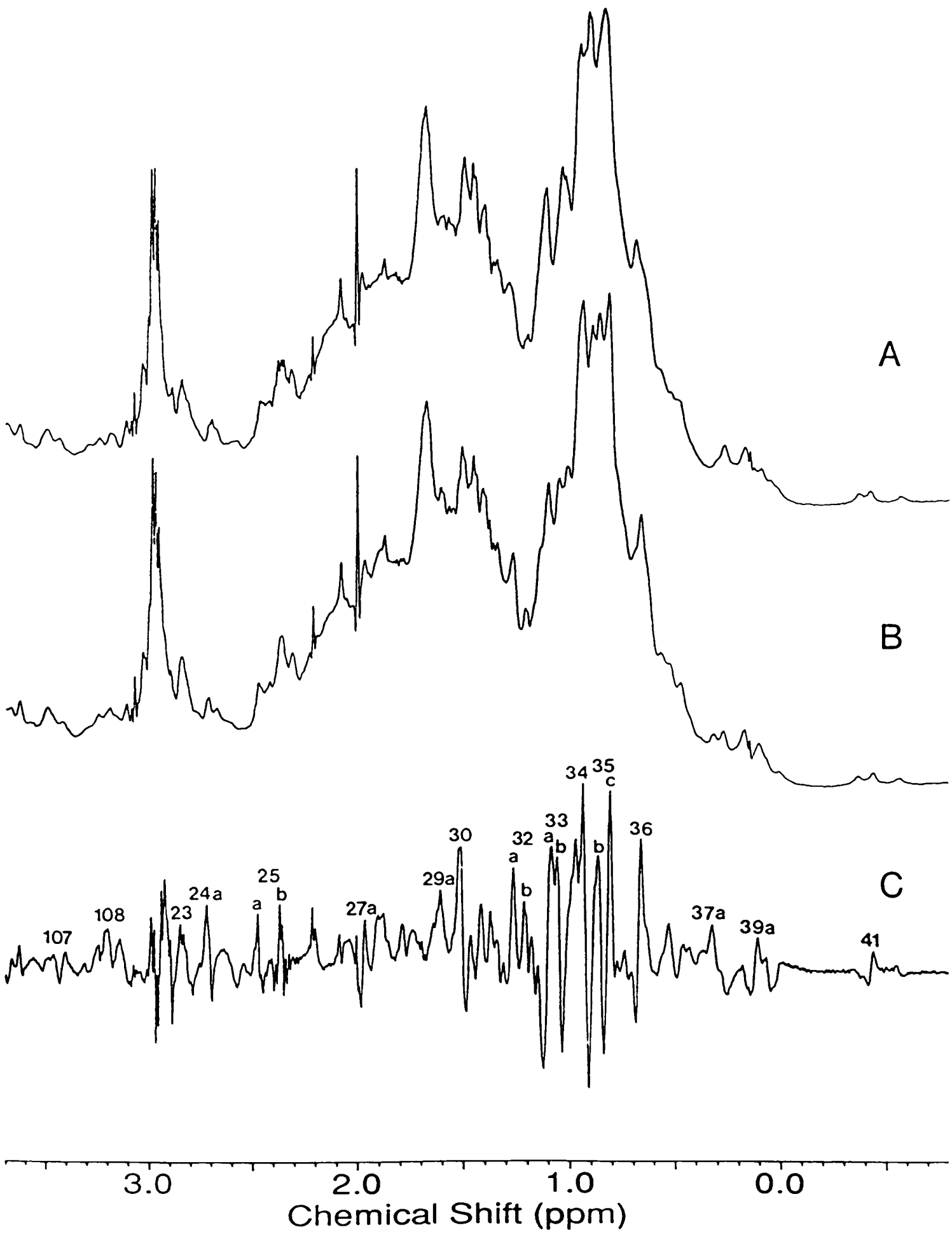

Figure 6-3B: Perturbation of the aliphatic region of the 500 MHz ^{1}H NMR spectrum of yeast PGK by ATP. (A) Spectrum in the presence of a 2.15:1 molar ratio of ATP:protein. (B) Spectrum in the absence of ATP. (C) The difference spectrum (B) - (A).

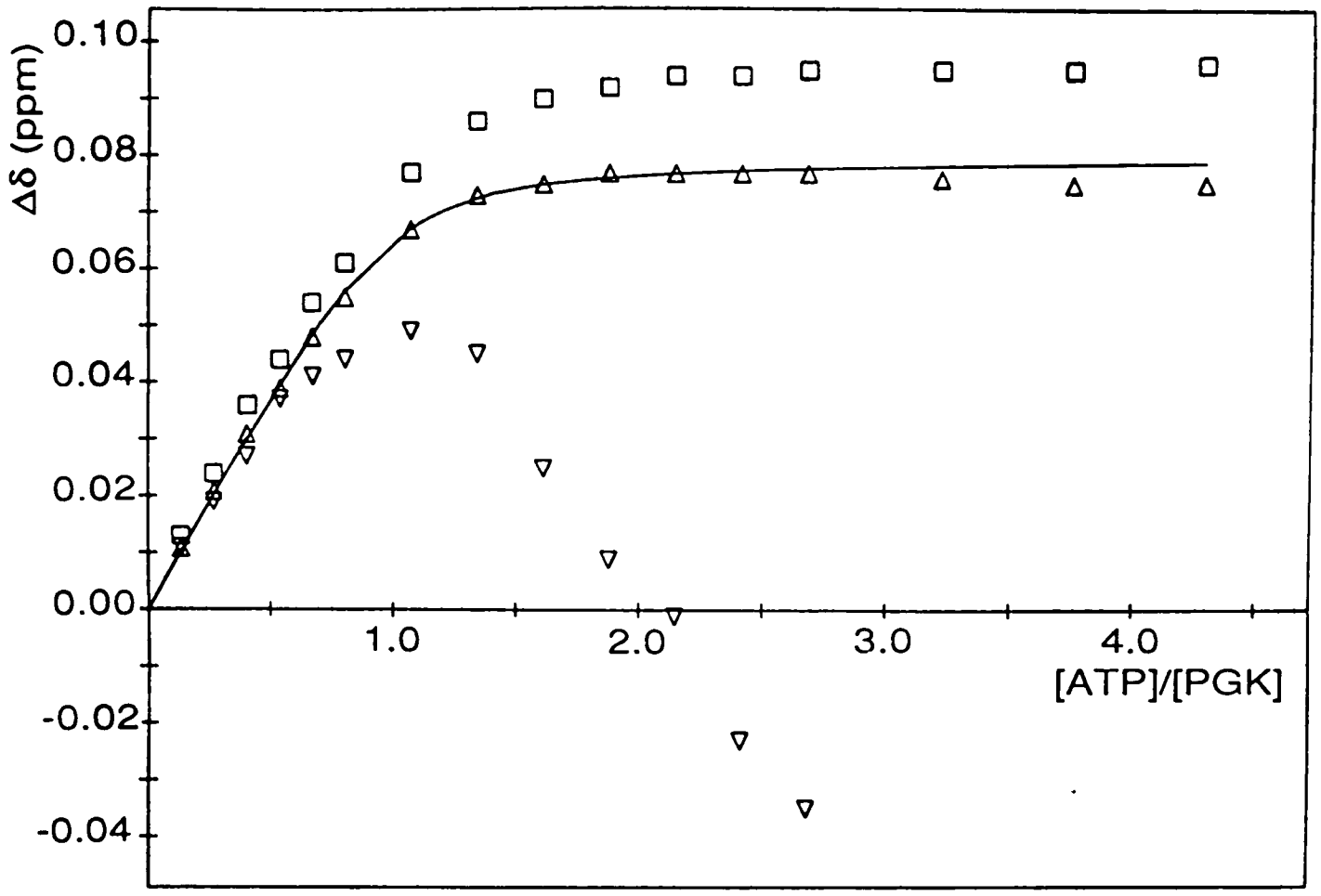

Figure 6-4: The change in chemical shifts of peaks 3 (□; His 62), 4 (∇; His 167) and 5a (Δ; His 170) plotted as a function of ATP:protein molar ratio. The continuous line represents a theoretical binding curve corresponding to a dissociation constant of 0.052 mM.

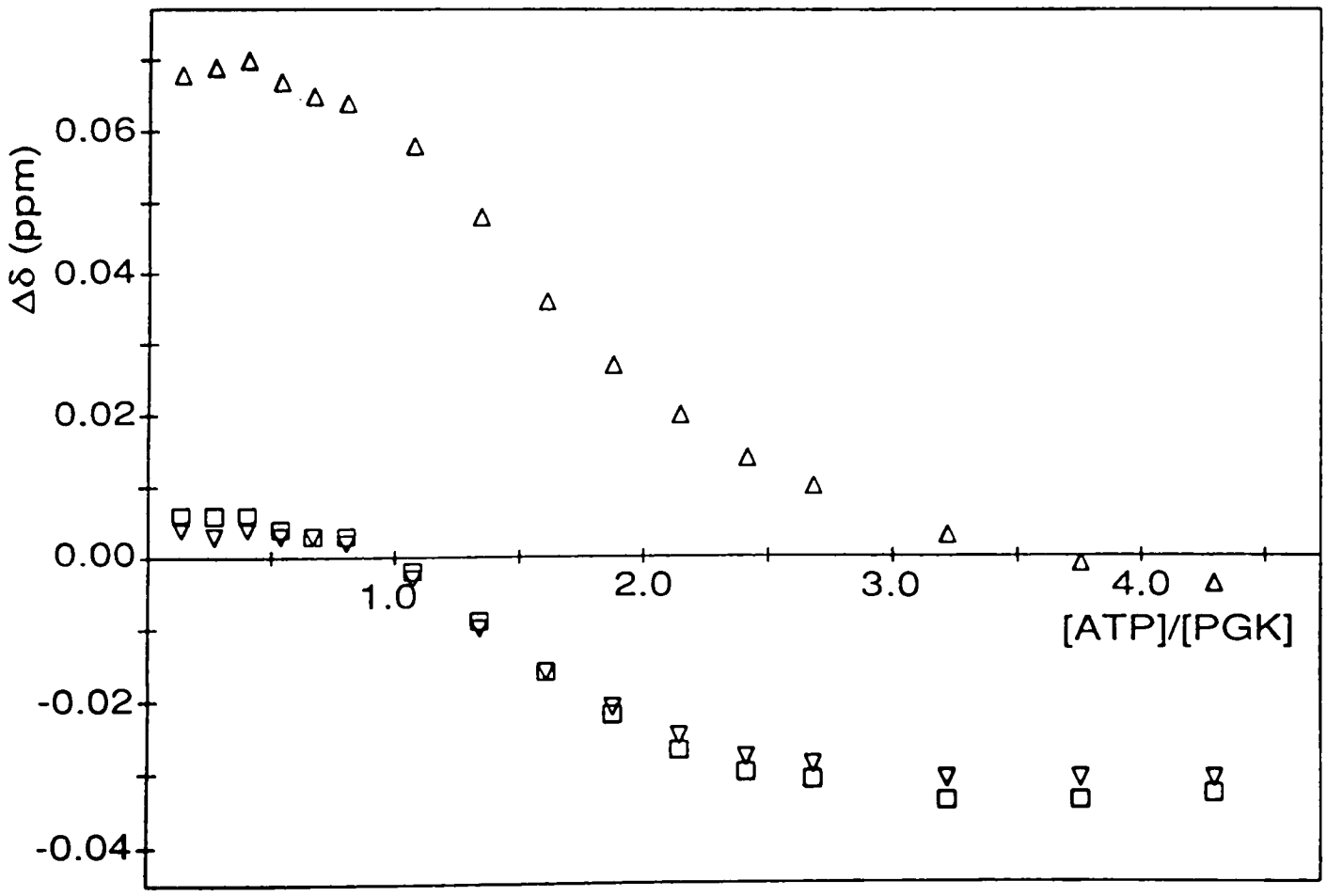

Figure 6-5: The change in chemical shifts of the C8-H (Δ), C2-H (□) and C1′-H (∇) resonances of ATP plotted as a function of ATP:protein molar ratio. The reference chemical shifts were determined from a 1 mM solution of ATP (pH 7.07) to be 8.53, 8.25 and 6.13 ppm respectively.

Table 6-1: Effects of ATP binding on resonances of the ^{1}H NMR spectrum of yeast PGK

Numbers are observed shifts in ppm, negative shifts are upfield. (B) = broadening, (Sp) = peak split, (-) = upfield shift, (+) = downfield shift, – = no observable effect, ? = possible effect.

Aromatic		Aliphatic	
Resonance	Effect	Resonance	Effect
1	–	107	(+)
2a	?	108	(-)(B)
2b	?	23	(-)
3	+0.10	24a	(-)(B)
4	(+,-)	25a	(-)
5a	+0.08	25b	(Sp)
6	-0.02	27a	(+)
5	–	28b	(B)
7a	-0.02(B)	29a	(B)
7b	–	30	(-)(B)
7c	(-)	32a	(+)(B)
8	(-)(B)	32b	(B)
8a	?	33a	(+)
8b	(B)	33b	(-)
8c	-0.04	33c	(+)
9	?	34	(-)
10	?	35b	(-)
11	?	35c	(+)(B)
12	see text	36	(+)
13a′	(+)	37a	(-)
13b′	+0.08	39a	(Sp)
14a′	(-)	39b	(+)
14a	(-)	41	(+)
14b	(+)		
15a	?		
15b′	(+)		
15b	(+,-)		
15c	(+)		
15d	(+)		
16	-0.02		
17	(B)		
18	–		

with Mg.ATP (see §§ 2.3.3 & 6.3.4) the perturbed components of peaks 8 and 13b have been assigned to Phe 289 and Phe 342 respectively. It is noted here that observable splitting of peak 8 in the 1D spectrum is not seen until the [ATP]:[PGK] ratio is greater than 1.3:1. Wilson *et al.* (1988) also reported adenosine specific effects at peaks 12 and 15a. In Figure 6-3 an upfield shift of a component of peak 12 is masked by peak 11. Later 2D experiments (§ 6.3.4), however, confirm that a component of peak 12, assigned to Phe 342, shifts upfield on binding Mg.ATP. The broadening previously reported for peak 15a appears now to be due to a downfield shift of peak 15b′ which is due to an unidentified Phe residue. Perturbations are also observed around peak 14a. From the difference spectrum (Figure 6-3A) it appears that peak 14a′ and a component of 14a shift slightly upfield while peak 14b moves slightly downfield.

A number of effects are also observed in the aliphatic region of the spectrum (Figures 6-2B & 6-3B; Table 6-1). All shifts in this region of the spectrum are less than about 0.03 ppm in magnitude. A number of the effects are also biphasic with [ATP]:[PGK] ratio, again reflecting the contribution of two binding sites. In particular, peak 37a which is due to an alanine or threonine residue in the vicinity of the general anion binding site (possibly Ala 395 which is close in space to His 167 in the crystal structure; § 5.3.1) is initially shifted downfield but at higher [ATP]:[PGK] ratios it broadens and moves upfield. Some of the aliphatic peaks affected by ATP binding were also perturbed by 3-PG binding (*c.f.* Table 3-1). The downfield shifts of peaks 27a and 41 observed on addition of ATP, however, were not seen on addition of 3-PG. Peak 27a has been tentatively assigned to Met 173 (Wilson, 1986) while peak 41 was earlier tentatively assigned to Thr 375 (§ 2.3.4). The downfield shift of resonance 36 is small compared to that induced by 3-PG. Peak 42, which was shifted 0.05 ppm upfield by 3-PG addition remains unperturbed.

As with 3-PG binding most of the effects described above are characteristic

of minor conformational changes in the protein as a result of ATP binding. Some effects may also be due to local field changes resulting from the aromatic nature of the adenine moiety. It is apparent, however, that the conformational changes induced by the two substrates are somewhat different although both appear to interact with the 'basic patch' region of the protein.

Further evidence for secondary binding is gained from the change in chemical shifts of the adenine and ribose protons (C8-H, C2-H and C1′-H) as a function of [ATP]:[PGK] ratio (Figure 6-5). The initial shifts of these resonances reflect the environment of ATP at the primary binding site. From Figure 6-5 it can be seen that the C8-H undergoes the largest change on going from free solution to being bound at the primary site. At ratios of [ATP]:[PGK] greater than ~ 0.5:1 all three resonances shift upfield. If only one binding site existed the chemical shifts would be expected to return towards their respective positions in free solution since all three resonances are in fast exchange *i.e.* the observed chemical shift is a weighted average of the free and bound chemical shifts. The adenine C2-H and ribose C1′-H resonances, however, shift upfield of their positions in free solution and reflect the environments of these protons in the secondary ATP binding site.

6.3.1.1. Dissociation constant for ATP^{4-} binding

The chemical shift of resonance 5a (His 170) as a function of [ATP]:[PGK] ratio (Figure 6-4) could be fitted to a 1:1 binding curve (see § 3.2.2) up to a ratio of ~ 2.7:1, indicating that the effect of secondary ATP binding on this resonance is minimal. The dissociation constant was thus calculated to be 0.052 ± 0.010 mM (I = 0.10 M, pH = 7.1, T = 300 K). The change in chemical shift of peak 3 (His 62) is also consistent with the above K_d.

6.3.2. *Effect of $Mg.ATP^{2-}$ binding on the 1D ^1H NMR spectrum of PGK*

The effect of Mg^{2+} on the mode of ATP binding to PGK was initially investigated by carrying out titrations of the protein with ATP solutions

containing 1:1 and 5:1 molar ratios of $MgCl_2$:ATP. Using a dissociation constant for Mg.ATP of 0.051 mM (Sigel *et al.*, 1987) these solutions correspond to 60-90% and > 95% $Mg.ATP^{2-}$ respectively at nucleotide concentrations in the range 0.2-5 mM (*i.e.* the concentration range during the titrations). In the latter case the proportion of Mg_2.ATP present will also increase with nucleotide concentration. For example, using a dissociation constant for Mg_2.ATP of 30 mM (Bishop *et al.*, 1981), a 5 mM solution of ATP containing 25 mM Mg^{2+} will contain approximately 3.1 mM $Mg.ATP^{2-}$ (62%) and 1.9 mM Mg_2.ATP (38%).

6.3.2.1. Interaction with Mg.ATP (1:1)

A 60 mM solution of ATP and $MgCl_2$ was titrated into a 1 mM solution of yeast PGK at pH 7.1 and monitored using 500 MHz ^1H NMR (Figure 6-6). Difference spectra corresponding to a [Mg.ATP]:[PGK] ratio of 2.04:1 are given in Figure 6-7. The observed shifts of 'basic patch' histidine peaks 3, 4 and 5a as a function of [ATP]:[PGK] ratio are plotted in Figure 6-8 and the shifts of nucleotide C8-H, C2-H and C1′-H resonances are plotted in Figure 6-9.

As observed in the titration with ATP the 'basic patch' histidine resonances are initially shifted downfield (Figure 6-8). The maximum downfield shifts, however, are less than those observed in the absence of the metal ion. At higher ratios of [ATP]:[PGK] peak 4 (His 167) broadens and shifts upfield. Resonance 3 (His 62) is also observed to shift upfield at higher nucleotide concentrations. This effect was not seen in the absence of Mg^{2+}. These results show that the metal ion alters the interaction between the nucleotide triphosphate and the 'basic patch' region of the N-terminal domain.

A summary of resonances perturbed by addition of 1:1 Mg.ATP to the protein is given in Table 6-2 (see also Figure 6-7). The resonances affected are practically the same as those affected in the absence of Mg^{2+} (*c.f.* Table

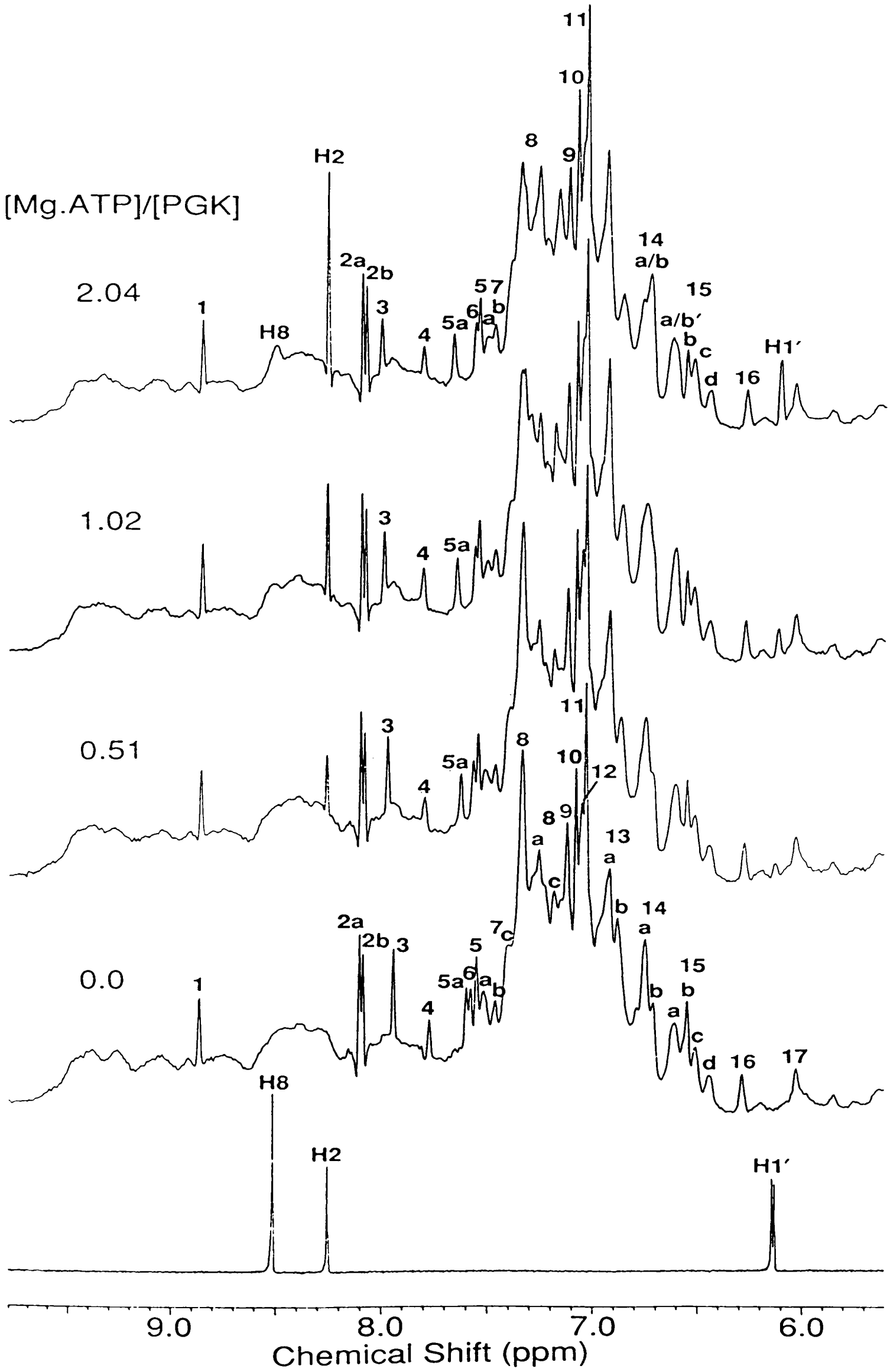

Figure 6-6A: Perturbations of the aromatic region of the 500 MHz ^{1}H NMR spectrum of yeast PGK by ATP at the ratios indicated and at a constant $[Mg^{2+}]$:[ATP] ratio of 1:1. The bottom spectrum is that obtained from a 2 mM solution of ATP and $MgCl_2$ (pH 7.10).

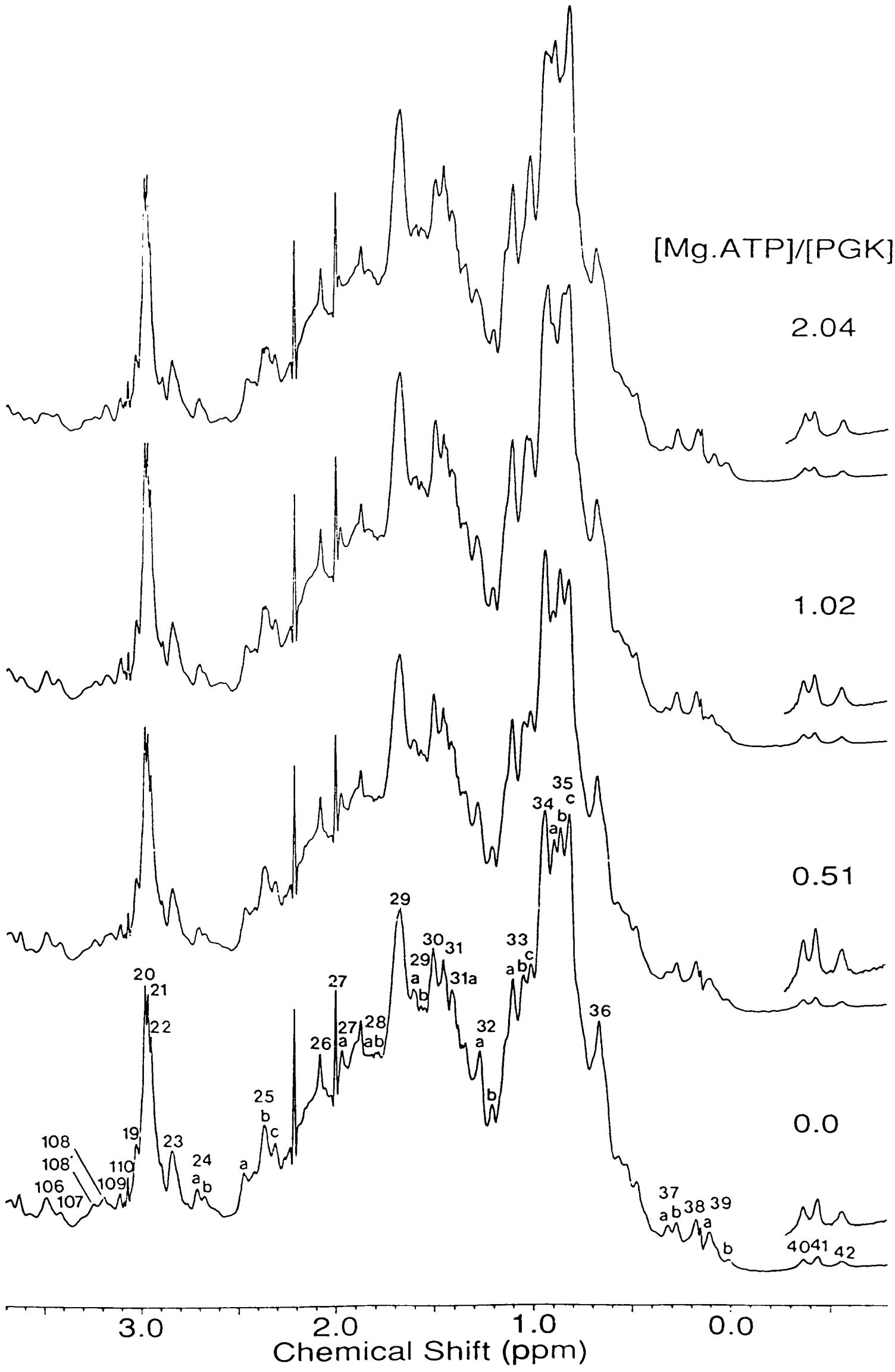

Figure 6-6B: Perturbations of the aliphatic region of the 500 MHz ^{1}H NMR spectrum of yeast PGK by ATP at the ratios indicated and a constant $[Mg^{2+}]$:[ATP] ratio of 1:1.

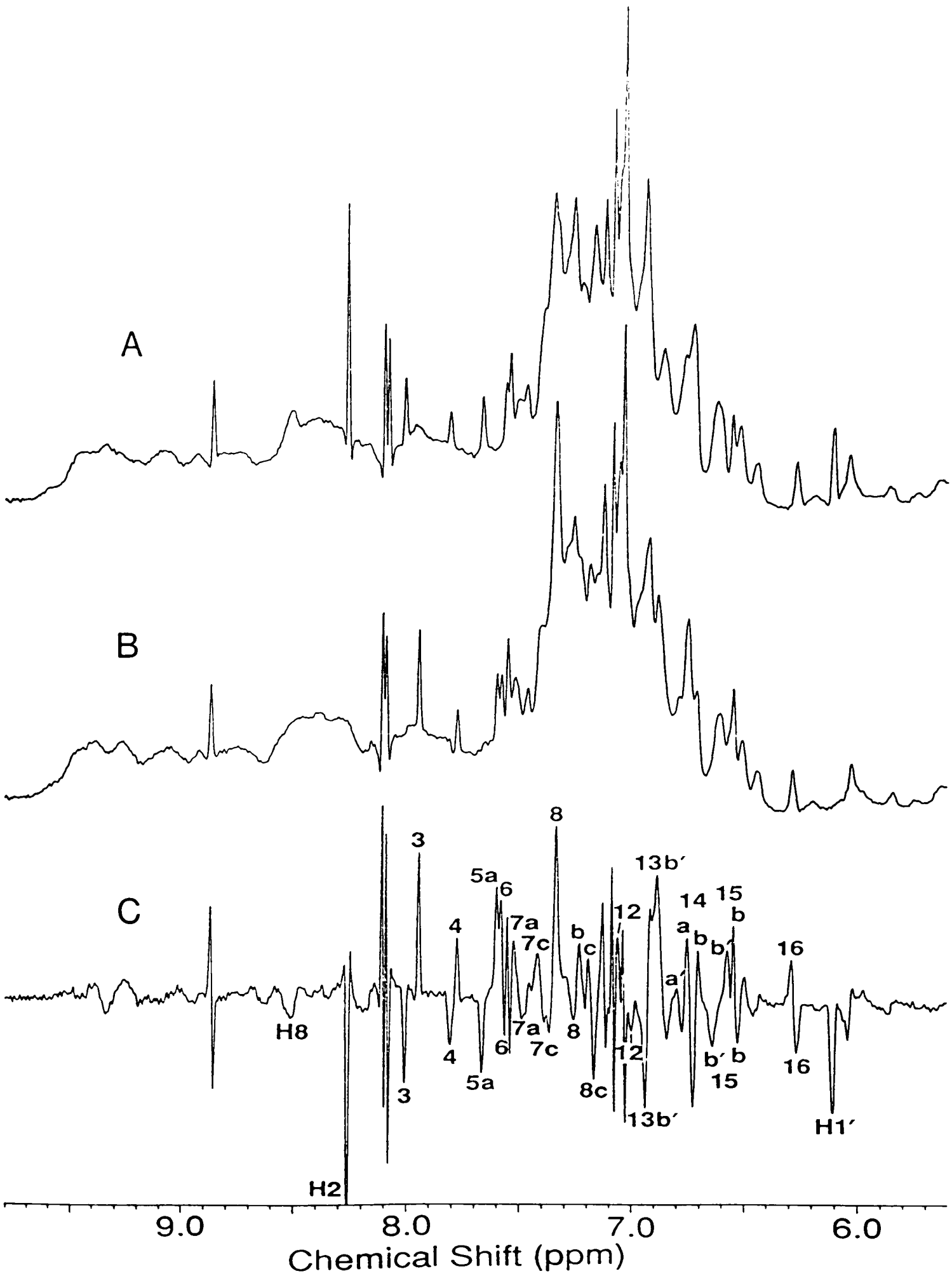

Figure 6-7A: Perturbation of the aromatic region of the 500 MHz ^1H NMR spectrum of yeast PGK by Mg.ATP. (A) Spectrum in the presence of a 2.04:2.04:1 molar ratio of Mg^{2+}:ATP:protein. (B) Spectrum in the absence of Mg^{2+} and ATP. (C) The difference spectrum (B) - (A).

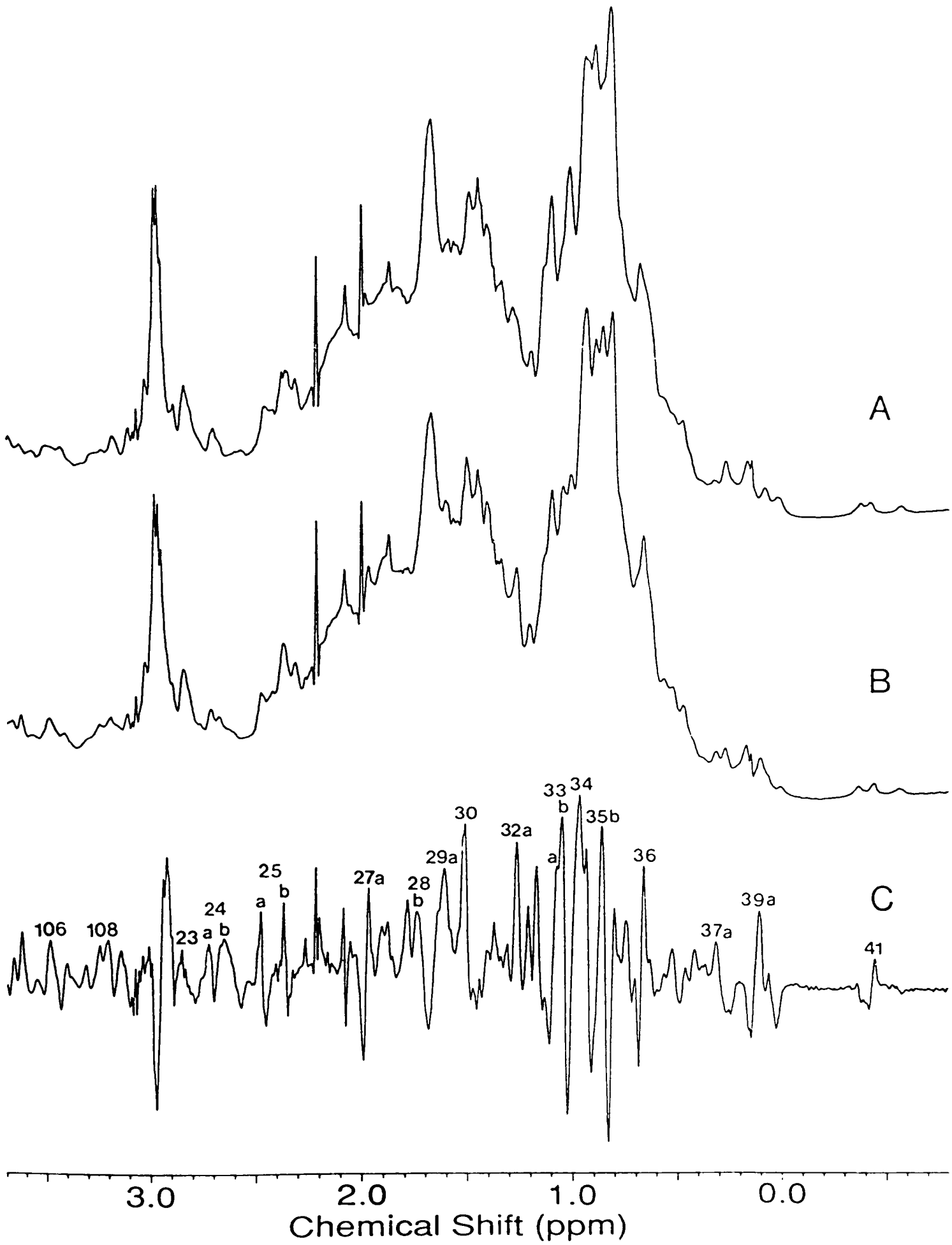

Figure 6-7B: Perturbation of the aliphatic region of the 500 MHz ^{1}H NMR spectrum of yeast PGK by Mg.ATP. (A) Spectrum in the presence of a 2.04:2.04:1 molar ratio of Mg^{2+}:ATP:protein. (B) Spectrum in the absence of Mg^{2+} and ATP. (C) The difference spectrum

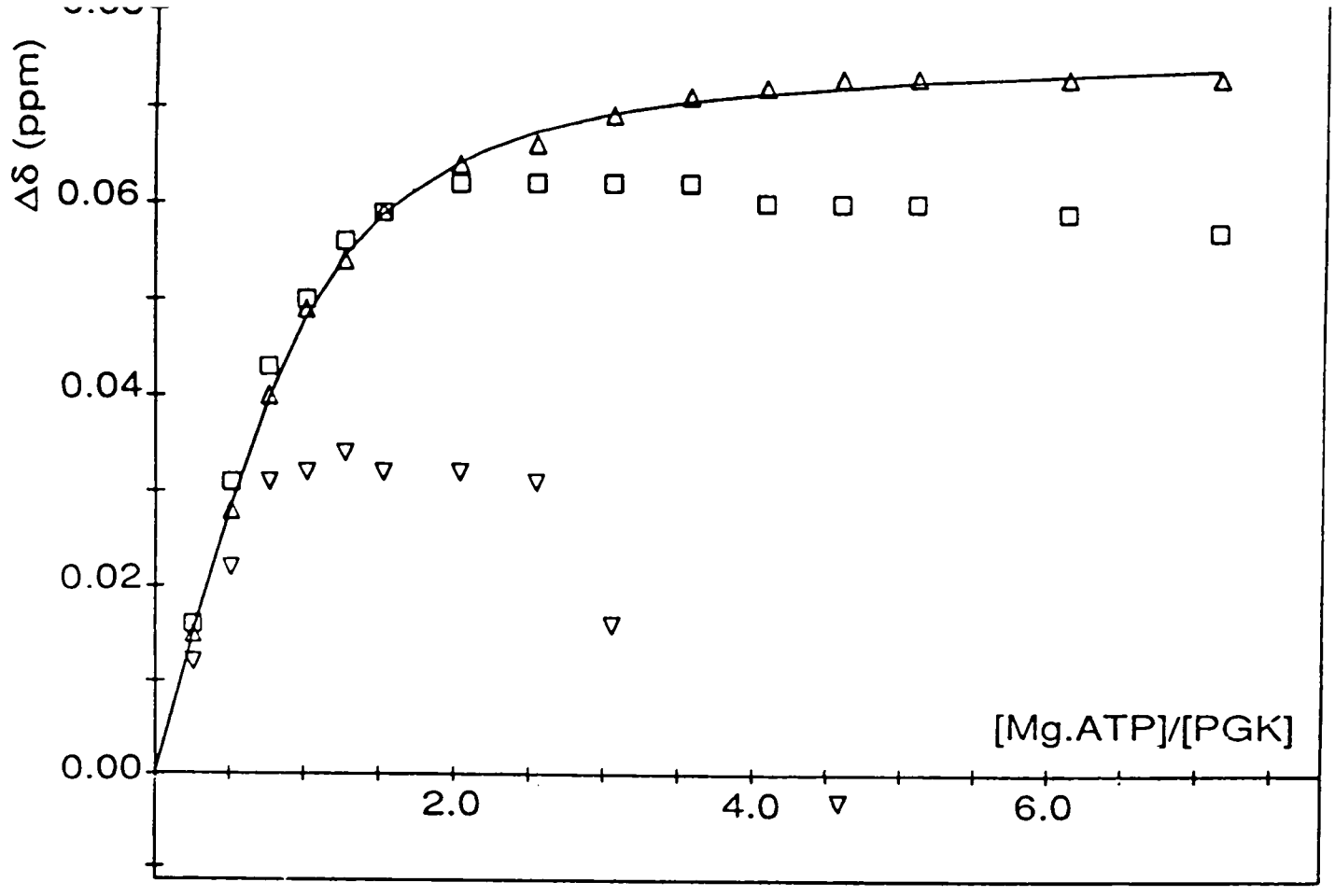

Figure 6-8: The change in the chemical shifts of peaks 3 (□; His 62), 4 (∇; His 167) and 5a (Δ; His 170) plotted as a function of ATP:protein molar ratio, at a constant $[Mg^{2+}]$:[ATP] ratio of 1:1. The continuous line represents a theoretical binding curve corresponding to a dissociation constant of 0.145 mM.

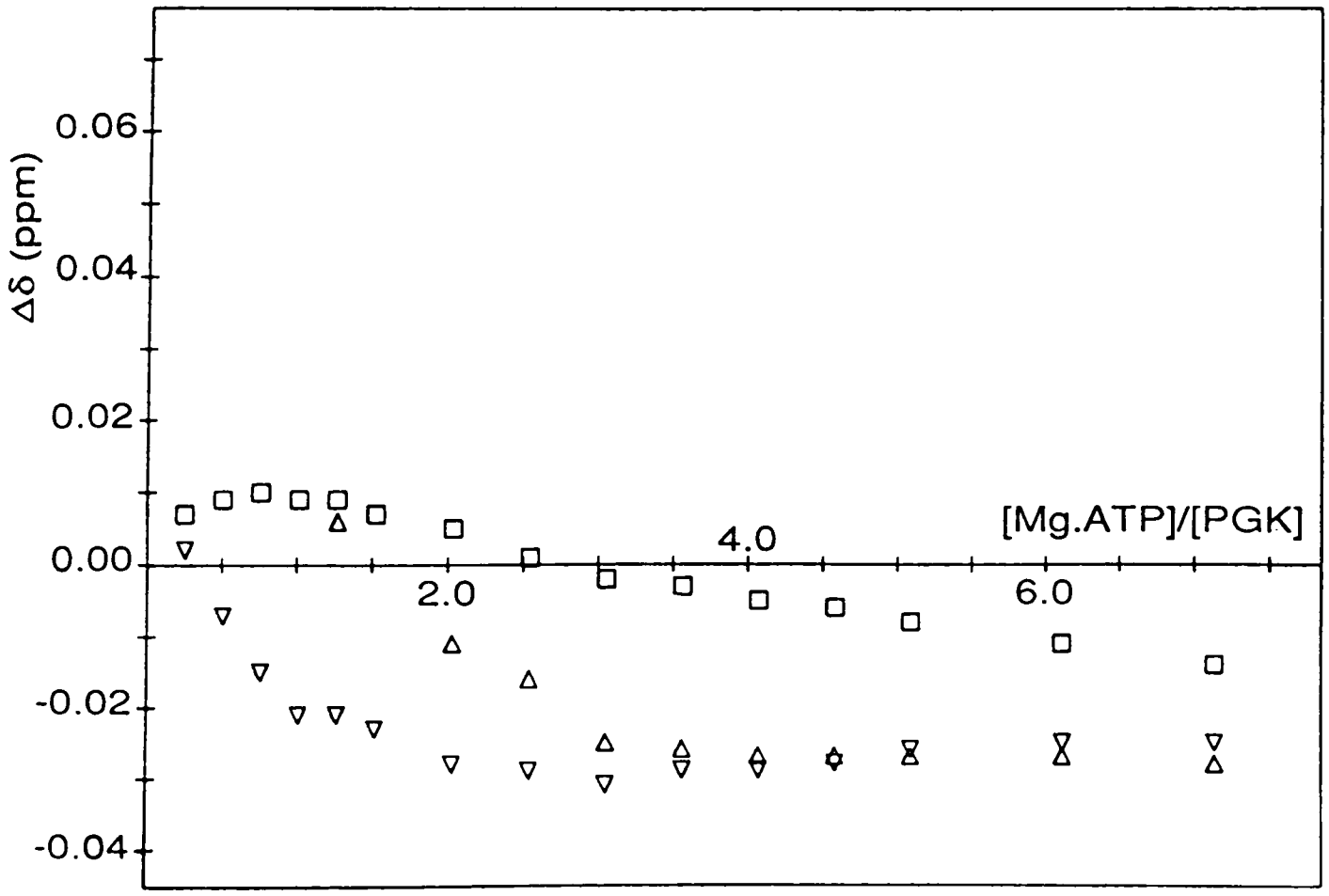

Figure 6-9: The change in the chemical shifts of the C8-H (Δ), C2-H (□) and C1′-H (∇) resonances of ATP plotted as a function of ATP:protein molar ratio, at a constant $[Mg^{2+}]$:[ATP] ratio of 1:1. The reference chemical shifts were determined from a 2 mM solution of Mg.ATP (1:1; pH 7.10) to be 8.51, 8.25 and 6.13 ppm respectively.

Table 6-2: Effects of 1:1 Mg.ATP binding on resonances of the ^1H NMR spectrum of yeast PGK

Numbers are observed shifts in ppm, negative shifts are upfield. (B) = broadening, (Sp) = peak split, (-) = upfield shift, (+) = downfield shift, – = no observable effect, ? = possible effect.

Aromatic		Aliphatic	
Resonance	Effect	Resonance	Effect
1	–	107	(+)
2a	–	108	(-)(B)
2b	–	23	?
3	+0.06	24a	(-)(B)
4	(+,-)	25a	(-)
5a	+0.07	25b	(Sp)
6	-0.02	27a	(+)
5	–	28b	(B)
7a	-0.02(B)	29a	(B)
7b	–	30	(-)(B)
7c	(-)	32a	(+)(B)
8	(-)(B)	32b	(B)
8a	?	33a	(+)
8b	(B)	33b	(-)
8c	-0.04	33c	(+)
9	–	34	(-)
10	–	35a	(+)(B)
11	–	35b	(-)
12	(-)	35c	(+)(B)
13a′	(+)	36	(+)
13b′	+0.08	37a	(+)(B)
14a′	(-)	39a	(Sp)
14a	(-)	39b	(+)
14b	(+)	41	(+)
15a	?		
15b′	(+)		
15b	(+)		
15c	(+)		
15d	(+)		
16	-0.02		
17	–		
18	–		

6-1 & Figure 6-3). Differences are, however, apparent when the concentration of nucleotide required to cause some effects is considered. As noted above the primary effect of 1:1 Mg.ATP on the 'basic patch' histidine resonances is reduced compared to the effect of ATP alone. The adenosine specific 'splitting' and broadening of peak 8 (due to an upfield shift of the component of peak 8 assigned to Phe 289) occurs at lower molar ratios of nucleotide:enzyme in the presence of Mg^{2+} than in its absence. These data alone suggest that the primary binding site of ATP involves electrostatic interactions between the triphosphate chain of the substrate and the 'basic patch' region of the N-terminal domain (*i.e.* the primary general anion binding site; see Chapter 5) while the secondary site involves hydrophobic interactions between adenosine and the hydrophobic pocket of the C-terminal domain (*i.e.* the crystallographically determined catalytic site). Addition of Mg^{2+} tends to reduce the affinity for the electrostatic site (presumably by lowering the overall negative charge associated with the triphosphate chain) and therefore increases the relative affinity for the predominantly hydrophobic catalytic site.

It is also noted that the chemical shifts of the nucleotide resonances (C8-H, C2-H and C1′-H) behave differently in the presence of a 1:1 molar ratio of Mg^{2+}:ATP (Figure 6-9). In particular the C8-H resonance appears to be in intermediate exchange and is therefore too broad to be observed until the nucleotide is in excess relative to the enzyme (Figure 6-6), above which it shifts upfield of its free position.

6.3.2.2. Dissociation constant for Mg.ATP (1:1) binding

The dissociation constant for Mg.ATP binding to yeast PGK was determined by following the chemical shift of resonance 5a (His 170) only, as a function of nucleotide:enzyme molar ratio (Figure 6-8). The biphasic data from peaks 3 (His 62) and 4 (His 167) cannot be fitted to a 1:1 ligand binding curve. The data for peak 5a were analysed using the 1:1 binding assumption (see § 3.2.2)

and the dissociation constant calculated to be 0.145 ± 0.020 mM (I = 0.10 M, pH = 7.1, T = 300 K), from two independent titrations. This value is very similar to previously reported dissociation constants for Mg.ATP (Tanswell *et al.*, 1974; Scopes, 1978; Tompa *et al.*, 1986).

6.3.2.3. Interaction with Mg.ATP (5:1)

The role of Mg^{2+} in nucleotide binding was further examined by titrating a 1.5 mM solution of yeast PGK at pH 7.1 with a 50 mM solution of ATP containing 250 mM $MgCl_2$ (*i.e.* a 5:1 excess of Mg^{2+} over ATP). As before the titration was monitored using 500 MHz ^1H NMR spectroscopy (Figure 6-10). Difference spectra corresponding to a [Mg.ATP]:[PGK] ratio of 0.47:1 are given in Figure 6-11. The change in chemical shifts of the 'basic patch' histidine resonances 3, 4 and 5a are plotted against the nucleotide:enzyme molar ratio in Figure 6-12, and the observed shifts of the nucleotide C8-H, C2-H and C1′-H resonances are plotted in Figure 6-13.

In the presence of a 5-fold excess of Mg^{2+} the effect of ATP binding on the resonances of the 'basic patch' histidines (Figure 6-12) is qualitatively similar to that observed when there is no metal ion present (Figure 6-4) or when there is an equimolar amount of Mg^{2+} relative to nucleotide (Figure 6-8). However, while the initial effect remains a downfield shift of peaks 3, 4 and 5a, the maximum shift attained decreases with increasing Mg^{2+} concentration (Figure 6-14). It is also noted that resonance 4 (His 167) does not appear to broaden to the same extent as observed in the previous cases, thereby allowing the chemical shift to be followed to higher [ATP]:[PGK] ratios. It was not possible to determine a dissociation constant in this case, because none of the observed shifts satisfied the 1:1 binding assumption *i.e.* they could not be fitted with theoretical 1:1 binding curves.

With the exception of peak 7a, which remains unshifted, all the peaks perturbed by addition of Mg.ATP in the ratio 1:1 (Table 6-2) are affected by

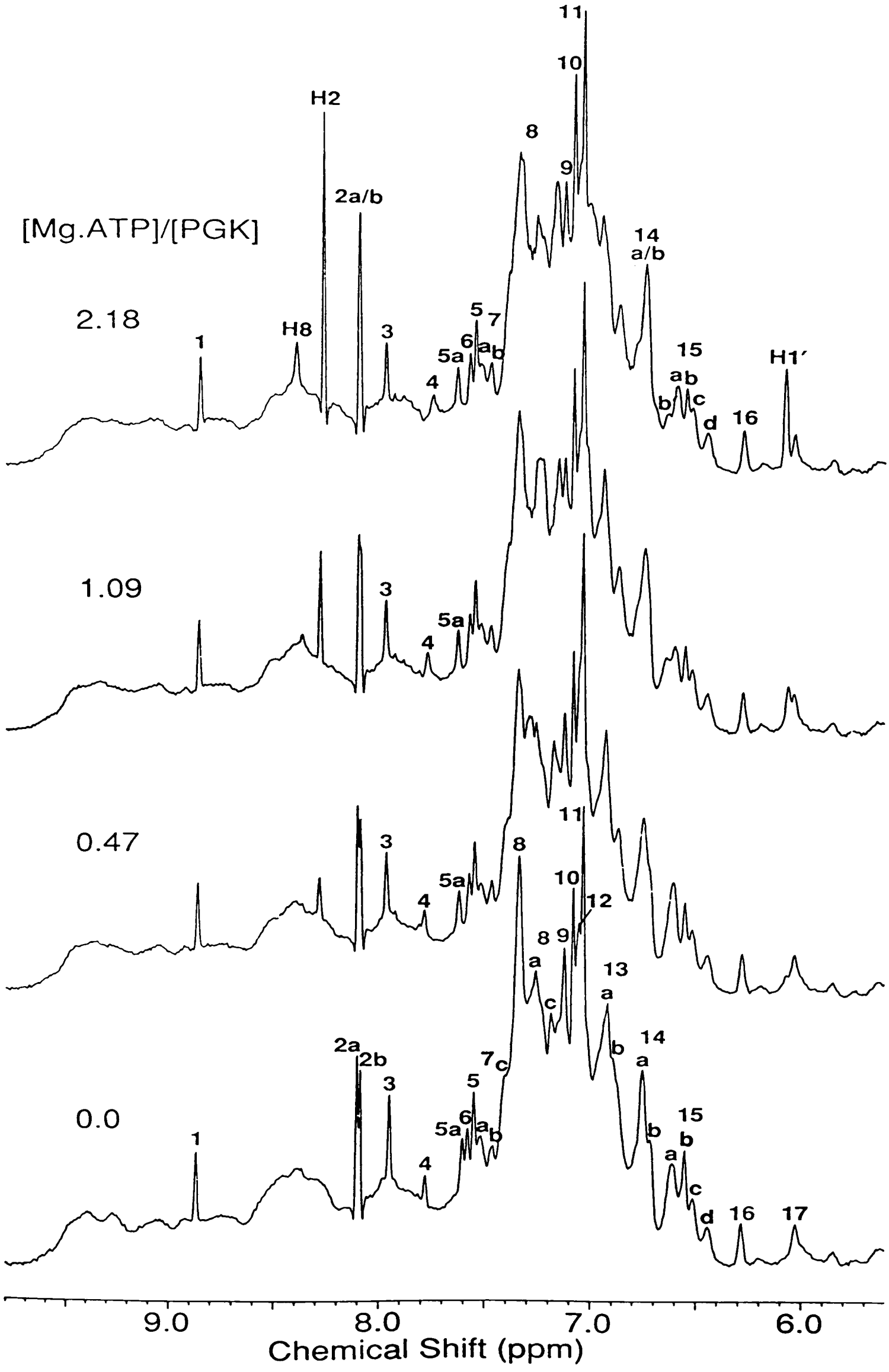

Figure 6-10A: Perturbations of the aromatic region of the 500 MHz ^{1}H NMR spectrum of yeast PGK by ATP at the ratios indicated and at a constant [Mg^{2+}]:[ATP] ratio of 5:1.

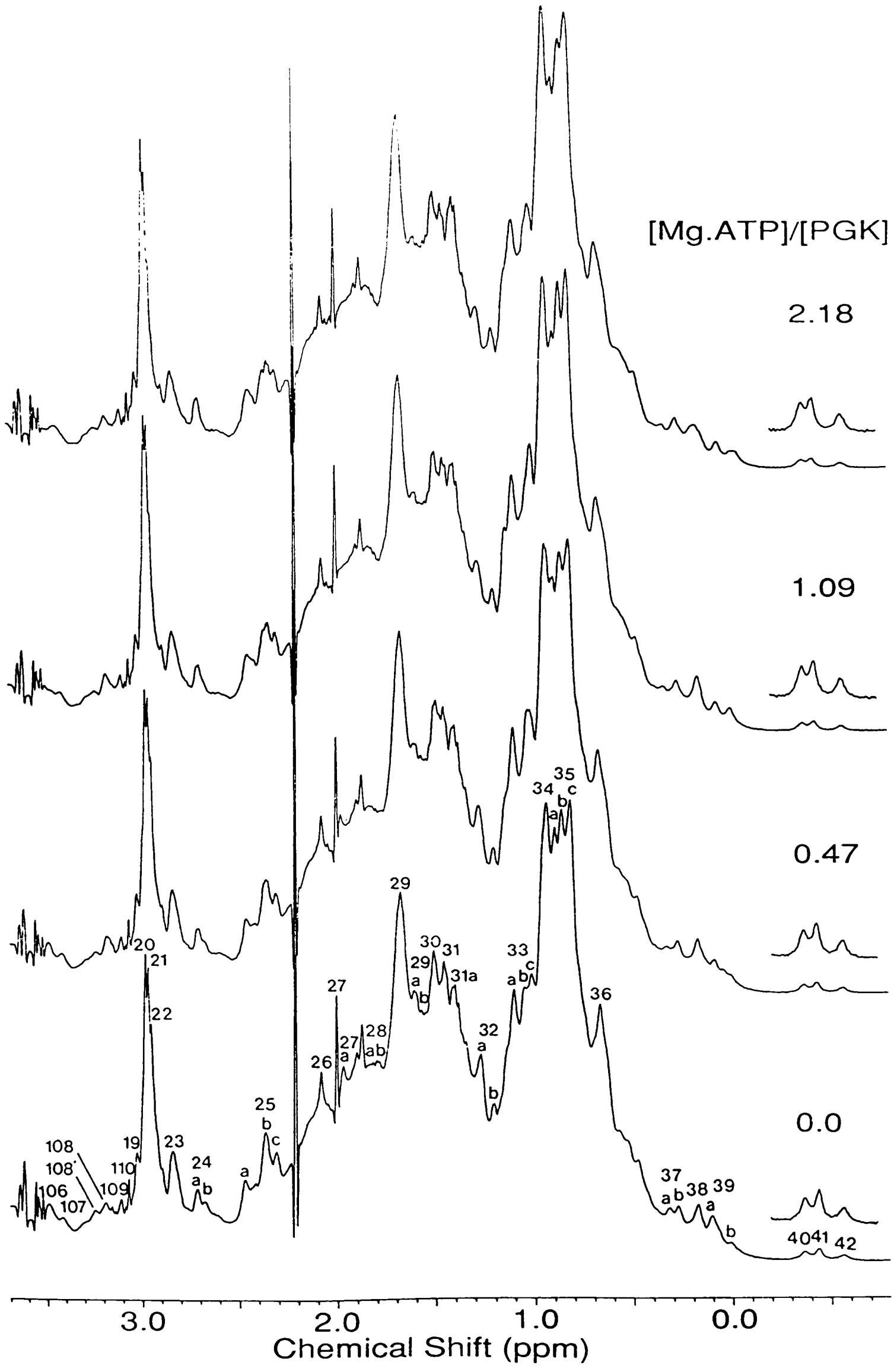

Figure 6-10B: Perturbations of the aliphatic region of the 500 MHz ^{1}H NMR spectrum of yeast PGK by ATP at the ratios indicated and a constant $[Mg^{2+}]$:[ATP] ratio of 5:1.

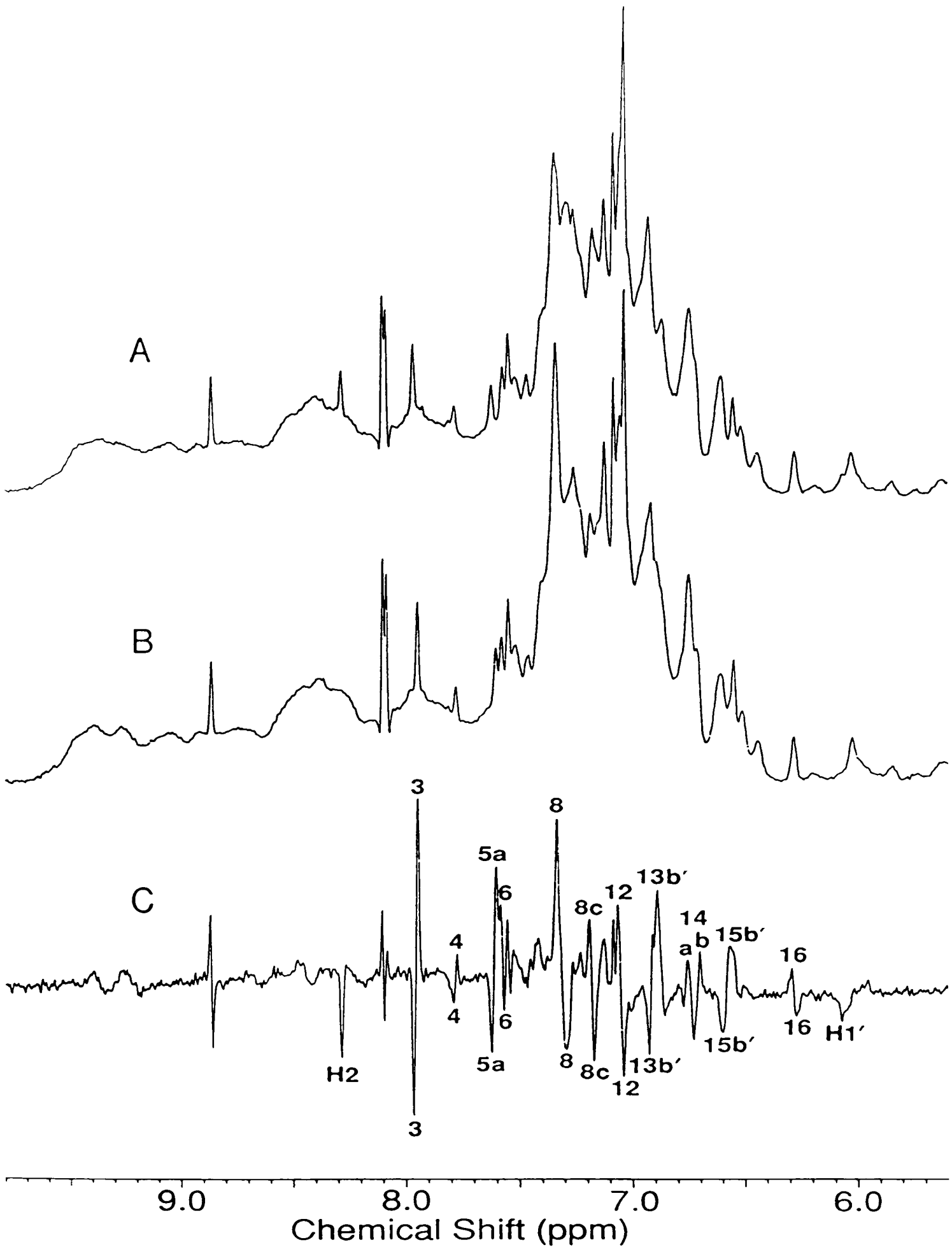

Figure 6-11A: Perturbation of the aromatic region of the 500 MHz ^1H NMR spectrum of yeast PGK by Mg.ATP. (A) Spectrum in the presence of a 2.35:0.47:1 molar ratio of Mg^{2+}:ATP:protein. (B) Spectrum in the absence of Mg^{2+} and ATP. (C) The difference spectrum (B) - (A).

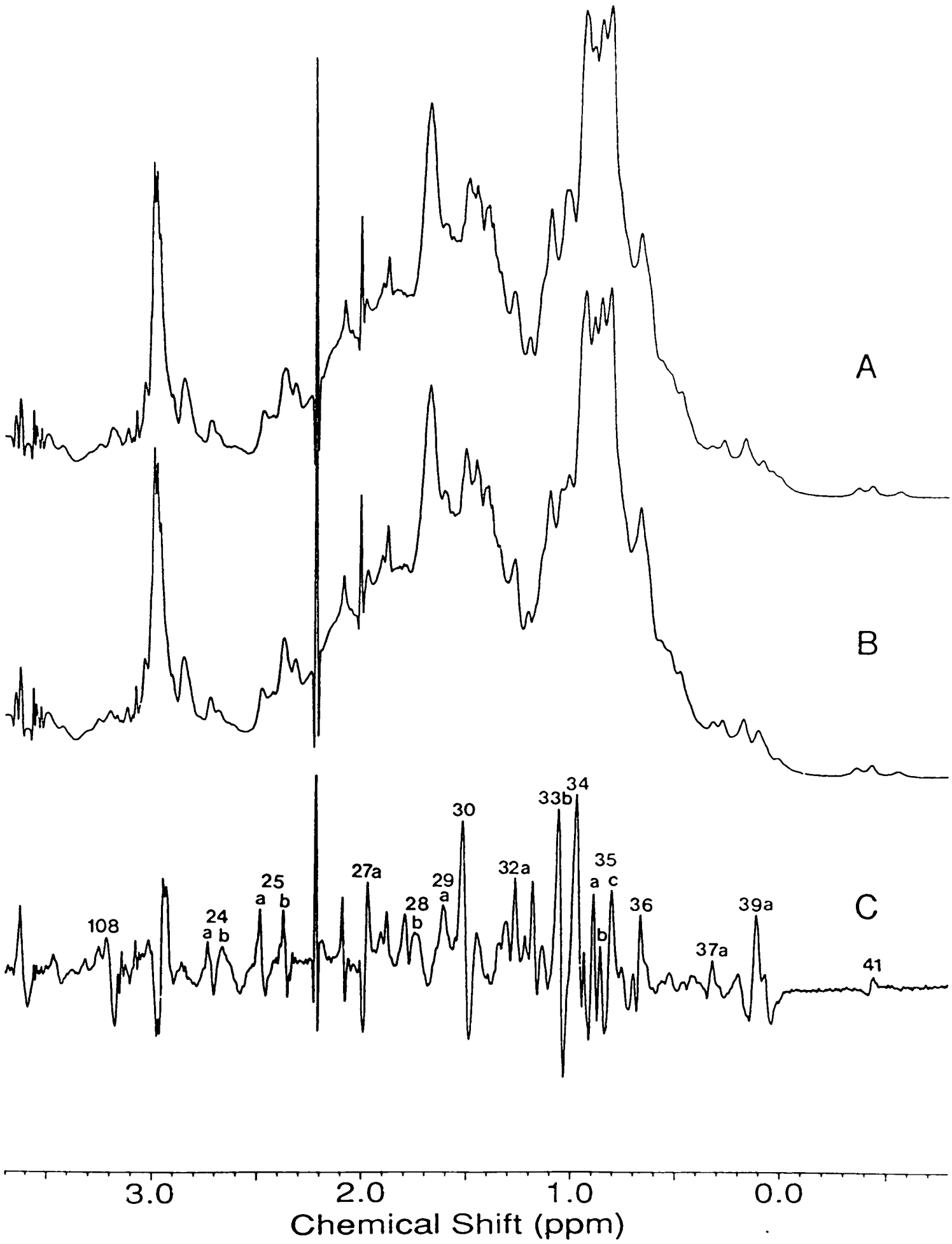

Figure 6-11B: Perturbation of the aliphatic region of the 500 MHz ^{1}H NMR spectrum of yeast PGK by Mg.ATP. (A) Spectrum in the presence of a 2.35:0.47:1 molar ratio of Mg^{2+}:ATP:protein. (B) Spectrum in the absence of Mg^{2+} and ATP. (C) The difference spectrum (B) - (A).

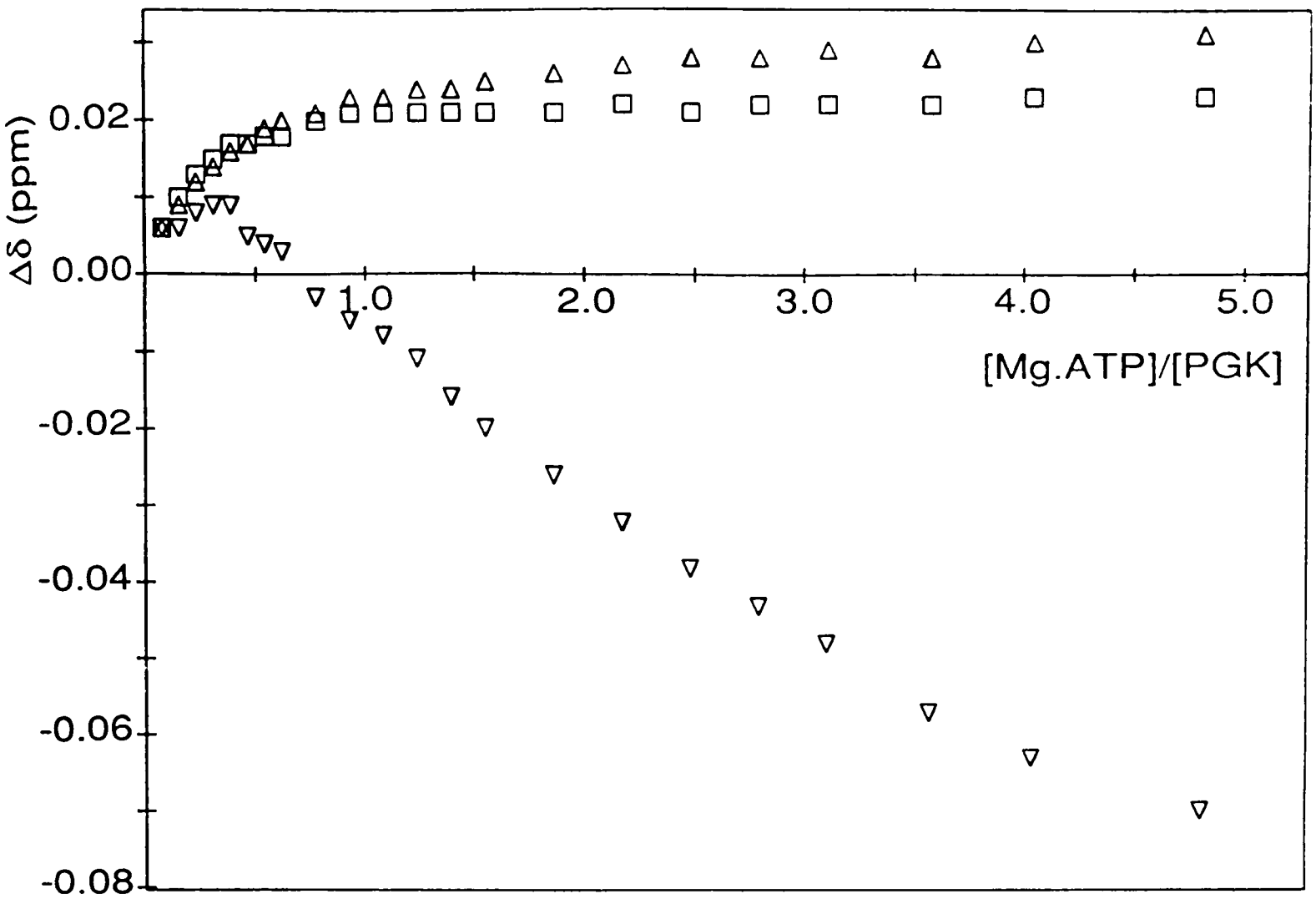

Figure 6-12: The change in the chemical shifts of resonances 3 (□; His 62), 4 (∇; His 167) and 5a (Δ; His 170) plotted as a function of ATP:protein molar ratio, at a constant $[Mg^{2+}]$:[ATP] ratio of 5:1.

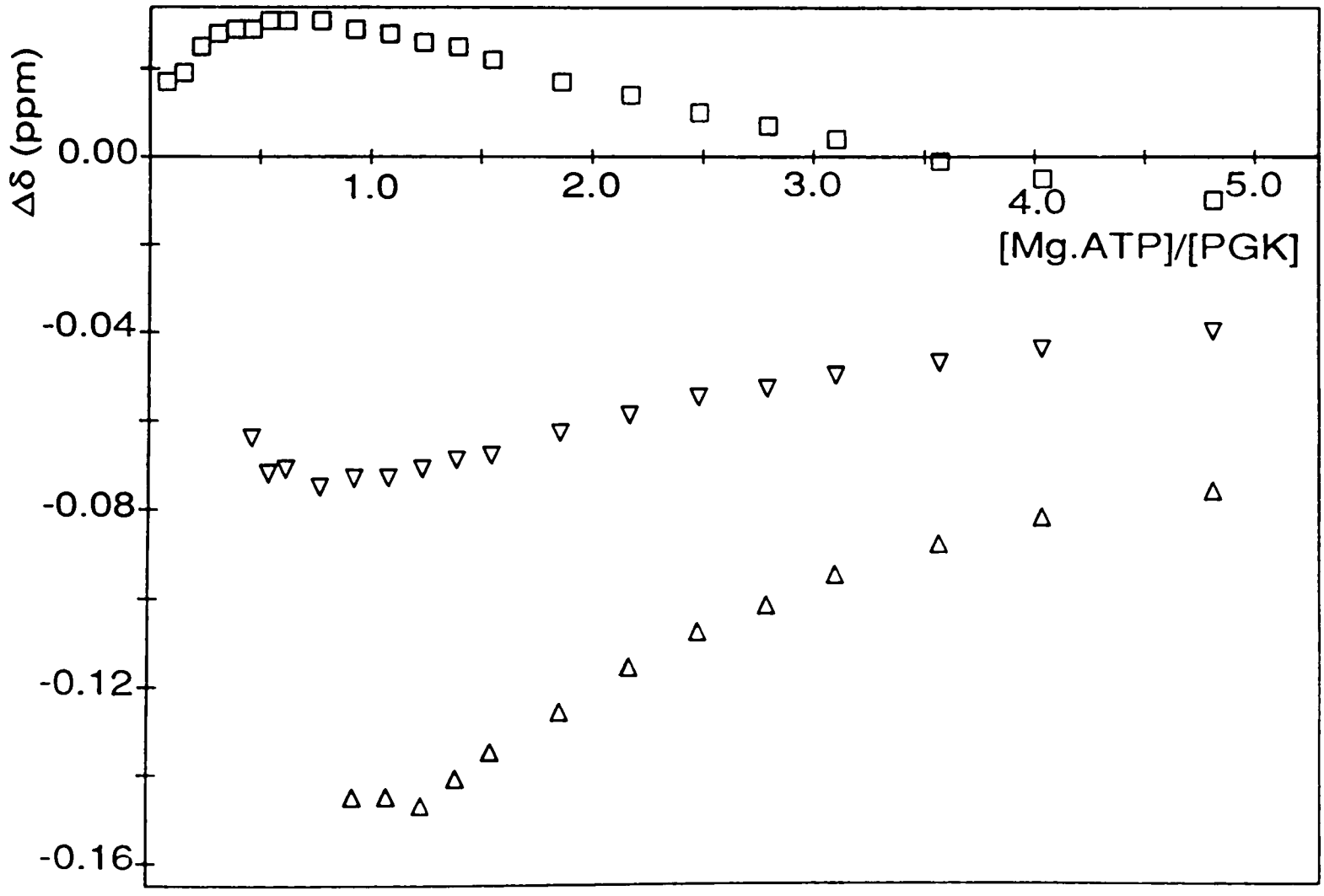

Figure 6-13: The change in the chemical shifts of the C8-H (Δ), C2-H (□) and C1′-H (∇) resonances of ATP plotted as a function of ATP:protein molar ratio, at a constant $[Mg^{2+}]$:[ATP] ratio of 5:1. The reference chemical shifts used are as in Figure 6-9.

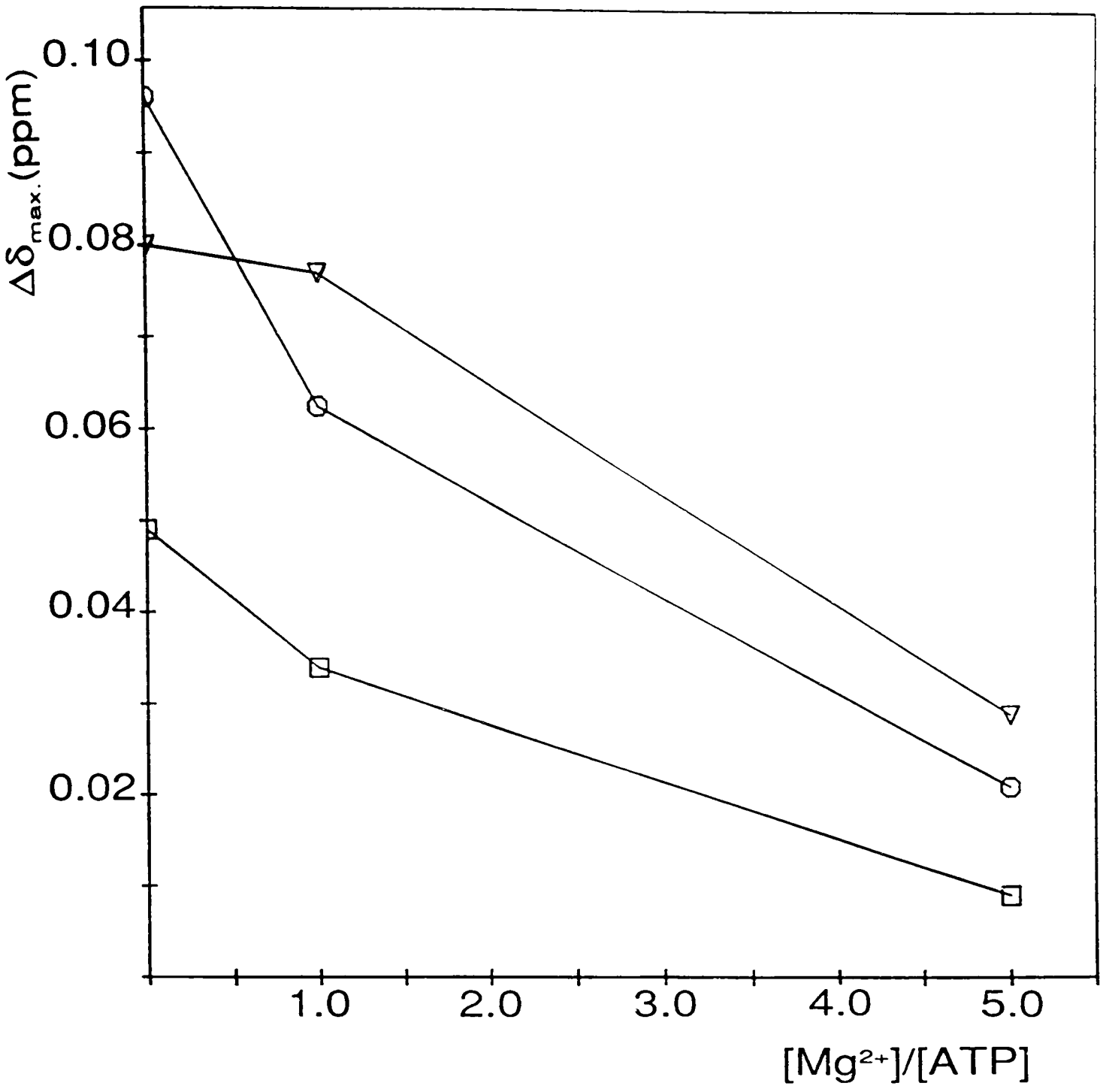

Figure 6-14: The maximum downfield change in chemical shift ($\Delta\delta_{max.}$) observed for the 'basic patch' histidine resonances 3 (○; His 62), 4 (□; His 167) and 5a (▽; His 170) on addition of ATP plotted as a function of the Mg^{2+}:ATP molar ratio.

Mg.ATP in the ratio 5:1. In the latter case, however, the adenosine specific 'splitting' of peak 8 is observed at an [ATP]:[PGK] ratio of ~ 0.3:1 (*c.f.* ~ 1.3:1 in the absence of metal ion) suggesting that the affinity of the nucleotide for the hydrophobic catalytic site has been increased further relative to the electrostatic anion binding site as the Mg^{2+} concentration, and hence the proportion of $Mg.ATP^{2-}$ and $Mg_2.ATP$ relative to ATP^{4-} in solution, has increased.

The chemical shifts of the nucleotide peaks as a function of [ATP]:[PGK] ratio are also different relative to the previous titrations (*c.f.* Figures 6-13, 6-9 and 6-5). As was observed on addition of 1:1 Mg.ATP the C8-H resonance is too broad to be observed at [ATP]:[PGK] ratios less than 1:1. At this ratio, however, the chemical shift of the C8-H resonance is ~ 0.14 ppm upfield of its position in a 2 mM solution of ATP and $MgCl_2$ (*i.e.* the reference chemical shifts in Figures 6-9 and 6-13). As the molar ratio of nucleotide:enzyme is increased from 1:1 to 5:1 the chemical shifts of the nucleotide C8-H, C2-H and C1′-H shifts towards their free positions. [Note that the chemical shifts of the free nucleotide peaks under these conditions are not expected to be identical to the reference values *i.e.* those measured from a 2 mM solution of ATP and $MgCl_2$, pH 7.1].

6.3.3. *Effect of Mg^{2+} on the binding of ATP to PGK*

In the preceding section it was shown that the mode of ATP binding to PGK is affected by the Mg^{2+} concentration. This affect has been further investigated by titrating ATP into a solution of PGK containing a large excess (~ 50 mM) of Mg^{2+} and by titrating a solution containing ATP and PGK with Mg^{2+}.

6.3.3.1. Effect of ATP binding on the 1D ^1H NMR spectrum of PGK in the presence of 50 mM $MgCl_2$

A 1 mM solution of PGK was made 50 mM in Mg^{2+} by addition of the

required volume of a 1 M $MgCl_2$ solution. The only significant effects observed in the aromatic region of the spectrum (Figure 6-15) are associated with His 123 and His 149 (peaks 1, 2a, 5 and 10 are shifted). These histidine residues are in close proximity to a weak cation binding site as can be demonstrated by addition of the relaxation probe, Mn^{2+}, to the free enzyme (see § 7.3.1). A 60 mM solution of ATP was then titrated into the ~ 1 mM PGK/50 mM Mg^{2+} solution and monitored using 500 MHz ^1H NMR (Figure 6-15). The shifts of 'basic patch' histidine resonances 3, 4 and 5a are plotted are plotted in Figure 6-16 and of nucleotide peaks C8-H, C2-H and C1′-H are plotted in Figure 6-17.

It is immediately seen that peak 4 (His 167) only shifts upfield and that the change in shift is approximately linear with nucleotide concentration up to an [ATP]:[PGK] ratio of ~ 6:1. The small downfield shifts observed for peaks 3 (His 62) and 5a (His 170) are also approximately linear in this range. The absence of a downfield shift of peak 4 indicates that interactions between the nucleotide and the general anion binding site are minimal under these conditions. In this experiment the concentration of ATP^{4-} in solution is negligible, thereby eliminating any contribution due to electrostatic binding of this species. Also, the proportion of nucleotide present as neutral Mg_2.ATP will be significant. For instance, using K_d(Mg.ATP^{2-}) = 0.051 mM (Sigel *et al.*, 1987) and K_d(Mg_2.ATP) = 30 mM (Bishop *et al.*, 1981) a 1 mM solution of ATP in 50 mM $MgCl_2$ will contain ~ 0.62 mM Mg_2.ATP and ~ 0.38 mM Mg.ATP^{2-}. The di-magnesium complex will clearly not bind in the electrostatic site and its affinity for the catalytic site is likely to be reduced due to competition between the Mg^{2+} ion and lysine residues 213 and 217 for the α- and β-phosphates.

Since a six-fold excess of nucleotide over protein is not sufficient to saturate the binding (as judged from the shifts of histidine resonances 3, 4 and 5a; Figure 6-16) it is not possible to calculate a dissociation constant

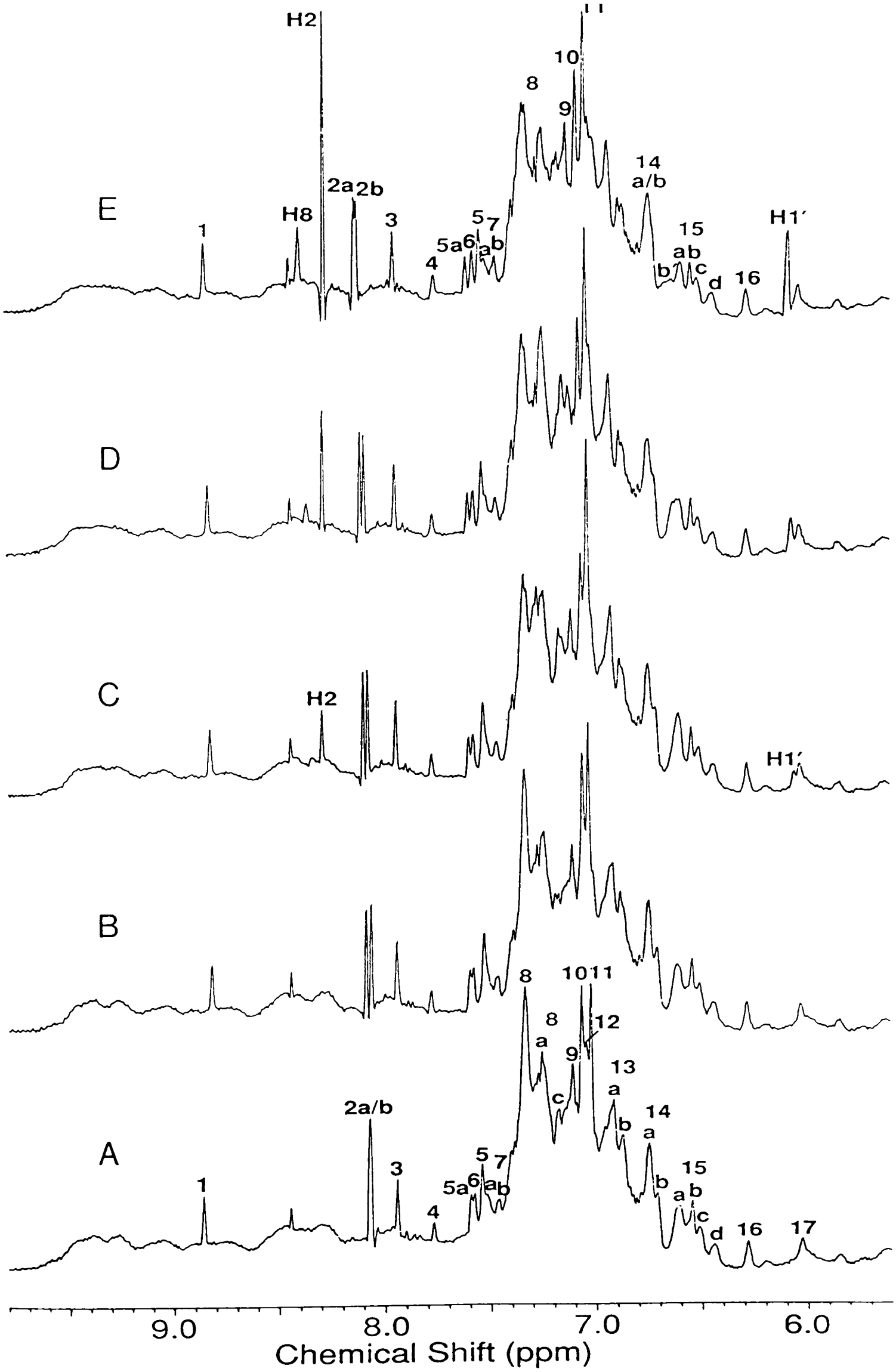

Figure 6-15: Perturbation of the aromatic region of the 500 MHz ^{1}H NMR spectrum of yeast PGK by ATP in the presence of 50 mM Mg^{2+}. (A) Spectrum in the absence of Mg^{2+} and ATP. (B) Spectrum in the presence of 50 mM $MgCl_2$. (C), (D) and (E) Spectrum as in (B) but with the addition of ATP to give molar ratios of ATP:PGK of 0.5:1, 1.0:1 and 2.0:1, respectively.

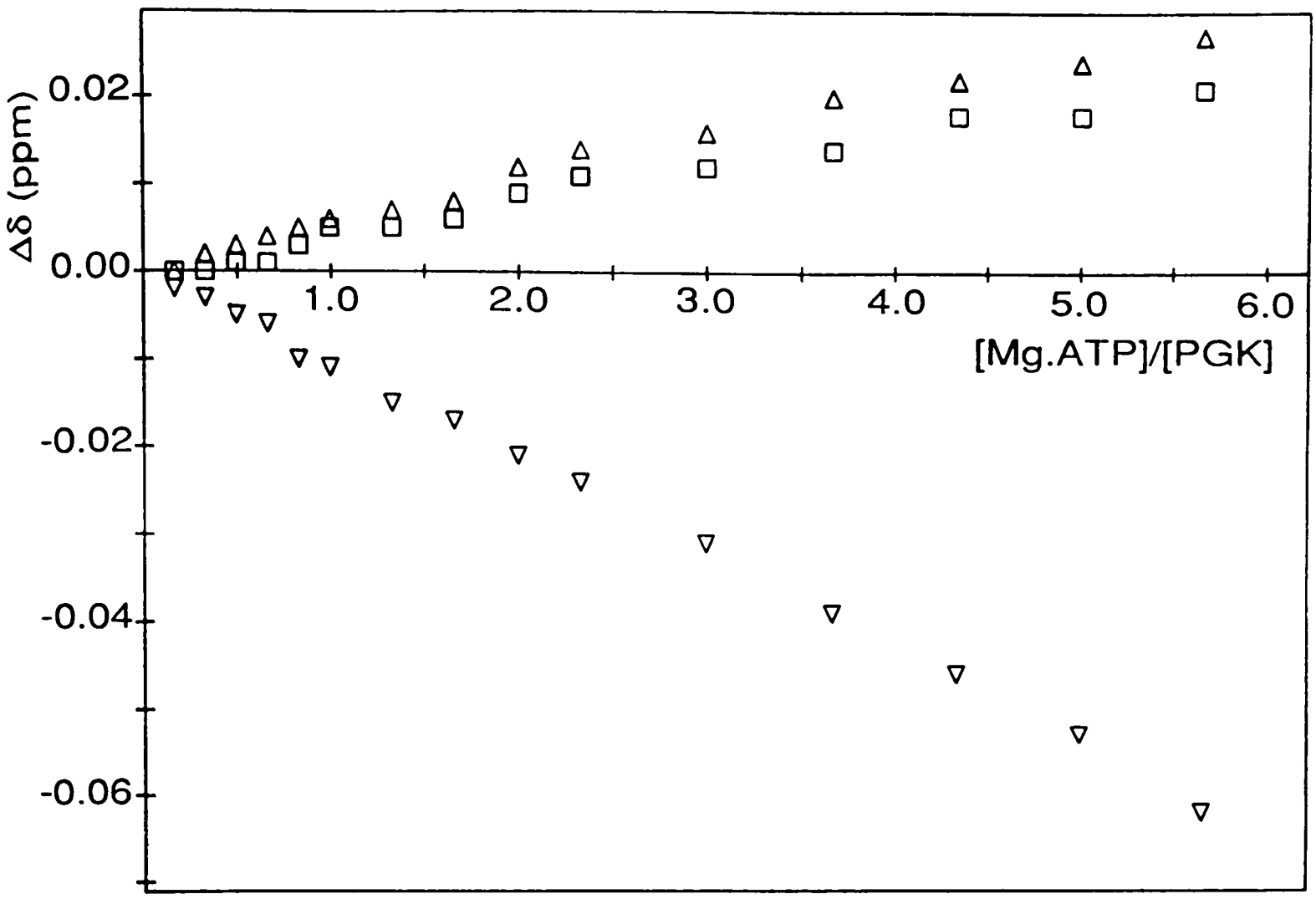

Figure 6-16: The change in the chemical shifts of peaks 3 (□; His 62), 4 (∇; His 167) and 5a (Δ; His 170) plotted as a function of ATP:protein molar ratio, in the presence of 50 mM $MgCl_2$.

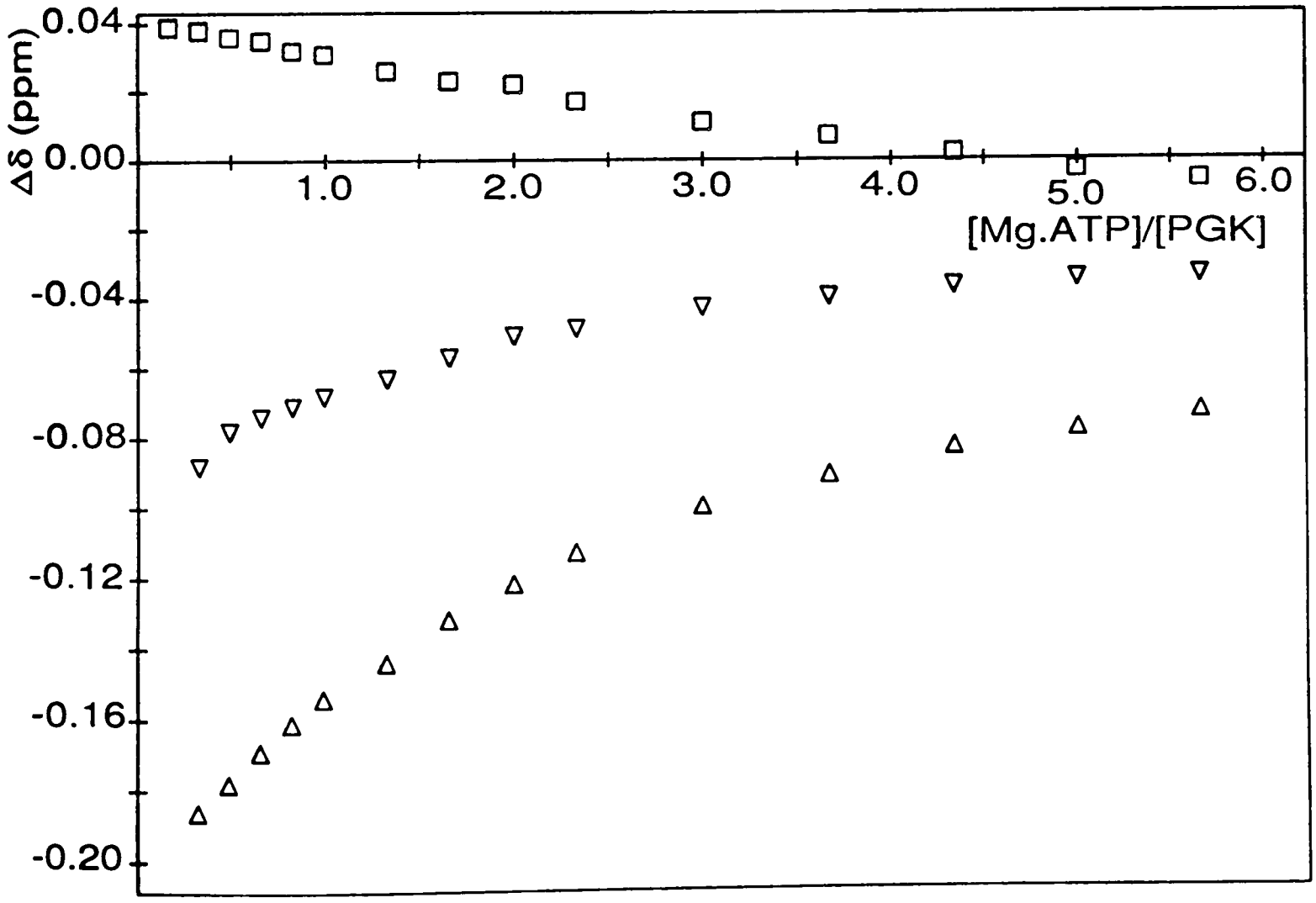

Figure 6-17: The change in the chemical shifts of the C8-H (Δ), C2-H (□) and C1′-H (∇) resonances of ATP plotted as a function of ATP:protein molar ratio, in the presence of 50 mM $MgCl_2$. The reference chemical shifts used are as in Figure 6-9.

for ATP under these conditions. It is evident, however, that the total affinity is less than that determined for binding of 1:1 Mg.ATP to the electrostatic site (by at least an order of magnitude).

Effects indicative of adenosine binding (particularly at peak 8) were observed in the aromatic region of the spectrum following the first addition of ATP, suggesting that under these conditions the nucleotide binds only at the hydrophobic site. The shifts observed for the nucleotide peaks (Figure 6-17) support this conclusion, with the initial shifts representing the environment of ATP bound at the hydrophobic site. As the ratio of [ATP]:[PGK] increases the nucleotide resonances shift towards their free positions, as expected for a two site (free and bound) system in the fast exchange limit. The 'free' chemical shift positions appear to be similar to those observed when 5:1 Mg.ATP was in excess relative to the protein (*c.f.* Figure 6-13).

6.3.3.2. Effect of Mg^{2+} on the 1D ^1H NMR spectrum of ATP.PGK

A solution of ATP and PGK in the ratio 1.5:1 was titrated with $MgCl_2$ until the ratio $[Mg^{2+}]$:[ATP] was ~ 36:1. The titration was monitored using 500 MHz ^1H NMR spectroscopy (Figure 6-18). A plot of the change in chemical shift of the 'basic patch' histidine peaks 3, 4 and 5a as a function of $[Mg^{2+}]$:[ATP] ratio is given in Figure 6-19. A plot of the chemical shifts of the nucleotide peaks C8-H, C2-H and C1′-H as a function of $[Mg^{2+}]$:[ATP] ratio is given in Figure 6-20.

As would be predicted from the previous experiments the 'basic patch' histidine resonances, which were initially shifted downfield as a result of ATP^{4-} binding, are shifted upfield with increasing Mg^{2+} concentration. Peak 4 (His 167) appears to reach a constant value at a $[Mg^{2+}]$:[ATP] ratio of ~ 10:1. Above this ratio the chemical shifts of peaks 3 (His 62) and 5a (His 170) appear to be independent of the presence of ATP with the small upfield shifts being similar to those observed in control experiments where $MgCl_2$ was titrated into a solution of free PGK. This point is demonstrated in Figure 6-21

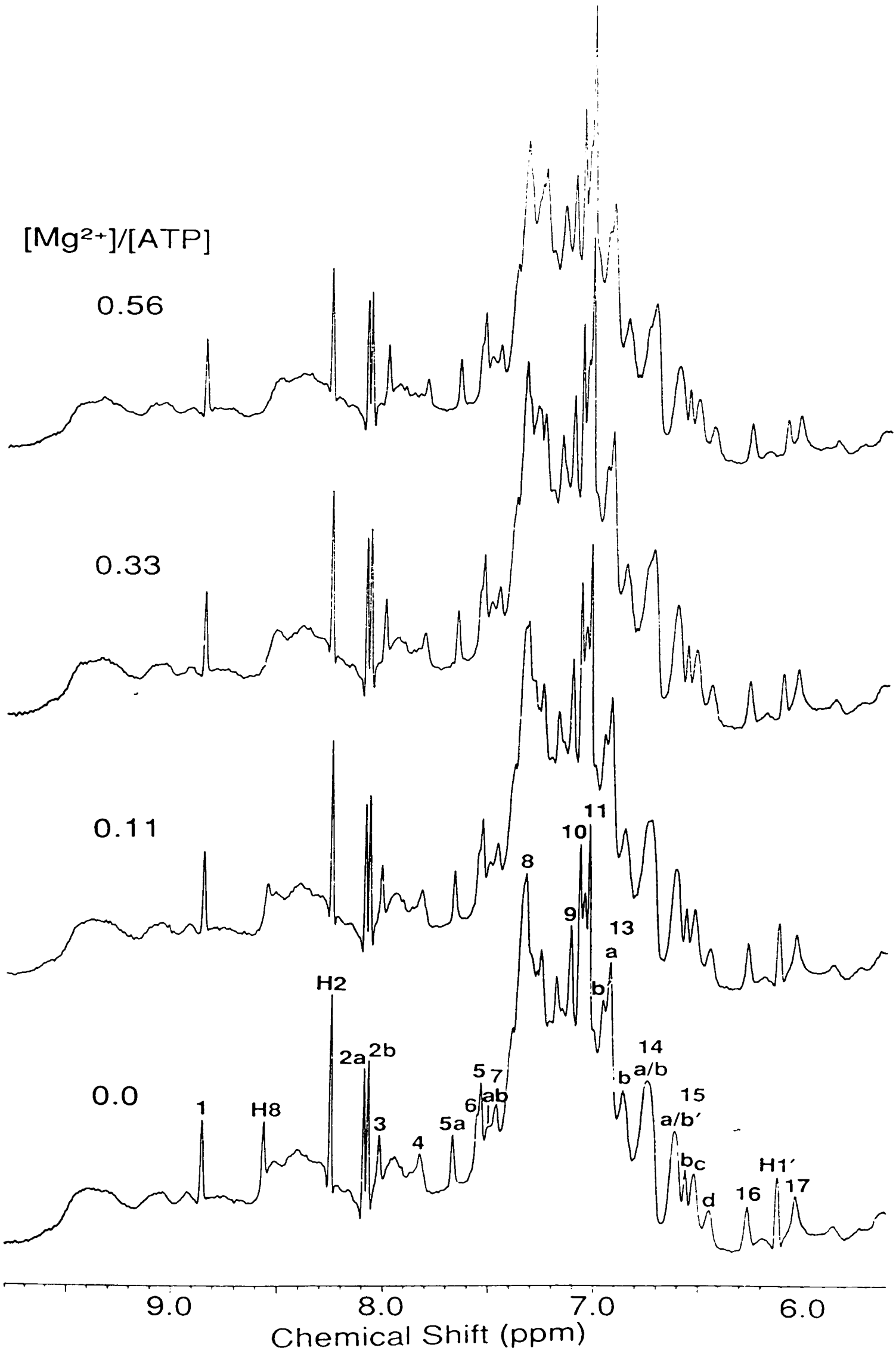

Figure 6-18: Perturbation of the aromatic region of the 500 MHz ^{1}H NMR spectrum of PGK in the presence of a 1.5:1 molar excess of ATP by Mg^{2+} at the $[Mg^{2+}]$:[ATP] ratios indicated.

(cont'd)

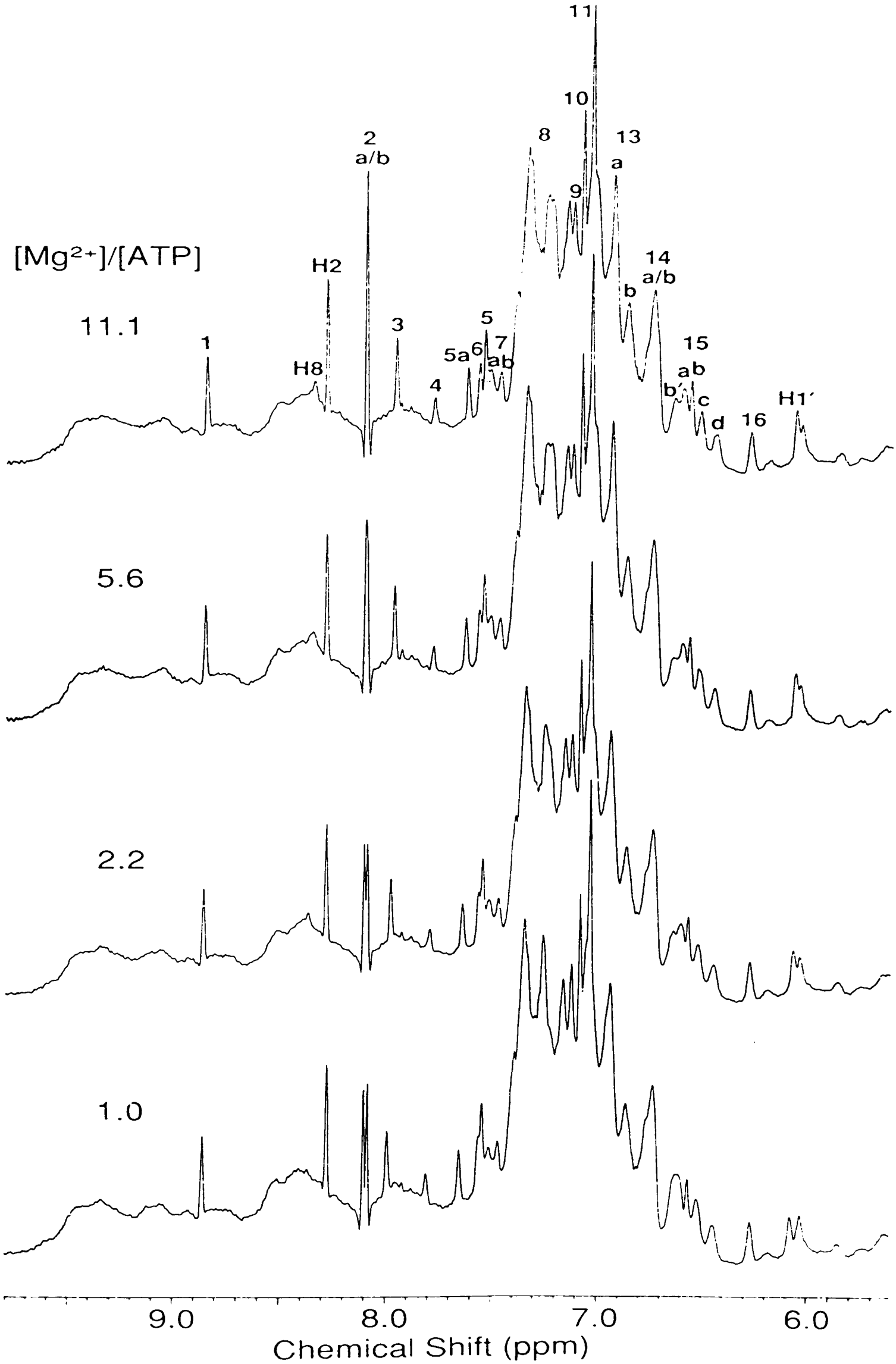

Figure 6-18 (cont'd)

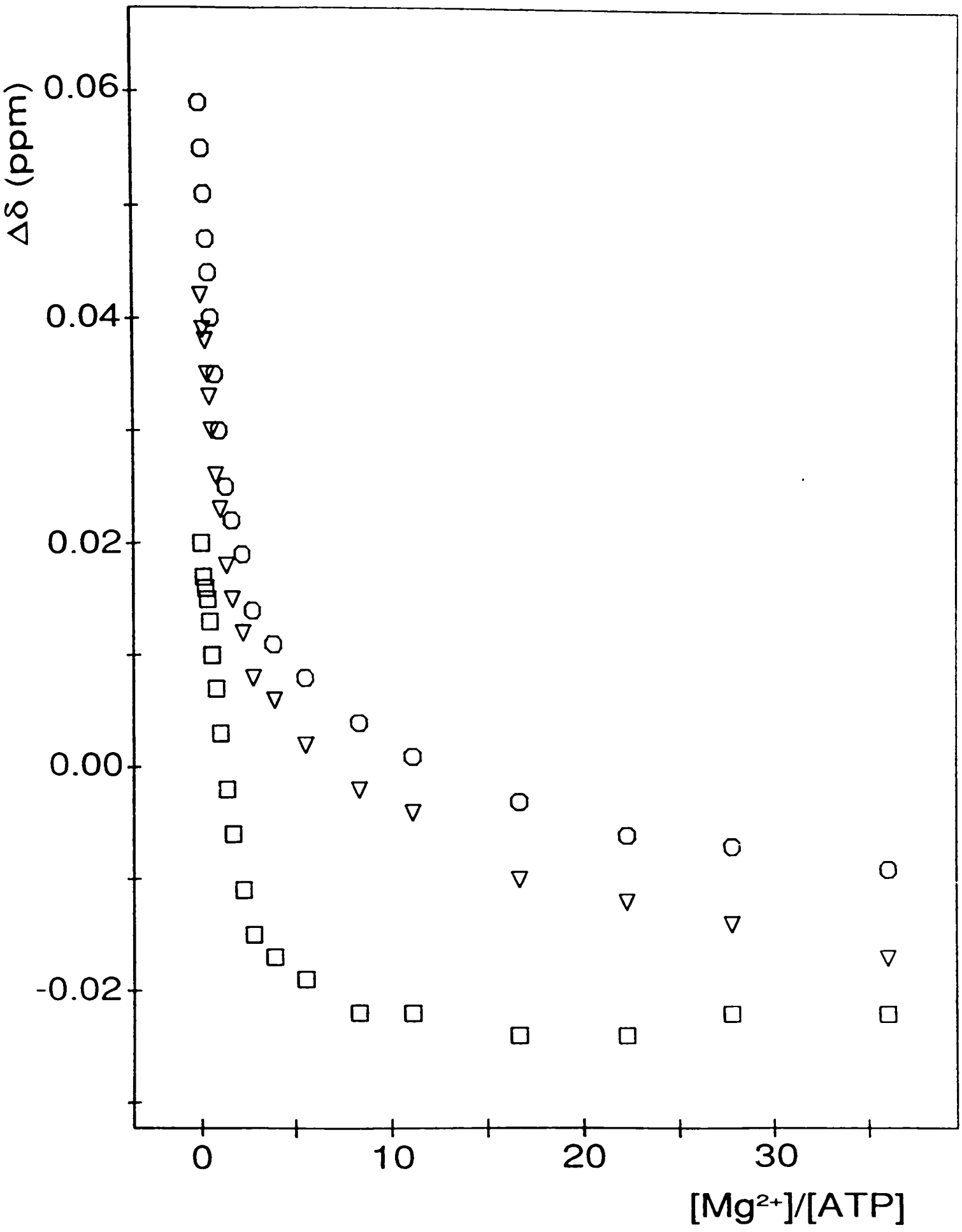

Figure 6-19: The change in the chemical shifts of peaks 3 (○; His 62), 4 (□; His 167) and 5a (▽; His 170) plotted as a function of Mg^{2+}:ATP molar ratio. The [ATP]:[PGK] ratio was constant at 1.5:1.

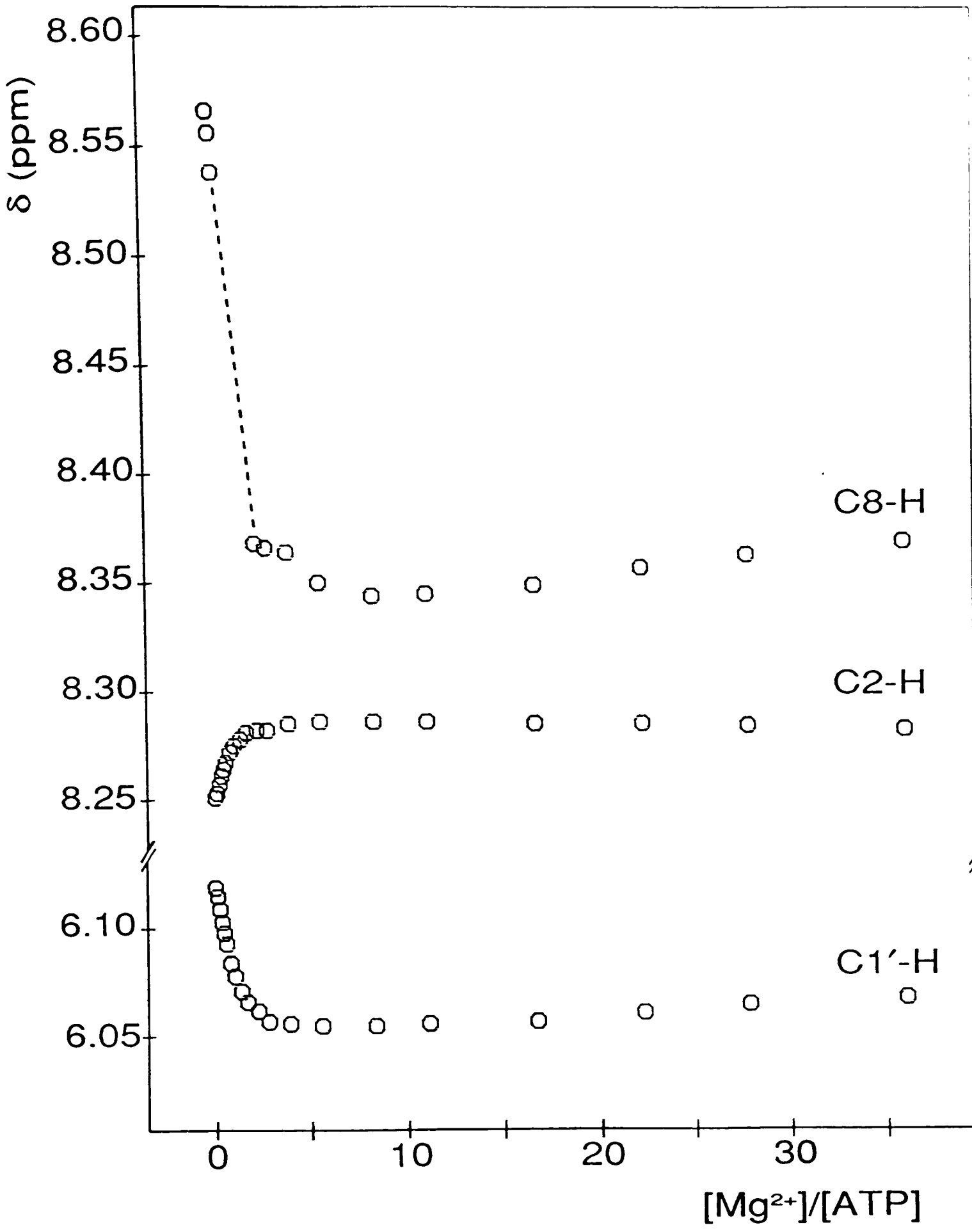

Figure 6-20: The chemical shifts of the C8-H, C2-H and C1′-H resonances of ATP plotted as a function of Mg^{2+}:ATP molar ratio. The [ATP]:[PGK] ratio was constant at 1.5:1.

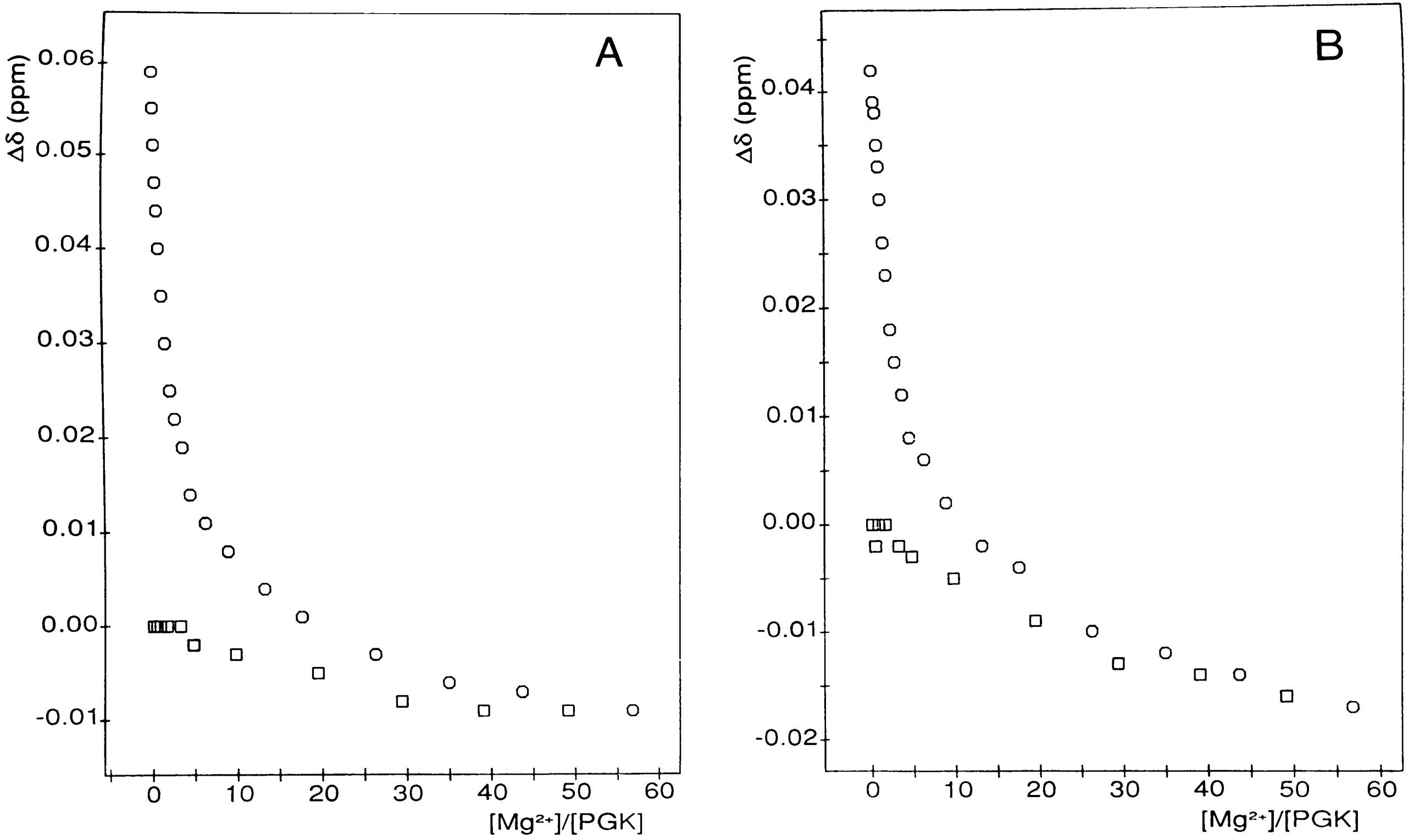

Figure 6-21: The change in the chemical shifts of peaks 3 (A) and 5a (B) plotted as a function of Mg^{2+}:protein molar ratio in the absence of (□) and the presence of (○) a 1.5:1 molar excess of ATP.

where the shifts of peaks 3 and 5a are plotted against [Mg^{2+}]:[PGK] ratio both in the presence and absence of ATP.

As the Mg^{2+} concentration increases a component of peak 8 is observed to broaden and shift upfield, peak 8c shifts upfield, a component of peak 12 shifts upfield and peak 15b′ shifts downfield (Figure 6-18). These effects are indicative of adenosine binding. The upfield shifts observed for the 'basic patch' histidine resonances are therefore due to a decrease in the occupancy of the primary electrostatic ATP^{4-} binding site and a concomitant increase in the occupancy of the hydrophobic (and presumably catalytic) site with increasing Mg^{2+} concentration. It is also noted that peak 7a shifts back downfield to its position in unliganded PGK as the Mg^{2+} concentration increases. The upfield shift of this resonance on binding ATP^{4-} is therefore an effect due to binding at the primary electrostatic site. An upfield shift of peak 7a was also observed on binding 3-PG (§ 3.3.1), $[Co(CN)_6]^{3-}$ (§ 5.3.2; Figure 5-7) and sulphate (H.C. Graham, personal communication) to the enzyme.

The nucleotide peaks C8-H, C2-H and C1′-H are all broadened by the addition of Mg^{2+} (Figure 6-18). In particular the C8-H resonances is too broad to be observed between [Mg^{2+}]:[ATP] ratios of ~ 0.2:1 to ~ 2:1. The change in chemical shifts observed for these nucleotide peaks (Figure 6-20) are consistent with the previous experiments. The shifts are linear with [Mg^{2+}]:[ATP] ratio up to ~ 2:1 and reach a maximum between 5:1 and 10:1. The observed changes in the chemical shifts of the nucleotide peaks reflect the changing environments of ATP as the Mg^{2+} concentration increases. Evidence from this and the previous experiments suggests that the change is from ATP^{4-} being predominantly bound via electrostatic interactions to the 'basic patch' region of the N-terminal domain to $Mg.ATP^{2-}$ being bound via hydrophobic (and some electrostatic) interactions to the catalytic site of the C-terminal domain. The small changes observed at [Mg^{2+}]:[ATP] ratios greater than ~ 10:1 are probably due to the increasing proportion of $Mg_2.ATP$.

6.3.4. *Effect of $Mg.ATP^{2-}$ binding on the 2D ^1H NMR spectrum of PGK*

The above 1D analysis of the effect of ATP binding on the ^1H NMR spectrum of PGK clearly demonstrates that two binding sites exist and that the occupancy of the two sites is dependent on the Mg^{2+} concentration. It was suggested that the primary site for ATP^{4-} binding involves electrostatic interactions between the triphosphate chain and the general anion binding site described in Chapter 5 (*i.e.* the 'basic patch' region of the N-terminal domain), while the secondary binding site involves predominantly hydrophobic interactions between the adenine and ribose moieties and the C-terminal domain (presumably the catalytic site determined crystallographically; see Figure 6-1). The affinity of the primary site for ATP is reduced as the concentration of Mg^{2+} increases. In order to compare the crystallographically determined nucleotide binding site with those observed using NMR, and to establish more clearly which aromatic resonances are being perturbed, a 2D NOESY spectrum of a solution containing 1.1 mM PGK, 2.2 mM ATP and 2.6 mM $MgCl_2$ was obtained and compared with that obtained for the free enzyme (Figure 6-22). The results reported here were discussed and used for assignment purposes earlier (§ 2.3.3).

As discussed in Chapter 2, if the intermolecular NOE connectivities observed between the C2-H resonance of ATP and the resonances of Phe I (Figure 6-22) are assumed to result from nucleotide binding at the crystallographically determined site then it is possible to assign Phe I to Phe 289. The peaks labelled Phe D were assigned to Phe 342 on the basis of the inter-residue NOE connectivities observed between these peaks and Phe 289 (§ 2.3.3). The above assignments are in accord with very similar ('non-random coil') cross-peaks which are observed in the 2D spectra of the isolated C-terminal domain (see § 9.3.2). Further evidence for Mg.ATP binding at the same (catalytic) site as in the crystal structure comes from intermolecular NOE connectivities

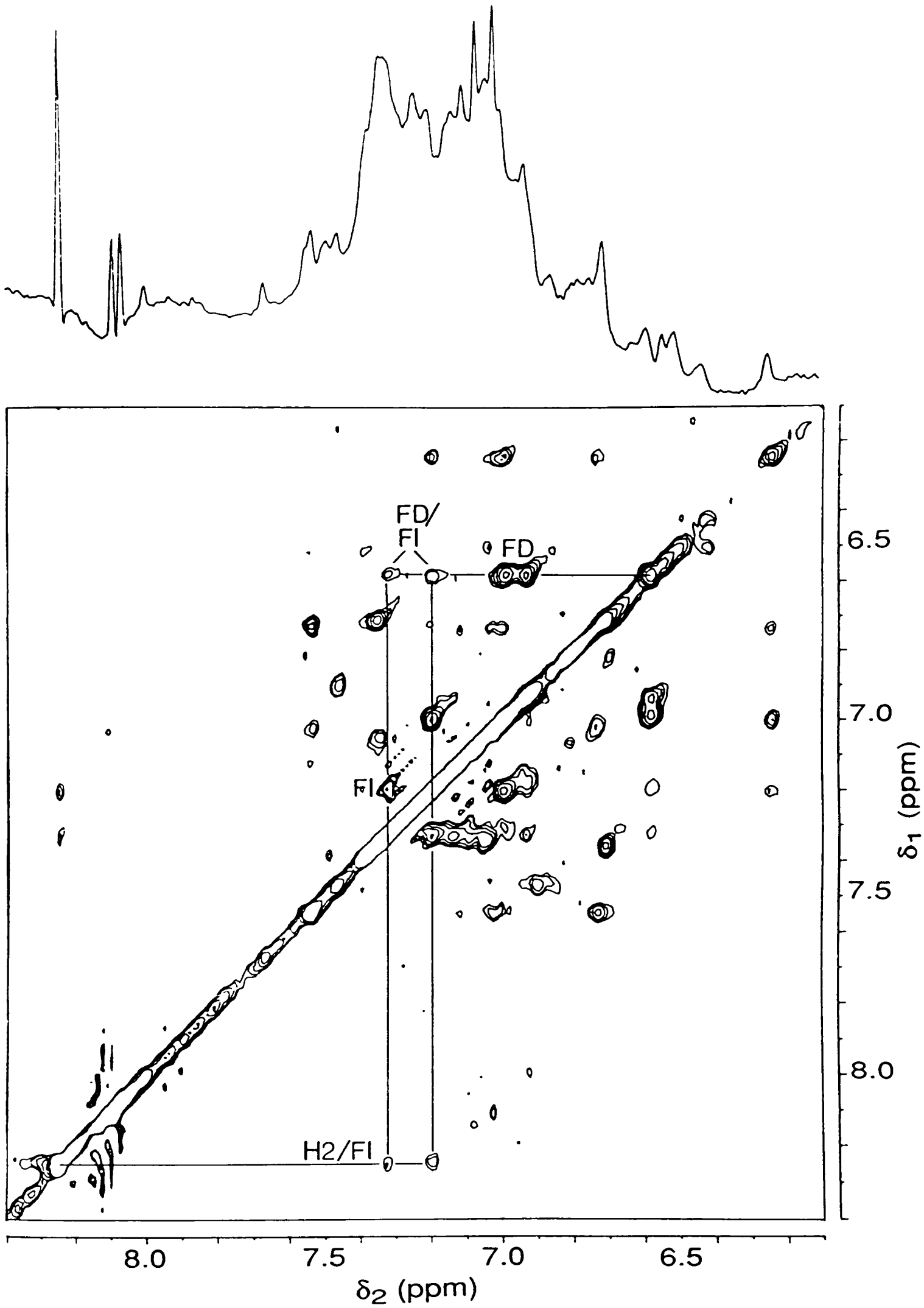

Figure 6-22A: Aromatic region of the 600 MHz NOESY spectrum of Mg.ATP.PGK ([Mg^{2+}]:[ATP]:[PGK] = 3:3:1). Inter-molecular NOE connectivities between the C2-H resonance of ATP and Phe I are labelled (H2/FI) as are inter-residue NOEs between Phe I and Phe D. Phe I and Phe D were assigned to Phe 289 and Phe 342 respectively (see § 2.3.3).

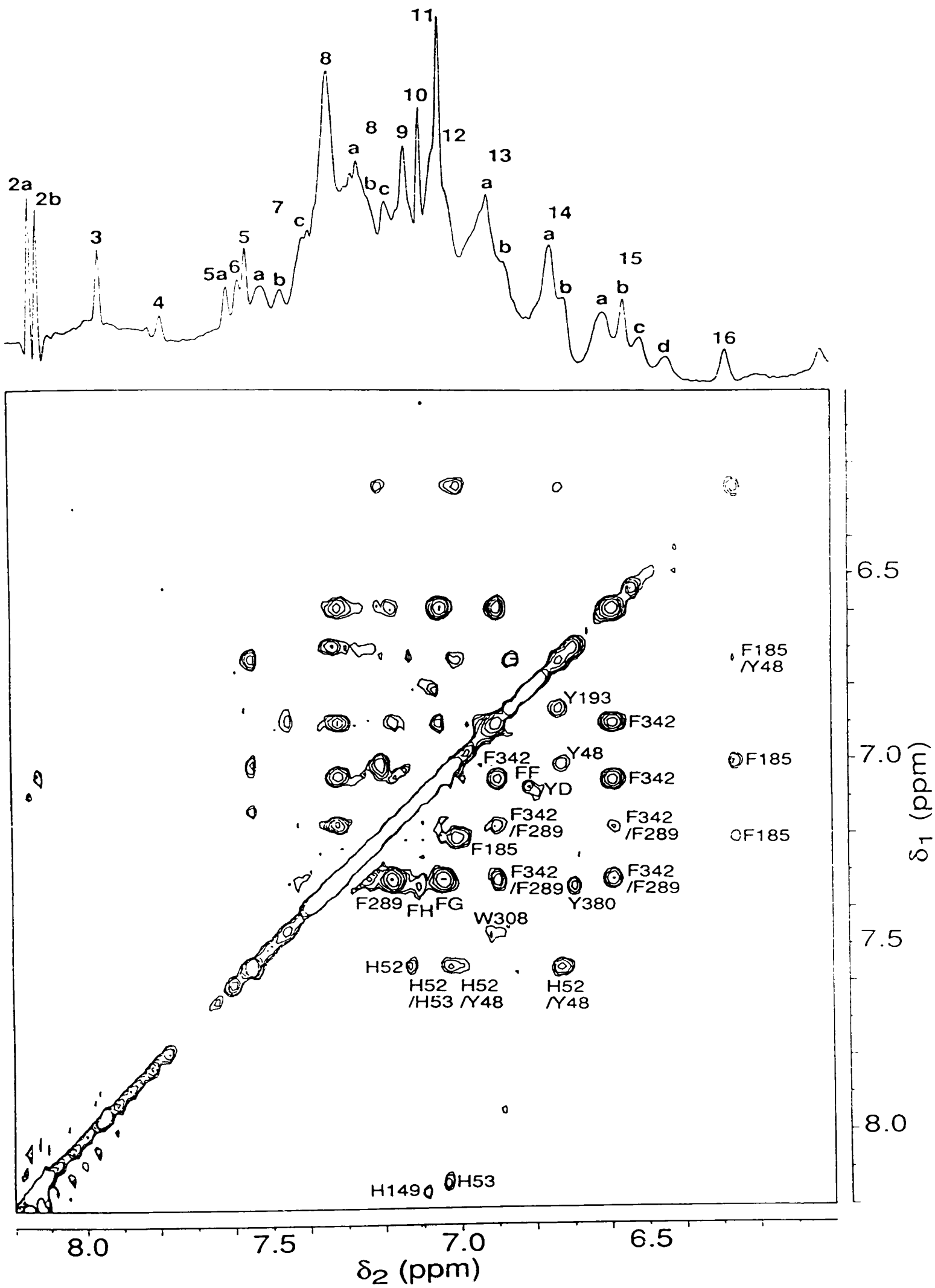

Figure 6-22B: Aromatic region of the 500 MHz NOESY spectrum of free PGK for comparison with Figure 6-22A.

observed between the C2-H resonance of ATP and aliphatic resonances between 0.8 ppm - 1.9 ppm (Figure 6-23). Observation of these cross-peaks is consistent with the proximity of the C2-H of bound ATP to Leu 311 and Val 339, as seen in the crystal structure (Figure 6-24).

From the 2D NOESY spectrum it is also possible to identify which residues give rise to some of the peaks observed to shift in the 1D spectra. In particular it can be seen that the adenosine specific effects observed at peaks 8, 8c, 12 and 13b are due to shifts of resonances assigned to Phe 289 and Phe 342. The upfield shift of a component of peak 12 and downfield shift of a component of peak 13b are seen most clearly since the cross-peaks labelled FD (intra-residue NOEs of Phe 342) shift closer together as a result of nucleotide binding (Figure 6-22).

In addition, the resonances assigned to Tyr 193 are both observed to shift upfield (~ 0.03 ppm), accounting for the upfield shift of a component of peak 14a seen in the 1D spectra. This, together with the observed upfield shift of peak 6 (His 388) in the 1D spectra (Table 6-2) suggests that the mutual orientation of Tyr 193 and His 388 in the interdomain region of the protein, has been altered slightly as a result of Mg.ATP binding. The aromatic resonances of Phe 185 also shift slightly as a result of Mg.ATP binding. A 0.02 ppm upfield shift of peak 16 (Phe 185, C4-H) was noted in the 1D spectra (Table 6-2). These differences can also be interpreted in terms of a small conformational change involving α-helix V (see Figure 6-1) in the interdomain region. The magnitudes of the shifts observed for these resonances are significantly less than those resulting from 3-PG binding to the enzyme (§§ 3.3.1 & 3.3.2). This indicates that the conformational changes in the interdomain region of the enzyme induced by 3-PG binding are larger in magnitude than those induced by Mg.ATP binding.

The cross-peaks assigned to Trp 308 (6.88, 7.46 ppm) remains unperturbed by Mg.ATP binding. This would not be expected from the X-ray

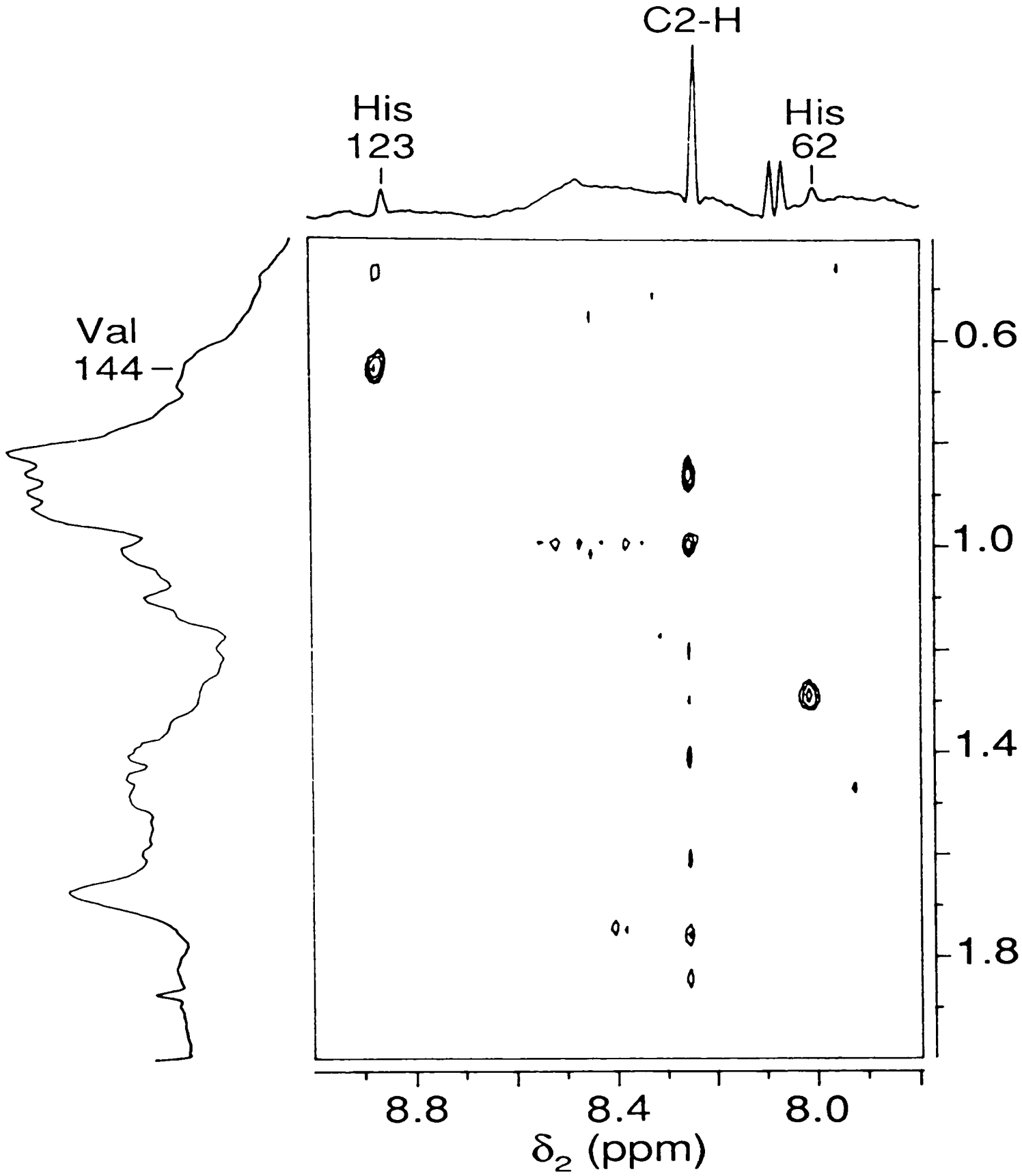

Figure 6-23: Region of the 600 MHz NOESY spectrum of Mg.ATP.PGK (as in Figure 6-22A) showing inter-molecular NOE connectivities between the C2-H resonance of the nucleotide and aliphatic resonances of the protein.

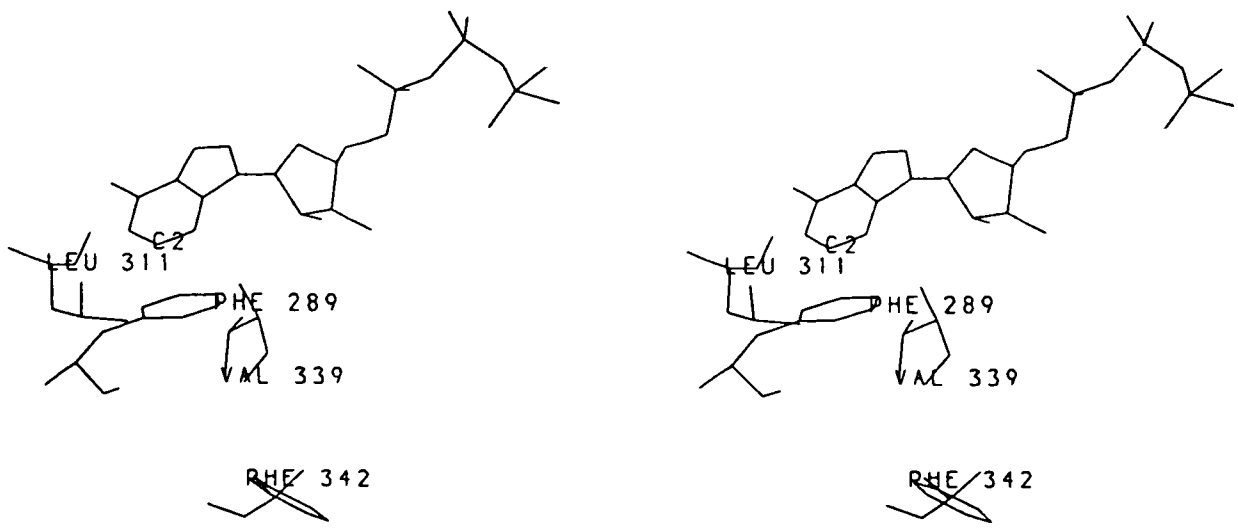

Figure 6-24: A stereo drawing illustrating the spatial proximity of Phe 289, Leu 311 and Val 339 to the C2 of bound ATP. The shortest inter-proton distances (in Å) from these residues to the C2-H of ATP are 1.4 (Leu 311; HD1), 2.1 (Phe 289; HE2), 2.2 (Leu 311; HD2) and 2.8 (Val 339; HB). The crystallographic coordinates are those of Watson *et al.* (1982), available from the Brookhaven Protein Data Bank.

crystallographic results (Watson *et al.*, 1982) which suggest that the indole ring of Trp 308 moves into a position adjacent to the adenine ring when ATP is bound to the enzyme.

6.4. Discussion

Earlier ATP binding studies (Tanswell *et al.*, 1976; Wilson *et al.*, 1988) have been extended and the role of Mg^{2+} in the mode of binding investigated. In contrast with the previous results the present study clearly indicates the presence of at least two ATP binding sites on the enzyme.

The downfield shifts observed for resonances of the 'basic patch' histidines at low nucleotide:enzyme molar ratios suggests that the primary binding site involves electrostatic interactions between the nucleotide triphosphate chain and arginines in the 'basic patch' region. This region was identified in Chapter 5 as being the primary general anion binding site. As the Mg^{2+} concentration is increased relative to ATP, adenosine specific effects in the ^1H NMR spectra are observed at lower nucleotide:enzyme molar ratios. This observation leads to the conclusion that the secondary binding site involves predominantly hydrophobic interactions between the adenosine moiety and the protein. Evidence from 2D NOESY experiments confirm that the secondary site is equivalent to the catalytic site observed by X-ray crystallographic studies (Watson *et al.*, 1982). The affinity of the catalytic site is increased relative to the primary electrostatic site with increasing Mg^{2+} concentration. It is also apparent that binding in the secondary (catalytic) site causes a conformational change at His 167 which results in an upfield shift of peak 4, but has little effect on His 62 or His 170. Binding of ATP^{4-} or $Mg.ATP^{2-}$ to the enzyme in the presence of 50 mM sulphate also results in an upfield shift of peak 4 (His 167) and only small (< 0.02 ppm) downfield shifts of peaks 3 (His 62) and 5a (His 170) (H.C. Graham, personal communication). It therefore appears that high levels of sulphate block the binding of ATP at the

primary electrostatic site (*i.e.* the nucleotide is competing for the same general anion binding site as sulphate).

The above qualitative conclusions disagree with those of Ray & Nageswara Rao (1988) who suggested that ATP^{4-} binds about 7-fold tighter at the catalytic site ($K_d \sim 0.070$ mM) compared to a secondary site ($K_d \sim 0.5$ mM), while $Mg.ATP^{2-}$ binds about 75-fold tighter at the catalytic site ($K_d \sim 0.065$ mM) compared to the same secondary site ($K_d \sim 5.0$ mM). The experimental conditions were different, however, with the ^{31}P NMR study being carried out at 5 °C in 0.2 M HEPES, pH 8.2 compared to the present ^{1}H NMR study at 27 °C in 0.1 M Na d_3-acetate, pH 7.1. These workers also assumed independent binding at the two sites. This is clearly not the case in the present study as can be illustrated by Figures 6-7 and 6-16. Figure 6-16 shows that the effect on resonance 3 of nucleotide binding at the hydrophobic site is a small downfield shift. The upfield shift observed at higher [ATP]:[PGK] ratios for peak 3 in Figure 6-7 shows that binding of nucleotide at the secondary site affects the binding at the primary site.

Since binding at the two sites are not independent no attempt has been made to interpret the results in more than a qualitative way, as discussed above. There are at least 10 different exchange processes occuring in the solution, with at least 7 different nucleotide environments contributing to the observed chemical shifts, *i.e.*

$$E + ATP \leftrightarrow E.ATP \qquad (1)$$

$$E' + ATP \leftrightarrow E'.ATP' \qquad (2)$$

$$E + Mg.ATP \leftrightarrow E.Mg.ATP \qquad (3)$$

$$E' + Mg.ATP \leftrightarrow E'.Mg'.ATP' \qquad (4)$$

$$E.ATP + Mg \leftrightarrow E.Mg.ATP \qquad (5)$$

$$E'.ATP' + Mg \leftrightarrow E'.Mg'.ATP' \qquad (6)$$

$$ATP + Mg \leftrightarrow Mg.ATP \qquad (7)$$

$$Mg.ATP + Mg \leftrightarrow Mg_2.ATP \qquad (8)$$

$$E' + Mg_2.ATP \leftrightarrow E'.Mg'_2.ATP' \qquad (9)$$

$$E'.Mg'.ATP' + Mg \leftrightarrow E'.Mg'_2.ATP' \qquad (10)$$

where the prime denotes binding to the hydrophobic catalytic site.

In the absence of Mg^{2+}, only equilibria (1) and (2) apply (§ 6.3.1), with $K_{d(1)}$ being less than $K_{d(2)}$. At a $[Mg^{2+}]$:[ATP] ratio of ~ 1:1 equilibria (1)-(7) are important (§ 6.3.2.1) and at higher ratios equilibria (8)-(10) contribute to the observed chemical shifts more and (1) and (2) less. The processes are clearly rapid enough to give a sharp averaged spectrum in the case of C2-H and C1′-H, but in the presence of Mg^{2+} the averaging is incomplete for C8-H on account of the greater chemical shift differences between the various free and bound states.

Larsson-Raźnikiewicz and Schierbeck (1977) have shown ATP^{4-} to be an activator of the enzyme at low concentrations (up to about 1 mM) and an inhibitor at higher concentrations. The inhibition was shown to be competitive with respect to both substrates ($Mg.ATP^{2-}$ and 3-PG). The data also indicated that there were at least two inhibitor molecules bound simultaneously to the enzyme. These results are consistent with the present study which suggests that the activatory site is equivalent to the general anion binding site, as discussed in Chapter 5. The activation and inhibition patterns of the PGK reaction by both substrates and products are complex (Larsson-Raźnikiewicz & Arvidsson, 1971; Larsson-Raźnikiewicz & Schierbeck, 1977; Schierbeck & Larsson-Raźnikiewicz, 1979), and offer the possibility of regulating the catalytic reaction *in vivo*. It is worth noting that the total cellular content of Mg^{2+} may be limiting compared with the number of Mg^{2+} binding sites (Gupta & Moore, 1980; Garfinkel & Garfinkel, 1984). Using ^{31}P NMR, Gupta & Moore (1980) have shown that the concentration of skeletal muscle cell ATP in the non-complexed form (*i.e.* ATP^{4-}) is ~ 0.4 mM (7 ± 1% of the total ATP present). This is within the range for activation of PGK in the direction

of gluconeogenesis *in vitro* (Larsson-Raźnikiewicz & Schierbeck, 1977).

Preliminary experiments have also been carried out with the nucleotide analogue adenosine 5′-(β,γ-difluoromethylene)triphosphate (APP(CF_2)P; Blackburn *et al.*, 1984; supplied by Dr G.M. Blackburn, Department of Chemistry, University of Sheffield). The primary effects of APP(CF_2)P and 1:1 Mg.APP(CF_2)P on the resonances of the 'basic patch' histidines are greater than observed with ATP and 1:1 Mg.ATP, with the maximum downfield shifts of peaks 3, 4 and 5a being 1.4-1.8 times greater. The secondary upfield shifts of peak 3 on binding APP(CF_2)P or Mg.APP(CF_2)P are also greater in magnitude than observed for the substrate. These observations may be due to a decreased flexibility in the β to γ-phosphate linkage of the analogue. Other effects of binding the analogue in the absence and presence of Mg^{2+} are qualitatively similar to those observed with ATP indicating that the mode of binding is similar. The dissociation constant for APP(CF_2)P was the same as that for ATP binding, within experimental error. Addition of 3-PG to a solution containing Mg.APP(CF_2)P and PGK in the ratio 0.8:1 appears to block the interaction of the nucleotide analogue with the 'basic patch' region. At saturating amounts of 3-PG the chemical shifts of peaks 3 (His 62), 4 (His 167) and 5a (His 170) are similar to those observed in Chapter 3 on formation of the 3-PG.PGK binary complex. Other effects in the spectrum, including broadening and shifting of the nucleotide C2-H and C1′-H resonances, indicate that the interaction between the nucleotide and the hydrophobic (catalytic) site increases with increasing 3-PG concentration.

6.5. References

Banks, R.D., Blake, C.C.F., Evans, P.R., Haser, R., Rice, D.W., Hardy, G.W., Merrett, M. & Phillips, A.W. (1979) *Nature (Lond.) 279,* 773-777.

Bishop, E.O., Kimber, S.J., Orchard, D. & Smith, B.E. (1981) *Biochim. Biophys. Acta 635,* 63-72.

Blackburn, G.M., Kent, D.E. & Kolkmann, F. (1984) *J. Chem. Soc. Perkin Trans, I,* 1119-1125.

Blake, C.C.F. & Rice, D.W. (1981) *Phil. Trans. R. Soc. Lond. A. 293,* 93-104.

Garfinkel, L. & Garfinkel, D. (1984) *Biochem. 23,* 3547-3552.

Gupta, R.K. & Moore, R.D. (1980) *J. Biol. Chem. 255,* 3987-3993.

Krietsch, W.K.G. & Bücher, T. (1970) *Eur. J. Biochem. 17,* 568-580.

Larsson-Raźnikiewicz, M. (1973) *Arch. Biochem. Biophys. 158,* 754-762.

Larsson-Raźnikiewicz, M. & Arvidsson, L. (1971) *Eur. J. Biochem. 22,* 506-512.

Larsson-Raźnikiewicz, M. & Schierbeck, B. (1977) *Biochim. Biophys. Acta 481,* 283-287.

Nageswara Rao, B.D., Cohn, M. & Scopes, R.K. (1978) *J. Biol. Chem. 253,* 8056-8060.

Ray, B.D. & Nageswara Rao, B.D. (1988) *Biochem. 27,* 5574-5578.

Roustan, C., Brevet, A., Pradel, L.-A. & van Thoai, N. (1973) *Eur. J. Biochem. 37,* 248-255.

Scheffler, J.E. & Cohn, M. (1986) *Biochem. 25,* 3788-3796.

Schierbeck, B. & Larsson-Raźnikiewicz, M. (1979) *Biochim. Biophys. Acta 568,* 195-204.

Scopes, R.K. (1978) *Eur. J. Biochem. 91,* 119-129.

Sigel, H., Tribolet, R., Malini-Balakrishnan, R. & Martin, R.B. (1987) *Inorg. Chem. 26,* 2149-2157.

Tanswell, P., Westhead, E.W. & Williams, R.J.P. (1974) *FEBS Lett. 48,* 60-63.

Tanswell, P., Westhead, E.W. & Williams, R.J.P. (1976) *Eur. J. Biochem. 63,* 249-262.

Tompa, P., Hong, P.T. & Vas, M. (1986) *Eur. J. Biochem. 154,* 643-649.

Watson, H.C. & Gamblin, S.J. (1985) *Proc. Int. Symp. Biomol. Struct. Interactions, Suppl. J. Biosci. 8,* 499-506.

Watson, H.C., Walker, N.P.C., Shaw, P.J., Bryant, T.N., Wendell, P.L., Fothergill, L.A., Perkins, R.E., Conroy, S.C., Dobson, M.J., Tuite, M.F., Kingsman, A.J. & Kingsman, S.M. (1982) *EMBO J. 1,* 1635-1640.

Wiksell, E. & Larsson-Raźnikiewicz, M. (1982) *J. Biol. Chem. 257,* 12672-12677.

Wilson, H.R. (1986) D. Phil. Thesis, University of Oxford.

Wilson, H.R., Williams, R.J.P., Littlechild, J.A. & Watson, H.C. (1988) *Eur. J. Biochem. 170,* 529-538.

Chapter 7

PROBING THE INTERACTION OF Mg.ATP WITH PGK USING THE PARAMAGNETIC CATION Mn^{2+}

7.1. Introduction

Using data from titrations with the paramagnetic relaxation probe Gd(III).ATP and the shift probes Pr(III).ATP and Eu(III).ATP, Tanswell *et al.* (1976) calculated distances of 5-6 Å between the bound metal ion and three histidine residues which have now been specifically assigned to the 'basic patch' histidines 62, 167 and 170. These distances are considerably less than the equivalent distances (14-18 Å) measured in the crystal structure of Watson *et al.* (1982) and have been widely quoted as evidence for the proposed 'hinge bending' motion in solution *i.e.* the NMR data reflect a 'closed' form of the enzyme. Care must, however, be taken in interpreting this result.

Firstly, the conformation of Ln.ATP binding to the enzyme was assumed to be equivalent to that determined in free solution (Tanswell *et al.*, 1975) with a metal ion to C8-H distance (used as a reference) of 6.1 Å. Subsequent determination of the crystal structure (Watson *et al.*, 1982) revealed that the triphosphate chain of coordinated Mg.ATP is in an extended conformation with a metal ion to C8-H distance of 9.6 Å. Substitution of this value into the previous calculations of metal ion to 'basic patch' histidine distances (Tanswell *et al.*, 1976) gives values of 8.3-10.2 Å.

Secondly, using relaxation data to obtain distances provides an average of all distances if the molecule being investigated is undergoing rapid conformational change. This average weights the positions relative to the probe, Gd^{3+}, by a factor proportional to r^{-6} (see Appendix 3). It is apparent that in solution the PGK molecule does fluctuate between many states, including 'open' and 'closed' forms (Wilson *et al.*, 1988). If for (say) 20% of

the time the three 'basic patch' histidines are close to the Gd^{3+} ion and for 80% of the time they are further away by a factor of two or more then the NMR data will be weighted by three or more fold in favour of the shorter distance and the form present in the minority.

A third problem is the presence of a secondary, electrostatic, ATP binding site in the 'basic patch' region, as identified in the preceding chapter. A relatively small proportion of Gd(III).ATP binding at this site would also have the effect of weighting the NMR data towards a shorter distance. It was established in Chapter 6, however, that the affinity of the general anion site for $Mg.ATP^{2-}$ is less than for ATP^{4-}. It is therefore likely that the affinity of this site for $Gd.ATP^{-}$ will be even lower.

In this chapter the line broadening reagent, Mn^{2+} (high-spin $3d^5$ ion, S = 5/2), is used to probe the area of interaction between the phosphate of ATP and the protein. Unlike $Gd.ATP^{-}$, which is a competitive inhibitor of PGK with respect to $Mg.ATP^{2-}$ (Tanswell *et al.*, 1974), $Mn.ATP^{2-}$ is a substrate of the enzyme (Larsson-Raźnikiewicz, 1970). In order to establish whether or not any of the observed broadening effects arise from $Mn.ATP^{2-}$ binding at the general anion site the experiments have been repeated under conditions which discriminate against such binding (*i.e.* high sulphate concentration).

7.2. Experimental methods

7.2.1. *Mn^{2+} titrations*

$MnCl_2.4H_2O$ (3 mM in 100 mM Na d_3-acetate/D_2O solution) was added in 0.1-1.0 µl aliquots to solutions of PGK (1 mM, prepared as described in § 2.2.5) in the presence or absence of 1.1 mM Mg.ATP, and the 1D ^1H NMR spectra recorded after each addition. The pH of the inorganic probe solution was adjusted to be the same as the protein solutions (7.10 ± 0.05) and the pH of the protein sample measured both before and after completion of the

titration. Similar titrations were also carried out on protein samples which were exchanged into D_2O containing 100 mM sodium d_3-acetate and 50 mM ammonium sulphate.

7.3. Results

7.3.1. *Interaction of Mn^{2+} with PGK*

In this preliminary experiment $MnCl_2$ was added to a 1 mM sample of PGK to give a final Mn^{2+} concentration of 15 μM. The effects on the aromatic region of the spectrum are illustrated in Figure 7-1.

The difference spectrum (Figure 7-1C) shows that a selected set of resonances, associated with the surface histidine residues 52, 53, 123 and 149, are broadened. This result indicates the presence of at least two cation binding sites on the protein surface, one in the vicinity of His 123 and His 149, and the other close to His 52 and His 53. From the relative broadenings it appears that Mn^{2+} binds either closer to His 123 and His 149 or with higher affinity than it does in the latter site. From the crystal structure (Watson *et al.*, 1982) the most likely groups for binding Mn^{2+} in close proximity to His 123 and His 149 are Asp 143 and Glu 150 (see Figure 2-17B), and in the vicinity of His 52 and His 53 are Asp 12 and Glu 51 (see Figure 2-17A). Glu 51 is situated at the C-terminal end of α-helix I. It is therefore possible that a cation-helix dipole interaction is also involved. In the aliphatic region of the spectrum the only significant broadenings observed are of peaks which can be associated with the side-chain protons of Asp and Glu residues, and a component of peak 36 (0.65 ppm) which has been assigned to a methyl group of Val 144 (§ 4.3.2).

Apart from very slight broadening of resonances 4 and 15b (His 167) there is no evidence of interaction between the metal ion and the 'basic patch' region of the protein. At higher Mn^{2+} concentrations peaks 4 and 15b broaden further indicating a third metal binding site. This site probably involves the totally

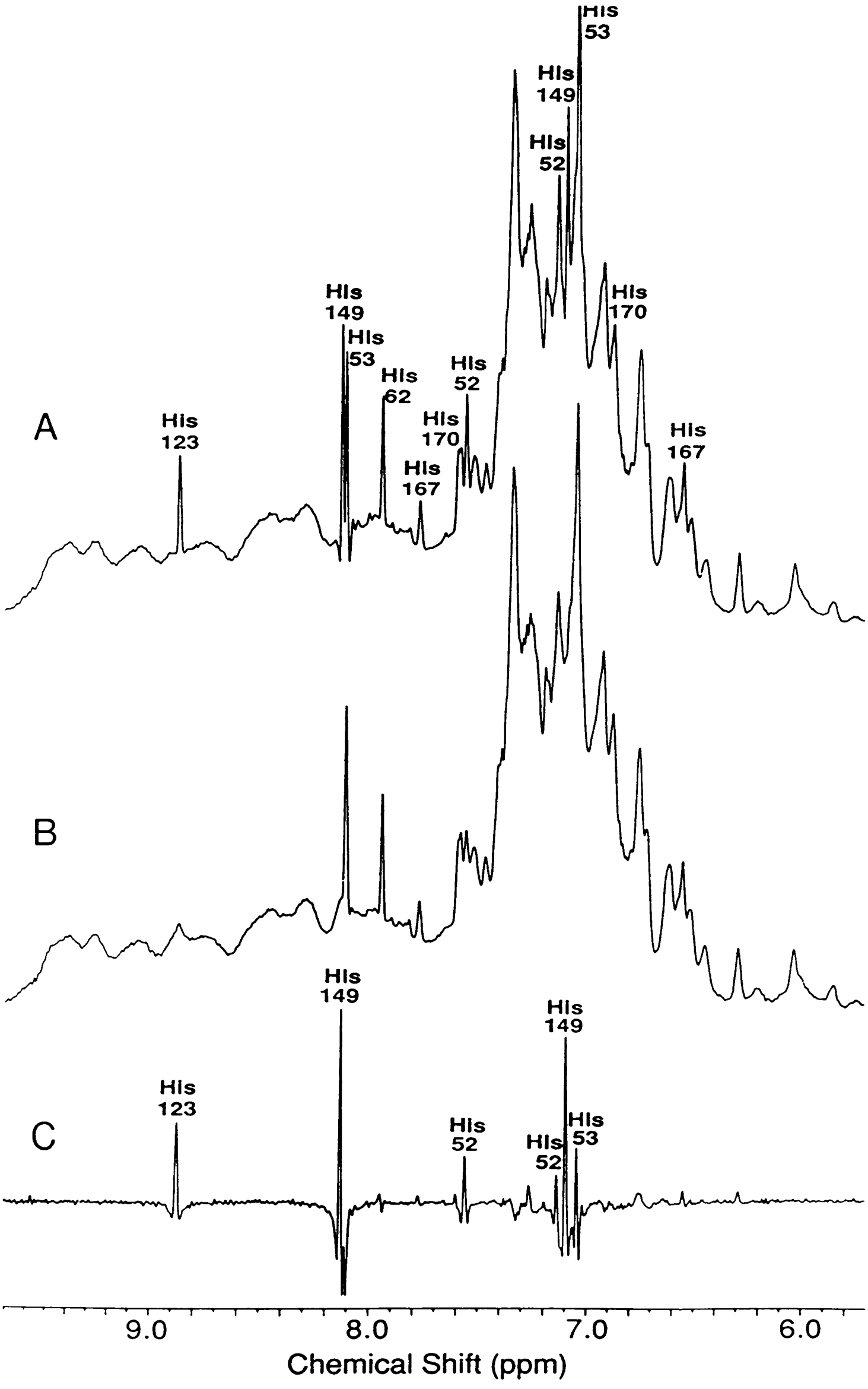

Figure 7-1: Perturbation of the aromatic region of the 500 MHz ^{1}H NMR spectrum of yeast PGK by Mn^{2+}. (A) Spectrum of 1 mM PGK in the absence of Mn^{2+}. (B) Spectrum of 1 mM PGK in the presence of 15 μM Mn^{2+}. (C) The difference spectrum (A) - (B).

conserved (see Appendix 1) Glu residues 398 and 401 situated at the C-terminal end of interdomain α-helix XIII.

7.3.2. *Interaction of Mn^{2+} with Mg.ATP.PGK*

A 3 mM solution of $MnCl_2$ was added to a solution containing 1 mM PGK, 1.1 mM $MgCl_2$ and 1.1 mM ATP, to give total Mn^{2+} concentrations of 0.7 μM, 3.7 μM, 7.3 μM, 14 μM and 29 μM. The effects on the aromatic and aliphatic regions of the spectrum are illustrated in Figures 7-2 and 7-3.

In contrast to the previous experiment, addition of Mn^{2+} in the presence of the nucleotide triphosphate selectively broadens those resonances assigned to the 'basic patch' histidines 62, 167 and 170 (*c.f.* Figures 7-1 & 7-2) in addition to the nucleotide C2-H and C1′-H peaks. This observation is in agreement with the previous studies using Gd^{3+} as a relaxation probe (Tanswell *et al.*, 1976; Wilson *et al.*, 1988).

At higher Mn^{2+} concentrations than shown in Figure 7-2 a component of peak 8, which was shifted upfield on binding Mg.ATP, and peak 8c are broadened significantly. These two peaks may correspond to Phe 289, whose ring protons are 10.8-14.9 Å from the metal ion in the crystal structure (Watson *et al.*, 1982). The closest aromatic group to the metal ion in the crystal is, however, Phe 340 with ring proton to metal distances between 6.4-11.3 Å. Components of peaks 12, 13a and 15a, corresponding to Phe 342, peaks 14a and 13b, corresponding to Tyr 193 and peaks 7a and 7c, corresponding to an unidentified Phe residue are also very slightly broadened at the highest Mn^{2+} concentration investigated. At the higher concentrations the peaks due to surface histidines 52, 53, 123 and 149 broadened by Mn^{2+} in the absence of nucleotide also begin to broaden slightly.

A number of resonances are also observed to broaden in the aliphatic region of the spectrum (Figure 7-3). Included are a number of peaks which were seen to broaden on addition of $[Cr(CN)_6]^{3-}$ to the substrate free protein (*e.g.* peaks

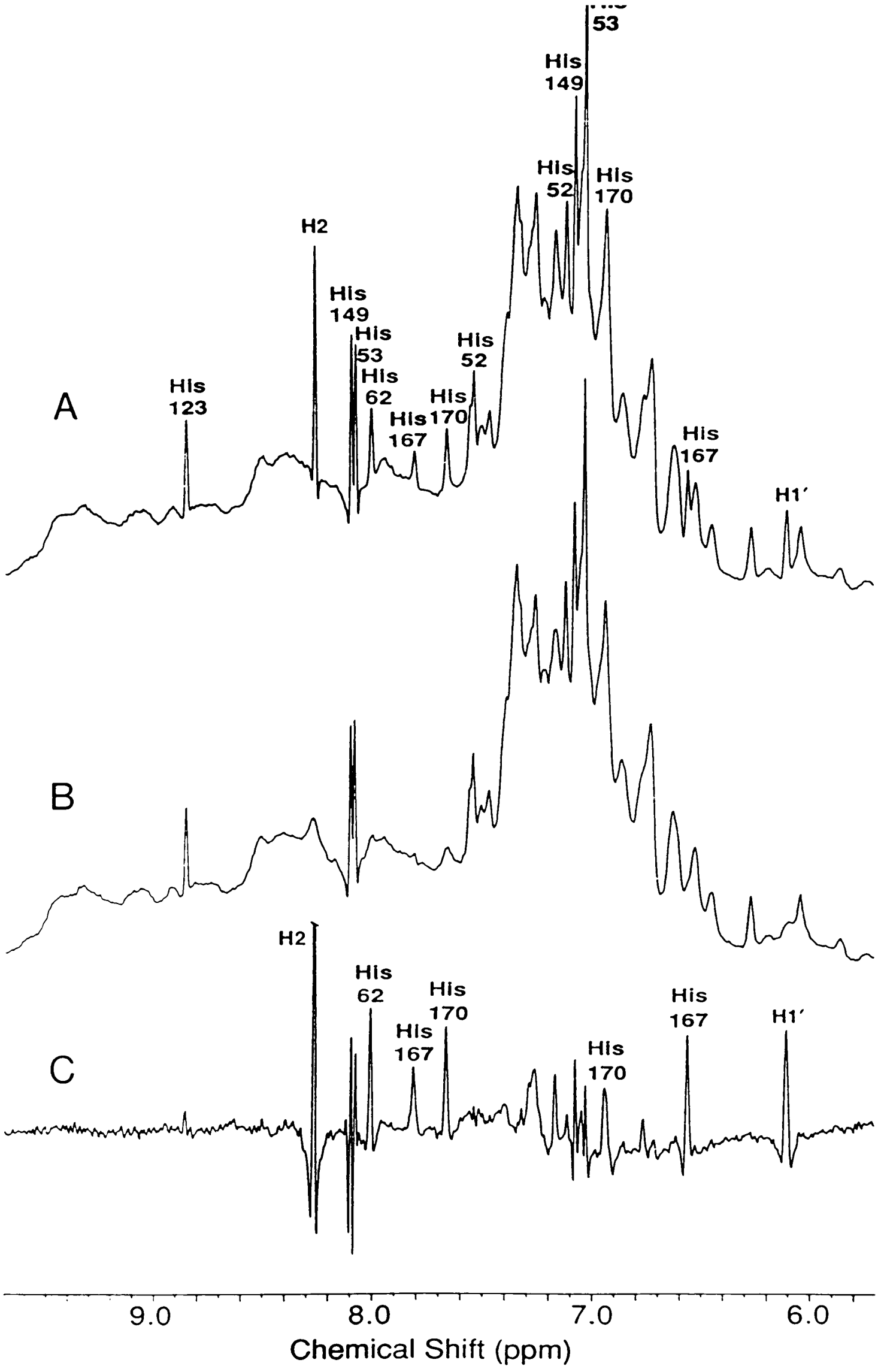

Figure 7-2: Perturbation of the aromatic region of the spectrum of Mg.ATP.PGK by Mn^{2+}. (A) Spectrum of 1 mM PGK in the presence of 1.1 mM ATP and 1.1 mM Mg^{2+}. (B) Spectrum as in (A) but with the addition of 7.3 μM Mn^{2+}. (C) The difference spectrum (A) - (B).

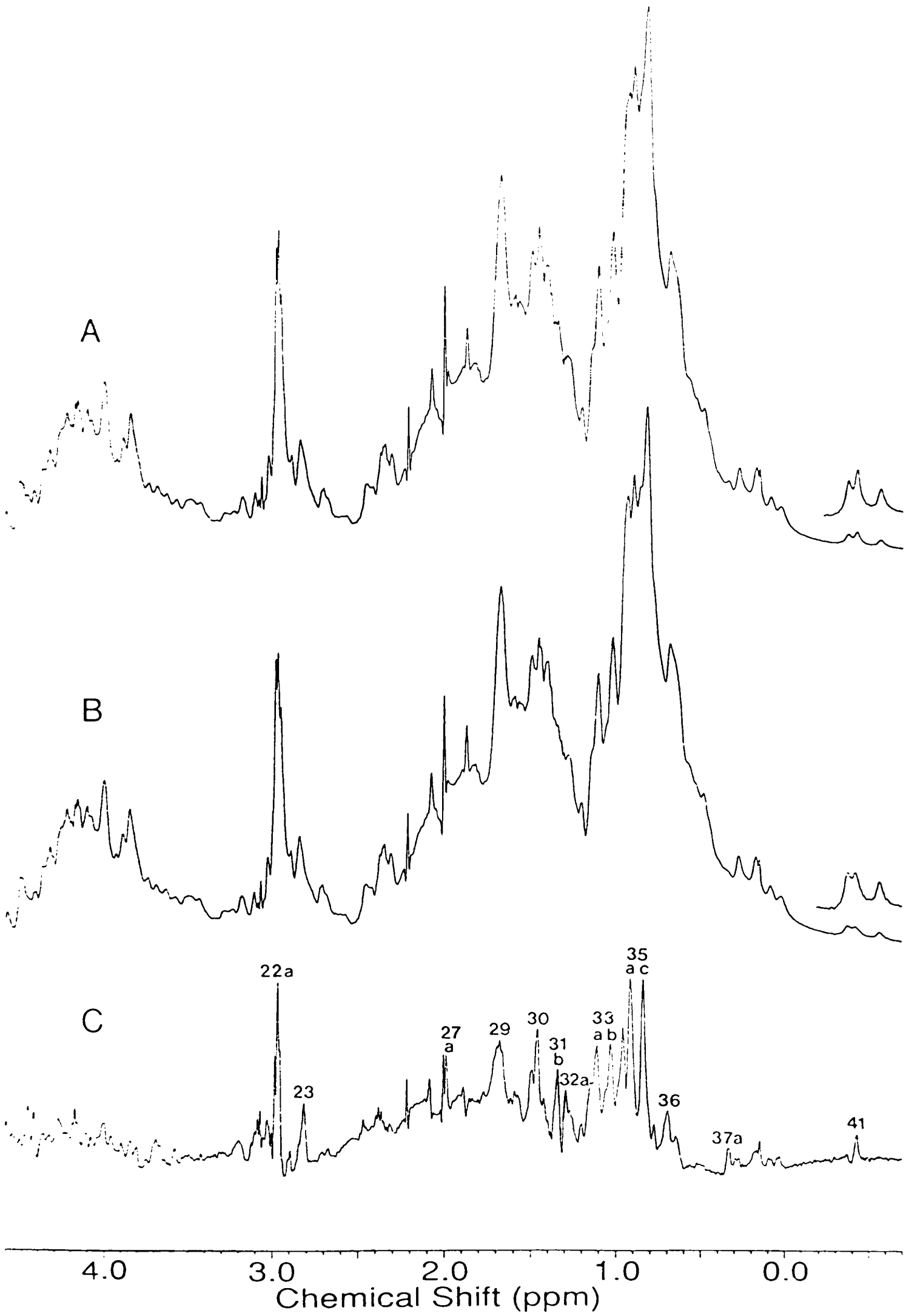

Figure 7-3: Perturbation of the aliphatic region of the spectrum of Mg.ATP.PGK by Mn^{2+}. (A) Spectrum of 1 mM PGK in the presence of 1.1 mM ATP and 1.1 mM Mg^{2+}. (B) Spectrum as in (A) but with the addition of 7.3 μM Mn^{2+}. (C) The difference spectrum (A) - (B).

22a, 23, 31b, 32a, 33a, 35a, 35c and 37a) and are presumably due to aliphatic protons in the 'basic patch' region (*c.f.* Figures 5-5 & 7-3). Also broadened is upfield methyl peak 41, consistent with the assignment of this resonance to Thr 375 (§ 2.3.4) which is ~ 9 Å from the metal binding site in the Mg.ATP.PGK crystal structure. In addition peaks which may be associated with Lys residues (1.5-1.8 ppm and ~ 3.0 ppm) are broadened. This is consistent with the proximity of Lys 213 and Lys 217 to the metal ion in the crystallographically determined catalytic site.

The broadening effect produced by replacing Mg^{2+} with Mn^{2+} falls off with the sixth power of the distance between the protons being affected and the bound metal ion. That the resonances of the 'basic patch' histidines are broadened at lower concentrations of $Mn.ATP^{2-}$ than other aromatic resonances indicates that on average these histidines are the closest aromatic groups to the bound metal. As has been pointed out previously (Watson & Gamblin, 1985; Wilson *et al.*, 1988) this result is inconsistent with the single ATP site observed in the crystal structure.

7.3.2.1. Estimation of distances between 'basic patch' histidines and the metal ion

An estimate of the upper limit of the mean distances between Mn^{2+} and the 'basic patch' histidines can be made if it is assumed that there is only one $Mn.ATP^{2-}$ binding site per molecule (see Appendix 3). A plot of the line-width, $\Delta\nu_{1/2}$, versus the Mn^{2+} concentration (Figure 7-4) yields slopes equivalent to $1/\pi(K_d + [E]_o)(T_{2,M} + \tau_M)$, where K_d is the dissociation constant for the complex, $[E]_o$ is the enzyme concentration, $T_{2,M}$ is the transverse relaxation time in the fully bound Mn.ATP.enzyme complex and τ_M is the life-time of the complex. K_d was assumed to be 0.15 mM (§ 6.3.2). Since different broadenings were observed for different histidine resonances (Figure 7-4) the term τ_M may be neglected and maximum values of $T_{2,M}$ calculated from the slopes in Figure 7-4 (Table 7-1).

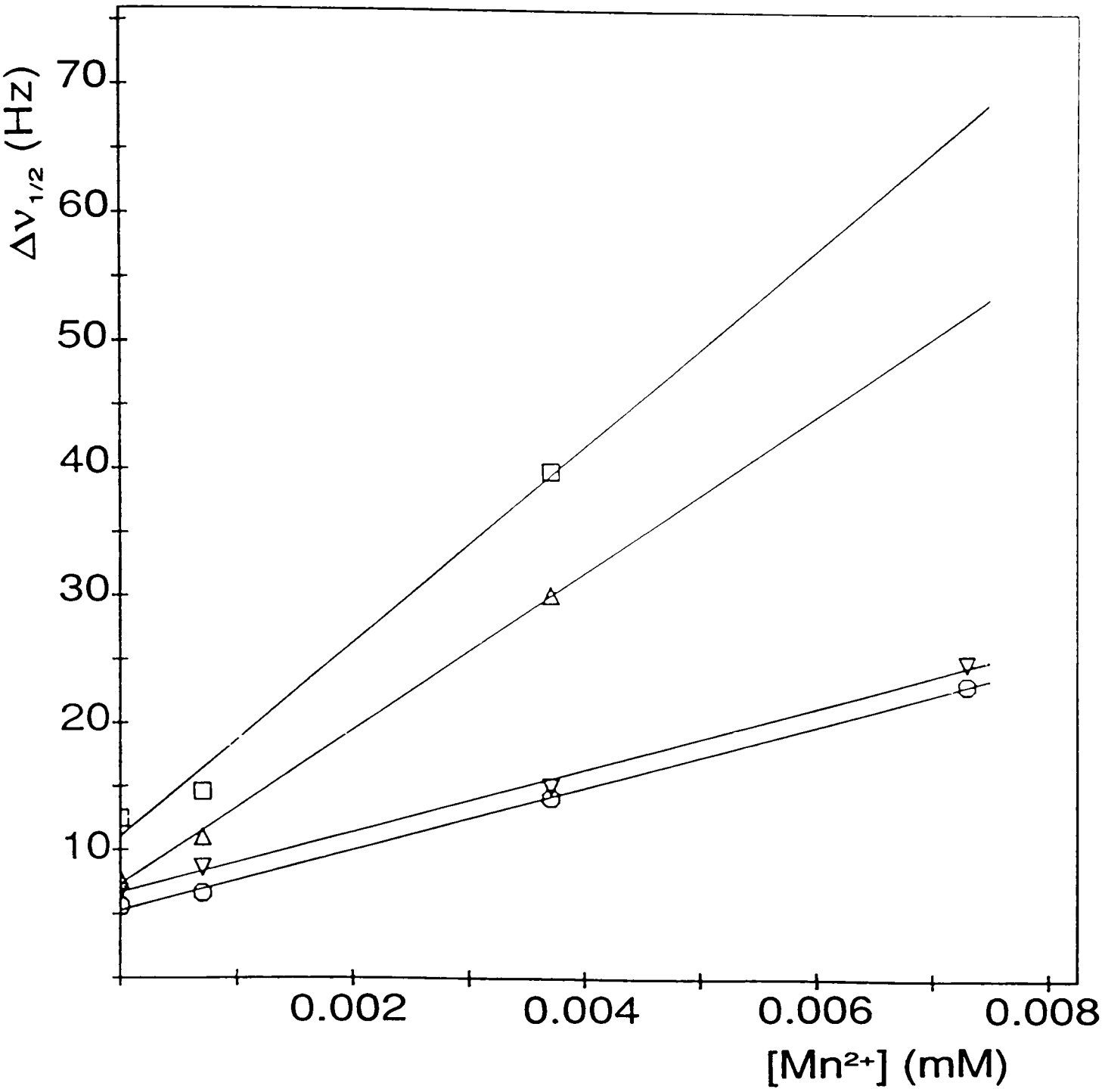

Figure 7-4: The line-widths ($\Delta\nu_{1/2}$) of peaks 3 (○; His 62), 4 (□; His 167), 5a (▽; His 170) and 15b (△; His 167) in the spectrum of Mg.ATP.PGK plotted as a function of Mn^{2+} concentration.

Table 7-1: Estimation of Mn^{2+} to 'basic patch' histidine distances from Mn.ATP.enzyme complex relaxation data.

Slopes were determined from Figure 7-4.

	Resonance			
Parameter	3 (His 62)	4 (His 167)	5a (His 170)	15b (His 167)
slope/Hz mM^{-1}	2458	7730	2472	6108
$(T_{2,M})_{max.}$/ms	0.113	0.036	0.112	0.045
$\langle r_i \rangle$/Å	9.4	7.8	9.4	8.0

A maximal value for the correlation time which modulates the proton-Mn dipolar interaction, τ_c, was obtained by equating it to τ_R, the rotational correlation time for the enzyme molecule. τ_R was calculated from the Stokes-Einstein equation (see Appendix 3) to be ~ 1.4×10^{-8} s. Maximum distances were thus calculated from

$$\frac{1}{T_{2,M}} = \frac{4}{20}\frac{\mu_o^2}{(4\pi)^2}\frac{\gamma_I^2 g^2 S(S+1)\beta^2}{r^6} \cdot \tau_c,$$

and are given in Table 7-1.

While these estimates are greater than those reported by Tanswell *et al.*, (1976) they are still significantly shorter than the 14-18 Å distances found in the 'open' crystal structure (Watson *et al.*, 1982).

7.3.3. *Interaction of Mn^{2+} with Mg.ATP.PGK in the presence of 50 mM sulphate*

In order to investigate whether there is a contribution to the observed broadening of the 'basic patch' histidine resonances from $Mn.ATP^{2-}$ binding directly to the general anion binding site, experiments have been carried out under conditions which discriminate against this possibility. In Chapter 6 it was established that the affinity of ATP for the hydrophobic catalytic site is increased relative to the primary electrostatic site with increasing Mg^{2+} concentration. It was also noted that high levels of sulphate block the binding of ATP to the electrostatic site (H.C. Graham, personal communication).

7.3.3.1. Interaction of ATP with PGK in the presence of excess Mg^{2+} and sulphate

Preliminary experiments have been carried out to determine the mode of interaction of ATP with PGK in the presence of 50 mM ammonium sulphate and a 10-fold excess of $MgCl_2$. A PGK solution containing 50 mM ammonium sulphate in addition to 100 mM sodium d_3-acetate was titrated with a 50 mM solution of ATP containing 500 mM $MgCl_2$ and monitored using 500 MHz ^1H

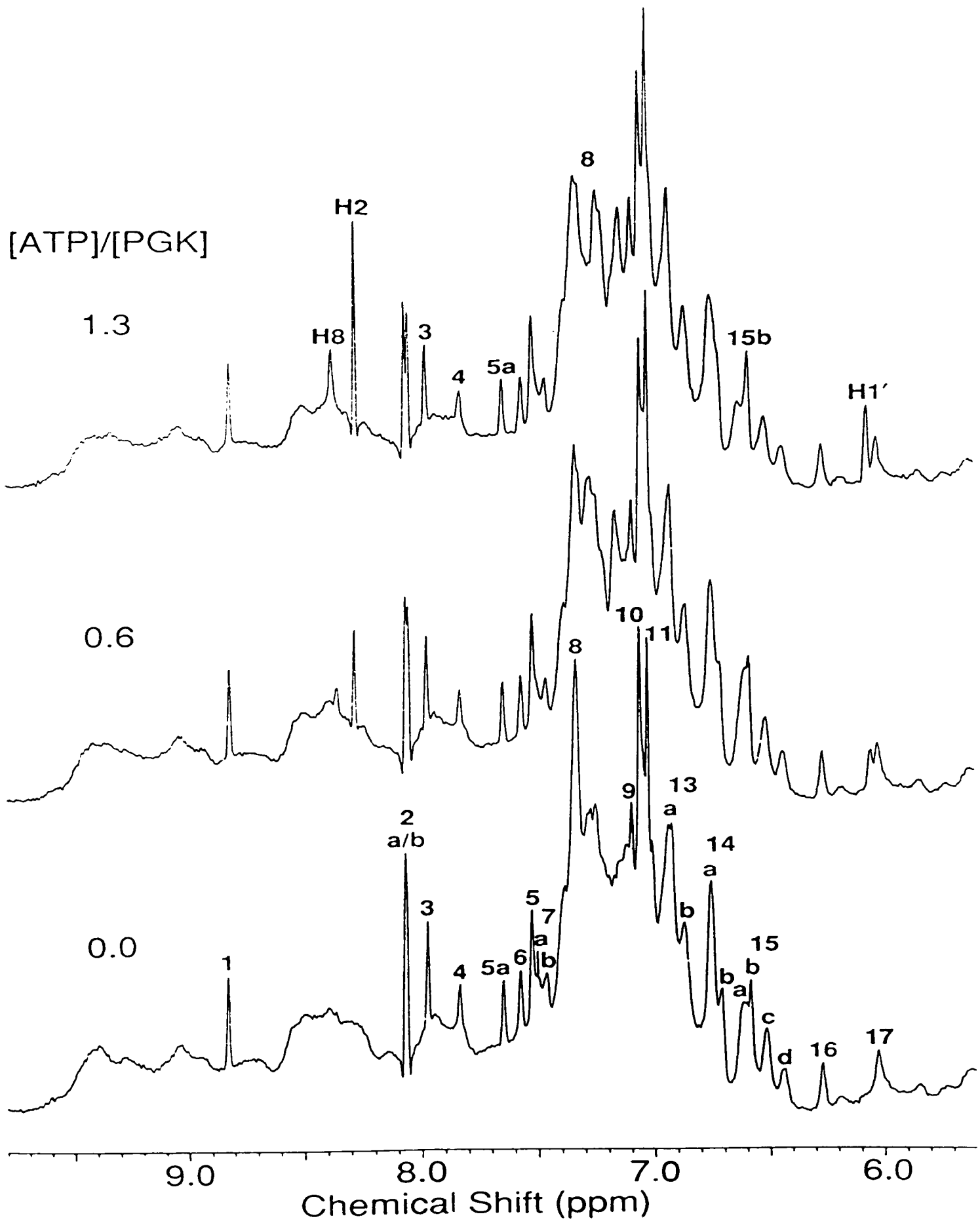

Figure 7-5: Perturbation of the aromatic region of the 500 MHz ^{1}H NMR spectrum of yeast PGK by ATP at the ratios indicated, and in the presence of 50 mM $(NH_4)_2SO_4$ and a constant $[Mg^{2+}]$:[ATP] ratio of 10:1.

NMR spectroscopy (Figure 7-5).

The observation that the 'basic patch' histidine resonances, 3, 4, 5a and 15b, are not significantly perturbed by addition of ATP (Figure 7-5) suggests that the nucleotide does not interact with the general anion site (either directly or indirectly) under these conditions. Perturbations at peaks 8, 12, 14b and 15a, however, are indicative of binding at the hydrophobic site. This is confirmed by observation of inter-molecular NOEs between the C2-H resonance of the nucleotide and peaks assigned to Phe 289, Leu 311 and Val 339 (Figures 7-6 and 7-7). Similar cross-peaks were observed in the NOESY spectrum of the Mg.ATP.PGK complex in the absence of sulphate and a 1.2:1 molar ratio of Mg^{2+} to ATP (*c.f.* Figures 6-22 and 6-23). It is notable that the changes observed for the resonances of Phe 289 and Phe 342 on adding nucleotide in the presence of 50 mM sulphate are different from those seen in Chapter 6 (*c.f.* Figure 6-22). In particular the third Phe 289 resonance is now observable and gives a weak NOE to the C3,5-H resonance of Phe 342 (Figure 7-6).

7.3.3.2. Effect of Mn^{2+}

A 3 mM solution of $MnCl_2$ was titrated into a solution containing 1 mM PGK, 0.7 mM $MgCl_2$ and 0.7 mM ATP, to give total Mn^{2+} concentrations between 1.3-40 μM. The effects on the aromatic and aliphatic regions of the spectrum at a Mn^{2+} concentration of 6.6 μM are illustrated in Figures 7-8 and 7-9.

Comparison of Figures 7-8 and 7-2 shows that the same aromatic resonances are affected in the presence and in the absence of sulphate. It is also apparent, however, that the degree of broadening of the 'basic patch' histidine resonances in Figure 7-8 is less than in Figure 7-2, despite there being a higher concentration of Mn^{2+} present. This is clearly demonstrated when the line-widths are plotted against $[Mn^{2+}]/\pi(K_d + [E]_o)$, as in Figure 7-10. Metal

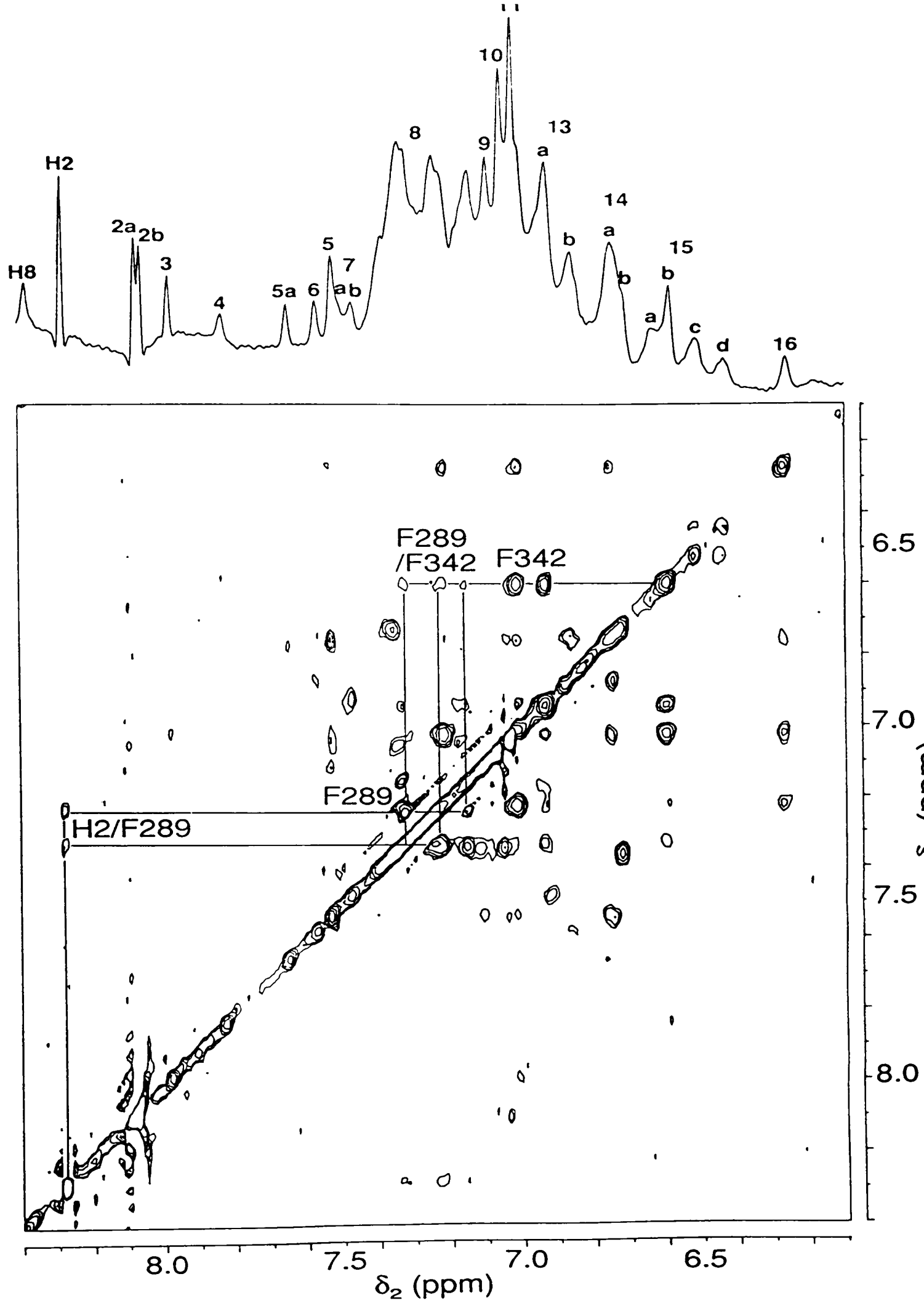

Figure 7-6: Aromatic region of the 500 MHz NOESY spectrum of PGK plus Mg.ATP (1.1 mM PGK, 1.3 mM ATP, 13 mM $MgCl_2$, 50 mM $(NH_4)_2SO_4$, 0.10 M Na d_3-acetate, pH 7.1, 27 °C). Inter-molecular NOE connectivities between the C2-H resonance of ATP and Phe 289 and inter-residue NOE connectivities between Phe 289 and Phe 342 are labelled.

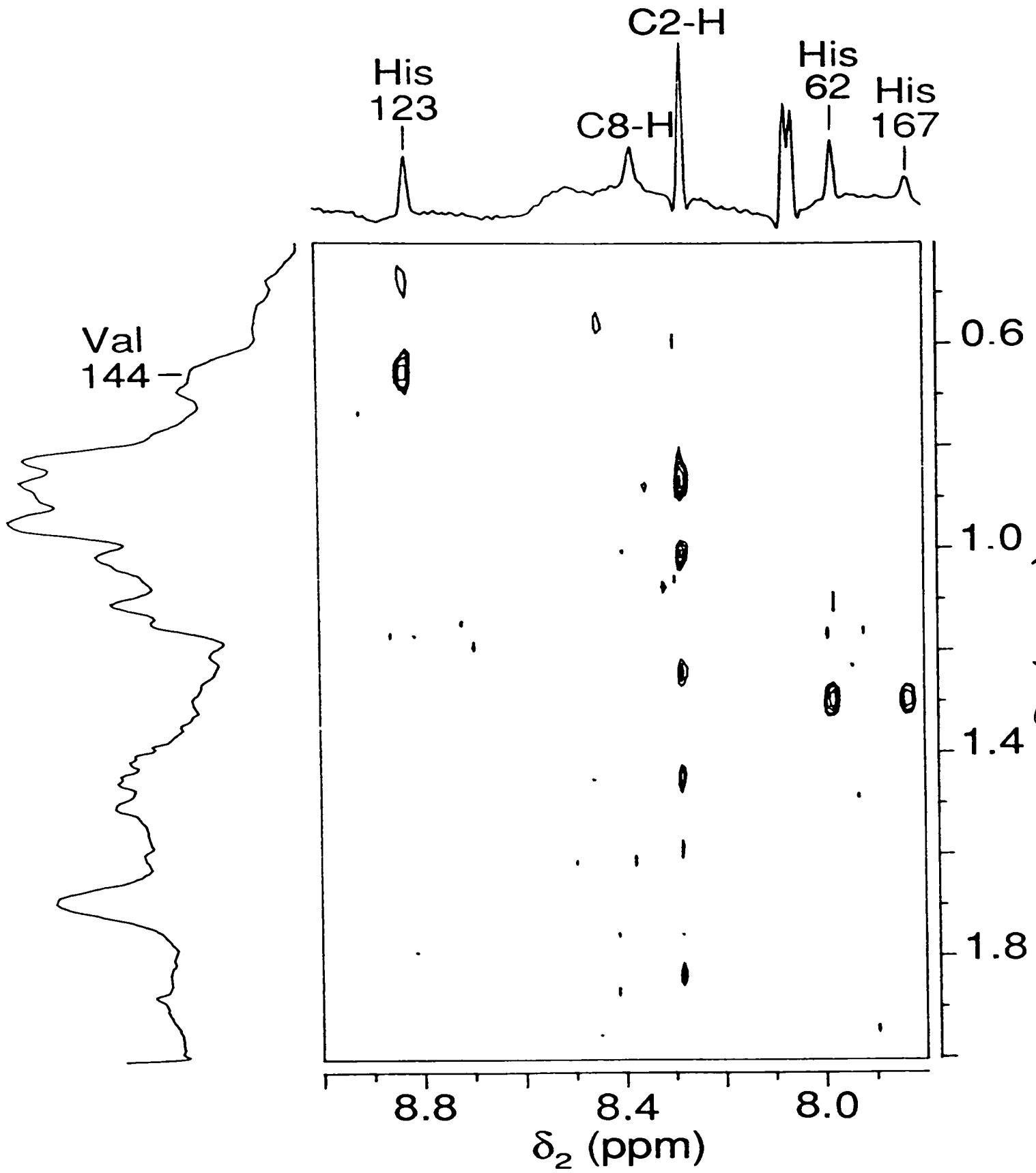

Figure 7-7: Region of the 500 MHz NOESY spectrum of PGK plus Mg.ATP (1.1 mM PGK, 1.3 mM ATP, 13 mM $MgCl_2$, 50 mM $(NH_4)_2SO_4$, 0.10 M Na d_3-acetate, pH 7.1, 27 °C) showing inter-molecular NOE connectivities between the C2-H resonance of the nucleotide and aliphatic resonances of the protein.

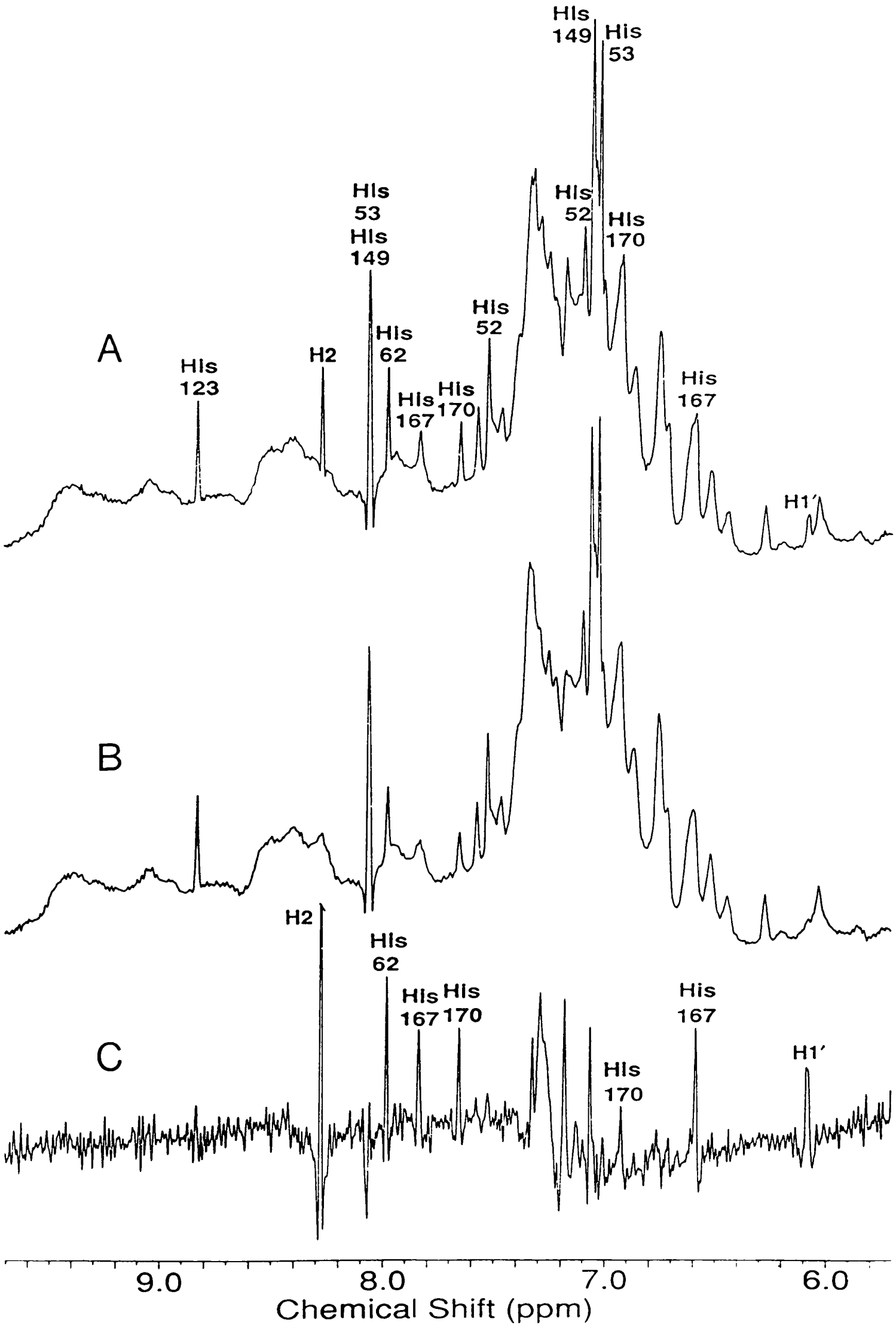

Figure 7-8: Perturbation of the aromatic region of the spectrum of Mg.ATP.PGK in the presence of 50 mM $(NH_4)_2SO_4$ by Mn^{2+}. (A) Spectrum of 1 mM PGK in the presence of 0.7 mM ATP, 0.7 mM Mg^{2+} and 50 mM $(NH_4)_2SO_4$. (B) Spectrum as in (A) but with the addition of 6.6 μM Mn^{2+}. (C) The difference spectrum (A) - (B).

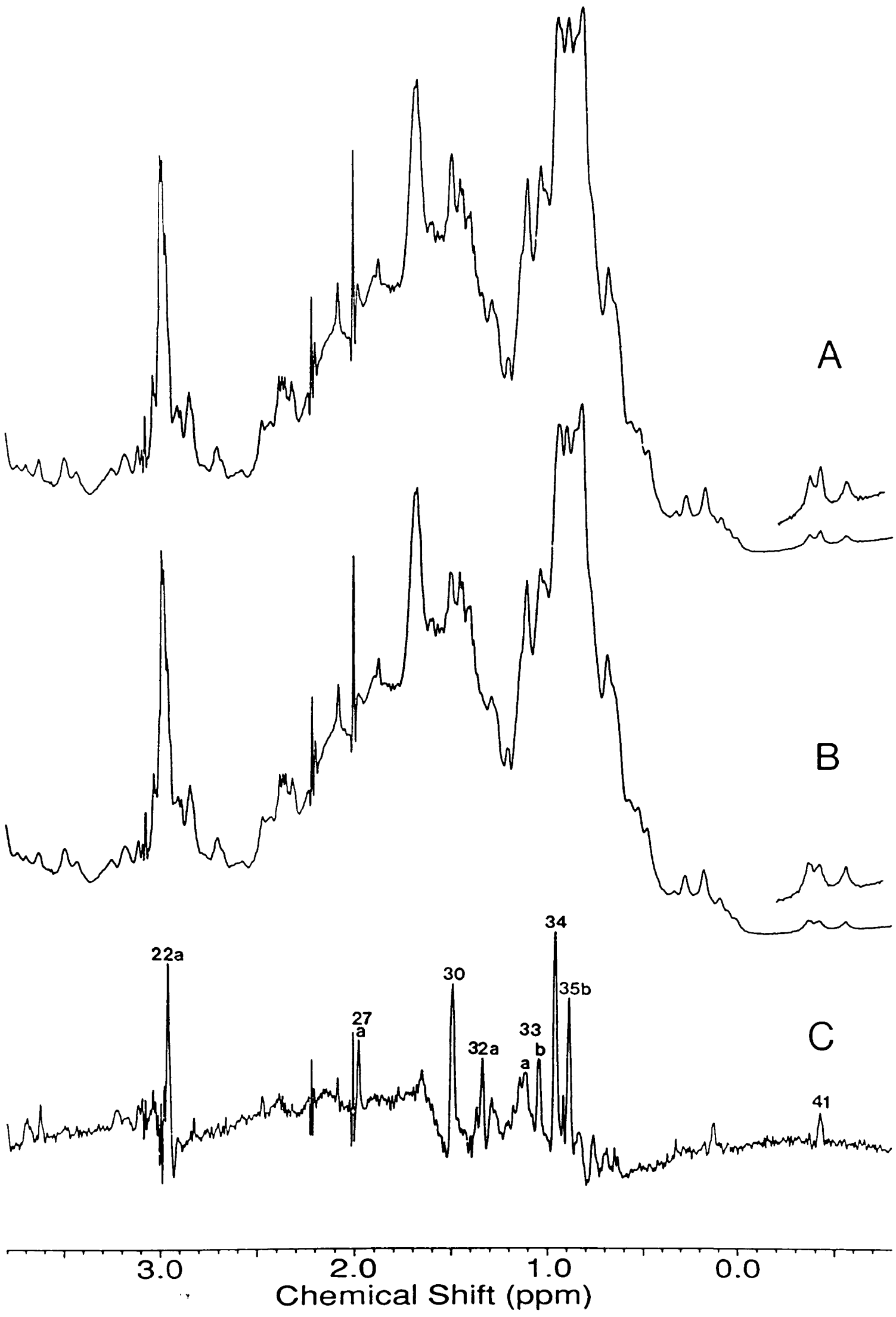

Figure 7-9: Perturbation of the aliphatic region of the spectrum of Mg.ATP.PGK in the presence of 50 mM $(NH_4)_2SO_4$ by Mn^{2+}. (A) Spectrum of 1 mM PGK in the presence of 0.7 mM ATP, 0.7 mM Mg^{2+} and 50 mM $(NH_4)_2SO_4$. (B) Spectrum as in (A) but with the addition of 6.6 μM Mn^{2+}. (C) The difference spectrum (A) - (B).

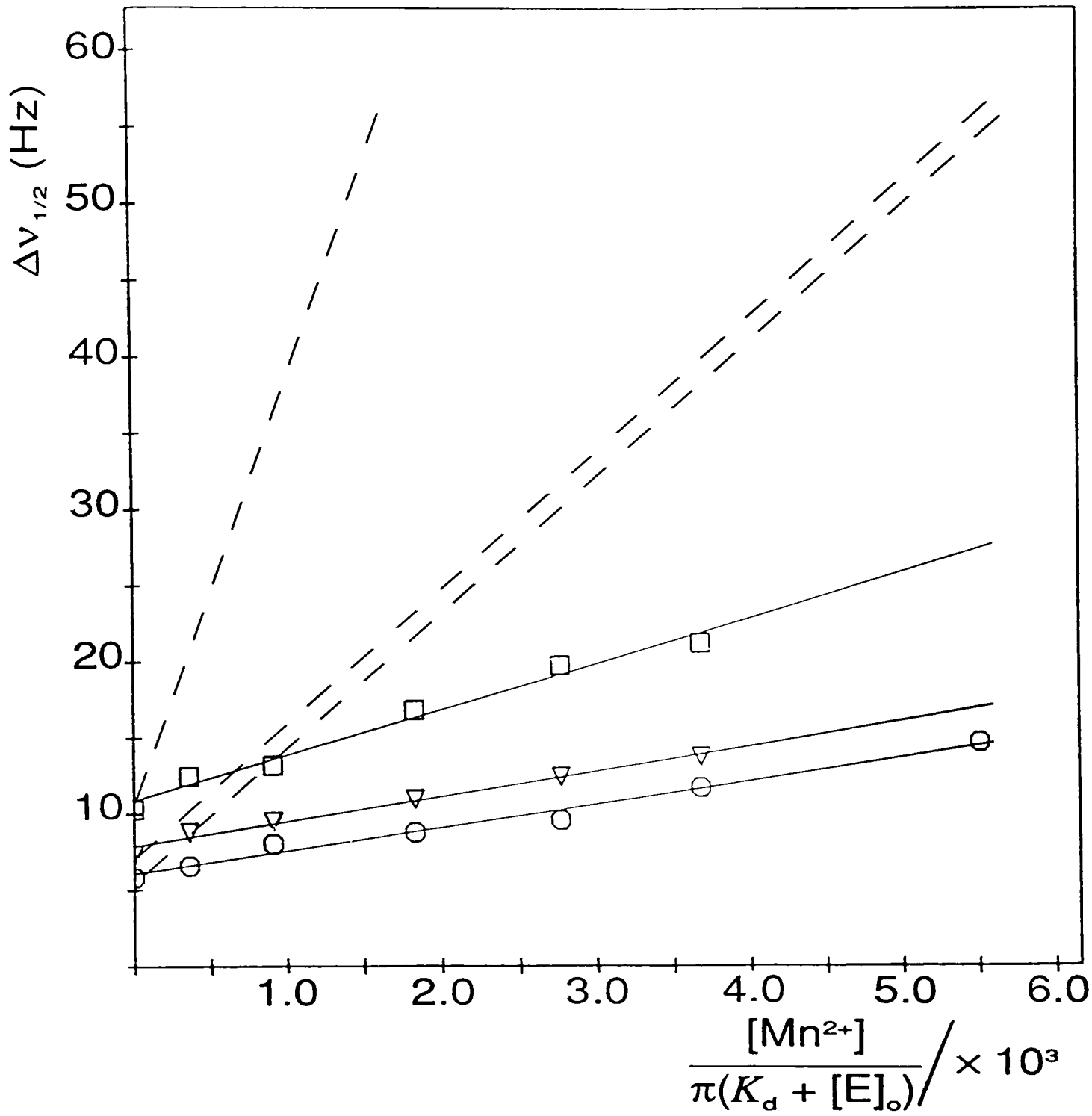

Figure 7-10: The line-widths ($\Delta\nu_{1/2}$) of peaks 3 (○; His 62), 4 (□; His 167) and 5a (▽; His 170) in the spectrum of Mg.ATP.PGK, in the presence of 50 mM $(NH_4)_2SO_4$, plotted as a function of $[Mn^{2+}]/\pi(K_d + [E]_o)$. The dashed lines represent the slopes obtained from a similar plot of data obtained in the absence of $(NH_4)_2SO_4$.

ion to histidine distances calculated from the slopes in Figure 7-10 (*i.e.* in the presence of 50 mM sulphate) are 3.2 ± 0.2 Å greater than those calculated in § 7.3.2 in the absence of sulphate (Table 7-2).

There are two possible explanations for the above result. The first is that in the absence of sulphate a significant proportion of the $Mn.ATP^{2-}$ binds directly to the 'basic patch' region via electrostatic interactions, thereby weighting the relaxation data towards the shorter distance. In the presence of sulphate there is competition for binding at the general anion site but not for binding at the hydrophobic site. A second explanation would be that in the presence of 50 mM sulphate the enzyme assumes a different conformation which, on average, places the 'basic patch' histidines ~ 3 Å further from the metal ion than in its absence.

7.4. Discussion

The results reported in this chapter confirm the observations made in previous studies (Tanswell *et al.*, 1976; Wilson *et al.*, 1988) that the average metal ion to 'basic patch' histidine distances in the presence of ATP are less than those observed crystallographically.

At least three binding sites for Mn^{2+} were identified on the surface of the protein. Wrobel & Stinson (1980) have shown that yeast PGK contains a strong Mn^{2+} binding site (K_d = 4-8 μM). This is probably the one involving Asp 143 and Glu 150, in the vicinity of His 123 and His 149, and Cys 97 (the thiol group monitored by Wrobel & Stinson, 1980). Binding of the paramagnetic cation to the protein did not significantly perturb the resonances of the 'basic patch' histidines.

That the maximal distances calculated from the Mn.ATP.enzyme complex broadening data in the presence of 50 mM ammonium sulphate are greater than in its absence indicates that direct binding of $Mn.ATP^{2-}$ to the 'basic patch' region of the protein cannot be ruled out as a possible reason for the

Table 7-2: Estimation of Mn^{2+} to 'basic patch' histidine distances from Mn.ATP.enzyme complex relaxation data in the presence of 50 mM ammonium sulphate.

Slopes were determined from Figure 7-10.

	Resonance		
Parameter	3 (His 62)	4 (His 167)	5a (His 170)
slope/Hz	1532	3012	1657
$(T_{2,M})_{max.}$/ms	0.653	0.332	0.604
$\langle r_i \rangle$/Å	12.6	11.2	12.4

discrepancy between the solution and the crystallographic results. It is interesting that a metal ion to ^{31}P(3-PG) distance of 11.1 ± 0.3 Å was determined for the Mn.ADP.3-PG.enzyme complex (Ray & Nageswara Rao, 1988), suggesting that this complex is in an 'open' conformation. It is possible that the Mn.ATP.SO_4.enzyme complex is also in a similar 'open' conformation.

One way of testing the two possibilities may be to photoaffinity label (Czarnecki *et al.*, 1979) the protein with an analogue of ATP (*e.g.* 8-azido-ATP or 2-azido-ATP) in the presence of sufficient concentrations of anions (*e.g.* SO_4^{2-}, $[Co(CN)_6]^{3-}$, $[Fe(CN)_6]^{4-}$) to prevent interaction with the general anion binding site. Once the nucleotide is covalently bound (hopefully only at the hydrophobic, catalytic site) the anions could be removed and the sample titrated with Mn^{2+} as before.

7.5. References

Czarnecki, J., Geahlen, R. & Haley, B. (1979) *Methods Enzymol. 46,* 642-653.

Larsson-Raźnikiewicz, M. (1970) *Eur. J. Biochem. 17,* 183-192.

Ray, B.D. & Nageswara Rao, B.D. (1988) *Biochem. 27,* 5579-5585.

Tanswell, P., Westhead, E.W. & Williams, R.J.P. (1974) *FEBS Lett. 48,* 60-63.

Tanswell, P., Thornton, J.M., Korda, A.V. & Williams, R.J.P. (1975) *Eur. J. Biochem. 57,* 135-145.

Tanswell, P., Westhead, E.W. & Williams, R.J.P. (1976) *Eur. J. Biochem. 63,* 249-262.

Watson, H.C., Walker, N.P.C., Shaw, P.J., Bryant, T.N., Wendell, P.L., Fothergill, L.A., Perkins, R.E., Conroy, S.C., Dobson, M.J., Tuite, M.F., Kingsman, A.J. & Kingsman, S.M. (1982) *EMBO J. 1,* 1635-1640.

Watson, H.C. & Gamblin, S.J. (1985) *Proc. Int. Symp. Biomol. Struct. Interactions, Suppl. J. Biosci. 8,* 499-506.

Wilson, H.R., Williams, R.J.P., Littlechild, J.A. & Watson, H.C. (1988) *Eur. J. Biochem. 170,* 529-538.

Wrobel, J.A. & Stinson, R.A. (1980) *Eur. J. Biochem. 104,* 249-254.

Chapter 8

NMR STUDIES OF ISOLATED STRUCTURAL DOMAINS OF YEAST PGK

8.1. Introduction

PGK is composed of two globular domains of approximately equal size, corresponding to the N-terminal and C-terminal halves of the protein (Blake & Rice, 1981; Watson *et al.*, 1982). Wetlaufer (1973) has suggested that protein domains, such as those of PGK, result from independent folding processes and that the folded domains may be kinetic intermediates which interact to form the native structure:

> Distinct structural regions have been found in several globular proteins composed of single polypeptide chains. The existence of such regions and the continuity of peptide chains within them, coupled with kinetic arguments, suggests that the early stages of the three-dimensional structure formation (nucleation) occur independently in separate parts of these molecules. A nucleus can grow rapidly by adding peptide chain segments that are close to the nucleus in amino acid sequence. Such a process would generate three-dimensional (native) protein structures that contain separate regions of continuous peptide chain.... One of the most searching experimental tests for an independent continuous region would be to demonstrate self-assembly of just that region, with a high degree of fidelity.

Support for this view comes from two sources. Firstly, studies of the unfolding-refolding processes of proteins, using different conformational probes, have shown the folding of domains to be intermediate in the folding of several proteins. In particular, studies of the unfolding-refolding of PGK have indicated independent refolding of each domain with different equilibrium constants, the most favourable being that for refolding of the C-terminal domain (Burgess & Pain, 1977; Betton *et al.*, 1984, 1985; Adams *et al.*, 1985; Mitraki *et al.*, 1987). Secondly, the folding of isolated protein fragments corresponding to structural domains, obtained by either limited proteolysis or by chemical cleavage, has been studied. Several such studies have provided evidence that domains can be considered as independent folding units

(Wetlaufer, 1981; Ghélis & Yon, 1982). In an attempt to provide direct evidence for the ability of the domains of PGK to fold independently, Adams *et al.* (1985) have investigated the folding of the N-terminal cyanogen bromide fragment (residues 1-173). This peptide does not correspond precisely to the N-terminal domain, in that it lacks the C-terminal β-strand F and its connection (~ 12 residues) to the interdomain α-helix V (in addition to the ~ 15 residue C-terminal peptide, including α-helix XIV, which folds back from the C-terminal domain on to the surface of the N-terminal domain; Figure 8-1). Despite this it was reported to fold into a native-like conformation, stabilised by specific dimer formation.

Site-directed mutagenesis now provides an alternative and specific general method for producing protein fragments corresponding to known structural domains, and has been used to produce isolated N- and C-domains of yeast PGK (Minard *et al.*, 1989). In this chapter, 1D and 2D NMR techniques are applied to the isolated domains in order to establish their structural integrity and to further investigate their substrate binding properties. Analysis of the isolated domains also offers an alternative method of resonance assignment in the ^{1}H NMR spectrum of native yeast PGK (see Chapter 2).

8.2. Experimental methods

8.2.1. *Mutagenesis*

The two domains of yeast PGK were produced by Dr P. Minard (Laboratoire d'Enzymologie Physico-chimique et Moléculaire, Groupe de Recherche du Centre National de la Recherche Scientifique associé à l'Université de Paris-Sud) using recombinant techniques as described by Minard *et al.* (1989). The N-domain was obtained by introduction of a termination codon at the position coding for Phe 185. The C-domain was obtained by deletion of the coding sequence between Ser 1 and Leu 186. C-terminal analysis by

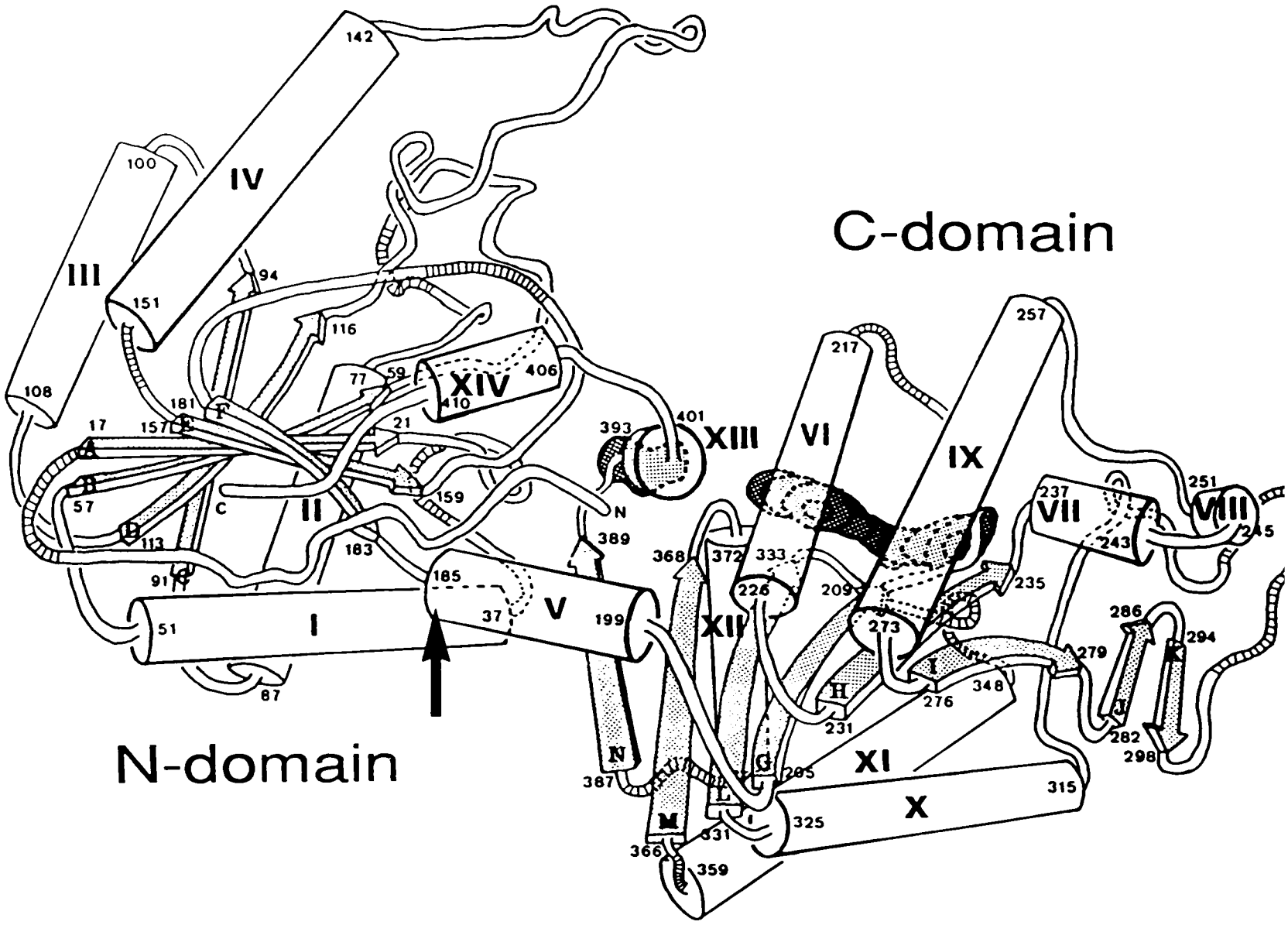

Figure 8-1: A schematic drawing of the crystal structure of yeast PGK from Watson *et al.* (1982). The position chosen as the domain cut-off, Phe 185, is indicated by an arrow.

carboxypeptidase digestion showed the two terminal Lys residues of the isolated C-domain to be absent (Minard *et al.*, 1989). The molecular masses of the N- and C-terminal domains, calculated from their amino acid sequences, are 20328 and 23866 Da respectively.

8.2.2. *Preparation of NMR samples*

Protein samples were stored as ammonium sulphate suspensions. Samples for NMR experiments were resuspended in a 100 mM sodium d_3-acetate/D_2O solution and concentrated using Amicon Centricon 10 microconcentrators to a volume of ~ 200 µl. The sample was washed 4-5 times with 2.5 ml of the sodium d_3-acetate/D_2O solution, on the Centricon concentrator, to effect sulphate removal and D_2O/H_2O exchange. The final volume was adjusted to 450-500 µl (concentration 1-3 mM, pH 6.5-7.5). Protein concentrations were determined using molar absorption coefficients ($A_{280\ nm}$) of 6544 and 15183 $M^{-1}\ cm^{-1}$ for the N- and C-domains respectively (Minard *et al.*, 1989).

8.2.3. *NMR spectroscopy*

NMR experiments were performed either on a Bruker AM500 or AM600 spectrometer as described in § 2.2.6. Two-dimensional (2D) NMR experiments (COSY, Aue *et al.*, 1976; NOESY, Jeener *et al.*, 1979; RCT, Eich *et al.*, 1982, King & Wright, 1983) were performed in the phase sensitive mode using the method of time-proportional phase incrementation (Marion & Wüthrich, 1983). NOESY spectra were recorded with mixing times of 150 and 250 ms and a random variation of ± 20 ms. RCT spectra were recorded with a total mixing time of 30 ms.

All spectra were recorded at a temperature of 27 °C. Acetone was used as an internal chemical shift reference (δ = 2.214 ppm).

8.2.4. *pH titrations*

pH adjustments of the protein samples were made either with NaOD or DCl

(0.4 % w/w). The pH values quoted are uncorrected meter readings taken on a Radiometer PHM 84 Research pH meter using an Ingold combination electrode, inserted directly into a 5mm NMR tube.

8.2.5. *Substrate binding*

The binding of 3-PG to the N-domain and Mg.ATP to the C-domain was investigated by titrating the protein samples (in the NMR tubes) with 1-4 µl aliquots of 60 mM substrate solutions and measuring the 1D ^{1}H NMR spectra. The pH of the 3-PG and Mg.ATP ($[Mg^{2+}]$:[ATP] ~ 1:1) solutions were initially adjusted to be the same (± 0.05) as the respective protein solutions. The pH of the protein sample was measured both before and after completion of the titration to ensure that any observed effects in the spectrum were not due to changes in pH.

8.3. Results

8.3.1. *N-Terminal domain*

The 500 MHz ^{1}H NMR spectrum of the isolated N-terminal domain (Figure 8-2) shows chemical shift dispersion (*i.e.* 'non-random coil' peaks) typical of a structured protein. In particular, the presence of slowly exchanging amide resonances (7.4 ppm - 9.7 ppm) indicates that certain parts of the protein back-bone are protected from solvent. Downfield shifted α-CH resonances (4.7 ppm - 5.6 ppm) are indicative of β-structures (Dalgarno *et al.*, 1983) and consistent with the circular dichroic results of Minard *et al.* (1989). All amide protons, however, exchange for deuterons in the solvent within 48 hours of completing the D_2O/H_2O solvent exchange (pH 7.1, 4 °C) indicating a significant degree of flexibility in the structure.

In the aromatic region of the spectrum 11 of the expected 14 histidine resonances (7 histidine residues) are observed. The pH dependence of these peaks is illustrated in Figure 8-3. It is notable that all the observable

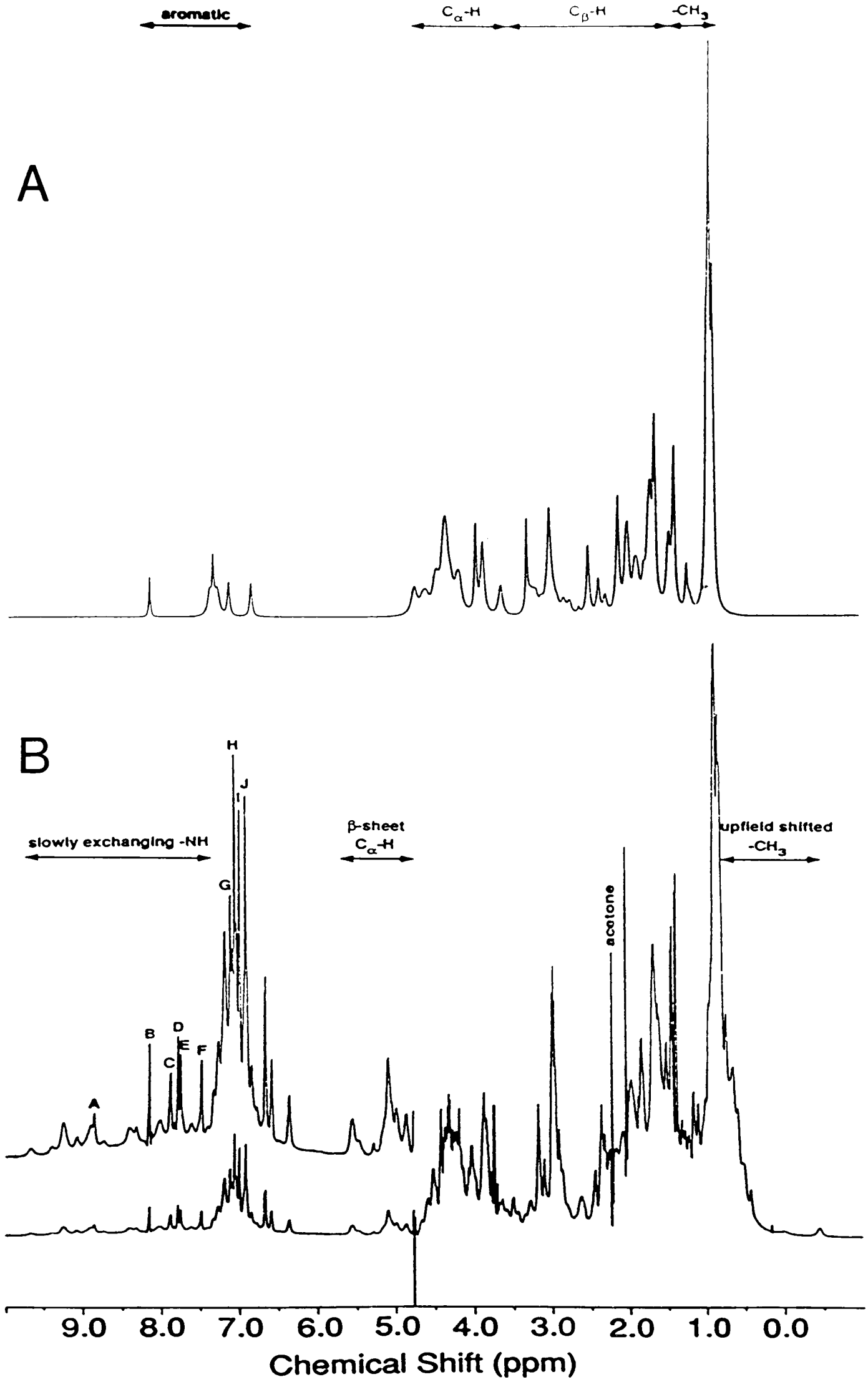

Figure 8-2: (A) A computed 'random coil' ^{1}H NMR spectrum of non-labile protons of the N-terminal domain of yeast PGK (pH 7.1, line width 10 Hz, 500 MHz). (B) ^{1}H NMR spectrum of a D_2O solution of the isolated N-terminal domain (3.0 mM, 0.10 M Na d_3-acetate, pH 7.09, 27 °C, 500 MHz). Spectral regions associated with various aspects of the protein tertiary fold are indicated. A four fold expansion of the downfield spectral region is inserted, with His C2-H and C4-H resonances labelled A-J.

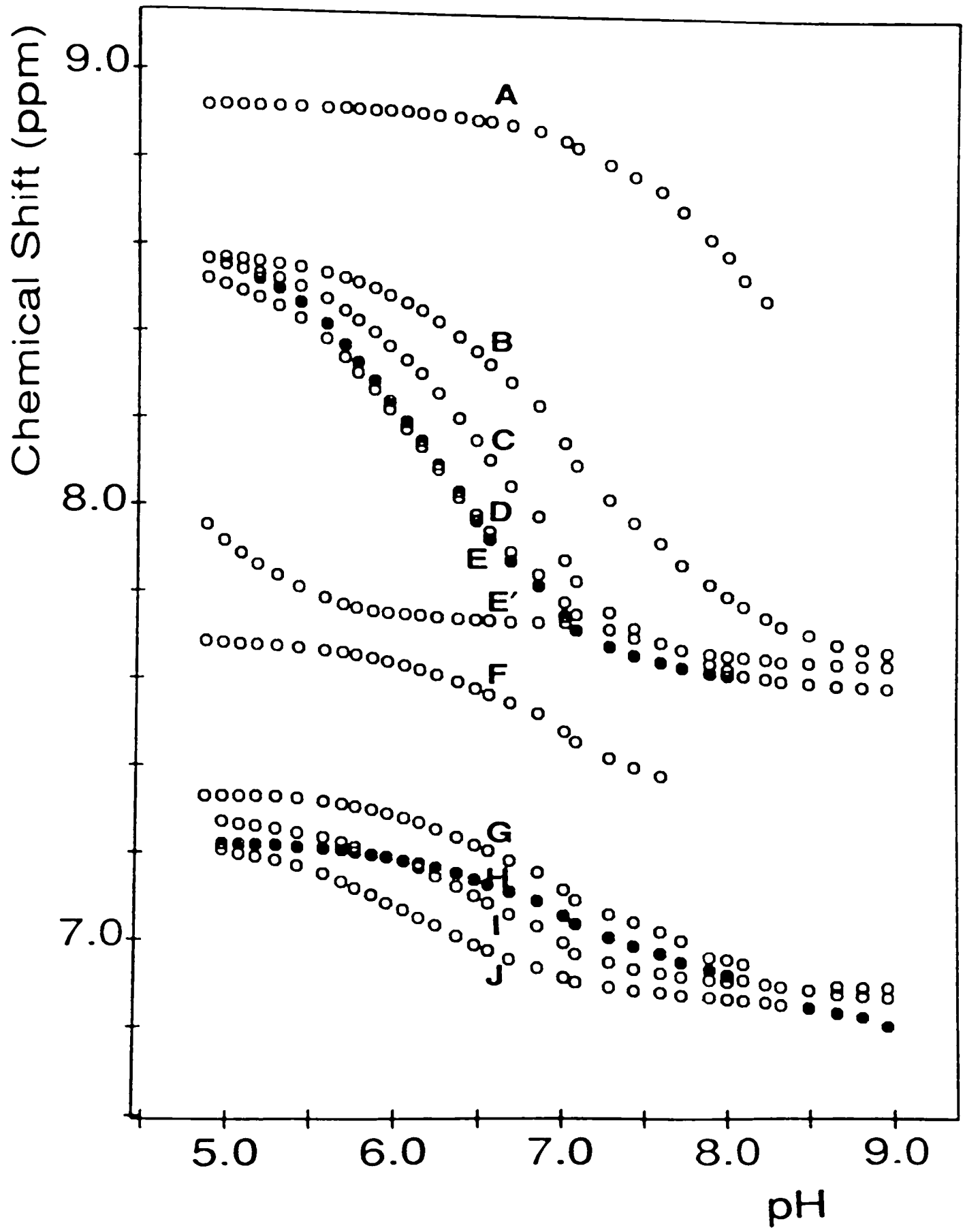

Figure 8-3: The pH dependence of chemical shifts for His C2-H and C4-H resonances of the isolated N-terminal domain. The peak labels (A-J) correspond to the peak labelling shown in Figure 8-2. The experimental points for peaks E and H are shaded for clarity.

histidine peaks shift within the pH range investigated (5.0 - 9.0), while in native PGK the resonances of His 62, 167 and 170 are independent of pH in this range (§ 2.3.6, Figure 2-16). These residues form part of the 3-PG binding site of the intact PGK molecule (Watson *et al.*, 1982; Walker *et al.*, 1989; see Chapter 3). This result therefore indicates a significant perturbation of this site in the isolated N-domain.

Some of the histidine peaks can be correlated with resonances which have been assigned in the native protein (Chapter 2), suggesting that regions of structural similarity do exist. For instance, the most downfield histidine resonance (His A) has a chemical shift and pH dependence very similar to peak 1 in the spectrum of native PGK, whilst peaks labelled "F" and "G" appear to correspond to resonances 5 and 9 respectively. In addition NOE connectivities are observed between peak "A" and a resonance at 0.66 ppm (*c.f.* NOE observed between peak 1 (His 123) and a resonance at 0.65 ppm (Val 144) in the spectrum of native PGK; § 4.3.2) and between peaks "F" and "G" (*c.f.* NOE observed between peak 5 (His 52; C2-H) and peak 9 (His 52; C4-H) in the spectrum of native PGK; § 2.3.2). Peak "F" also gives NOE cross-peaks to resonances at 6.97 ppm and 6.65 ppm which appear to correspond to a Tyr residue (Figure 8-4). This is consistent with the observed NOE connectivities between His 52 and Tyr 48 in the NOESY spectrum of native PGK (§ 2.3.2; Figure 2-10).

8.3.1.1. 3-Phosphoglycerate binding

A titration of the N-domain with 3-PG resulted in only very small perturbations of the 1D ^{1}H NMR spectrum of the protein, indicating that this substrate does not bind to the isolated domain with any significant affinity. This result is in contrast with the extensive perturbations (particularly of resonances assigned to residues in the N-domain) observed when 3-PG is added to samples of native PGK (Chapter 3), but in agreement with the 3-PG binding study of the N-terminal domain reported by Minard *et al.* (1989).

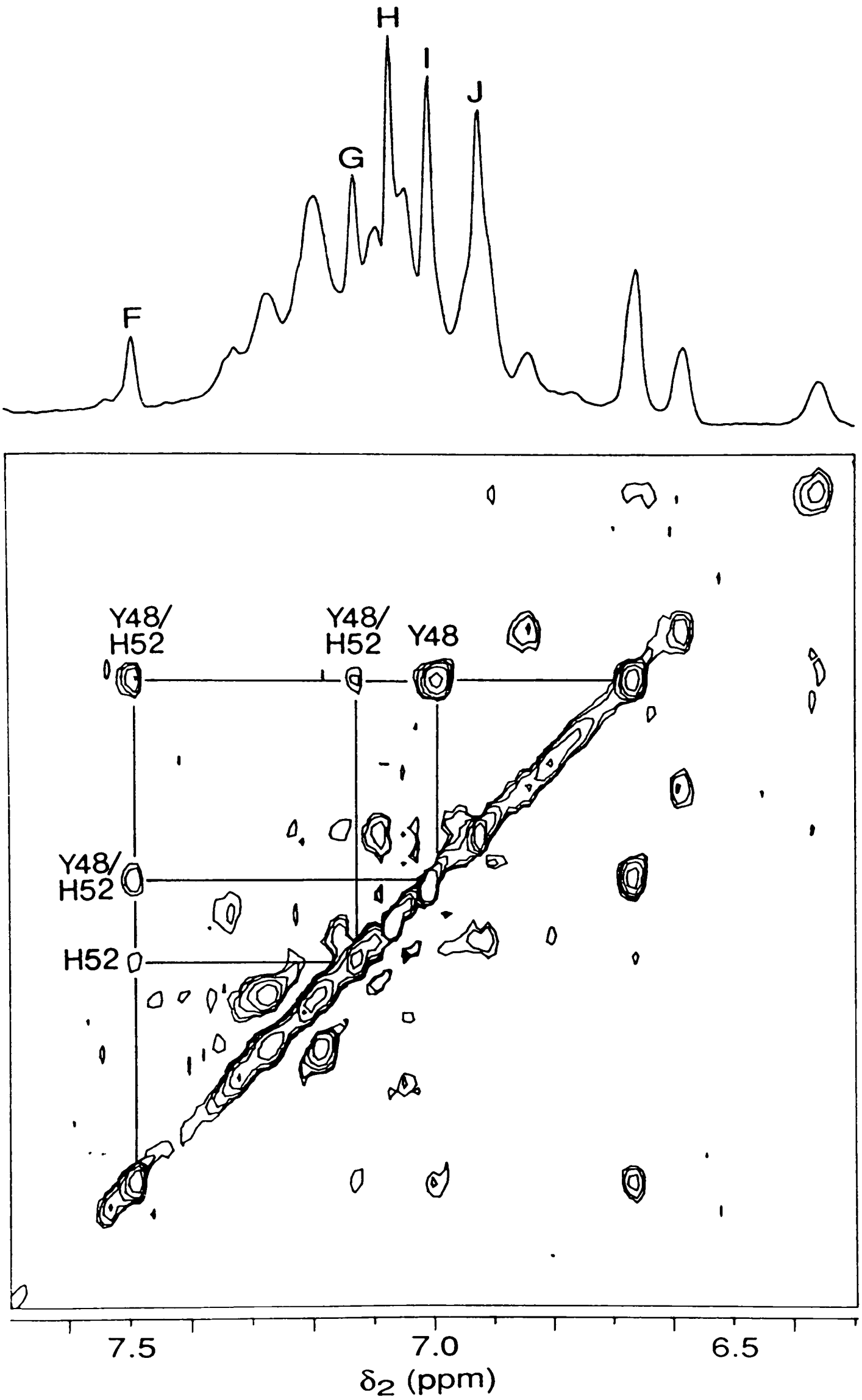

Figure 8-4: Aromatic region of the 500 MHz NOESY spectrum of the isolated N-terminal domain (3.0 mM, 0.10 M Na d_3-acetate, pH 7.1, 27 °C). The mixing time was 200 ms.

8.3.2. *C-Terminal domain*

As seen for the N-terminal domain, the 500 MHz ^{1}H NMR spectrum of the C-domain (Figure 8-5) shows the protein to be folded (*i.e.* there are a number of well resolved upfield shifted methyl resonances ($\delta < 0.8$ ppm), downfield shifted α-CH resonances ($\delta > 4.7$ ppm) and slowly or non-exchanging amide peaks (7.5 ppm - 9.5 ppm)). A large proportion of the amide resonances are retained after storage in D_2O solution (pH 6.6, 4 °C) for 3 weeks, indicating that the fold (and particularly the β-structure) is very stable.

8.3.2.1. Histidine 388

The C2-H and C4-H resonances of His 388 can be clearly identified from their pH dependence (Figure 8-6) which shows that in the isolated C-domain this histidine has a pK_a of about 6.6. This value is close to that expected for a histidine in a 'random peptide' (Markley, 1975). Two other resonances (peaks 13 and 16a) were also observed to shift with an apparent pK_a similar to that of the histidine, indicating that the chemical environments of the protons responsible for these peaks change as the protonation state of His 388 is altered. This is probably due to direct electronic effects of the histidine (rather than a relayed conformational effect), thus on average the protons must be in close proximity to His 388.

8.3.2.2. Tyrosines 193 and 380

The pH dependence of peaks 16a and 16b (Figure 8-6) indicates that these resonances are due to tyrosine side-chains. The COSY spectrum of the C-domain (Figure 8-7A) shows that at pH ~ 6.6 peak 16a (6.70 ppm) is coupled to peak 13 (6.87 ppm) and peak 16b (6.71 ppm) is coupled to a peak at 7.29 ppm (COSY spectra were also obtained at pH ~ 7.1 and pH ~ 10.5). Tyrosine cross-peaks have been identified with very similar ('non-random coil') chemical shifts in the COSY spectrum of native PGK (Figure 8-7B)

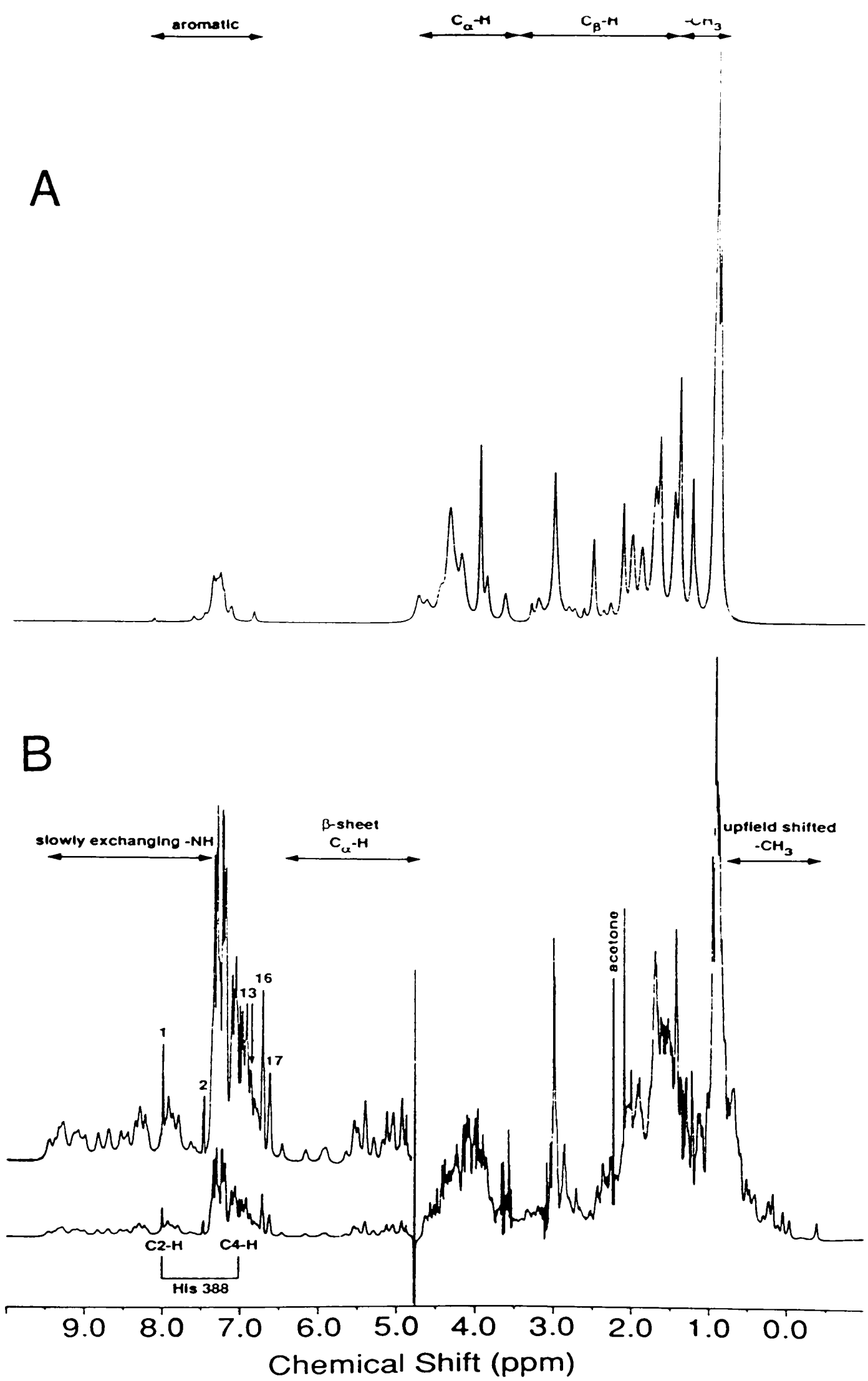

Figure 8-5: (A) A computed 'random coil' ^{1}H NMR spectrum of non-labile protons of the C-terminal domain of yeast PGK (pH 7.1, line width 10 Hz, 500 MHz). (B) ^{1}H NMR spectrum of a D_2O solution of the isolated C-terminal domain (1.9 mM, 0.10 M Na d_3-acetate, pH 7.08, 27 °C, 500 MHz). Spectral regions associated with various aspects of the protein tertiary fold are indicated. A four fold expansion of the downfield spectral region is inserted, with aromatic peaks referred to in the text labelled.

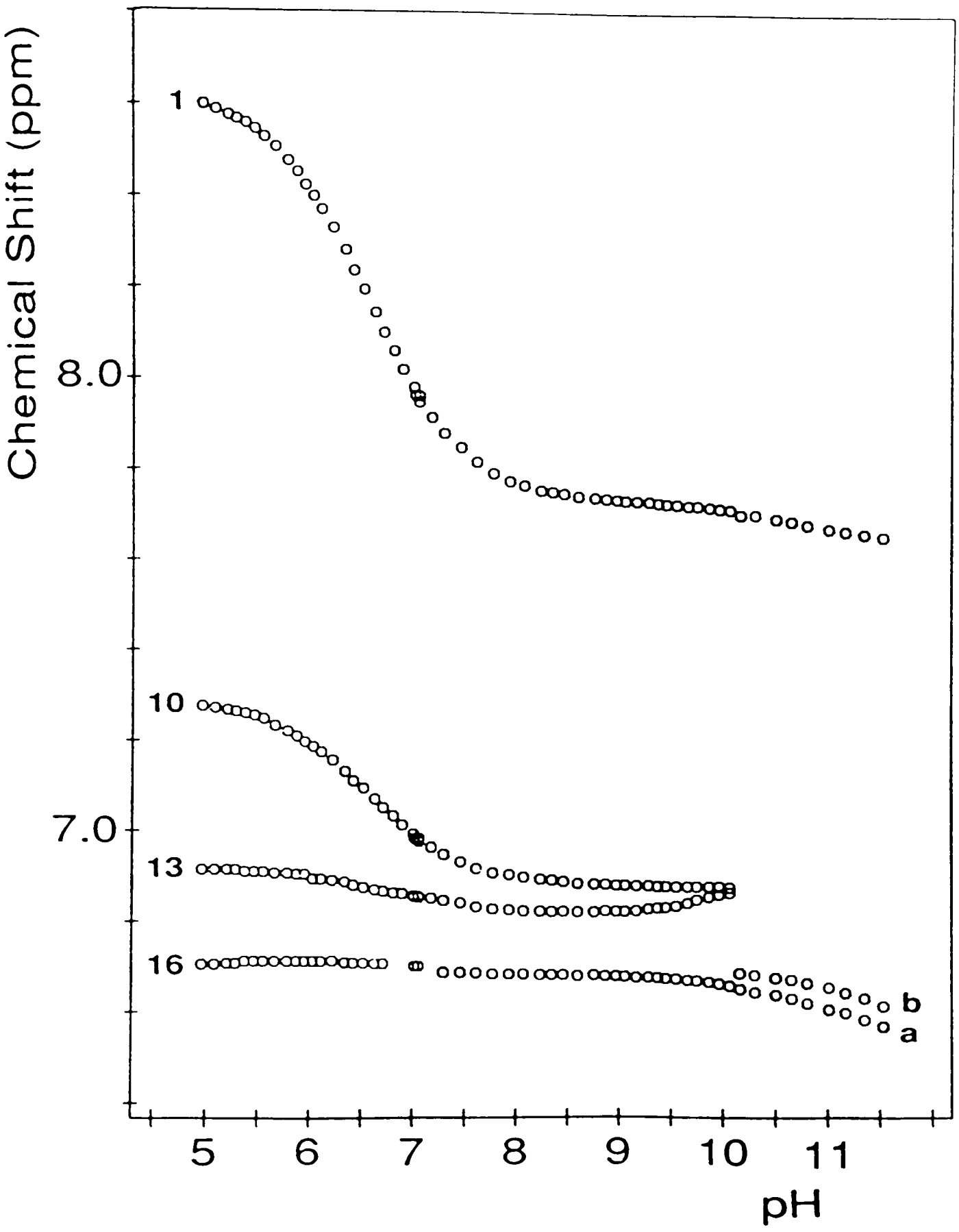

Figure 8-6: The pH dependence of chemical shifts for some aromatic resonances of the isolated C-terminal domain. The numbers correspond to the peak labels in Figure 8-5. Peaks 1 and 10 are assigned to C2-H and C4-H of His 388 respectively and titrate with a pK_a of 6.57 ± 0.02.

indicating that the environments of Tyr 193 and Tyr 380 in the isolated C-domain are similar to those found in the whole protein. In the crystal structure of native PGK (Watson *et al.*, 1982) the closest tyrosine side-chain to His 388 is Tyr 193. Peaks 13 and 16a (which titrate with His 388; see above) have therefore been assigned to Tyr 193 and peak 16b and the resonance at ~ 7.3 ppm to the remaining Tyr 380. It is noted, however, that the weak NOE observed between His 388 and Tyr 193 in the NOESY spectrum of native PGK is not seen in the NOESY spectrum of the isolated C-domain (Figure 8-11).

8.3.2.3. Comparison of the 2D ^{1}H NMR spectra of the C-domain and native PGK

Several other cross-peaks observed in the COSY spectrum of the C-terminal domain correlate with cross-peaks observed in the COSY spectrum of native PGK (in both the aliphatic and aromatic regions of the spectrum). Six such cross-peaks in the aromatic region of the spectrum are indicated in Figure 8-7. These include the resonances assigned above to Tyr 193 (YA) and Tyr 380 (YB). In addition, the cross-peaks labelled FA compare well with peaks assigned to Phe 342 in the spectrum of native PGK (§ 2.3.3) and the cross-peak at 6.91 ppm/7.46 ppm (WA) is in a very similar position to that tentatively assigned to Trp 308 (§ 2.3.2). The two cross-peaks labelled FB are unassigned (one cross-peak is almost coincident with one of the cross-peaks of Phe A; the spin system of Phe B was confirmed in a relayed coherence transfer (RCT) experiment; Figure 8-8). Comparison of COSY cross-peaks closer to the diagonal is complicated by the greater degree of overlap in the spectrum of the entire protein. In the aliphatic region of the spectrum there are also a number of cross-peaks in 'non-random coil' positions which can be correlated with cross-peaks observed in the COSY spectrum of intact PGK. Examples are shown in Figure 8-9.

From a comparison of the two COSY spectra it is apparent that the spectral

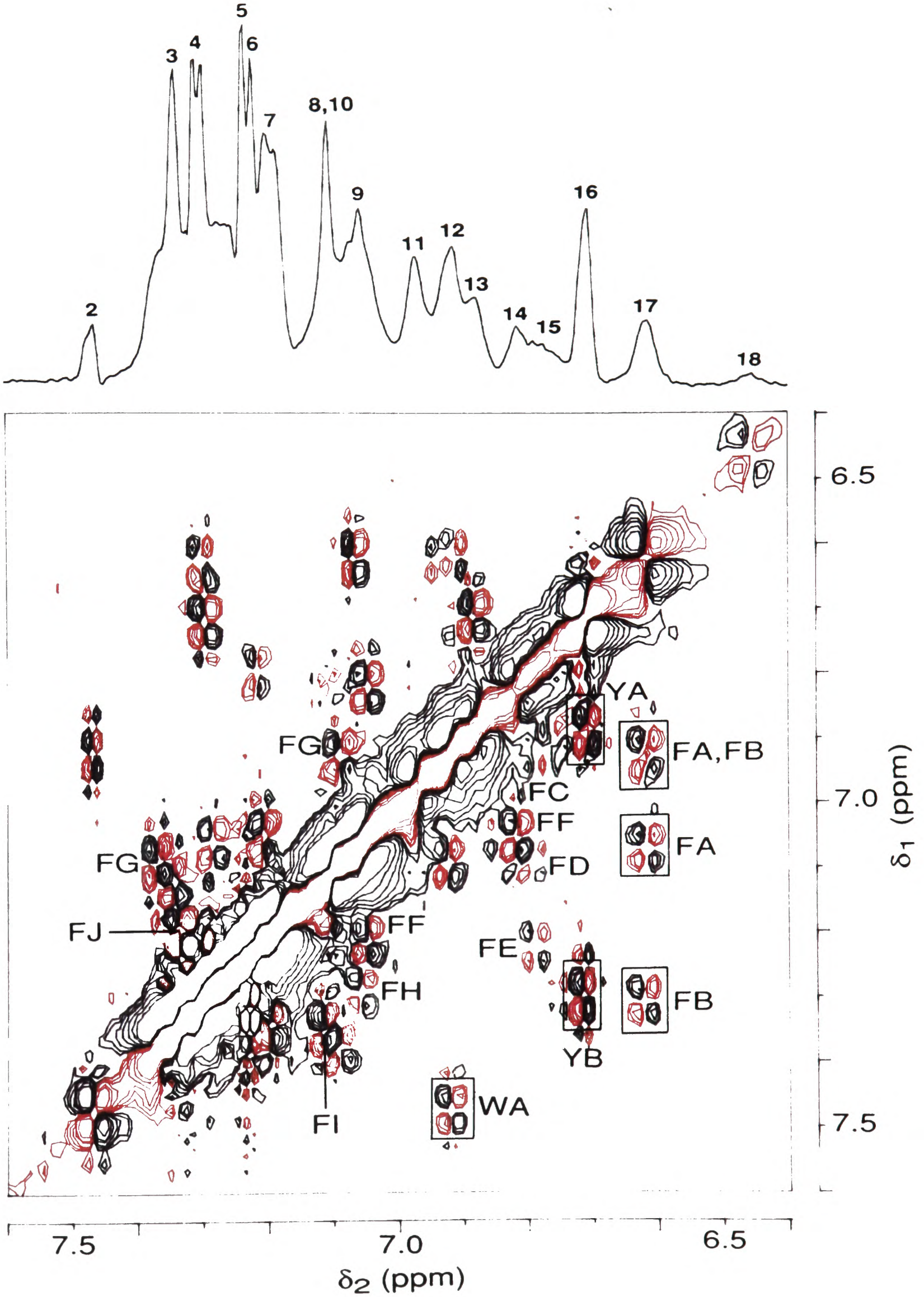

Figure 8-7A: Aromatic region of the 600 MHz COSY spectrum of the isolated C-terminal domain (1.9 mM, 0.10 M Na d_3-acetate, pH 6.63, 27 °C). The cross-peaks are labelled by spin-system. Cross-peaks which are also observed in the COSY spectrum of whole PGK are boxed.

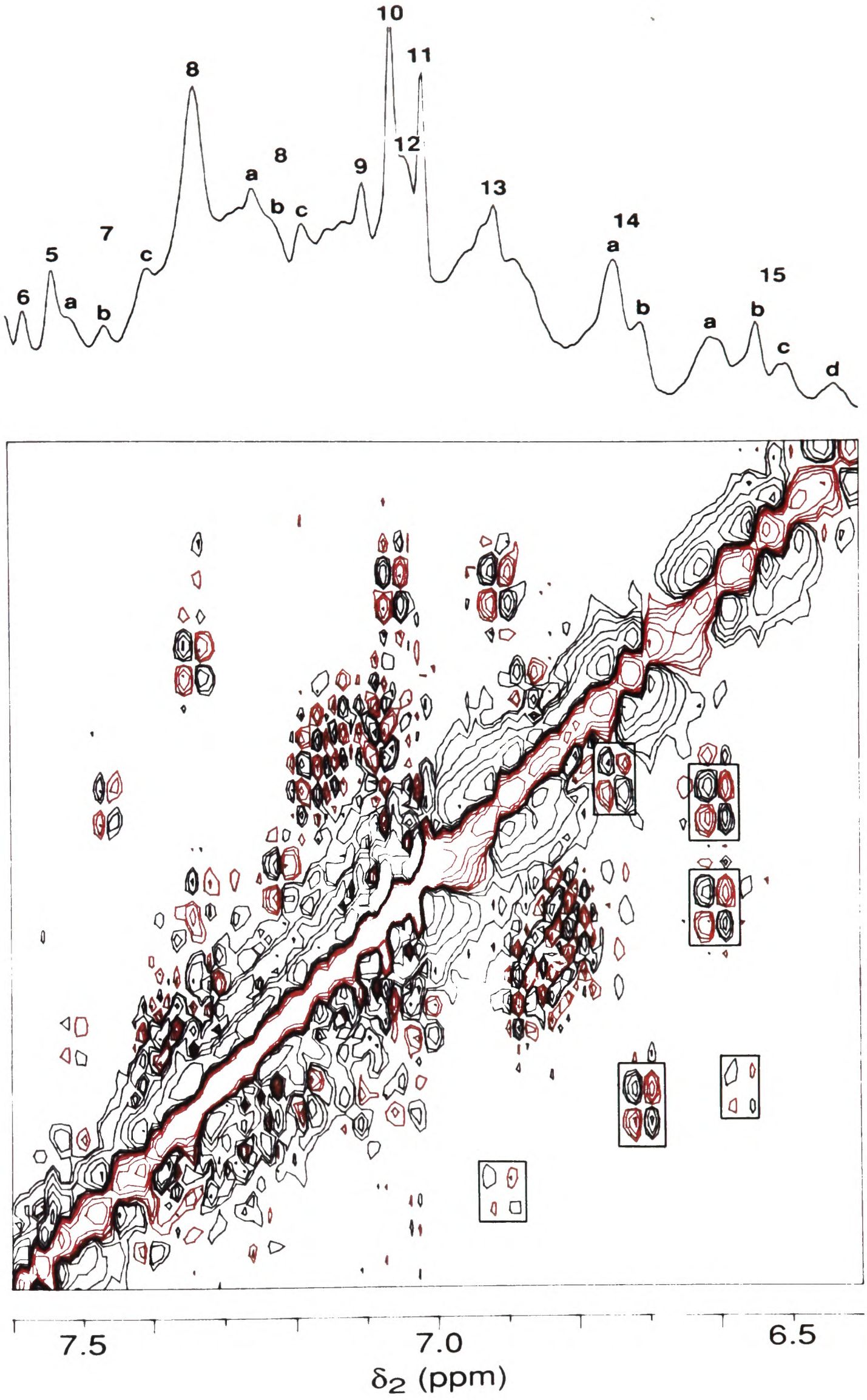

Figure 8-7B: The corresponding aromatic region of the 500 MHz COSY spectrum of whole PGK (1.2 mM, 0.10 M Na d_3-acetate, pH 7.10, 27 °C). Cross-peaks observed in the COSY spectrum of the isolated C-domain are boxed.

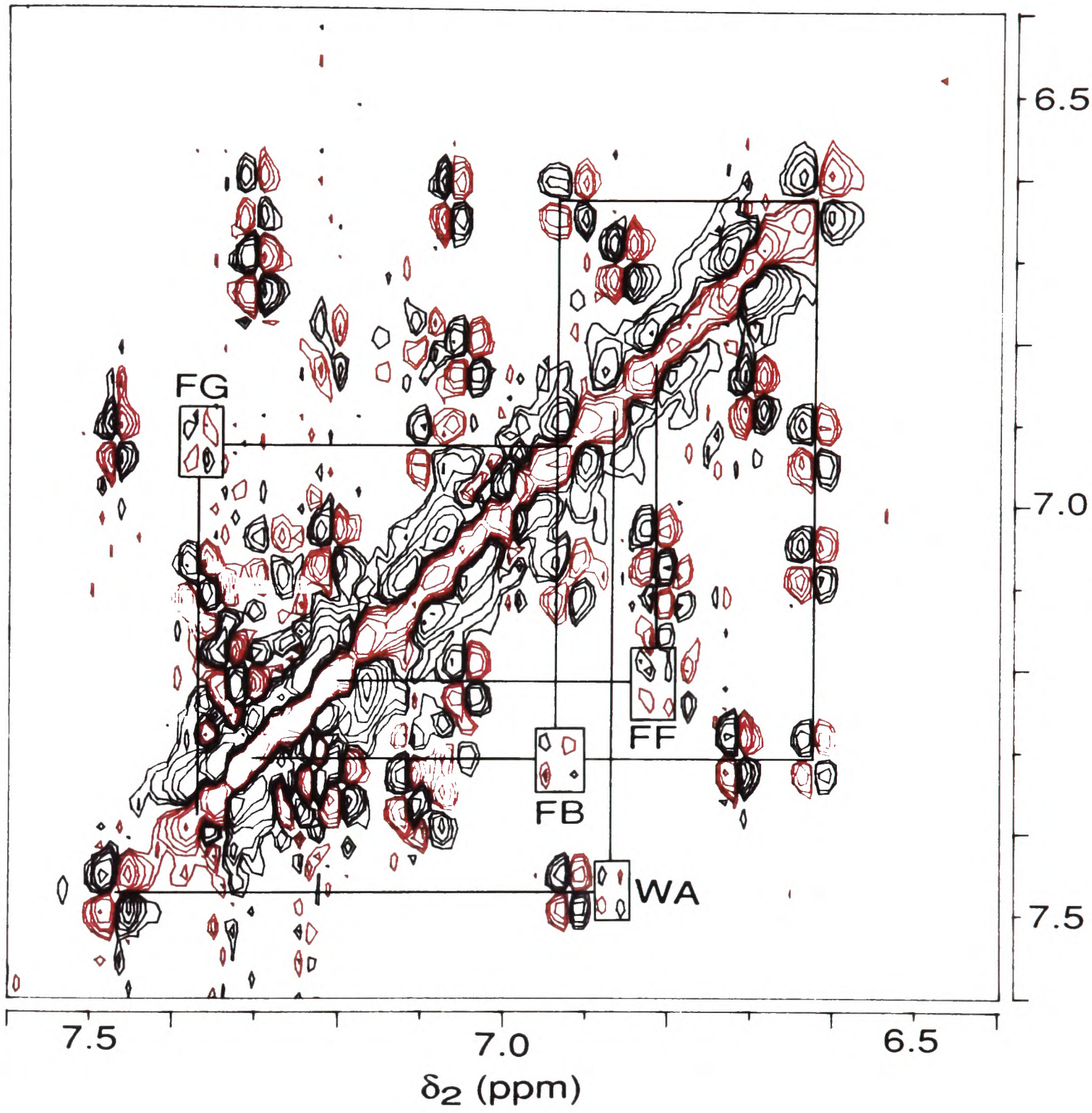

Figure 8-8: Aromatic region of the 600 MHz RCT spectrum of the isolated C-terminal domain (1.5 mM, 0.10 M Na d_3-acetate, pH 7.07, 27 °C). Selected RCT cross-peaks are boxed and labelled according to spin-system.

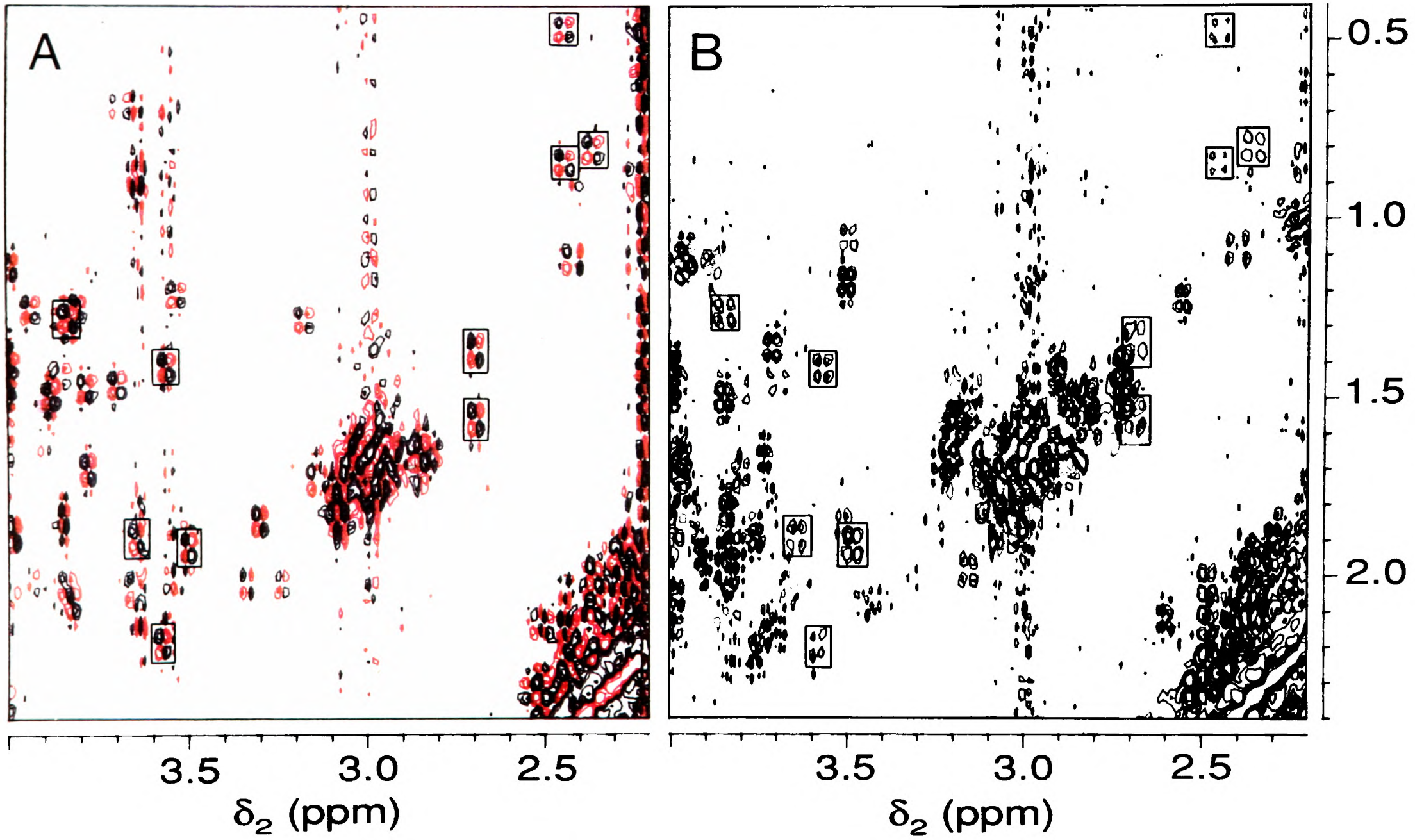

Figure 8-9: Comparison of sections of the aliphatic regions of the 600 MHz COSY spectrum of the isolated C-terminal domain (A) and the 500 MHz COSY spectrum of whole PGK (B). Cross-peaks which are observed in both spectra are boxed.

resolution has improved on going from whole PGK to the isolated C-domain. This is seen particularly in the upfield methyl region of the spectrum (Figure 8-10) where cross-peaks are observed from most of the resonances in the C-domain but from only a few resonances in intact PGK (*c.f.* Figure 2-8). This improvement in resolution is as expected on halving the molecular mass (~ 45 kDa to ~ 24 kDa) and consequently reducing the rotational correlation time of the molecule. The improved resolution also offers the possibility of specific assignment of aliphatic resonances, although no effort has yet been made in this direction. A number of cross-peaks have, however, been assigned to specific amino acid types with the aid of RCT spectra, as indicated in Figure 8-10.

Nevertheless, the correlation observed between the COSY spectrum of the isolated C-domain and that of native PGK indicates that the environments of Tyr 193, Phe 289, Trp 308, Phe 342, Tyr 380, an unidentified Phe side-chain and a number of aliphatic groups are similar in both cases (*i.e.* there are regions of structural similarity between the free C-domain and the C-domain in the entire protein).

In total, cross-peaks due to 10 out of 12 Phe, both Tyr and 1 out of 2 Trp side-chains have been identified in the aromatic region of the COSY spectrum of the isolated C-domain. A summary of the side-chain specific assignments in the aromatic region is given in Table 8-1.

8.3.2.4. NOESY spectrum of the C-domain

Further evidence for regions of structural similarity between the isolated C-domain and the C-domain of intact PGK is found by comparing the NOESY spectra of the two proteins. In particular, the NOE connectivities previously observed between Phe 289 and Phe 342 in the NOESY spectrum of native PGK (§ 2.3.2) are also seen for the isolated C-domain (Figure 8-11) showing that this region of the protein, which is close to the adenine binding site

Figure 8-10: Methyl region of the 600 MHz COSY spectrum of the isolated C-terminal domain (1.9 mM, 0.10 M Na d_3-acetate, pH 6.63, 27 °C). The upfield region of the corresponding 1D spectrum is also shown.

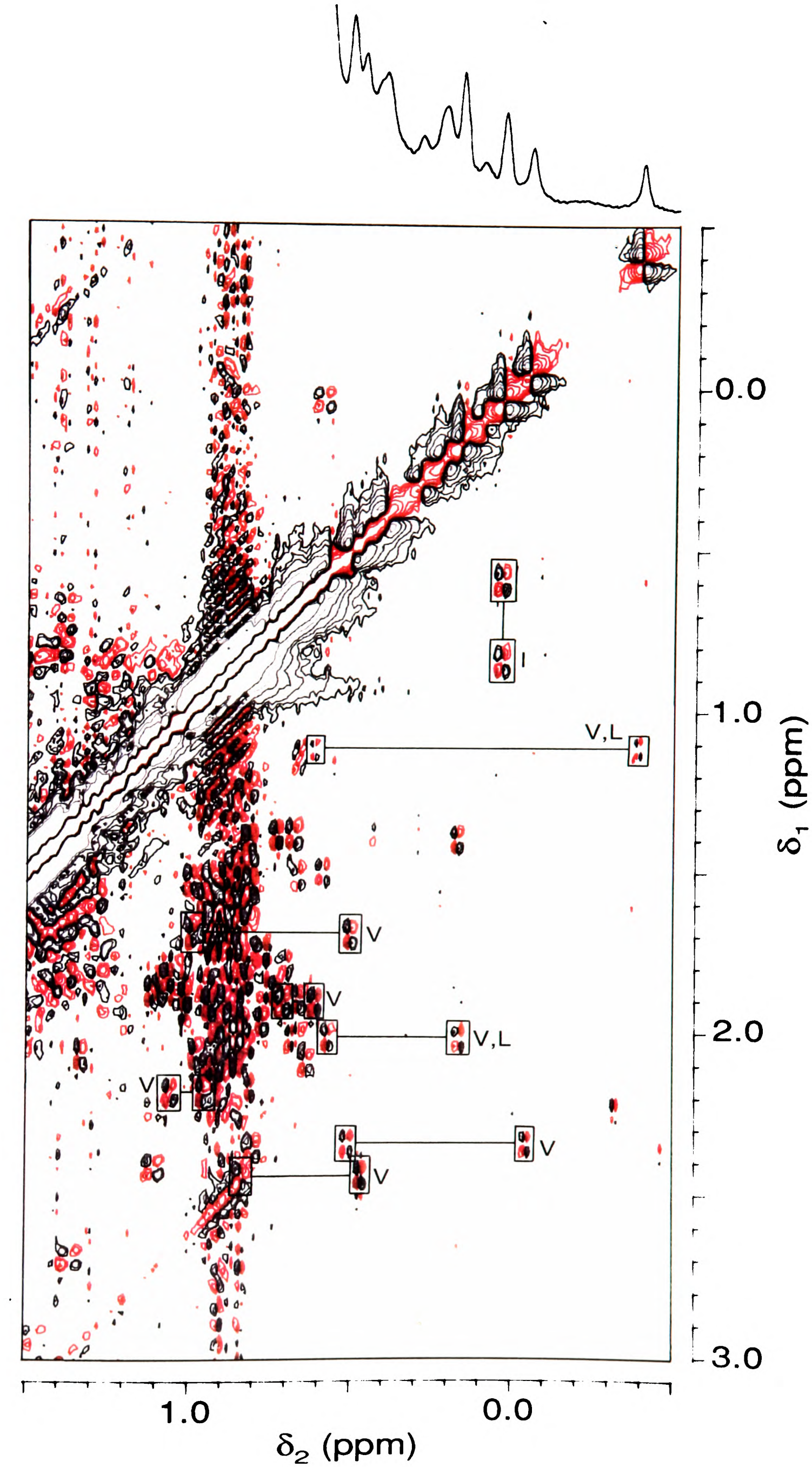

Figure 8-10

Table 8-1: Side-chain specific assignments of observable aromatic resonances in the ^1H NMR spectrum of the isolated C-domain.

pH = 6.6, 0.10 M Na d_3-acetate/D_2O, T = 300 K.

The meta proton resonances for Phe side-chains are indicated (m) where known. Numbers in parentheses are the chemical shifts of corresponding resonances in the ^1H NMR spectrum of whole PGK at pH 7.1 (*c.f.* Table 2-2). The chemical shifts of Phe D and Phe E are not coincident in the presence of Mg.ATP (data not shown).

Amino acid type	Chemical shift of ring protons (ppm)			Assignment
Phe A	6.61 (m)(6.59),	6.91 (6.88),	7.06 (7.04)	Phe 342
Phe B	6.62 (m)(6.55),	6.93,	7.30 (7.32)	
Phe C	6.76,	6.90		
Phe D	6.78,	7.08		
Phe E	6.78,	7.22		
Phe F	6.81,	7.04 (m),	7.20	
Phe G	6.92,	7.08 (m),	7.37	
Phe H	7.05,	7.28		
Phe I	7.10 (m),	7.24,	7.34	
Phe J	7.19 (7.17),	7.33 (7.30)		Phe 289
Tyr A	6.70 (6.73),	6.87 (6.86)		Tyr 193
Tyr B	6.71 (6.69),	7.29 (7.33)		Tyr 380
Trp A	6.85,	6.91 (6.88),	7.46 (7.46)	Trp 308
His A	7.11,	8.22 (7.58)		His 388

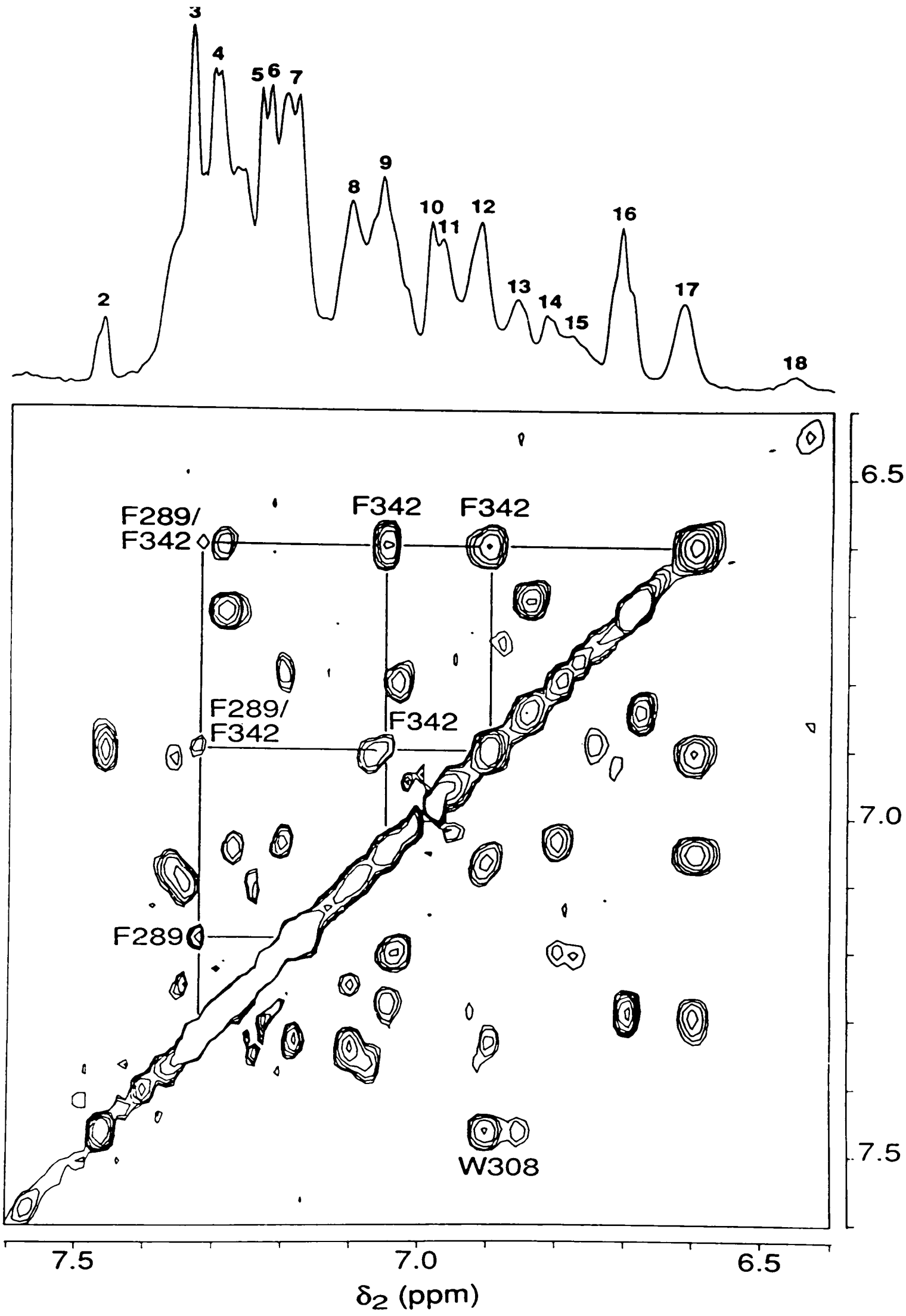

Figure 8-11: Aromatic region of the 600 MHz NOESY spectrum of the isolated C-terminal domain (2.2 mM, 0.10 M Na d_3-acetate, pH 7.11, 27 °C). The mixing time was 150 ms. Intra- and inter-residue NOE connectivities of Phe 289 and Phe 342 are labelled.

(Watson *et al.*, 1982; see also Chapter 6), is not greatly perturbed by the absence of the N-terminal domain.

A weak NOE cross-peak is observed between the resonance at 7.46 ppm (which is tentatively assigned to Trp 308; Scheffler & Cohn, 1986; § 2.3.2) and a peak at 6.85 ppm. Confirmation of the assignment to a Trp residue has been gained from RCT experiments (Figure 8-8) in which a weak RCT peak is observed between 7.46 ppm and 6.85 ppm, in addition to the COSY peak between 7.46 ppm and 6.91 ppm. Experiments using native PGK in which all the Phe rings are deuterated (§ 2.3.1) have clearly shown that the peak at 7.46 ppm is not due to a Phe side-chain. Observation of the RCT peak can therefore only be interpreted if the resonances at 7.46 ppm (peak 2), 6.91 ppm and 6.85 ppm are assigned to a Trp side-chain. The multiplicity of peak 2 was found to be even from 1D Hahn echo experiments, indicating that it is due to either the C4-H or the C7-H of the Trp indole ring.

8.3.2.5. Mg.ATP binding

A titration of the C-terminal domain with Mg.ATP at pH 7.1 was monitored using 500 MHz ^{1}H NMR spectroscopy (Figure 8-12). The addition of nucleotide results in changes throughout the spectrum. Changes in chemical shift position are most clearly observed in the upfield -CH_3 region (Figure 8-12B), the downfield α-CH region (Figure 8-12A) and the amide region (Figure 8-12A). Such shifts arise from changes in the chemical environment of these groups, most frequently due to their reorientation with respect to neighbouring aromatic and/or carbonyl moieties. Of course, the binding of Mg.ATP to the C-domain is expected to affect protons in the immediate vicinity of the binding site as a direct result of the aromatic and charged nature of the ligand. However, the large number of small shifts observed (particularly of back-bone α-CH and NH resonances) indicates extensive, though probably very small, conformational changes throughout the protein as a result of Mg.ATP binding.

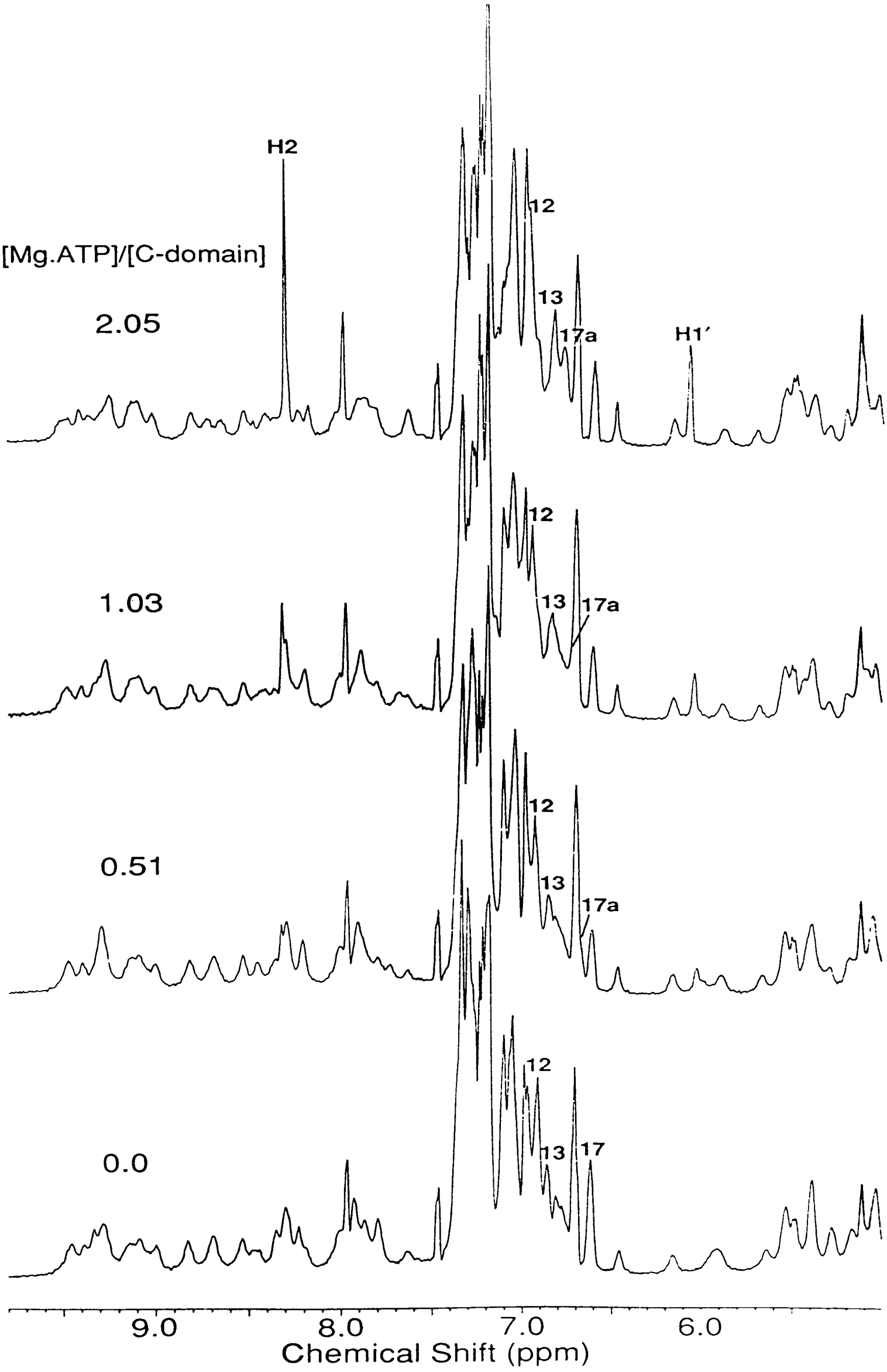

Figure 8-12A: Perturbations of the aromatic region of the 600 MHz ^{1}H NMR spectrum of the isolated C-terminal domain by Mg.ATP at the ratios indicated and pH 7.1.

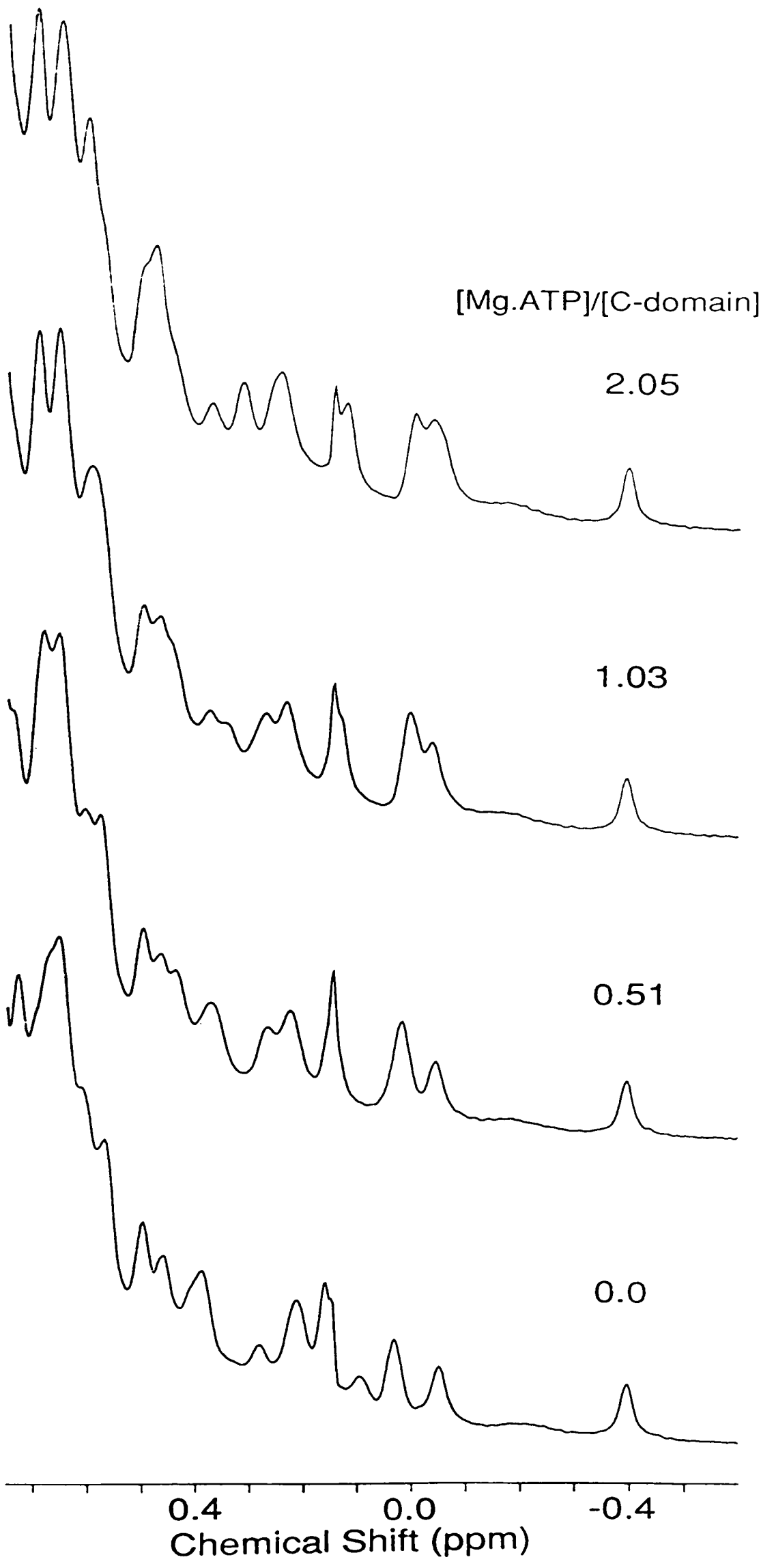

Figure 8-12B: Perturbations of the upfield methyl region of the 600 MHz ^{1}H NMR spectrum of the isolated C-terminal domain by Mg.ATP at the ratios indicated and pH 7.1.

The change in chemical shift of three aromatic resonances could be followed unambiguously in the 1D spectrum (Figure 8-12A) and are plotted in Figure 8-13. Two-dimensional ^{1}H NMR spectra of both 'free' and Mg.ATP bound C-terminal domain show that peak 13 is due to Tyr 193, peak 12 is due to Phe 342 and peak 17a to the unassigned Phe B (Figures 8-7, 8-8, 8-11 & 8-15). The shifts of these resonances were fitted to theoretical 1:1 binding curves, yielding a dissociation constant, $K_d = 0.35 \pm 0.05$ mM. This value is similar to that obtained in equilibrium dialysis experiments (0.33 mM; Minard *et al.*, 1989) and about 3 times that reported for the whole protein at ionic strength, I = 0.15 M (Scopes, 1978). Similar NMR experiments with native PGK resulted in a dissociation constant for Mg.ATP of ~ 0.15 mM (§ 6.3.2).

The shifts of the C2-H and C1′-H of the nucleotide (Figure 8-14) are consistent with a single binding site, in that they shift towards their 'free' positions with increasing [ATP]:[C-domain] ratio. The chemical shifts observed for these resonances are notably different from those seen on titrating Mg.ATP into a solution of PGK (*c.f.* Figure 6-9) indicating differences in the time averaged environments of the C2-H and C1′-H in the two systems. [Note that the C8-H resonance is in intermediate exchange and is therefore not observed].

8.3.2.6. NOESY spectrum of Mg.ATP bound C-domain

Some of the effects of Mg.ATP on aromatic resonances of the C-domain can be seen by comparing the NOESY spectra of the complexed (Figure 8-15) and uncomplexed (Figure 8-11) proteins. These include shifts of resonances due to Tyr 193, Phe 342 and the unassigned Phe B, as discussed above. The resonances of Phe 342 are affected in a very similar way following nucleotide binding to native PGK (§ 6.3.4). The resonances equivalent to Phe B in the spectrum of whole PGK are broadened by addition of Mg.ATP and, as a result, are not observed in the 2D spectra of the Mg.ATP.PGK complex

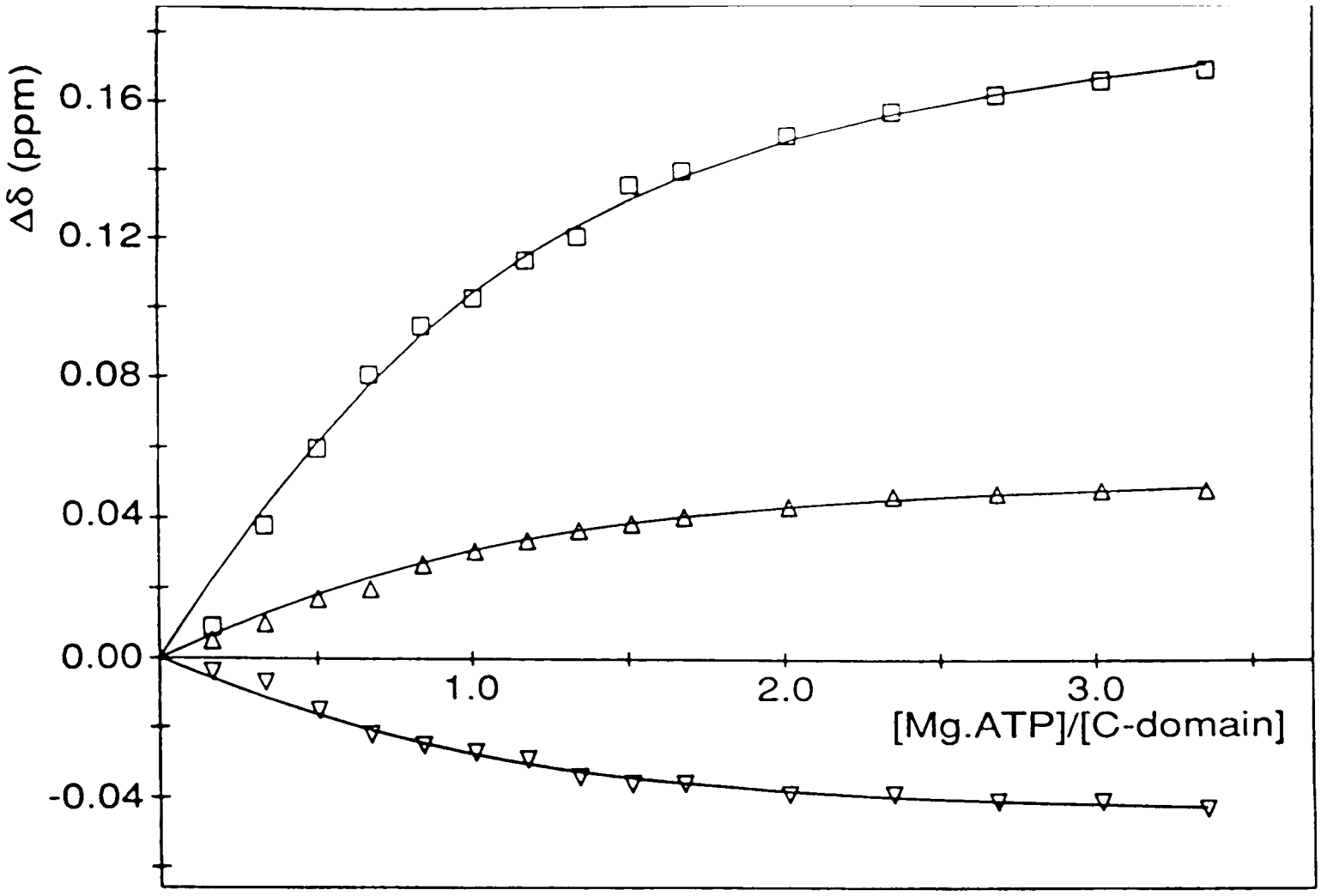

Figure 8-13: The change in the chemical shifts of peaks 12 (Δ), 13 (∇) and 17a (□) plotted as a function of Mg.ATP:protein molar ratio. The continuous lines represent theoretical binding curves corresponding to a dissociation constant, K_d = 0.35 mM.

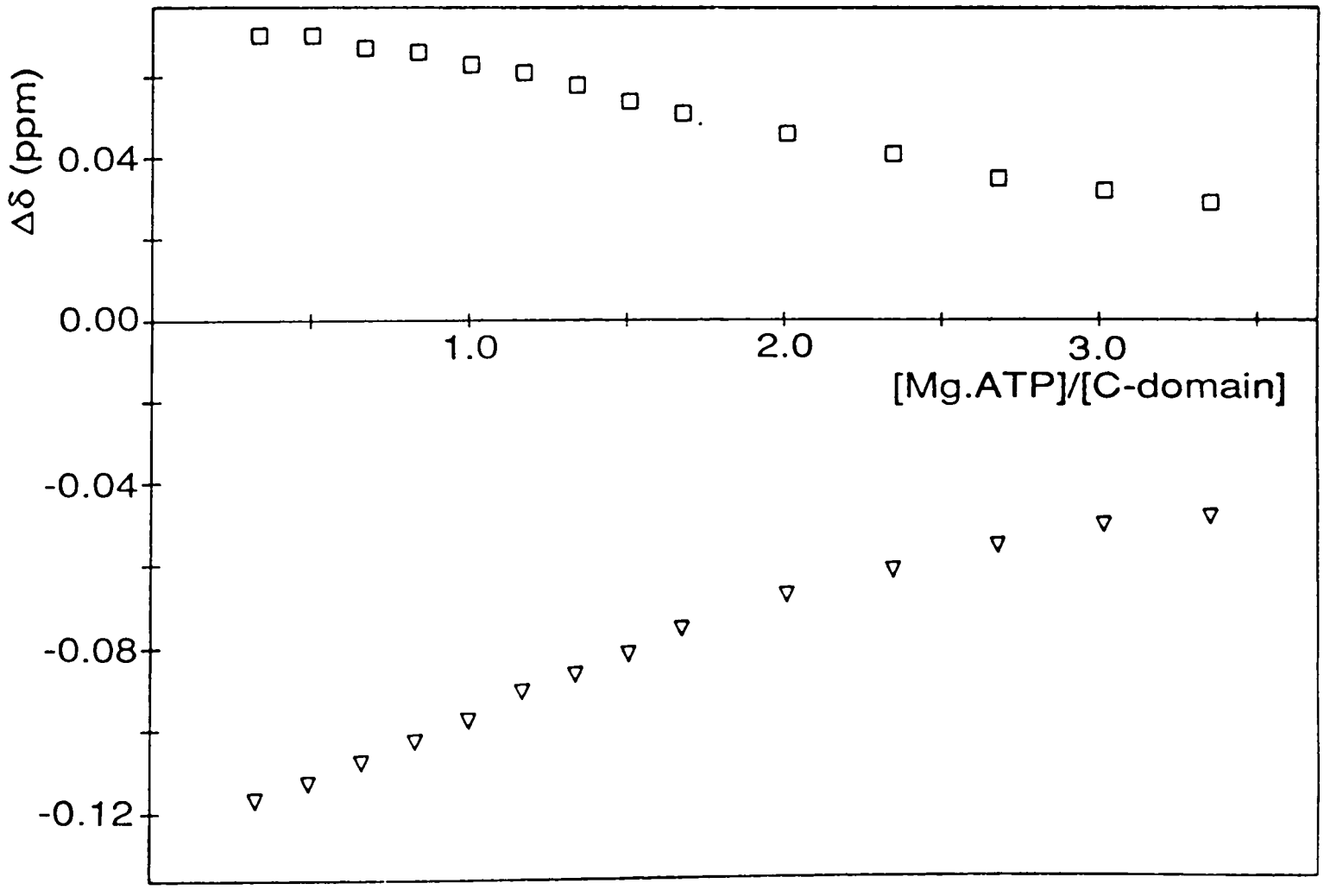

Figure 8-14: The change in the chemical shifts of the C2-H (□) and C1′-H (∇) resonances of ATP plotted as a function of Mg.ATP:protein molar ratio.

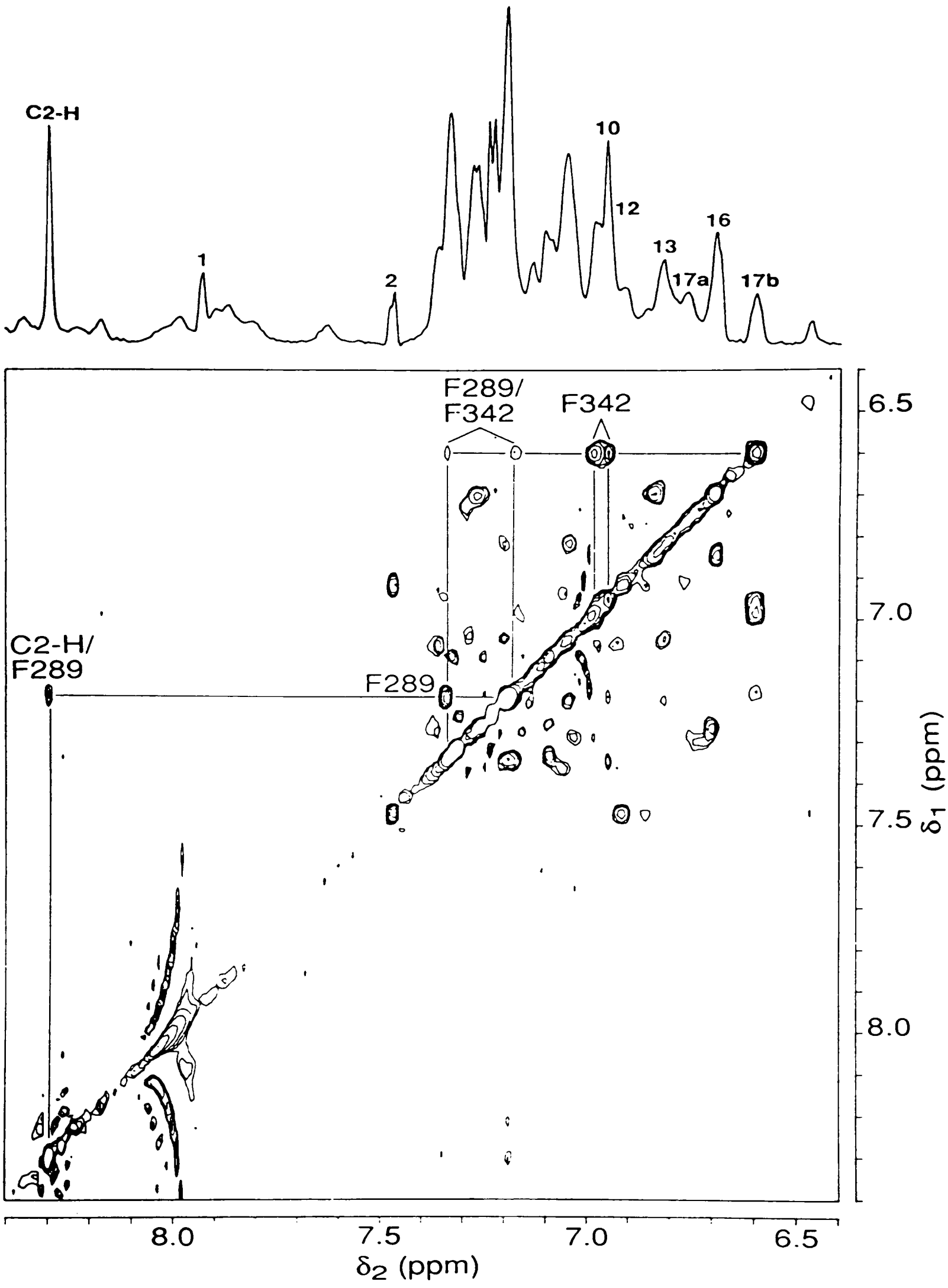

Figure 8-15: Aromatic region of the 600 MHz NOESY spectrum of the isolated C-terminal domain plus Mg.ATP (1.8 mM C-domain, 5.5 mM Mg.ATP, 0.10 M Na d_3-acetate, pH 7.1, 27 °C). Inter-molecular NOE connectivities between the C2-H resonance of ATP and Phe 289 and inter-residue NOE connectivities between Phe 289 and Phe 342 are labelled.

(although the most upfield peak, 15b′, is observed to shift downfield in 1D spectra). Other similarities between the NOESY spectra of nucleotide bound C-domain and entire PGK include the observation of inter-molecular NOE connectivities between the C2-H resonance of the adenine ring and Phe 289 (Figure 8-13) and aliphatic resonances thought to correspond to Leu 311 and Val 339 (Figure 8-16). It may also be significant that the peaks assigned to the indole ring of Trp 308 are unperturbed in both cases.

8.4. Discussion

^{1}H NMR spectroscopy provides direct evidence that the two domains of yeast PGK, obtained by site-directed mutagenesis (Minard *et al.*, 1989), are capable of independent folding. The C-domain is more stable with respect to amide H/D exchange than the N-domain suggesting that the conformational flexibility of the latter is greater.

While there is evidence for structural similarity between regions of the N-domain and folded PGK, it is clear that the 'basic patch' region, which forms part of the active site of native PGK (Watson *et al.*, 1982; Walker *et al.*, 1989) is perturbed (*i.e.* the environments of His 62, His 167 and His 170 have been altered as indicated by the fact that their chemical shifts are pH dependent in the isolated N-domain but independent of pH in intact PGK). This observation accounts for the fact that 3-PG does not bind to the isolated N-domain (this work and Minard *et al.*, 1989). Rearrangement of the 'basic patch' region probably comes about because the C-terminal end of PGK, which in the full protein folds back from the C-domain and packs against the N-domain, is absent (see Figure 8-1). Mas and Resplandor (1988) have recently reported that the C-terminal peptide is important for maintaining the structural integrity and function of PGK. Without the stabilising contribution of the C-terminal peptide (including α-helices XIII and XIV) it seems likely that the positively charged Arg side-chains 21, 38 and 168, of the 'basic

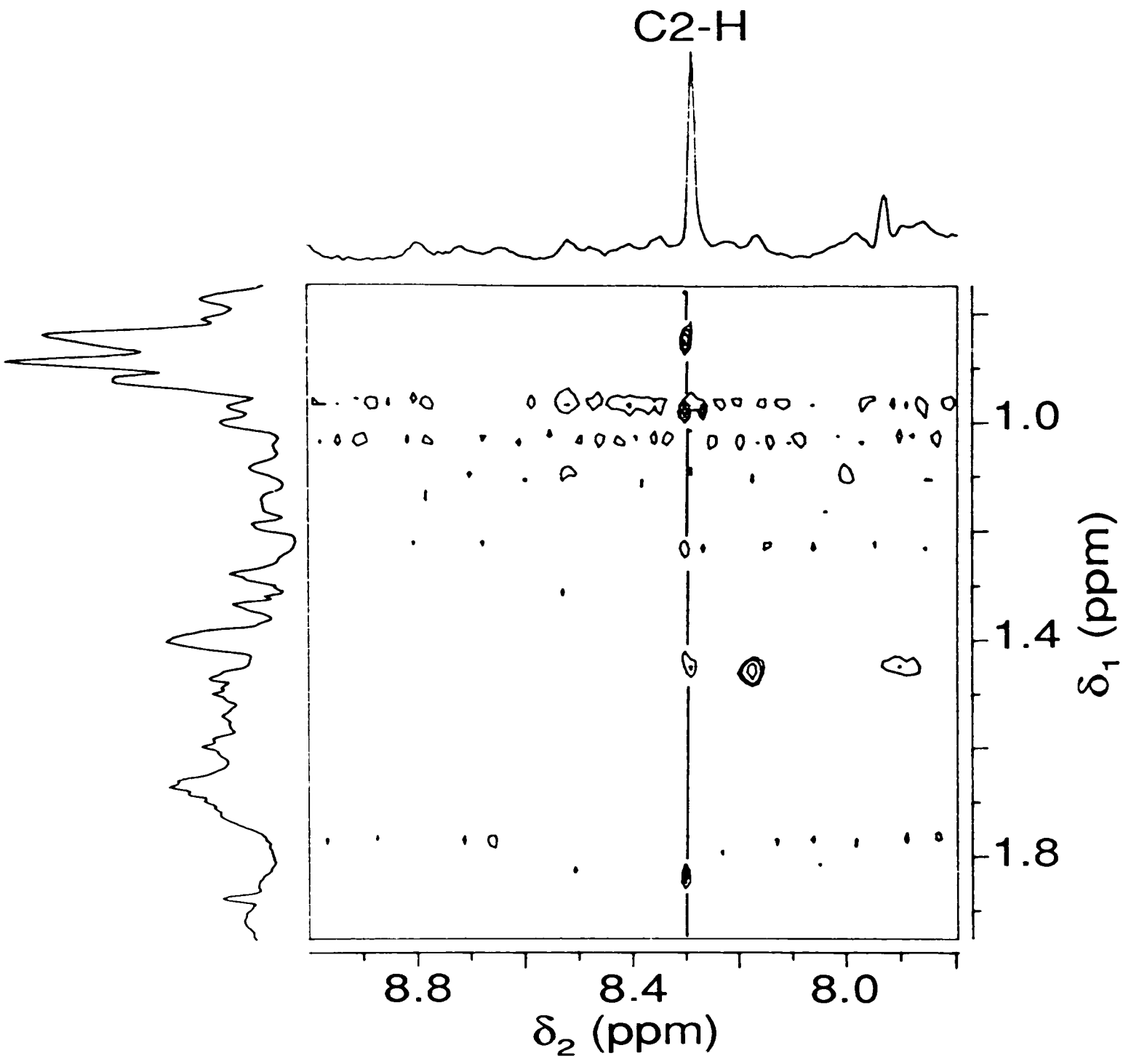

Figure 8-16: Region of the 600 MHz NOESY spectrum of the isolated C-terminal domain plus Mg.ATP (as in Figure 8-15) showing inter-molecular NOE connectivities between the C2-H resonance of the nucleotide and aliphatic resonances of the protein.

patch' will repel each other, thus altering the environments of neighbouring His residues 62, 167 and 170, as is observed. It is also possible that 3-PG binding to PGK requires interactions with the amino end of interdomain helix XIII (as in the crystallographic structure of Watson *et al.*, 1982), in addition to those identified in the 'basic patch' region.

The degree of correlation between the 2D ^{1}H NMR spectra of the C-domain and native PGK is high, suggesting that extensive regions of the isolated domain have a native-like structure. A significant exception to this is the environment of His 388. In the crystal structure this histidine residue appears to interact with Glu 190 (Watson *et al.*, 1982). Earlier NMR results suggest, however, that in solution His 388 may in fact be interacting with Lys 189 (§ 2.3.6). The pK_a of ~ 6.6 found for His 388 in the present study (Figure 8-6) indicates that in the isolated C-domain it is not interacting with any charged groups. The environment of His 388 in the isolated C-domain is, therefore, clearly modified with respect to the full protein. In view of the above, the observation that the environment of Tyr 193 in the isolated C-domain is similar to that found in native PGK is somewhat surprising. For Tyr 193 to be sufficiently close to His 388 to experience a field which is dependent on the protonation state of the histidine, and to have 'non-random' ring proton chemical shifts similar to those observed in the spectrum of the full protein, it is necessary to assume that at least residues 193-199 are folded in an α-helical conformation equivalent to the carboxy end of α-helix V. It is unlikely that the amino end of interdomain α–helix V (residues 186-190) is correctly folded since there are close contacts between this region and the N-domain in the full protein (*c.f.* NOEs observed between Phe 185 and Tyr 48; § 2.3.2).

Further evidence for regions of structural similarity between the C-domain and native PGK comes from the ability of the C-domain to bind Mg.ATP with an affinity only 3 times lower than that of the native protein. The results

from NOESY spectra provide direct evidence that the adenine of ATP binds to the same region of the C-domain as it does to native PGK.

The differences in chemical shift of the ATP C2-H and C1′-H resonances in the presence of the C-domain and native PGK, however, shows that the average environment experienced by the nucleotide is not exactly the same in each case. The results reported here and by Minard *et al.* (1989) indicate only one Mg.ATP binding site on the isolated C-domain, while two sites have been reported for native PGK (Scopes, 1978; Nageswara Rao *et al.*, 1978). ^{1}H NMR evidence (see Chapter 6) suggests that the second binding site involves interactions of the phosphate groups of ATP with the 'basic patch' region of the N-terminal domain. These interactions are dependent on both Mg^{2+} concentration and ionic strength. The absence of a secondary ATP binding site on the isolated C-domain would therefore account for different chemical shifts observed for the fast-exchanging ATP resonances.

The observation that Mg.ATP binding affinity to the C-domain is independent of ionic strength (Minard *et al.*, 1989) suggests that interactions between positively charged groups of the protein and the triphosphate chain of the nucleotide are unimportant. It therefore appears that removal of the N-domain has perturbed the region of the C-domain responsible for phosphate binding while leaving the adenine binding pocket intact. If the observed increase in the Mg.ATP dissociation constant, relative to native PGK, is due solely to the loss of interactions between the protein and the triphosphate chain then these interactions are only contributing about 2.2 kJ mol^{-1} (~ 10 %) to the free energy of binding of this substrate to PGK. It is also noted that the dissociation constant for Mg.ATP binding to the C-domain is about equal to the K_m for this substrate of PGK.

The above analysis shows that the C-domain of PGK is well folded and that it undergoes only minor changes on binding nucleotide. The phosphate binding site, however, is dependent on the presence of the N-domain. The

N-terminal domain is more flexible and destruction of the 'hinge region' by removal of the C-domain destroys the binding site for the substrate, 3-PG. Although both domains are capable of independent folding the 'hinge region' appears to be highly disordered in each case. Interactions between the folded (covalently linked) domains are therefore essential for formation of the active site. These interactions include extensive non-covalent contacts between the C-terminal peptide (including α-helices XIII and XIV) and the N-domain (see Figure 8-1). The N-terminal domain and the 'hinge region' are, therefore, not independent. This is in accord with NMR studies of the intact protein which showed that the so-called 'hinge movement' was linked to stretches of at least 3 helices (I, V and XIII) from both the N-domain and the interdomain region (Chapter 3). The possible role of the C-terminal α-helix XIV in domain movement has been discussed previously (Blake *et al.*, 1986; Mas & Resplandor, 1988). It is notable that the interdomain region is α-helical while the 'cores' of the two domains are largely β-sheets.

8.5. References

Adams, B., Burgess, R.J. & Pain, R.H. (1985) *Eur. J. Biochem. 152,* 715-720.

Aue, W.P., Bartholdi, E. & Ernst, R.R. (1976) *J. Chem. Phys. 64,* 2229-2246.

Banks, R.D., Blake, C.C.F., Evans, P.R., Haser, R., Rice, D.W., Hardy,G.W., Merrett, M. & Phillips, A.W. (1979) *Nature (Lond.) 279,* 773-777.

Betton, J.-M., Desmadril, M., Mitraki, A. & Yon, J.M. (1984) *Biochem. 23,* 6654-6661.

Betton, J.-M., Desmadril, M., Mitraki, A. & Yon, J.M. (1985) *Biochem. 24,* 4570-4577.

Blake, C.C.F. & Rice, D.W. (1981) *Phil. Trans. R. Soc. Lond. A. 293,* 93-104.

Blake, C.C.F., Rice, D.W. & Cohen, F.E. (1986) *Int. J. Pep. Protein Res. 27,* 443-448.

Burgess, R.J. & Pain, R.H. (1977) *Biochem. Soc. Trans. 5,* 692-694.

Dalgarno, D.C., Levine, B.A. & Williams, R.J.P. (1983) *Biosci. Reports 3,* 443-452.

Eich, G., Bodenhausen, G. & Ernst, R.R. (1982) *J. Am. Chem. Soc. 104,* 3731-3732.

Ghélis, C. & Yon, J.M. (1982) *Protein Folding,* Academic Press, New York.

Jeener, J., Meier, B.H., Bachmann, P. & Ernst, R.R. (1979) *J. Chem. Phys. 71,* 4546-4553.

King, G. & Wright, P.E. (1983) *J. Magn. Reson. 54,* 328-332.

Marion, D. & Wüthrich, K. (1983) *Biochem. Biophys. Res. Comm. 113,*

967-974.

Markley, J.L. (1975) *Acc. Chem. Res. 8,* 70-80.

Mas, M.T. & Resplandor, Z.E. (1988) *Proteins 4,* 56-62.

Minard, P., Hall, L., Betton, J.-M., Missiakas, D. & Yon, J.M. (1989) *Protein Eng.,* submitted for publication.

Mitraki, A., Betton, J.-M., Desmadril, M. & Yon, J.M. (1987) *Eur. J. Biochem. 163,* 29-34.

Nageswara Rao, B.D., Cohn, M. & Scopes, R.K. (1978) *J. Biol. Chem. 253,* 8056-8060.

Scheffler, J.E. & Cohn, M. (1986) *Biochem. 25,* 3788-3796.

Scopes, R.K. (1978) *Eur. J. Biochem. 91,* 119-129.

Walker, P.A., Littlechild, J.A., Hall, L. & Watson, H.C. (1989) *Eur. J. Biochem.,* in press.

Watson, H.C., Walker, N.P.C., Shaw, P.J., Bryant, T.N., Wendell, P.L., Fothergill, L.A., Perkins, R.E., Conroy, S.C., Dobson, M.J., Tuite, M.F., Kingsman, A.J. & Kingsman, S.M. (1982) *EMBO J. 1,* 1635-1640.

Wetlaufer, D.B. (1973) *Proc. Nat. Acad. Sci. USA, 70,* 697-701.

Wetlaufer, D.B. (1981) *Adv. Protein Chem. 34,* 61-92.

Wilson, H.A., Williams, R.J.P., Littlechild, J.A. & Watson, H.C. (1988) *Eur. J. Biochem. 170,* 529-538.

Chapter 9

CONCLUSIONS

9.1. Structural studies

Structural aspects of yeast PGK in solution have been investigated using three different approaches: (a) comparison of NMR parameters of native yeast PGK with the observed crystal structure, (b) investigation of the effects of site-specific mutations on the solution state NMR spectra and (c) investigation of the individual isolated domains as produced by site-specific mutagenesis.

For the purposes of this discussion the C-domain is defined as including residues 200-386 and does not include residues found in the interdomain region or the N-domain (see Figure 9-1). The interdomain region can be defined as including α-helix V (residues 185-199) and residues 387-405 (including β-sheet strand N and α-helix XIII). The N-domain includes residues 1-184 (as isolated using site-directed mutagenesis by Minard *et al.* (1989) and investigated in Chapter 8) and, in native PGK, the C-terminal peptide 406-415 (including α-helix XIV; see Figure 9-1).

In the preceding chapter it was demonstrated that the isolated C-terminal domain (residues 185-415 *i.e.* including the interdomain residues and the C-terminal peptide) has a native-like structure and is capable of binding ATP with an affinity comparable to that observed for the intact protein. This result is entirely consistent with the crystallographic observation that the C-terminal domain functions as a nucleotide binding domain. In addition, the NMR results indicate that the nucleotide binding site on the isolated C-terminal domain is the same as that observed crystallographically for the whole molecule. Thus the separation of this domain from the N-domain has little or no effect on the C-domain structure. The interdomain region, however, did not appear to be folded in the same way as in the native protein, as

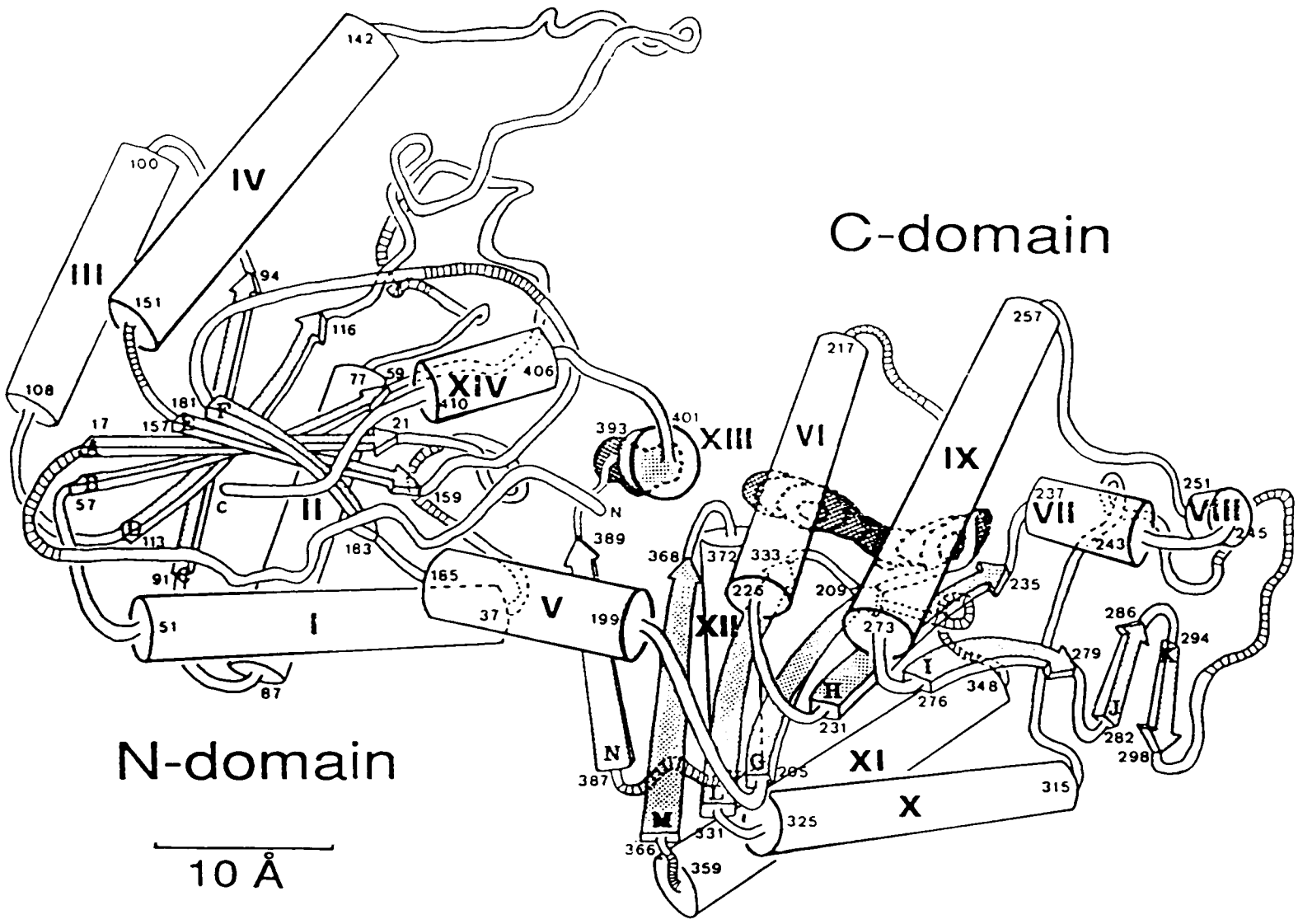

Figure 9-1: A schematic drawing of the crystal structure of yeast PGK. The α-helices are denoted by cylinders and the β-sheet strands by arrows. The crystallographically determined binding position for Mg.ATP is shown behind α-helices VI and IX, while that for 3-PG is behind helix XIII. (After Watson *et al.*, 1982).

indicated by the 'random coil' like pK_a of His 388.

In contrast to the C-domain, the second fragment investigated (residues 1-184) did not bind substrate (3-PG) indicating that the 3-PG binding site is intimately associated with the interdomain region. It is clear from the pH dependence of the NMR spectra that the environments of histidine residues 62 and 167, which form part of the 3-PG binding site in intact PGK, have been greatly perturbed. The most likely explanation for this observation is the absence of the C-terminal peptide (residues 406-415), which has extensive noncovalent interactions with the N-terminal domain and is covalently connected to interdomain α-helix XIII in native PGK (*c.f.* Mas & Resplandor, 1988). In regions remote from the 'basic patch' there are, however, structural similarities between the isolated N-terminal domain and intact PGK. Of the assigned residues His 52 and His 123 appear to be in similar environments in the two proteins.

It has also been found that the isolated C-domain is more stable with respect to amide H/D exchange than the N-domain peptide, indicating that the conformational flexibility of the N-domain may be greater than the C-domain.

1D and 2D ^{1}H NMR studies on intact native PGK have resulted in an increased number of specific assignments (*c.f.* Tables 2-2 & 2-3; Scheffler & Cohn, 1986; Wilson *et al.*, 1988), thus allowing a qualitative comparison to be made between the solution structure and the observed crystal structure of yeast PGK. In general, given that most assignments were made on the basis of correlations with the X-ray structure (with some being confirmed by the use of site-specific mutagenesis), it can be said that the NMR derived data are consistent with this structure. In particular chemical shift, NOE and pK_a data for resonances assigned to Tyr 48, His 52, His 53, His 123, His 149, His 170, Phe 185, Tyr 193, Phe 289, Phe 342 and Tyr 380 are consistent with their crystallographically determined environments.

Despite the generally observed similarity between the crystal and solution

structures a few significant differences are found in the time averaged environments of histidine residues in the 'basic patch' and the interdomain regions of the protein. While the pH dependence of the chemical shifts of resonances assigned to His 62 and His 167 are consistent with their positions relative to positively charged arginine residues 21, 38 and 168, the observation of an NOE connectivity from both histidines to a resonance at 1.26 ppm (see Table 4-3) cannot be accounted for using the crystal structure. The average conformation of this region of the protein in solution must therefore differ in some way from that of the X-ray crystal structure of Watson *et al.* (1982).

The pH dependence of peak 6, which was assigned to His 388 in the interdomain region, indicated that in solution this histidine interacts with positively charged Lys 189 rather than the acidic Glu 190 as deduced from the crystal structure. The crystallographically determined salt link was implicated as being important in controlling the proposed substrate induced conformational transition from the 'open' to the 'closed' form of the enzyme (Watson *et al.*, 1982). It was also proposed that these residues may mediate activation of the enzyme by sulphate and other anions (Watson *et al.*, 1982). The results of several site-directed mutagenesis studies in which Glu 190 and His 388 have been replaced (Wilson *et al.*, 1987; Mas *et al.*, 1987; Mas *et al.*, 1988) suggest that while the totally conserved residue (see Appendix 1) Glu 190 is essential for sulphate induced activation, the critical role cannot be ascribed to specific interactions with His 388. This conclusion is consistent with the above NMR finding that in solution His 388 does not interact with Glu 190. Since completing the earlier chapters of this thesis, NMR experiments have been carried out, in collaboration with Dr J.A. Littlechild (Department of Biochemistry, University of Bristol), on one of the above mutant enzymes in which His 388 has been replaced by a glutamine residue (H388Q; Wilson *et al.*, 1987). NMR spectra of this mutant form of

yeast PGK confirm the assignment of peak 6 to His 388, and also indicate that the mutation results in some relatively long-range conformational changes within the interdomain region. The mutant enzyme H388Q has a $k_{cat.}$ reduced by 5-fold relative to wild-type PGK, while the K_m for ATP is lowered by ~ 3-fold and the K_m for 3-PG is unaffected (Wilson *et al.*, 1987). It is likely that the conformational changes in the interdomain region induced by this substitution interfere with the efficiency of the substrate-induced conformational transitions and thereby reduce the catalytic activity of the enzyme without significantly perturbing substrate binding. Further experiments with the mutant enzyme are required to test this hypothesis.

The other site-directed mutant forms of yeast PGK investigated (Δ51-56, H62Q, R168K, R168M, H170D and D372N) appeared to undergo only small local changes in conformation as a result of the substitutions. Structural studies of the 'basic patch' mutants become more significant in the substrate bound states.

9.2. Ligand binding

Extensive ATP binding studies with wild-type yeast PGK show that, in solution, the adenine moiety binds to the same hydrophobic site on the surface of the C-terminal domain of the enzyme as observed by X-ray crystallographic studies (Watson *et al.*, 1982). Two binding sites were found for the phosphate groups of ATP. The primary phosphate binding site involves electrostatic interactions between the anionic groups and the positively charged arginine residues in the 'basic patch' region of the N-terminal domain (*i.e.* Arg 21, 38, 65 and 168). The second site is equivalent to the crystallographically determined catalytic site and presumably involves interactions between the triphosphate chain and conserved lysine residues 213 and 217, in addition to specific interactions between Mg^{2+} (when present) and Asp 372 (Watson & Gamblin, 1985). The affinity of ATP for the catalytic site, which involves both

hydrophobic (predominantly) and electrostatic interactions, is increased relative to the primary electrostatic site with increasing Mg^{2+} concentration.

Conformational changes resulting from ATP binding at either of the two sites were minor and localised, apart from a slight change observed in the interdomain region (as indicated by small changes in the chemical shifts of resonances assigned to Phe 185, Tyr 193 and His 388; see Table 9-1).

In contrast to the binding of ATP, the triose substrate, 3-PG, was found to bind to a single site in the 'basic patch' region of the N-terminal domain. Binding of 3-PG results in highly selective short- and long-range conformational changes in the N-domain and the interdomain region which are significantly greater in magnitude than those induced by ATP binding (Table 9-1).

The use of paramagnetic and diamagnetic anions has enabled the determination of a general anion binding site in the 'basic patch' region of the N-terminal domain. The site thus determined shares at least two residues which were shown to interact with 3-PG, namely His 62 and Arg 168, and is probably identical to the electrostatic binding site of ATP. Binding of anions other than 3-PG [*e.g.* $[Co(CN)_6]^{3-}$, $[Fe(CN)_6]^{3-}$, ATP^{4-} (this work); SO_4^{2-}, $[Fe(CN)_6]^{4-}$ (H.C. Graham, personal communication)] to the general anion binding site appear to cause only minor conformational changes (Table 9-1) which are localised within the binding area and the interdomain region (*i.e.* there are no detectable effects at remote histidines 52, 123 and 149, as observed on binding 3-PG). The effect of anions on the rate of reaction of the single cysteine of yeast PGK with 5,5′-dithiobis(2-nitrobenzoic acid) (Wrobel & Stinson, 1978) indicates, however, that significant delocalisation of anion induced conformational transitions may occur (Cys 97 is ~ 16 Å from His 62 and ~ 22 Å from Arg 168).

As with ATP binding the presence of a secondary general anion binding site has also been noted. It can be postulated that the primary anion site is

Table 9-1: Effects of ligand binding on the resonances of selected amino acids of yeast PGK.

\+ $0 < \Delta\delta \leq 0.04$ ppm

++ 0.04 ppm $< \Delta\delta <$ 0.10 ppm

+++ $\Delta\delta \geq 0.10$ ppm

	Ligand			
Residue	ATP^{4-}	$Mg.ATP^{2-}$	3-PG	$[Co(CN)_6]^{3-}$
Tyr 48	+	+	+	
His 52			++	
His 53			+	
His 62	++	+	+++	+
His 123			++	
His 149			++	
Phe 163			+++	
His 167	+	++	+++	++
His 170	++	+	+	+
Phe 185	+	+	+++	+
Tyr 193	+	+	++	
Phe 289	+	++		
Trp 308				
Phe 342	++	++		
Thr 375	+	+		
Tyr 380	+	+		
His 388	+	+	+++	
Phe J	+		+	+

responsible for the observed activatory effect of anions (including ATP^{4-}; Larsson-Raźnikiewicz & Schierbeck, 1977) at low concentrations (Larsson-Raźnikiewicz & Jansson, 1973; Scopes, 1978; Khamis & Larsson-Raźnikiewicz, 1981) while the secondary anion binding site leads to inhibition at higher concentrations.

Induction of the longer range conformational changes are very specific to the triose substrate, 3-PG. That these changes are closely related to activity is illustrated by the fact that the analogue 2-hydroxy-4-phosphonobutanoic acid acts as a relatively efficient substrate (Orr & Knowles, 1974) but 2-hydroxy-4-arsonobutanoic acid does not (Adams *et al.*, 1983). Both substrate analogues have binding affinities comparable with 3-PG. The maximum displacement of the phosphonate oxygens and the arsonate oxygens relative to the corresponding phosphoryl oxygens of 3-PG are ~ 0.3 Å and ~ 0.6 Å respectively (Kamiya *et al.*, 1983). In addition the mutation of 'basic patch' Arg 168 to either a lysine (R168K) or a methionine (R168M) residue was shown to prevent the 3-PG induced conformational changes. In the case of R168K the positive charge of the side-chain at position 168 was only displaced by ~ 1 Å, and did not significantly effect the binding affinity for 3-PG. A critical role can thus be attributed to the totally conserved (see Appendix 1) residue Arg 168 in propagating the 3-PG induced conformational changes.

The other 'basic patch' mutant enzymes investigated (H62Q and H170D) underwent the same conformational transitions on binding 3-PG as the wild-type enzyme. Results with wild-type PGK indicate that the triose substrate interacts with the 'basic patch' histidines in the order 62 >167 >> 170. It is possible that Gln 62 in mutant H62Q functions in an analogous way to His 62 in the wild-type protein. The fact that mutation of His 170 to an Asp has little effect on the propagation of the 3-PG induced conformational changes or the enzymatic activity (Fairbrother *et al.*, 1989) confirms that this

residue is of little importance in substrate binding or catalysis.

The effects of 3-PG binding on the ^{1}H NMR spectrum of mutant Δ51-56 are also very similar to those observed for the wild-type enzyme. The dissociation constant for 3-PG binding to this mutant has also been determined and was found to be similar to that of wild-type PGK (K_d = 0.014 mM compared to 0.011 mM for wild-type PGK). These results indicate that the transmission of conformational effects from the triose binding site is not dependent on the composition of the loop which joins α-helix I with β-strand B.

The conformational change induced by 3-PG binding deviates from the rigid-body motion of the domains assumed in the simple 'hinge-bending' models of Pickover *et al.* (1979), Blake *et al.* (1986) and Ptitsyn *et al.* (1986), as indicated by effects observed at His 52, 123 and 149 remote from both the substrate binding site and the interdomain region (*i.e.* there appears to be an interdependence of movements in the interdomain region and within the N-domain on binding 3-PG). There is little or no movement, however, of the cores of the two domains which are held by β-sheets.

As pointed out by Mas and Resplandor (1988), the most suitable existing model to describe the mechanism of domain movement in PGK is the *helix interface shear* mechanism (Lesk & Chothia, 1984). This model involves the cumulative effects of small shifts and rotations at the interfaces between packed helices within and between the two domains, which are accommodated by small conformational changes in the side-chains. Conformational changes in proteins involving the relative motions of packed α-helices have been demonstrated in a number of other cases (Table 9-2). A detailed analysis of insulin, in which different high resolution (~ 1.5 Å) and well-refined crystal structures were compared, has led to the suggestion of several general principles for the relative motions of packed helices (Chothia *et al.*, 1983). (a) The backbones of helices tend to move as rigid rods during conformational changes. Conformational changes within helices, when they do occur, tend to

Table 9-2: Proteins in which conformational changes involving the relative reorientations of packed α-helices have been described.

Protein	Reference
Adenylate kinase	Sachsenheimer & Schulz, 1977
Alcohol dehydrogenase	Lesk & Chothia, 1984
Calmodulin	Levine *et al.*, 1983
Citrate synthase	Lesk & Chothia, 1984
Haemoglobin	Baldwin & Chothia, 1979
Hexokinase	Lesk & Chothia, 1984
Insulin	Chothia *et al.*, 1983

be localised rather than spread out *i.e.* helices 'kink' rather than bend smoothly. (b) The small relative displacements of packed helices (up to ~ 1.5 Å) are readily accommodated by small adjustments in torsion angles (up to ~ 15°) without the repacking of interfaces. (c) Such low energy adjustments can accommodate shifts of up to no more than ~ 1.5 Å, which limits the extent to which conformational changes can be dissipated locally and causes their transmission over longer distances.

In the case of PGK the conformational transitions induced by 3-PG binding involve mutual reorientations of, at least, helices V and XIII in the interdomain region and helix I in the N-terminal domain, but do not appear to be communicated to the C-terminal domain. It is apparent from this and previous (Wilson *et al.*, 1988) studies that PGK is mobile in certain regions. The protein does not adopt a single conformation in solution but rather fluctuates between a range of conformations, including several 'open' or substrate binding forms and a 'closed' and supposedly catalytically competent form. The position of the conformational equilibrium is affected by several anions including the substrates and their analogues. The largest and most specific effects are observed for triose substrate (3-PG) binding. It may well be that the 'open' form of the enzyme, which is predominant when no substrates are bound, is held open by electrostatic repulsions. Any neutralisation of the positive charge, by adding anions, including substrates, then brings about some reorientation. The spatial charge-charge complementarity between 3-PG and the 'basic patch' region of the protein results not only in the largest conformational readjustments but specific changes which allow phosphoryl transfer. These involve at least three helices, including those in the interdomain ('hinge') region, allowing the domains to move together and thus generate the active site when both substrates are bound.

9.3. References

Adams, S.R., Sparkes, M.J. & Dixon, H.B.F. (1983) *Biochem. J. 213,* 211-215.

Baldwin, J. & Chothia, C.J. (1979) *J. Mol. Biol. 129,* 175-220.

Blake, C.C.F., Rice, D.W. & Cohen, F.E. (1986) *Int. J. Peptide Protein Res. 27,* 443-448.

Chothia, C., Lesk, A.M., Dodson, G.G. & Hodgkin, D.C. (1983) *Nature (Lond.) 302,* 500-505.

Fairbrother, W.J., Walker, P.A., Minard, P., Littlechild, J.A., Watson, H.C. & Williams, R.J.P. (1989) *Eur. J. Biochem.,* in press.

Kamiya, K., Cruse, W.B.T. & Kennard, O. (1983) *Biochem. J. 213,* 217-223.

Khamis, M.M. & Larsson-Raźnikiewicz, M. (1981) *Biochim. Biophys. Acta 657,* 190-194.

Larsson-Raźnikiewicz, M. & Jansson, J.R. (1973) *FEBS Lett. 29,* 345-347.

Larsson-Raźnikiewicz, M. & Schierbeck, B. (1977) *Biochim. Biophys. Acta 481,* 283-287.

Lesk, A.M. & Chothia, C. (1984) *J Mol. Biol. 174,* 175-191.

Levine, B.A., Dalgarno, D.C., Esnouf, M.P., Klevitt, R.E., Scott, G.M.M. & Williams, R.J.P. (1983) in *Mobility and Function in Proteins and Nucleic Acids* (Ciba Foundation Symp. 93) pp. 72-90, Pitman, London.

Mas, M.T., Resplandor, Z.E. & Riggs, A.D. (1987) *Biochem. 26,* 5369-5377.

Mas, M.T., Bailey, J.M. & Resplandor, Z.E. (1988) *Biochem. 27,* 1168-1172.

Mas, M.T. & Resplandor. Z.E. (1988) *Proteins 4,* 56-62.

Minard, P., Hall, L., Betton, J.-M., Missiakas, D. & Yon, J.M. (1989) *Protein Eng. 3,* in press.

Orr, G.A. & Knowles, J.R. (1974) *Biochem. J. 141,* 721-723.

Pickover, C.A., McKay, D.B., Engelman, D.M. & Steitz, T.A. (1979) *J. Biol. Chem. 254,* 11323-11329.

Ptitsyn, O.B., Pavlov, M.Y., Sinev, M.A. & Timchenko, A.A. (1986) in *Multidomain Proteins,* (Patthy, L. & Friedrich, P. eds) pp. 9-25, Akadémiai Kiadó, Budapest.

Sachsenheimer, W. & Schulz, G.E. (1977) *J. Mol. Biol. 114,* 23-36.

Scheffler, J.E. & Cohn, M. (1986) *Biochem. 25,* 3788-3796.

Scopes, R.K. (1978) *Eur. J. Biochem. 85,* 503-516.

Wilson, C.A.B., Hardman, N., Fothergill-Gilmore, L.A., Gamblin, S.J. & Watson, H.C. (1987) *Biochem. J. 241,* 609-614.

Wilson, H.R., Williams, R.J.P., Littlechild, J.A. & Watson, H.C. (1988) *Eur. J. Biochem. 170,* 529-538.

Watson, H.C., Walker, N.P.C., Shaw, P.J., Bryant, T.N., Wendell, P.L., Fothergill, L.A., Perkins, R.E., Conroy, S.C., Dobson, M.J., Tuite, M.F., Kingsman, A.J. & Kingsman, S.M. (1982) *EMBO J. 1,* 1635-1640.

Watson, H.C. & Gamblin, S.J. (1985) *Proc. Int. Symp. Biomol. Struct. Interactions, Suppl. J. Biosci. 8,* 499-506.

Wrobel, J.A. & Stinson, R.A. (1978) *Eur. J. Biochem. 85,* 345-350.

Appendix 1

AMINO ACID SEQUENCE OF YEAST PGK

The amino acid sequence of yeast PGK (Watson *et al.*, 1982). Residues forming helices (***), parallel (+++) and anti-parallel (+-+) β-sheets and β-turns(^^^) are indicated. The helices and β-sheets are labelled according to Figure 1-1. Bold, underlined residues are totally conserved in the PGK sequences of horse (Merrett, 1981), human (Michelson *et al.*, 1983), *Trypanosoma brucei* (B & C; Osinga *et al.*, 1985), mouse (Mori *et al.*, 1986), *Aspergillus nidulans* (Clements & Roberts, 1986), *Thermus thermophilus* (Bowen *et al.*, 1988), *Zymomonus mobilis* (Conway & Ingram, 1988), *Crithidia fasciculata* (Swinkels *et al.*, 1988), *Penicillium chrysogenum* (van Solingen *et al.*, 1988), *Bacillus stearothermophilus* (Davies *et al.*, 1989) and *Escherichia coli* (Alexander & Perham, 1989).

```
1                   10                  20                  30                  40
                                        A
                    ^ ^ ^ ^ + + + + +                   ^ ^ ^ ^         * * * *
SLSSKLSVQDLDLKDKRVFIRVDFNVPLDGKKITSNQRIV

41                  50                  60                  70                  80
      I                                 B
* * * * * * * * * * * *               + + +                 ^ ^ ^ ^         * * * *
AALPTIKYVLEHHPRYVVLASHLGRPNGERNEKYSLAPVA

81                  90                  100                 110                 120
  II                        C                   III                 D
* * * * * * *         + + + +         * * * * * * * * *           + + + +
KELQSLLGKDVTFLNDCVGPEVEAAVKASAPGSVILLENL

121                 130                 140                 150                 160
                                                    IV                      E
                                        * * * * * * * * * * ^ ^ ^           + + +
RYHIEEEGSRKVDGQKVKASKEDVQKFRHELSSLADVYIN

161                 170                 180                 190                 200
                                            F                   V
                    ^ ^ ^ ^               + + +   * * * * * * * * * * * * * * * *
DAFGTAHRAHSSMVGFDLPQRAAGFLLEKELKYFGKALEN
```

```
201                 210                 220                 230                 240
                  G                   VI                  H                  VII
          + + + + +         ^ ^ ^ * * * * * * * * * *         + + + + +   * * * *
PTRPFLAILGGGAKVADKIQLIDNLLDKVDSIIIGGGMAFT

241                 250                 260                 270                 280
                VIII                                    IX                   I
* * *   * * * * * * *         * * * * * * * * * * * * * * * * *     + + + +
FKKVLENTEIGDSIFDKAGAEIVPKLMEKAKAKGVEVVLP

281                 290                 300                 310                 320
      J                             K                                         X
  + - + - +                 + - + - +         ^ ^ ^ ^ ^ ^ ^         * * * * * *
VDFIIADAFSADANTKTVTDKEGIPAGWQGLDNGPESRKL

321                 330                 340                 350                 360
                      L                                       XI
* * * * *           + + +         ^ ^ ^ ^ ^ ^ ^     * * * * * * * * * * * * ^
FAATVAKAKTIVWNGPPGVFEFEKFAAGTKALLDEVVKSS

361                 370                 380                 390                 400
            M                   XII                 N                  XIII
^ ^       + + +       * * * * * * * * *   ^ ^ ^ ^     + + +       * * * * * * * *
AAGNTVIIGGGDTATVAKKYGVTDKISHVSTGGGASLELL

401                 410
                  XIV
*           * * * * * *
EGKELPGVAFLSEKK
```

Amino acid composition:

Ala, A	43	Gly, G	37	Pro, P	17
Arg, R	13	His, H	8	Ser, S	27
Asn, N	14	Ile, I	23	Thr, T	18
Asp, D	25	Leu, L	41	Trp, W	2
Cys, C	1	Lys, K	42	Tyr, Y	7
Glu, E	29	Met, M	3	Val, V	38
Gln, Q	8	Phe, F	19		
				Total	415

References:

Alexander, P.R. & Perham, R.N. (1989) *Mol. Microbiol.*, in press.

Bowen, D., Littlechild, J.A., Fothergill, J.E., Watson, H.C. & Hall, L. (1988) *Biochem. J. 254,* 509-517.

Clements, J.M. & Roberts, C.F. (1986) *Gene 44,* 97-105.

Conway, T. & Ingram, L.O. (1988) *J. Bacteriol. 170,* 1926-1933.

Davies, G.J., Watson, H.C. & Hall, L. (1989) in preparation.

Merrett, M. (1981) *J. Biol. Chem. 256,* 10293-10305.

Michelson, A.M., Markham, A.F. & Orkin, S.H. (1983) *Proc. Natl. Acad. Sci. USA 80,* 472-476.

Mori, N., Singer-Sam, J. & Riggs, A.D. (1986) *FEBS Lett. 204,* 313-317.

Osinga, K.A., Swinkels, B.W., Gibson, W.C., Borst, P., Veeneman, G.H., van Boom, J.H., Michels, P.A.M. & Opperdoes, F.R. (1985) *EMBO J. 4,* 3811-3817.

Swinkels, B.W., Evers, R. & Borst, P. (1988) *EMBO J. 7,* 1159-1165.

Watson, H.C., Walker, N.P.C., Shaw, P.J., Bryant, T.N., Wendell, P.L., Fothergill, L.A., Perkins, R.E., Conroy, S.C., Dobson, M.J., Tuite, M.F., Kingsman, A.J. & Kingsman, S.M. (1982) *EMBO J. 1,* 1635-1640.

van Solingen, P., Muurling, H., Koekman, B. & van den Berg, J. (1988) *Nucleic Acid Res. 16,* 11823.

Appendix 2

K_d CALCULATION FROM CHANGE IN CHEMICAL SHIFT

For a 1:1 ligand/enzyme interaction,

$$E + S \rightleftharpoons ES,$$

the dissociation constant K_d is given by

$$K_d = \frac{[E].[S]}{[ES]}$$

$$= \frac{([E]_i - [ES])([S]_i - [ES])}{[ES]} \qquad \textbf{(A2-1)}$$

where $[E]_i$ and $[S]_i$ are the total concentrations of enzyme and substrate (ligand) present, respectively, and [E], [S] and [ES] are the equilibrium concentrations of enzyme, substrate (ligand) and 1:1 complex respectively.

The ratio of substrate to enzyme concentration is given by,

$$\frac{[S]_i}{[E]_i} = R_i = \frac{[S]_a.V_i}{[E]_0.V_0} \qquad \textbf{(A2-2)}$$

$$\text{where} \quad [S]_i = \frac{[S]_a.V_i}{V_0 + V_i.} \qquad \textbf{(A2-3)}$$

and $[S]_a$ = concentration of added substrate (ligand)

V_i = volume of substrate solution added

V_0 = initial volume of enzyme solution

$[E]_0$ = initial concentration of enzyme solution

It is assumed that

$$\frac{\Delta\delta_i}{\Delta\delta_{max}} = \frac{[ES]}{[E]_i} \qquad \textbf{(A2-4)}$$

where $\Delta\delta_i$ is the change in chemical shift and $\Delta\delta_{max}$ is the maximum change at saturating amounts of substrate (ligand).

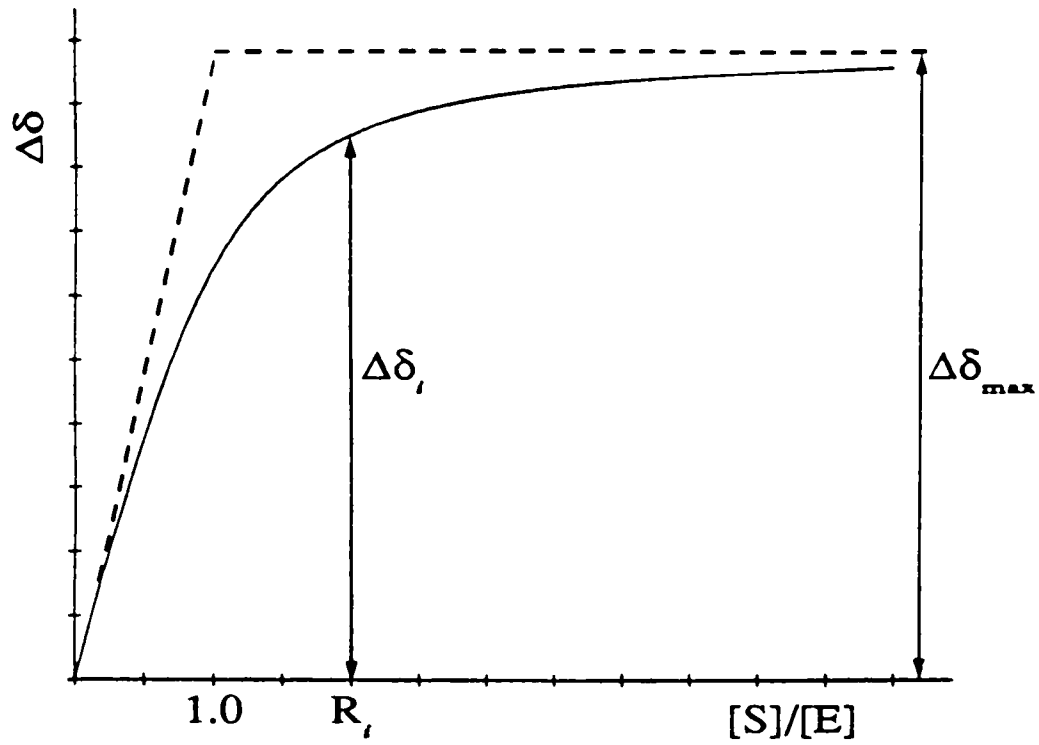

(A2-1) $\Rightarrow$ $0 = [ES]^2 - ([E]_i + K_d + [S]_i)[ES] + [E]_i.[S]_i$

$$\Rightarrow [ES] = \frac{([E]_i + K_d + [S]_i) \pm \{([E]_i + K_d + [S]_i)^2 - 4.[E]_i.[S]_i\}^{1/2}}{2}$$

(A2-4) $\Rightarrow$ $[ES] = \frac{\Delta\delta_i}{\Delta\delta_{max}} [E]_i$

$$\therefore \Delta\delta_i = \frac{\Delta\delta_{max}}{2[E]_i}[([E]_i + K_d + [S]_i) \pm \{([E]_i + K_d + [S]_i)^2 + 4.[E]_i.[S]_i\}^{1/2}$$

rearranging and combining with **(A2-2)** gives,

$$\Delta\delta_i = \frac{\Delta\delta_{max}}{2}\left[\left(1 + \frac{K_d.R_i}{[S]_i} + R_i\right) - \left\{\left(1 + \frac{K_d.R_i}{[S]_i} + R_i\right)^2 - 4.R_i\right\}^{1/2}\right]$$

Using $\Delta\delta_i$ versus V_i as input to a non-linear regression routine (NAG routine E04FDF; NAG Library, 1987) this equation can be fitted to give K_d, $\Delta\delta_{max}$ and $[E]_0$.

References:

NAG Library (1987) *The NAG Fortran Library Manual-Mark 12*, Numerical Algorithms Group.

Appendix 3

RELAXATION AND SHIFT PROBES

The magnetic moment of an unpaired electron is ~ 10^3 times greater than that of a nucleus. Since fluctuation of local fields leads to relaxation, the larger fields resulting from the presence of a paramagnetic species gives rise to very efficient nuclear spin relaxation provided their electron spin relaxation is not too fast (see below). The strong local fields produced by an unpaired electron can be coupled to the nuclei by dipole-dipole interactions or (more rarely) by scalar coupling via a chemical bond. For a nucleus bound near a paramagnetic centre the relaxation times can be represented by the Solomon-Bloembergen equations (Solomon, 1955; Bloembergen, 1957). In this study the line-widths and hence the transverse relaxation times (T_2) are of interest:

$$\frac{1}{T_{2,M}} = \frac{1}{20}\frac{\mu_o^2}{(4\pi)^2}\frac{\gamma_I^2 g^2 S(S+1)\beta^2}{r^6}\left(4\tau_c + \frac{3\tau_c}{1+\omega_I^2\tau_c^2} + \frac{13\tau_c}{1+\omega_S^2\tau_c^2} \right)$$

$$+ \frac{1}{3} S(S+1)\left(\frac{A}{\hbar} \right)^2 \left(\tau_e + \frac{\tau_e}{1+\omega_S^2\tau_e^2} \right) \quad \textbf{(A3-1)}$$

where $T_{2,M}$ is the transverse relaxation time of a nucleus in the protein to which the paramagnetic species is fully bound,

ω_I and ω_S are the Larmor angular precession frequencies for the nuclear spins and electron spins respectively,

τ_c and τ_e are the correlation times for the dipolar and scalar interactions respectively,

γ_I is the magnetogyric ratio,

g is the Landé g-factor,

S is the total electron spin,

β is the Bohr magneton,

r is the distance between the paramagnetic centre and the nucleus and

$A/\hbar$ is the hyperfine coupling constant.

The first term arises from the dipole-dipole interaction between the electron spin (S) and the nuclear spin (I) which is modulated by a correlation time τ_c. The correlation time for the dipolar term is defined as

$$\frac{1}{\tau_c} = \frac{1}{\tau_R} + \frac{1}{\tau_S} + \frac{1}{\tau_M} \qquad \textbf{(A3-2)}$$

where τ_R is the rotational correlation time of the bound paramagnetic species,

τ_S is the electron spin relaxation time and

τ_M is the life-time of the nucleus in a bound state.

Paramagnetic metal ions can be classified as relaxation probes or shift probes on the basis of these correlation times. In general paramagnetic ions which give rise to easily measurable shifts have short electron spin relaxation times, therefore $1/\tau_c$ is dominated by the contribution from $1/\tau_S$, with $\tau_S \approx 10^{-12}$-10^{-13} s. In this case the relaxation induced by the paramagnetic ion is relatively inefficient and the line-widths are correspondingly narrow. Examples include most lanthanide(III) ion complexes and of importance in this thesis, low-spin Fe(III). Those metal ions in which $1/\tau_c$ is dominated by $1/\tau_R$ ($\tau_S > \tau_R$), with $\tau_c \approx 10^{-10}$-10^{-11} s are far more effective at causing relaxation and are thus used as relaxation probes. Examples include Cr(III), Mn(II) and Gd(III).

The shift of the magnetic resonances of nuclei in a paramagnetic complex from their corresponding positions in diamagnetic complexes generally result from two types of interaction with the unpaired electron. A contact (Fermi) shift contribution arises from delocalisation of unpaired electron spin density at the resonating nucleus. The interaction is transmitted through chemical bonds and is given by (McConnell & Chestnut, 1958)

$$\frac{\Delta\omega_M}{\omega_I} = -\left(\frac{A}{\hbar}\right)\frac{g\beta S(S+1)}{3kT\gamma_I} \qquad \textbf{(A3-3)}$$

where ω_I is the irradiating frequency.

Equation (A3-3) is only valid for systems with isotropic g-values and is therefore of no value in evaluating shifts due to octahedral low-spin Fe(III) (*e.g.* for $[Fe(CN)_6]^{3-}$ $|g_x| = 2.35$, $|g_y| = 2.10$ and $|g_z| = 0.915$; Bleaney and O'Brien, 1956).

The second contribution is the dipolar or pseudo-contact shift which results from the dipolar interaction between the nuclear spin and the unpaired electron spin. For anisotropic electron distribution the dipolar interaction does not average to zero. If possible effects of spin delocalisation on dipolar interactions are ignored the pseudo-contact shift is given by (Kurland & McGarvey, 1970)

$$\frac{\Delta\omega_M}{\omega_I} = \frac{\beta^2 S(S+1)}{9kTr^3}\left\{[g_z^2 - 1/2(g_x^2 + g_y^2)](3\cos^2\theta - 1) + 3/2(g_y^2 - g_x^2).\sin^2\theta.\cos 2\psi\right\} \qquad \textbf{(A3-4)}$$

where r is the distance between the nucleus and the paramagnetic centre,

θ is the angle between the vector $\boldsymbol{r}$ and the principal symmetry axis (z) of the complex and

ψ is the angle between the projection of the vector $\boldsymbol{r}$ in the xy plane and the x axis.

For the case of axial symmetry ($g_z = g_{\parallel}$ and $g_x = g_y = g_{\perp}$) then the contribution to chemical shift is given by (McConnell & Robertson, 1958; Bleaney, 1972)

$$\frac{\Delta\omega_M}{\omega_I} = \frac{\beta^2 S(S+1)}{9kT}(g_{\parallel}^2 - g_{\perp}^2)\frac{(3\cos^2\theta - 1)}{r^3} \qquad \textbf{(A3-5)}$$

In solution the values of r and θ will be the result of averaging of motions which are rapid on the NMR time scale. Equation (A3-5) is therefore more

commonly written as

$$\frac{\Delta\omega_M}{\omega_I} = D\left(\frac{(3\cos^2\theta - 1)}{r^3} \right)_{av.} \qquad \textbf{(A3-6)}$$

Calculation of distance ratios from $[Cr(CN)_6]^{3-}$ relaxation data:

At the Larmor frequency of protons ($\omega_I \approx 3.1 \times 10^9$ rad s^{-1} at 500 MHz) $\omega_I^2\tau_c^2 >> 1$, therefore, in the absence of scalar interactions, $T_{2,M}$ can be approximated by (from equation (A3-1))

$$\frac{1}{T_{2,M}} = \frac{4}{20}\frac{\mu_o^2}{(4\pi)^2}\frac{\gamma_I^2 g^2 S(S+1)\beta^2}{r^6} \cdot \tau_c$$

$$= f(\tau_c)\frac{1}{r^6} \qquad \textbf{(A3-7)}$$

In the absence of bound paramagnetic ion the peak height, p_A, is directly proportional to the transverse relaxation time of the unbound nucleus

$$p_A = \frac{A}{\Delta\nu_{1/2,A}} = B.T_{2,A} \qquad \textbf{(A3-8)}$$

The observed peak height in the presence of the paramagnetic ion is similarly dependent on T_2

$$p_{A,obs} = \frac{A}{\Delta\nu_{1/2,obs}} = B.T_{2,obs} \qquad \textbf{(A3-9)}$$

Under conditions of fast exchange between unbound ligand molecules (protein) and those bound by the paramagnetic ion the observed relaxation rate can be considered to arise from two contributions: (a) the relaxation rate in the absence of the paramagnetic ion, $1/T_{2,A}$ and (b) the relaxation rate arising from dipolar interaction with the bound paramagnetic ion, $1/T_{2,M}$

$$\frac{1}{T_{2,obs}} = \frac{(1 - f)}{T_{2,A}} + \frac{f}{T_{2,M}} \qquad \textbf{(A3-10)}$$

where f is the fraction of bound ligand,

$$f = \frac{[EI]}{[E]_o} \qquad \textbf{(A3-11)}$$

[EI] is the concentration of $[Cr(CN)_6]^{3-}$.enzyme complex and $[E]_o$ is the total enzyme concentration.

If the total $[Cr(CN)_6]^{3-}$ concentration, $[I]_o << [E]_o$, then

$$f \approx \frac{[I]_o}{[E]_o} << 1$$

$\therefore$ from equation (A3-10)

$$\frac{1}{T_{2,obs}} \approx \frac{1}{T_{2,A}} + \frac{[I]_o}{[E]_o.T_{2,M}} \qquad \textbf{(A3-12)}$$

$$\therefore \quad T_{2,obs} \approx \frac{[E]_o.T_{2,A}.T_{2,M}}{[I]_0.T_{2,A} + [E]_o.T_{2,M}} \qquad \textbf{(A3-13)}$$

The change in peak height is

$$\Delta p = p_A - p_{obs} = B(T_{2,A} - T_{2,obs})$$

Combining with equation (A3-13) gives

$$\Delta p = B\left(T_{2,A} - \frac{[E]_o.T_{2,A}.T_{2,M}}{[I]_o.T_{2,A} + [E]_o.T_{2,M}} \right) \qquad \textbf{(A3-14)}$$

$$\therefore \Delta p = \frac{B.[I]_o.T_{2,A}^2}{[I]_o.T_{2,A} + [E]_o.T_{2,M}}$$

$$= \frac{B.T_{2,A}^2}{T_{2,A} + ([E]_o/[I]_o).T_{2,M}} \qquad \textbf{(A3-15)}$$

$\therefore$ from equation (A3-7)

$$\therefore \Delta p = B.T_{2,A}^2 \left(T_{2,A} + \frac{[E]_o}{[I]_o} \frac{r^6}{f(\tau_c)} \right)^{-1} \qquad \textbf{(A3-16)}$$

if τ_c is assumed to be constant

$$\frac{1}{\Delta p} = \frac{1}{B.T_{2,A}^2}\left(T_{2,A} + \frac{[E]_o}{[I]_o}\frac{r^6}{C} \right)$$

$$= \frac{1}{B.T_{2,A}} + \frac{[E]_o}{[I]_0}\frac{r^6}{B.C.T_{2,A}^2}$$

$$\therefore \quad \frac{1}{\Delta p} = \frac{1}{p_A} + \frac{[E]_o}{[I]_o}\frac{r^6}{D} \qquad \textbf{(A3-17)}$$

A plot of $1/\Delta p$ versus $[E]_o/[I]_o$ will therefore have a slope proportional to r^6 and an intercept equal to $1/p_A$.

Estimation of maximum distances from Mn^{2+} relaxation data:

The paramagnetic contribution to the observed transverse relaxation rate, $1/T_{2,P}$, is defined by

$$\frac{1}{T_{2,P}} = \frac{f}{T_{2,M} + \tau_M} \qquad \textbf{(A3-18)}$$

Under conditions of fast exchange $1/T_{2,P}$ is approximated by $f/T_{2,M}$ as in equation (A3-10).

Given equation (A3-11) and

$$K_d = \frac{[E][I]}{[EI]} = \frac{([E]_o - [EI])([I]_o - [EI])}{[EI]} \qquad \textbf{(A3-19)}$$

if $[E]_o >> [I]_o$

$$[EI] = \frac{[E]_o.[I]_o}{K_d + [E]_o} \qquad \textbf{(A3-20)}$$

$$\therefore \quad f = \frac{[I]_o}{K_d + [E]_o} \qquad \textbf{(A3-21)}$$

Combining equations (A3-18) and (A3-21) gives

$$\frac{1}{T_{2,P}} = \frac{[I]_o}{(T_{2,M} + \tau_M)(K_d + [E]_o)}$$

$$\approx \frac{[I]_o}{T_{2,M}.(K_d + [E]_o)} \qquad \textbf{(A3-22)}$$

The linewidth at half-height, $\Delta\nu_P$, is related to $1/T_{2,P}$ by

$$\pi.\Delta\nu_P = 1/T_{2,P} \qquad \textbf{(A3-23)}$$

$$\therefore \quad \Delta\nu \approx \frac{[I]_o}{\pi.T_{2,M}.(K_d + [E]_o)} \qquad \textbf{(A3-24)}$$

By measuring the line-width as a function of Mn^{2+} concentration an upper limit for $T_{2,M}$ can be obtained. $T_{2,M}$ is related to the Mn^{2+}-proton distance by equation (A3-7).

A maximum value for τ_c can be obtained by equating it to τ_R (equation A3-2). τ_R can be calculated from the Stokes-Einstein equation

$$\tau_R = M\bar{V}\eta/RT$$

where M is the molecular mass of the complex (~ 45 kDa),
$\bar{V}$ is the partial specific volume (~ 0.749 $cm^3\ g^{-1}$ from Sinev *et al.*, 1989; calculated on the basis of chemical composition, Lee & Timasheff, 1974),
η is the viscosity (~ 1.047 cp for D_2O at 300 K).

In using the above approximation it is assumed that τ_R is isotropic and that the 'basic patch' histidines have no extra mobility.

References:

Bleaney, B. & O'Brien, M.C.M. (1956) *Proc. Phys. Soc. B. 69,* 1216-1230.

Bleaney, B. (1972) *J. Magn. Reson. 8,* 91-100.

Bloembergen, N. (1957) *J. Chem. Phys. 27,* 572-573.

Kurland, R.J. & McGarvey, B.R. (1970) *J. Magn. Reson. 2,* 286-301.

Lee, J.C. & Timasheff, S.N. (1974) *Arch. Biochem. Biophys. 165,* 268-273.

McConnell, H.M. & Chestnut, D.B. (1958) *J. Chem. Phys. 28,* 107-117.

McConnell, H.M. & Robertson, R.E. (1958) *J. Chem. Phys. 29,* 1361-1365.

Sinev, M.A., Razgulyaev, O.I., Vas, M., Timchenko, A.A. & Ptitsyn, O.B. (1989) *Eur. J. Biochem. 180,* 61-66.

Solomon, I. (1955) *Phys. Rev. 99,* 559-565.